Organocatalytic Synthesis of Pentafulvene Derivatives and Kinetic Analysis of Copper Catalyzed 1,4-Addition

Ryan Nouch

ID: 4246743

Supervised by Prof. Simon Woodward

Submitted January 2020

School of Chemistry

University of Nottingham

I hereby declare that this thesis is all my own work, except as indicated in the text.

Abstract

Chapter 1 discloses a novel organocatalytic method for the synthesis of pentafulvenes bearing chiral pendant groups. Despite the widespread utility of pentafulvenes, synthetic methods towards them have not developed significantly since their initial discovery in 1900. More specifically, syntheses of pentafulvenes bearing pendant chiral groups are extremely uncommon. The primary aim of this work was to develop the asymmetric synthesis of pentafulvene **1.162a**. Novel pentafulvene (±)-**1.162a** was observed to form in the pyrrolidine catalyzed reaction between 2-acetylbenzaldehyde (**1.160a**) and CpH. It was envisaged that an enantioselective variant of this reaction could help to furnish **1.162a** as a single enantiomer, utilizing the fact that **1.162a** was found to crystallize as a conglomerate. This resulted in the chiral amplification of scalemic mixtures of **1.162a** to enantiopure **1.162a** during crystallization. The reduction of enantiopure **1.162a** to the corresponding CpH derivative could then be performed in a diastereoselective manner. This provided a novel, facile method to afford a structurally diverse library of chiral CpH derivatives.

Chapter 2 discloses a data intensive investigation into the kinetics of copper catalyzed 1,4-asymmetric addition using organoaluminium and diorganozinc reagents. Copper catalyzed asymmetric conjugate addition reactions are among the most common methods for enantioselective carbon-carbon bond formation. However there remains little mechanistic evidence to support the structure of their key, rate-determining transition states. The aim of this project was to provide high quality kinetic data on the copper catalyzed asymmetric conjugate addition of organoaluminium and diorganozinc reagents to 2-cyclohexen-1-one. This also lead to the development of a novel copper(I) complex that proved to be an extremely effective catalyst for the asymmetric conjugate addition of organozinc reagents to a variety of α,β-unsaturated ketones. Studies of the copper(II) acetate catalyzed addition of triethylaluminium and the copper(I) tetrakisacetonitrile trifluoroacetate catalyzed addition of diethyl zinc to 2-cyclohexen-1-one were performed.

Acknowledgements

First, I should like to thank Prof. Simon Woodward for trusting me with such a varied and interesting project. It has had its challenges, just like any PhD, but the experience has been invaluable to me. A massive thank you for all of the support and guidance you have given me over the past 5 years.

I should also like to thank all members of the Woodward group, past and present, for their help and friendship. I would especially like to thank Laurence Burroughs for his patience and guidance throughout my undergraduate research project and the beginning of my PhD. Thanks to John Ritchie for his continued friendship, advice and help with the preparation of my thesis. I miss your problems of the day but at least you still get to school me at bouldering every week. I also owe thanks to Melchior Cini, Marc Magre and Darren Willcox for their early contributions to this project. *Shukran lak* to Mohammed Abid for his contributions to my project and for the Arabic lessons.

I got to share a lab for two years with the Ball group, so many thanks to all of you. Thanks to Mark Jurrat for letting me beat you so often at badminton and hopefully we will get to open that inappropriately named emu sanctuary one day. Sorry that my smidges bothered you so much! Thanks to Tom Barber for being a continual source of top-quality memes and for being a very reliable conference buddy. Another thank you to Lorenzo Maggi for the Italian lessons and for making great espressos! *Buon pomeriggio*!

This PhD couldn't have happened without the help of the analytical services team, so a massive thank you to the whole team and especially to Mick Cooper, Kevin Butler, Ben Pointer-Gleadhill, Tong Liu and William Lewis for all of their help. I also would like to thank the aforementioned Simon Woodward, the University of Nottingham and Aesica for their financial contributions towards this project.

Last, but certainly not least, I need to thank all of my friends and family for their love and support throughout my life. My love and gratitude to the three most important people in my life: my girlfriend Ashley, my fiancé Ashley and my wife Ashley; all of whom supported and loved me during my PhD. Thanks to my top-notch best man Patrick Whitelaw. I know we thought our friendship would end after Star Wars IX but I think optimistically we could make it all the way to Star Wars XII. A massive thank you to Charlotte Gidman for the past eight years of friendship.

I still think you would have looked great in a top hat and tails if I was allowed a best woman at the wedding, sorry you had to settle for being a bridesmaid instead. Thank you to Helen Powell for her friendship over those eight years also. I have forgiven you now for not setting up my job interview with your Dad.

Thanks to my Mum, Dad, Pete and Rachel for their love and support throughout my life. I would need to write a second thesis to fit in all the things I have to thank you all for. Thanks to Rachel for helping change me from a very scuzzy child into only a semi-scuzzy adult (sorry I had quite so many bad habits!). Thanks to Pete for the badminton lessons and for teaching me to always wear a gumshield when being passed things from a loft. Thanks to my Dad for teaching me how to properly clean a car and for motivating me to start going to the gym as a teenager. And thanks to my Mum for giving me my great music taste starting with those concerts you took me to whilst pregnant and for being the coolest mum (as agreed unanimously by all my friends in school).

I have one last thank you to write. If I was going to dedicate my thesis to anyone, it would be to my Grandad. He was there to see me start my PhD but is not here to see me finish it. I miss you every day and hope that you would still be proud of me. Thanks for being everything I could have wanted from a Grandad. Lots of love.

Abbreviations

Standard abbreviations of the *Journal of Organic Chemistry* are used.[*] Any that are undefined in that source are listed below:

A	Triethylaluminium
ACA	Asymmetric conjugate addition
BIPHEP	2,2'-Bis(diphenylphosphino)biphenyl
Cu_a	Copper(II) acetate
Cu_b	$Cu(MeCN)_4TFA{\cdot}TFAH$
CX	2-Cyclohexen-1-one
CX·A	2-Cyclohexen-1-one triethylaluminium adduct
CX·Zn	2-Cyclohexen-1-one diethylzinc adduct
DIC	*N,N'*-Diisopropylcarbodiimide
DMS	Dimethylsulfide
DTBP	2,6-Di-*tert*-butylpyridine
E	Enolate product of 1,4-addition
EDC	*N*-(3-Dimethylaminopropyl)-*N'*-ethylcarbodiimide hydrochloride
ee	Enantiomeric excess
ICP-OES	Inductively coupled plasma optical emission spectrometry
L	(*R,S,S*)-Feringa's ligand or (11b*R*)-*N,N*-Bis((1*S*)-1-phenylethyl)dinaptho (2,1-*d*:1',2'-*f*)(1,3,2)dioxaphosphephin-4-amine
NFSI	*N*-Fluorobenzenesulfonimide
P	(*R*)-3-Ethyl-cyclohexanone
PG	Protecting group
RT	Room temperature
TFA	Trifluoroacetate
TFAA	Trifluoroacetic anhydride
TFAH	Trifluoroacetic acid
p-TSA	*para*-Toluenesulfonic acid
ZACA	Zirconium-catalyzed asymmetric carboalumination
Zn	Diethylzinc

[*] Obtained from http://pubs.acs.org/paragonplus/submission/joceah/joceah_authguide.pdf on 13/09/2018.

Contents

1 Organocatalytic Synthesis of Pentafulvene Derivatives

1.1 Introduction

1.1.1 Introduction to Organocatalysis

Organocatalysis refers to the use of sub-stoichiometric quantities of organic molecules to catalyze chemical transformations.[1] Whilst the term organocatalysis is a relatively new one, the concept is not. As far back as the 19th century organic molecules were used to accelerate chemical transformations, with the first known example being the acetaldehyde catalyzed conversion of cyanogen (**1.1**) to oxamide (**1.2**) (Scheme 1a).[2][3] Later in the same century, Knoevenagel reported that the condensation of formaldehyde with diethyl malonate (**1.3**) is catalyzed by ethylamine (Scheme 1b).[4] Though not named as such at the time, organocatalytic reactions continued to be reported throughout the next century, one example being the Morita-Baylis-Hillman reaction. In this transformation, sub-stoichiometric quantities of amines or phosphines (*e.g.* DABCO or triphenylphosphine) are commonly used to accelerate, and control the regioselectivity of, the reaction between aldehydes and ethyl acrylate (**1.6**), to afford the corresponding α-hydroxyethylated product (**1.7**) (Scheme 1c).[5]

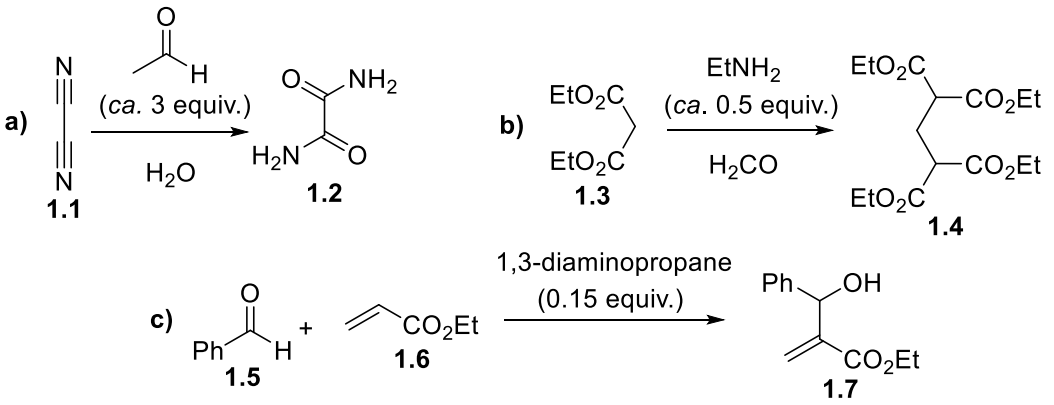

Scheme 1: Examples of early organocatalytic reactions: ***a)*** *Reaction between cyanogen (**1.1**) and acetaldehyde to form oxamide (**1.2**);*[2] ***b)*** *Knoevenagel condensation of diethyl malonate (**1.3**) and formaldehyde (2:1);*[4] ***c)*** *Morita-Baylis-Hillman reaction between benzaldehyde (**1.5**) and ethyl acrylate (**1.6**).*[5]

Prior to the 21st century, the field of asymmetric organocatalysis was largely unknown. It wasn't until the late 1990s that the potential of small organic molecules to catalyze enantioselective transformations began to become more widely recognised. Before this, only a few examples of asymmetric organocatalysis existed. Notable amongst these is the *O*-acetylquinine (**1.9**) mediated synthesis of ester **1.10** by Pracejus in 1960, one of the oldest organocatalytic transformations affording synthetically useful levels of enantioselectivity (Scheme 2a).[6] Another early example of note is the (*S*)-proline ($\mathbf{L_a}$) catalyzed Hajos-Parrish-Eder-Sauer-Wiechert reaction, discovered independently by two groups in 1971 (Scheme 2b).[7][8] Initially described as a unique chemical reaction, rather than a new field of catalysis, this reaction not only afforded a product with exceptionally high enantiopurity, but also became the centre of later mechanistic studies which helped bring organocatalysis into prominence. Towards the end of the 1990s, more examples of enantioselective organocatalysis began to appear. Several groups demonstrated the ability of organic molecules to catalyze the asymmetric epoxidation of alkenes, one example of which is the use of fructose-derived ketone **1.14** by Shi and co-workers (Scheme 2c).[9] Other types of transformation also proved possible, for example the asymmetric Strecker reaction, catalyzed by Schiff's base **1.17**, was developed by Sigman and Jacobsen in 1998 (Scheme 2d).[10]

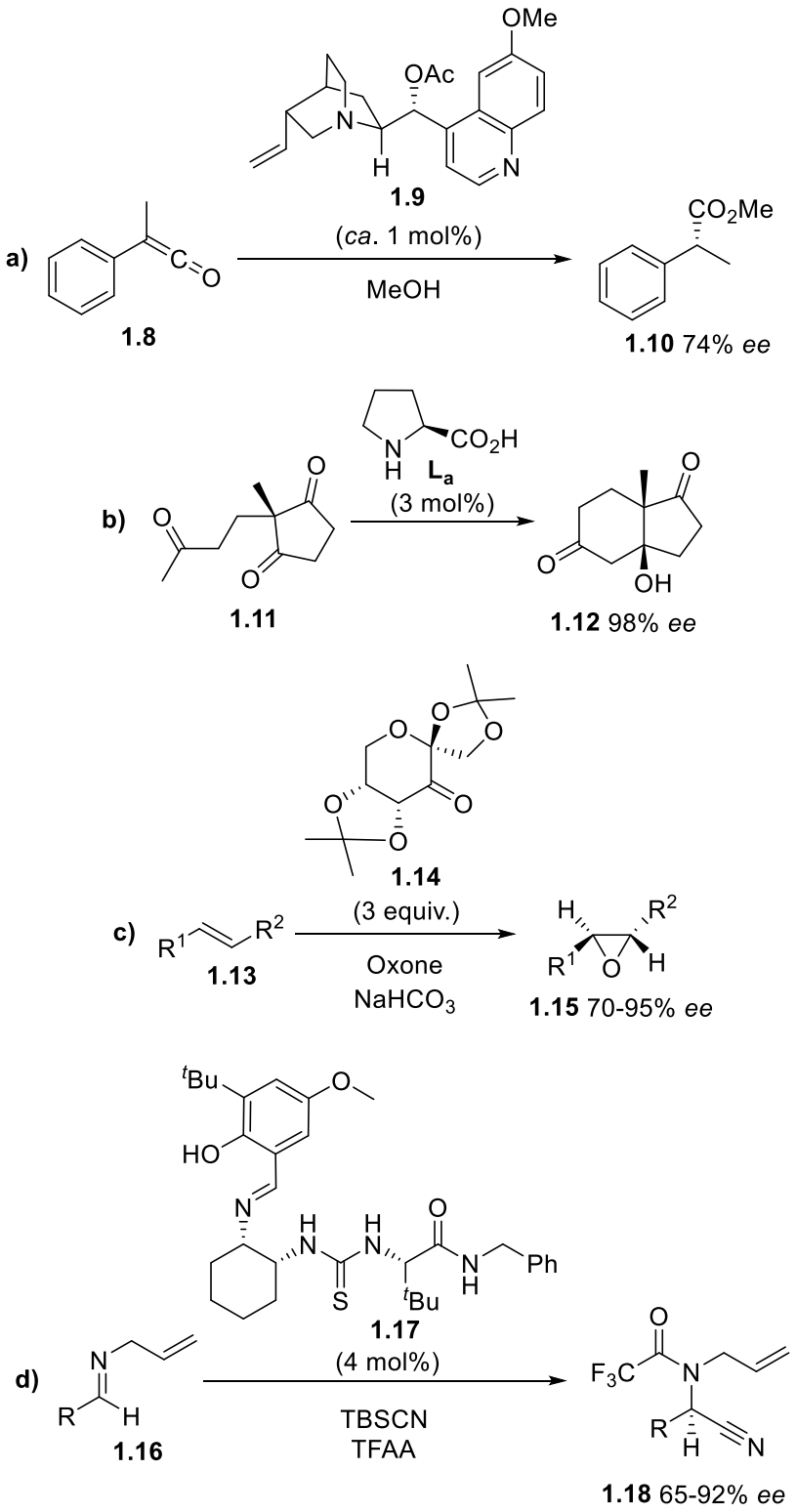

Scheme 2: Examples of early enantioselective organocatalytic reactions: ***a)*** *Synthesis of ester* ***1.10*** *from methyl phenyl ketene (****1.8****);*[6] ***b)*** *Hajos-Parrish-Eder-Sauer-Wiechert reaction;*[7] ***c)*** *Epoxidation of trans-alkenes mediated by fructose-derived ketone* ***1.14****;*[9] ***d)*** *Asymmetric Strecker reaction catalyzed by Schiff base* ***1.17****.*[10]

It was not until the year 2000 that the field of organocatalysis came into prominence, primarily though the work of two groups. Benjamin List and co-workers published an (*S*)-proline catalyzed asymmetric intermolecular aldol reaction between acetone and various aldehydes (Scheme 3a).[11] Based upon the principles of recently described aldolase[12] and chiral lanthanum complex catalysis,[13] as well as the intramolecular Hajos-Parrish-Eder-Sauer-Wiechert reaction, it demonstrated the potential utility of small organic molecules as asymmetric catalysts. Meanwhile, MacMillan and co-workers published an enantioselective 1,3-dipolar cycloaddition, between crotonaldehyde and a nitrone, catalyzed by a chiral imidazolidinone (**1.23**) (Scheme 3b).[14] This paper was not just one of the first published uses of the term organocatalysis, but also demonstrated the ability of organic molecules to catalyze transformations traditionally requiring chiral metal catalysts (*i.e.* Lewis acids). These organic molecules possess numerous advantages over metal catalysts: ease of handling, insensitivity to air/moisture, lower toxicity and environmental impact and the potential for extremely cheap sourcing from the chiral pool (*i.e.* utilizing the built-in chirality of biologically occurring molecules such as amino acids or monosaccharides).[15] As a result, the number of articles published focussing on organocatalysis has grown exponentially (Figure 1).

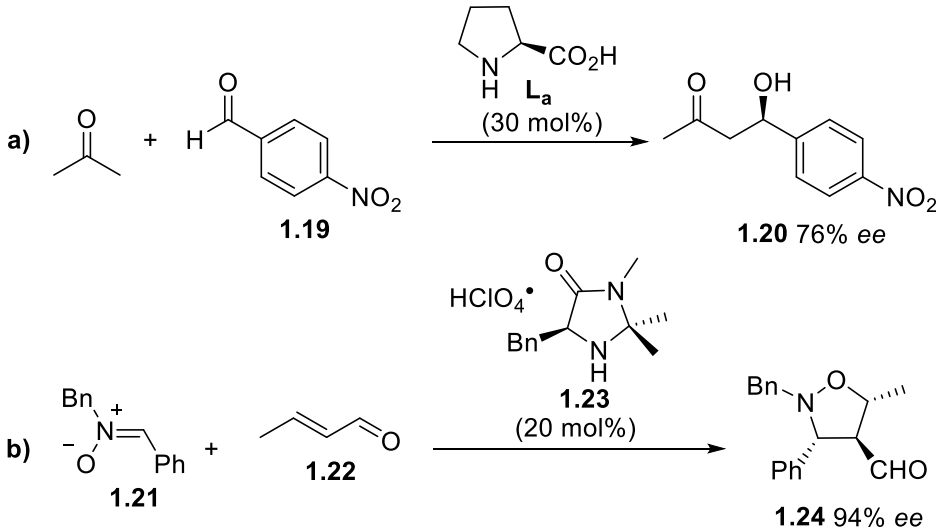

Scheme 3: Key publications from the year 2000: ***a)*** *List and co-workers' intermolecular aldol reaction;*[11] ***b)*** *MacMillan and co-workers' 1,3-dipolar cycloaddition.*[14]

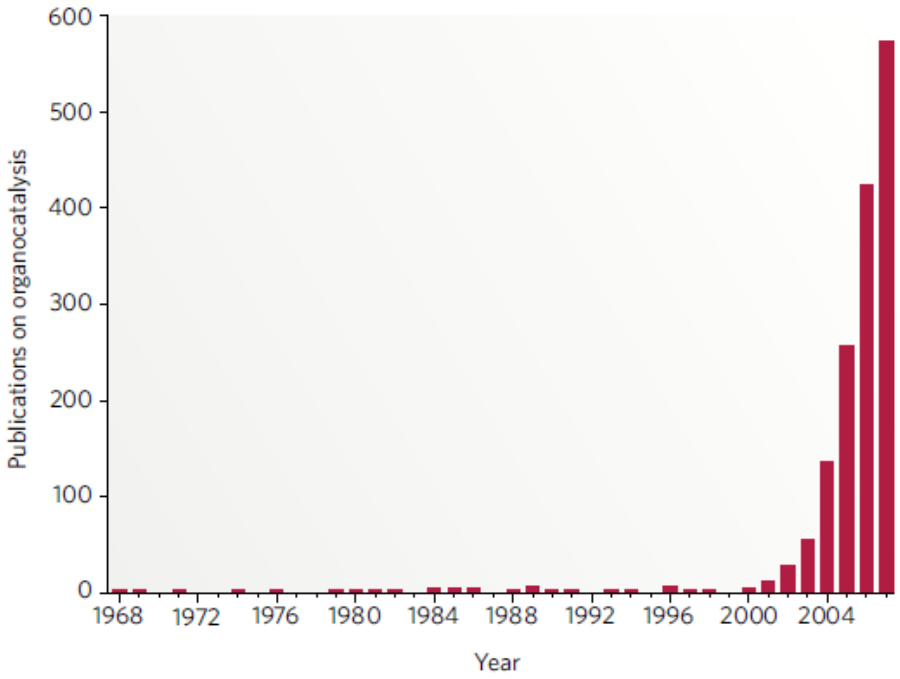

Figure 1: Graph showing the number of publications, per year, focussing on organocatalysis between 1968 and 2008 from MacMillan's 2008 review.[15]

1.1.2 Enamine and Iminium Organocatalysis

The transformations published by List and MacMillan, mentioned above (Scheme 3), both require a secondary amine catalyst but form either nucleophilic or electrophilic species. List's (*S*)-proline (**L**$_a$) uses enamine catalysis whilst MacMillan's imidazolidinone **1.23** functions *via* iminium catalysis. Enamines (**1.26**) are a more nucleophilic equivalent of an enol, in which the HOMO has been raised in energy, first discovered by Wittig and co-workers in 1927[16] and their versatility later demonstrated by the groups of Mannich[17] and Stork[18] among others. Iminium ions (1.25), however, are a more electrophilic equivalent of a carbonyl, in which the LUMO has been lowered in energy. These were first discovered by Schiff in 1864[19] and later utilized by Vilsmeier and Haack[20] among others.

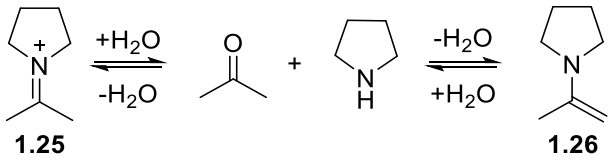

*Scheme 4: The formation of enamine **1.26** and iminium **1.25** in the condensation between acetone and pyrrolidine.*

List and co-workers theorized that their intermolecular aldol reaction, as well as the intramolecular Hajos-Parrish-Eder-Sauer-Wiechert reaction, proceeded *via* an enamine intermediate. Following further computational and kinetic studies, in collaboration with Houk, the Houk-List intermediate (**1.28**) was proposed in which the enamine formed from the condensation of (*S*)-proline and a ketone generated a six-membered ring intermediate (Scheme 5).[21][22] It was proposed that this intermediate was the origin of the stereoselectivity in these reactions and has since been further investigated and has proven useful in the prediction of the stereochemical outcome of other related reactions.[23]

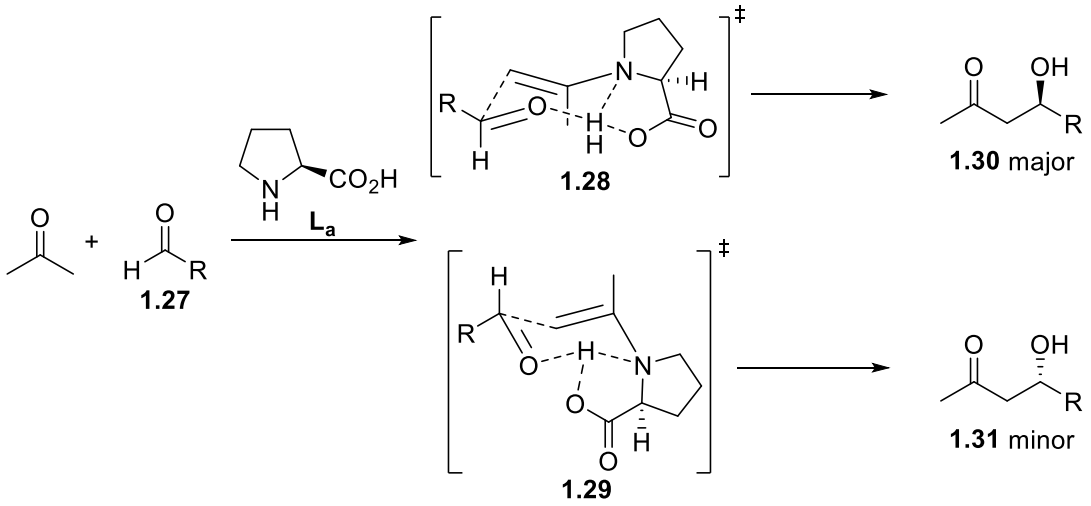

*Scheme 5: The two potential Houk-List intermediates in the (S)-proline (**L**$_a$) catalyzed aldol reaction between acetone and various aldehydes. Kinetic studies confirm the presence of only one proline molecule in the transition state and computational studies predict the energy difference between the potential intermediates **1.28** and **1.29**.*[21][22]

Enamine catalysis has been utilized, within the group of Karl Jørgensen, in the formation of various medicinally useful chiral heterocycles. Using hindered silyl-protected pyrrolidinemethanol derivative **1.34**, an intramolecular Povarov reaction affords octahydroacridine **1.36** derivatives with high levels of enantioselectivity (Scheme 6a).[24] Another example is the use of C_2-symmetric pyrrolidine derivative **1.38** to synthesize optically active 1,2-dihydroisoquinoline **1.39** derivatives, *via* an intramolecular addition of an enamine into a quinolinium salt, with high enantioselectivity and diastereoselectivity (Scheme 6b).[25]

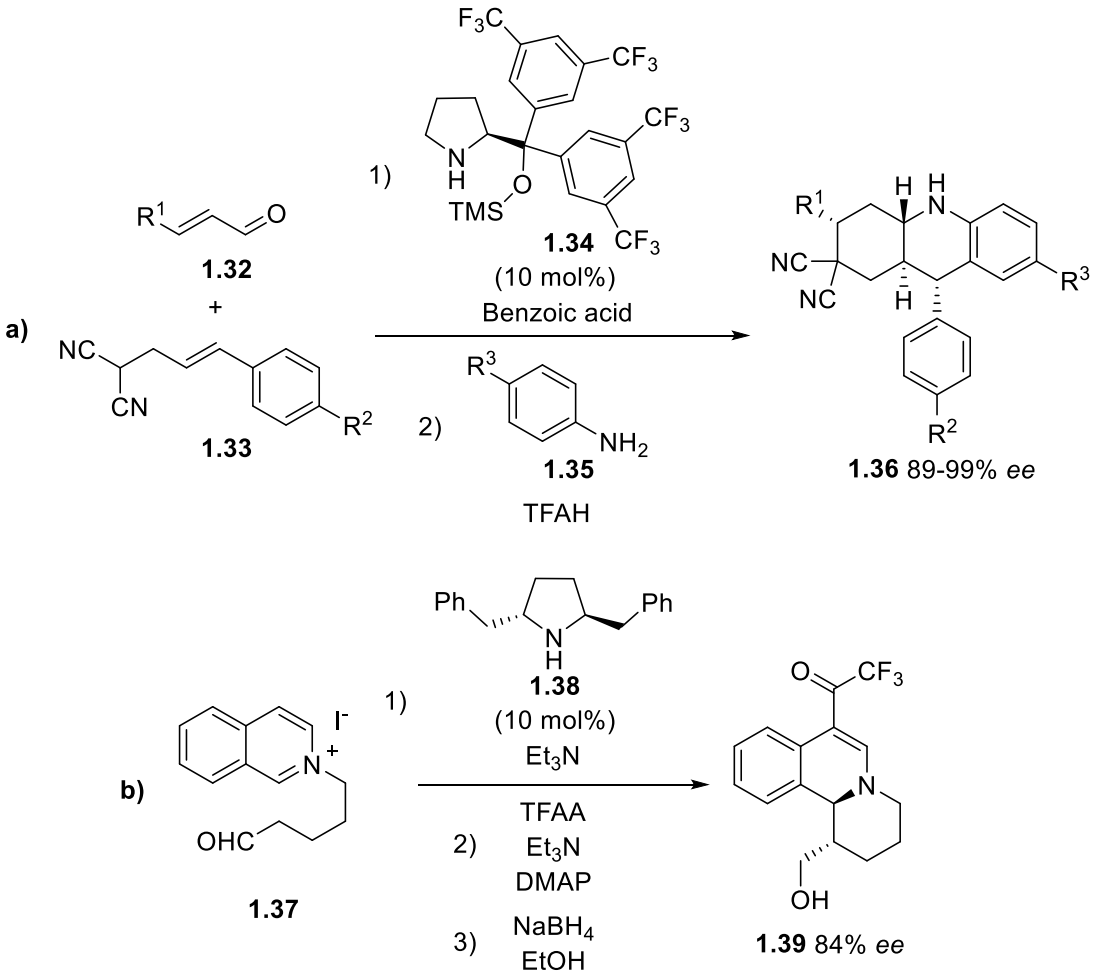

*Scheme 6: Examples of chiral heterocycle synthesis from the Jørgensen group: a) Synthesis of octahydroacridine **1.36** derivatives;[24] b) Synthesis of 1,2-dihydroisoquinoline **1.39** derivatives.[25]*

This mode of catalysis can also be used to enable the formation of several carbon-heteroatom bonds. Of these, an important example is the α-oxidation of aldehydes. Installation of groups containing oxygen, nitrogen, chlorine and fluorine (among others) can all be achieved *via* the interception of an enamine with various electrophiles.[26] Zhong achieved the (*S*)-proline (**L$_a$**) catalyzed α-aminoxylation of aldehydes by the use of nitrosobenzene (**1.40**) as the oxygen source (Scheme 7a).[27] In a similar manner, List achieved α-amination using azodicarboxylate (**1.43**) derived electrophiles (Scheme 7b).[28] Another similar example of α-fluorination comes from the Jørgensen group, using the same bulky silyl-protected pyrrolidinemethanol derivative (**1.34**) mentioned previously (Scheme 7c).[29]

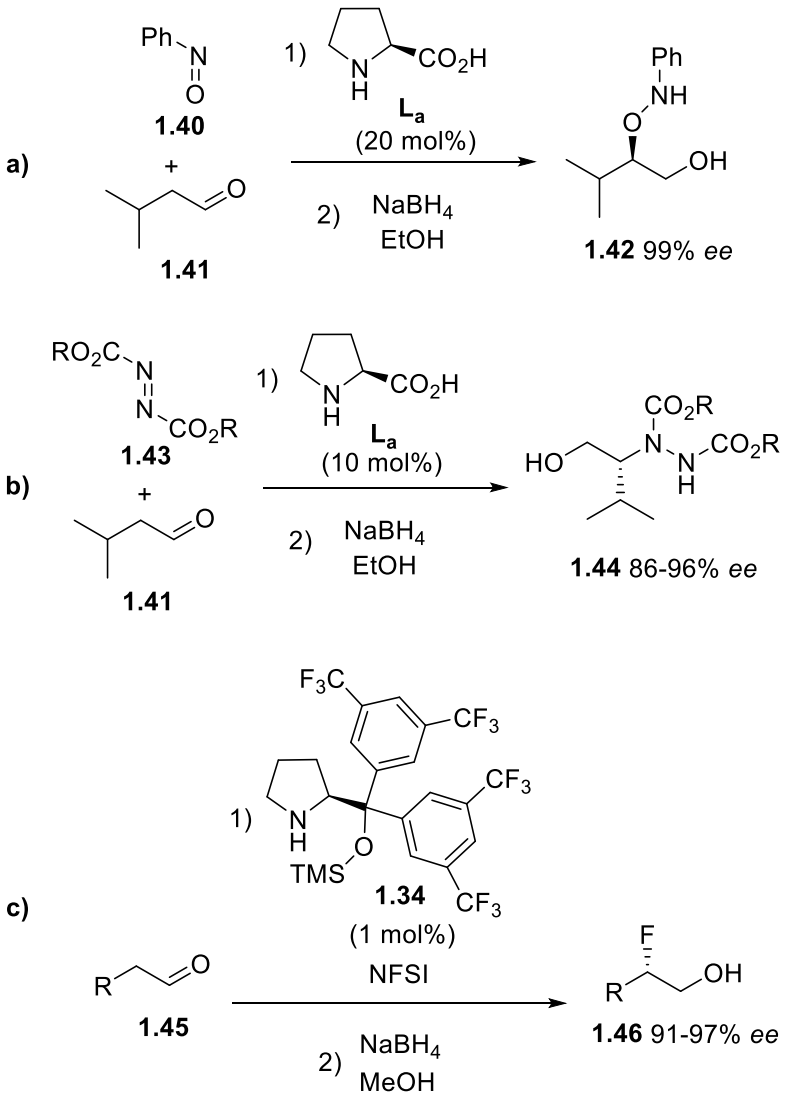

Scheme 7: Examples of enamine catalyzed α-oxidation of aldehydes: ***a)*** *Zhong's α-aminoxylation;*[27] ***b)*** *List's α-amination;*[28] ***c)*** *Jørgensen's α-fluorination.*[29]

Enantioselective chlorination at the α-position of an aldehyde is perhaps one of the more important examples of α-oxidation, as it provides a reactive handle enabling further functionalization. α-Chlorination was achieved within the groups of MacMillan[30] and Jørgensen.[31] MacMillan's route used imidazolidinone catalyst **1.48** with quinone-derived electrophile **1.47** (Scheme 8a) whilst Jørgensen's used C_2-symmetric pyrrolidine-derived catalyst **1.50** with NCS as the electrophile (Scheme 8b), with similar levels of success. To highlight the importance of this transformation, Jørgensen also then further functionalized the resulting product (Scheme 8c). Initial oxidation/reduction of the product enabled the synthesis of the corresponding epoxide (**1.51**) or amine (**1.52**) derivative, among other transformations.[31] This provides an important route to terminal epoxides, with high enantiopurity, which often prove challenging to synthesize by traditional methods. For

comparison, Jacobsen's Mn(II) salen complexes[32][33] or Shi's expoxidation,[9] seen earlier (Scheme 2c), both provide little/no stereoselectivity for terminal epoxides.

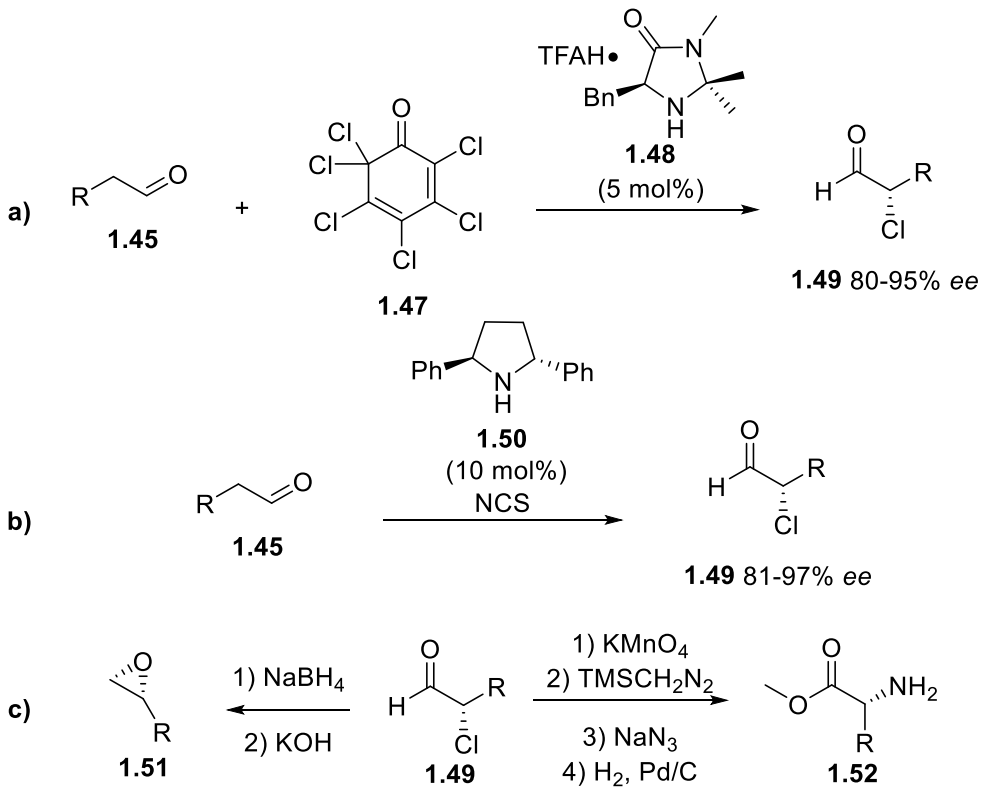

Scheme 8: α-Chlorination of aldehydes, methods and further functionalization: ***a)*** *MacMillan's α-chlorination;[30]* ***b)*** *Jørgensen's α-chlorination;[31]* ***c)*** *Jørgensen's further functionalization of the α-chlorinated aldehyde* ***1.49****.[31]*

As mentioned above, iminium organocatalysis functions in a similar way to traditional metal Lewis acid catalysis (*i.e.* by lowering the energy of the LUMO). Commonly, two main classes of transformation are catalyzed in this manner: Pericyclic reactions (*i.e.* cycloadditions) and 1,4-additions (Michael additions) to α,β-unsaturated compounds.[26] MacMillan's key paper in 2000, mentioned previously (Scheme 3b), reports a [3+2] cycloaddition between a nitrone (**1.21**) and an α,β-unsaturated aldehyde (**1.22**). The origin of the stereoselectivity is proposed to be due to the (*E*)-geometry of the iminium ion **1.53** (which was observed crystallographically) and the position of the pendant benzyl group effectively promote cycloaddition on the *Si* face in a mechanism that is common throughout iminium organocatalysis (Figure 2).[14]

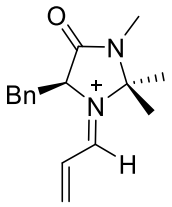

1.53

Figure 2: Structure of the key, stereochemistry determining iminium intermediate.[14]

The ability of iminium organocatalysis to catalyze cycloadditions is not limited to [3+2] but is also applicable to a range of other transformations. Diels-Alder [4+2] cycloadditions can be facilitated by iminium catalysis, for example the reaction between cyclopenta-1,3-diene (CpH) and *trans*-cinnamaldehyde (**1.54**) (Scheme 9a).[34] Additionally, the more unusual formal [4+3] cycloaddition between substituted furans (**1.58**) and 4-trialkylsiloxypentadienal (**1.57**) derivatives can be achieved using an imidazolidinone (**1.59**) related to those popularised by MacMillan (Scheme 9b).[35]

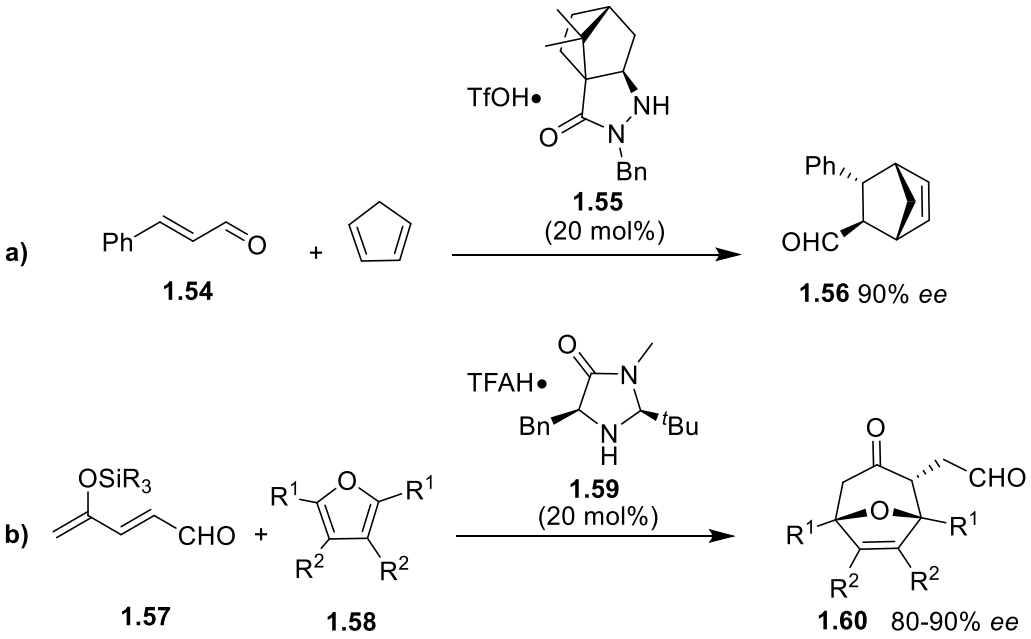

*Scheme 9: Cycloaddition examples: **a)** Diels-Alder [4+2] cycloaddition catalyzed by hydrazide **1.55**;[34] **b)** Asymmetric [4+3] cycloaddition.[35]*

The asymmetric 1,4-addition of a wide range of nucleophiles can be facilitated by iminium catalysis including, but not limited to: carbon (*i.e.* heterocycles), sulfur, nitrogen and oxygen-derived nucleophiles.[36] Meng and co-workers used this powerful approach in the synthesis of a potent selective serotonin reuptake inhibitor using indole as the nucleophile (Scheme 10a).[37] In Jørgensen's group, many heteroatom derived nucleophiles have been employed in these

additions; thio,[38] aza[39] and oxo-Michael additions[40] have all been achieved with high levels of success (Scheme 10b-d).

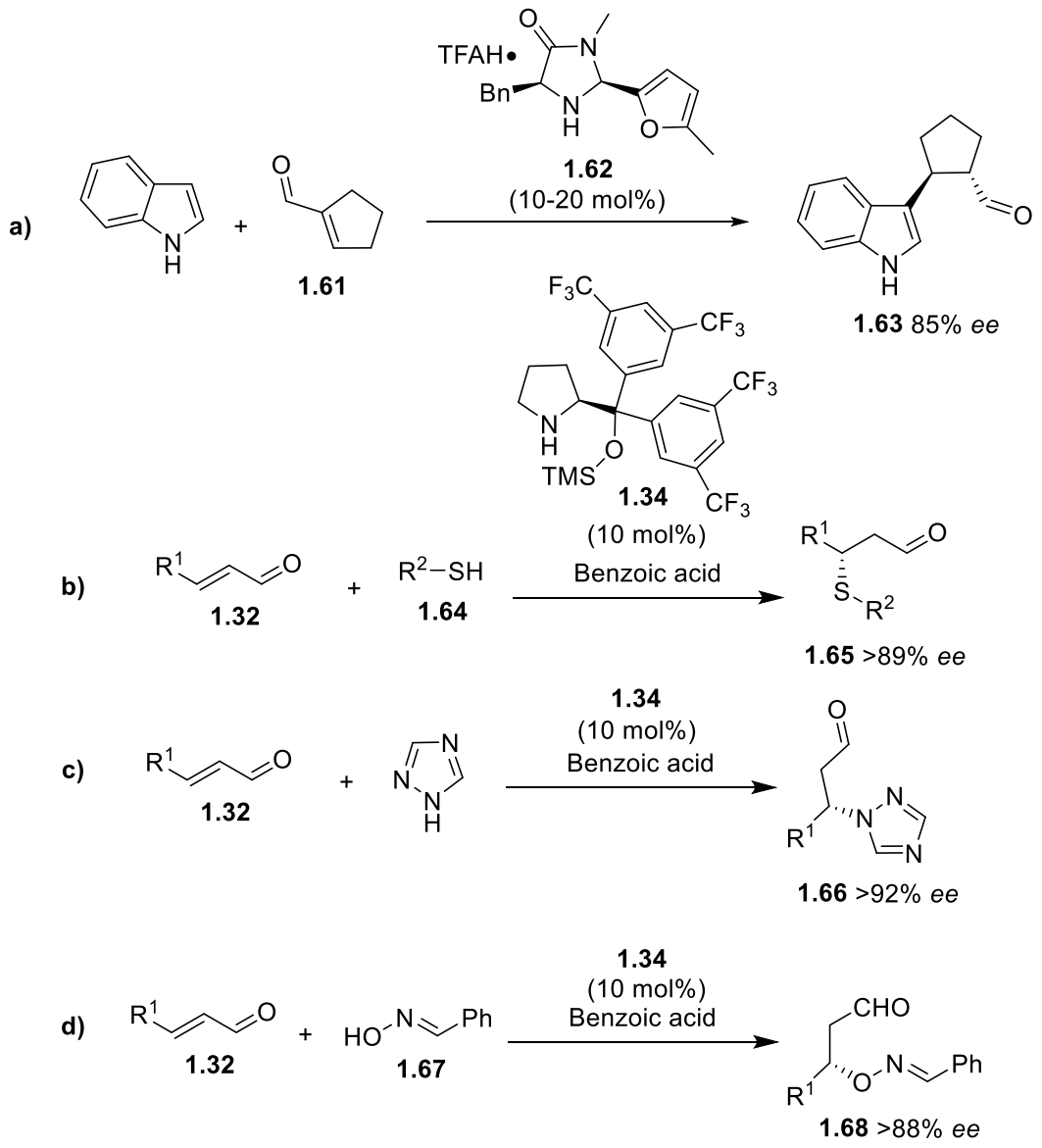

Scheme 10: Examples of iminium catalyzed 1,4-addition: ***a)*** *1,4-Addition of indole to an α,β-unsaturated aldehyde (**1.61**);[37]* ***b)*** *Thio-Michael addition with a range of thiol derived nucleophiles (**1.64**);[38]* ***c)*** *Aza-Michael addition using triazole;[39]* ***d)*** *Oxo-Michael addition with hydroxylamine **1.67**.[40]*

Combinations of enamine and iminium catalysis into multi-component cascade reactions have also been designed, allowing generation of chemical complexity in one-pot approaches. An example of this is the aza-Diels-Alder cascade reaction of an enone, aniline and formaldehyde to generate bridgehead amines moieties (Scheme 11a).[41] A more complex example is the generation of a key intermediate in the total synthesis of (+)-aromadendranediol, which combines ruthenium catalyzed cross-metathesis with enamine and iminium catalysis (Scheme 11b).[42]

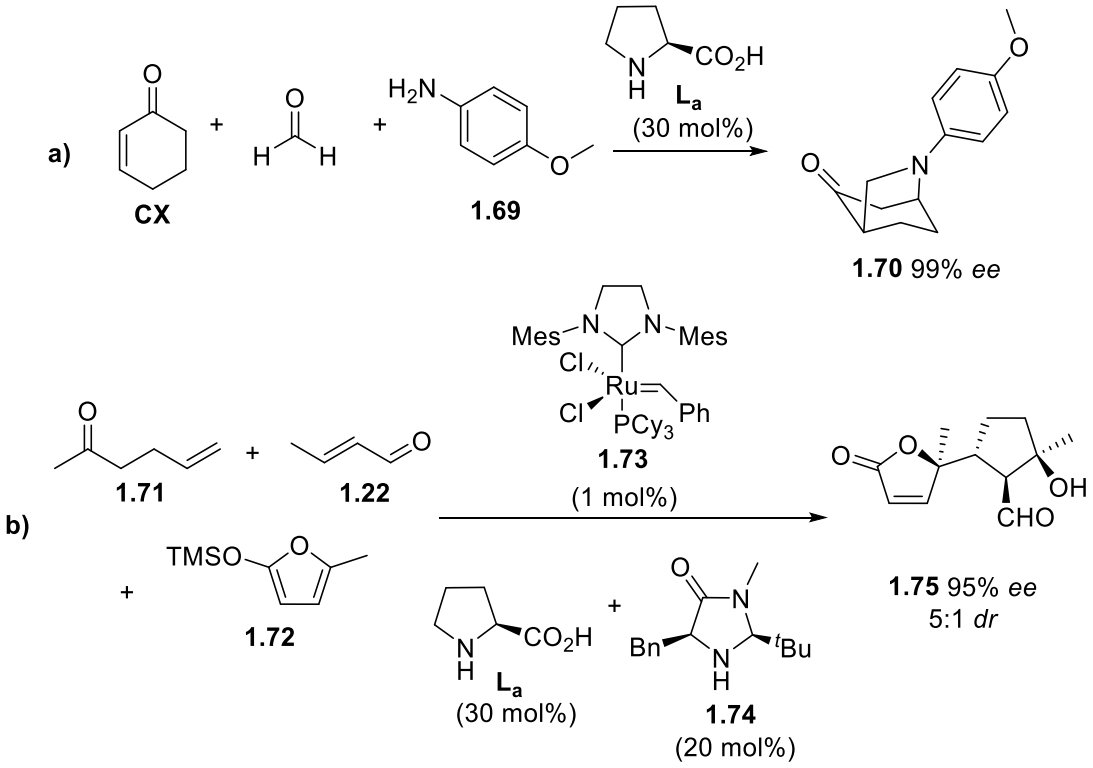

Scheme 11: Examples of enamine-iminium cascade reactions: ***a)*** *(S)-Proline catalyzed aza-Diels-Alder reaction;*[41] ***b)*** *Cascade reaction combining cross-metathesis (**1.73**), iminium (**1.74**) and enamine (**L_a**) catalysis.*[42]

1.1.3 Other Modes of Action in Organocatalysis

Many alternative classes of organocatalysis have been discovered, often acting in a complementary manner with iminium or enamine catalysis, including: Singly occupied molecular orbital (SOMO), hydrogen bonding, counterion and *N*-heterocyclic carbene (NHC) mediated catalysis.[43]

Discovered in 2007 by MacMillan and co-workers, SOMO catalysis functions *via* the generation of an enamine intermediate followed by its oxidation to afford 3π-electron SOMO activated species **1.76**. This can then be intercepted by a range of 'somophiles' in a highly enantioselective manner, in which the bulky pendant group of the amine catalyst blocks one face of the SOMO activated species (Scheme 12).[44][45]

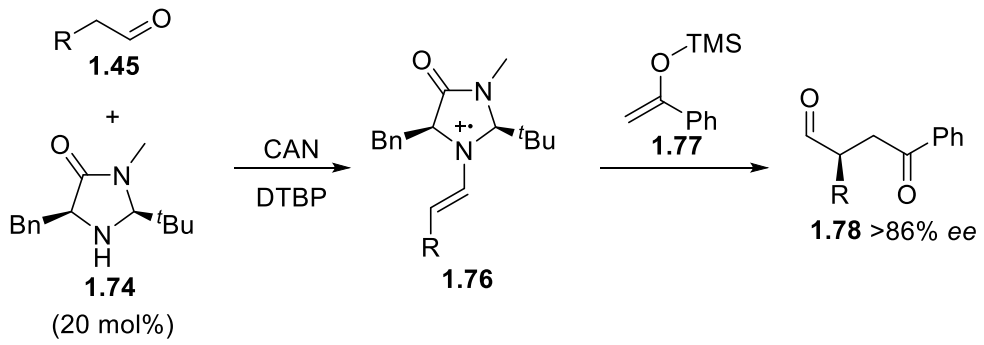

*Scheme 12: Example of SOMO catalysis using MacMillan's imidazolidinone catalyst **1.74** and an oxidant to form SOMO activated species **1.76** which can then react with 'somophile' **1.77**.*[44][45]

An example of hydrogen bonding catalysis was shown previously in Scheme 2d, with the use of a chiral thiourea to catalyze an asymmetric Strecker reaction by Sigman and Jacobsen. Functioning in a similar manner to traditional Lewis acid catalysis, hydrogen bonding catalysis utilizes its hydrogen bond donor sites to lower the LUMO energy of a target carbonyl. Jacobsen later went on to apply this type of catalysis to other asymmetric transformations, for example the Mannich reaction (Scheme 13).[46] It is worth noting that hydrogen bonding catalysis often requires much lower catalyst loadings (typically less than 5 mol%) than covalent modes of organocatalysis.

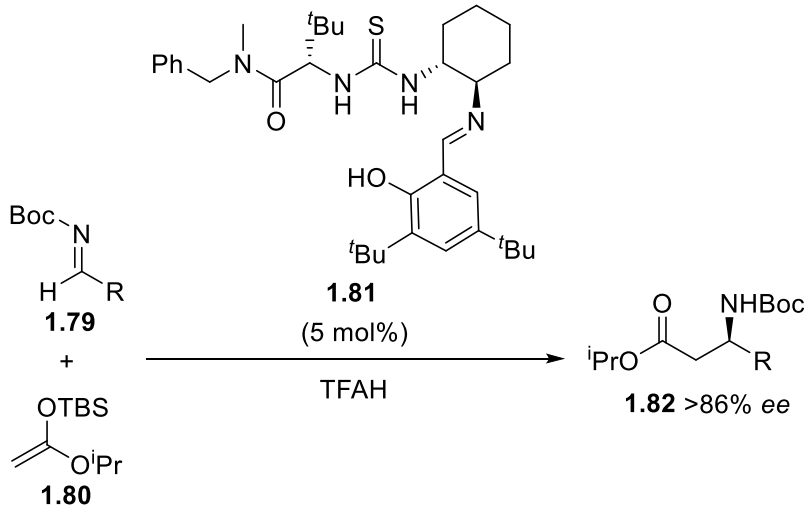

*Scheme 13: Asymmetric Mannich reaction catalyzed by Schiff's base **1.81** as an example of hydrogen bonding catalysis.*[46]

Following on from the discovery of hydrogen bond donors capable of asymmetric catalysis, Jacobsen reported that when combined with a chloride source (often trimethylsilyl chloride) thioureas could also be used to promote enantioselective reactions involving cationic intermediates.[47] These reactions are facilitated by the interaction between the anionic thiourea-chloride complex and a cationic iminium species forming the ion pair **1.86**, for example in the addition of indole to hydroxylactam-derived *N*-acyliminium **1.84** (Scheme 14). Formation of this ion-pair brings the chiral information of the catalyst into proximity with the reactive species, giving the reaction its enantioselectivity.[48]

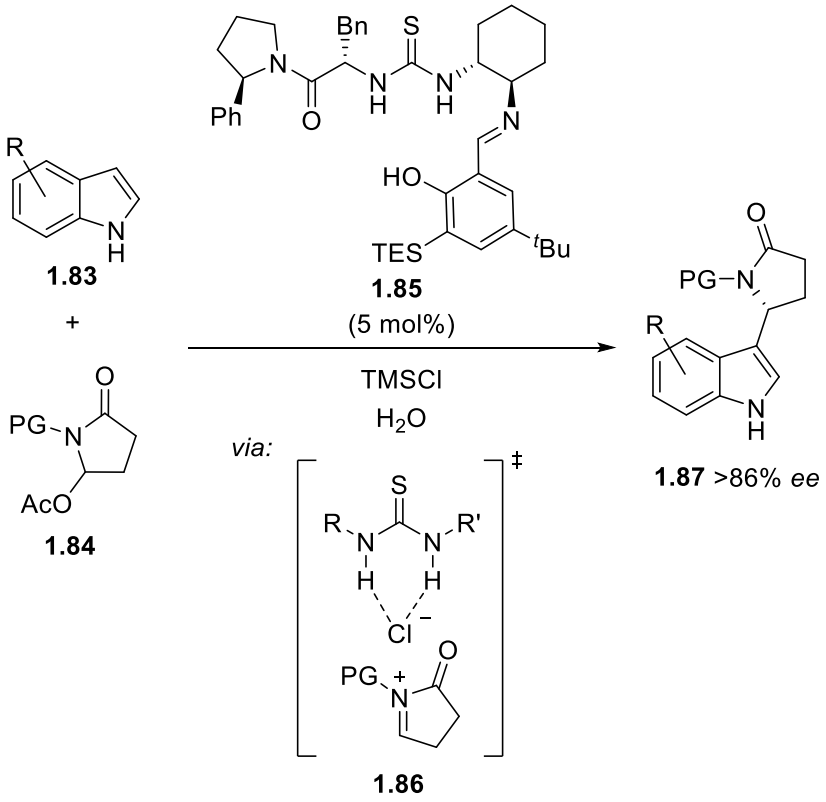

*Scheme 14: Example of counterion catalysis using Schiff's base **1.85** and trimethylsilyl chloride to facilitate the addition of indoles to hydroxylactam **1.84** derivatives.*[48]

NHC-mediated organocatalysis requires the conversion of an aldehyde from an electrophile to a nucleophile (umpolung), which can then in turn react with another electrophile. This is achieved *via* the formation of the Breslow intermediate **1.91** (Scheme 15a).[49] Examples of this can be seen in a variety of benzoin condensations and cyclizations which vary from moderate to excellent selectivity, depending on the system used (Scheme 15b).[50][51]

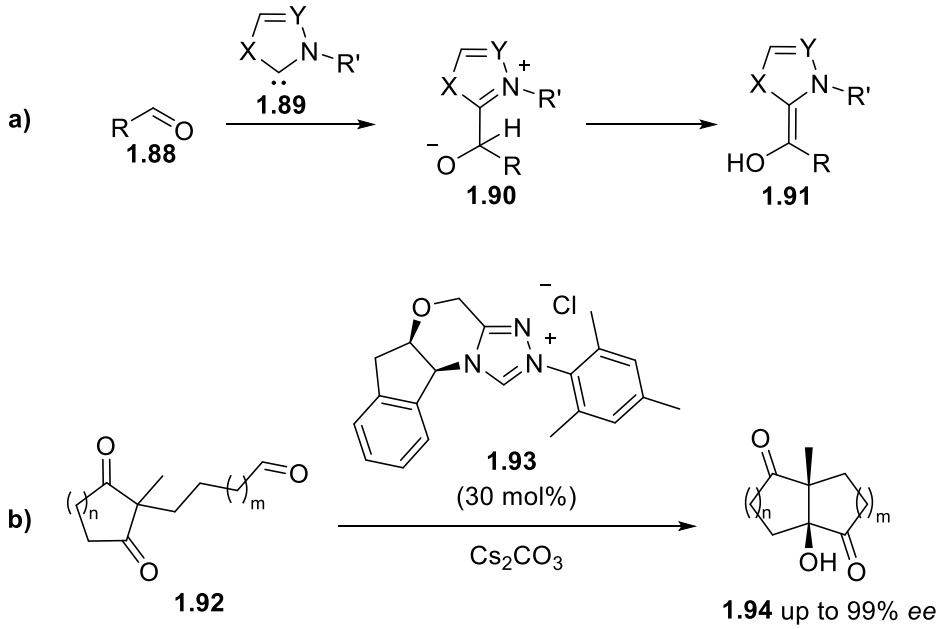

*Scheme 15: **a)** Formation of the Breslow intermediate **1.91** enabling the umpolung reactivity;[49] **b)** Example of an intramolecular benzoin condensation achieved utilising NHC-mediated catalysis.[51]*

One common feature for many organocatalytic reactions is the need for an additive. For the majority, these are acids (both organic and inorganic). However, there are many other potential additives which can have a significant impact on the outcome of a reaction. These can include, but are not limited to: amines, salts, alcohols, water or molecular sieves. Enamine and iminium catalysis are areas of organocatalysis in which an acid additive is often vital. Initially, it was believed that this was because the acid would increase the rate of amine condensation and hydrolysis.[52] Whilst this is true, more recently it has been shown that the nature of the acid can also have a marked effect on the enantioselectivity of a reaction through its interaction with the iminium ion transition state (Scheme 16).[53]

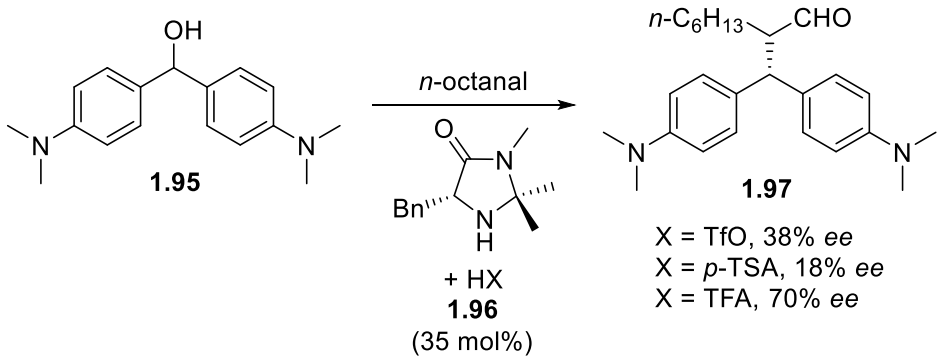

Scheme 16: Asymmetric alkylation of aldehydes demonstrating the large effect, on the enantioselectivity, the nature of the acid additive can have.[53]

1.1.4 Introduction to Fulvenes

The simplest fulvene, pentafulvene (**1.98**), is a structural isomer of benzene consisting of a cyclopenta-1,3-diene unit with an exocyclic carbon-carbon double bond. Various related fulvenes have been synthesized, including: indene-derived benzofulvene **1.99**, fluorene-derived dibenzofulvene **1.100** and cyclohepta-1,3,5-triene-derived heptafulvene **1.101** (Scheme 17a). Pentafulvene (**1.98**) is aromatic, possesses 6π electrons and is isoelectronic with pyrrole where the exocyclic double bond donates two electrons to the π system (rather than pyrrole's nitrogen lone pair).[54] Fulvenes are brightly colored, are electrophilic at C-6 (the terminal carbon) and demonstrate several possible modes of reactivity (Scheme 17b).[55]

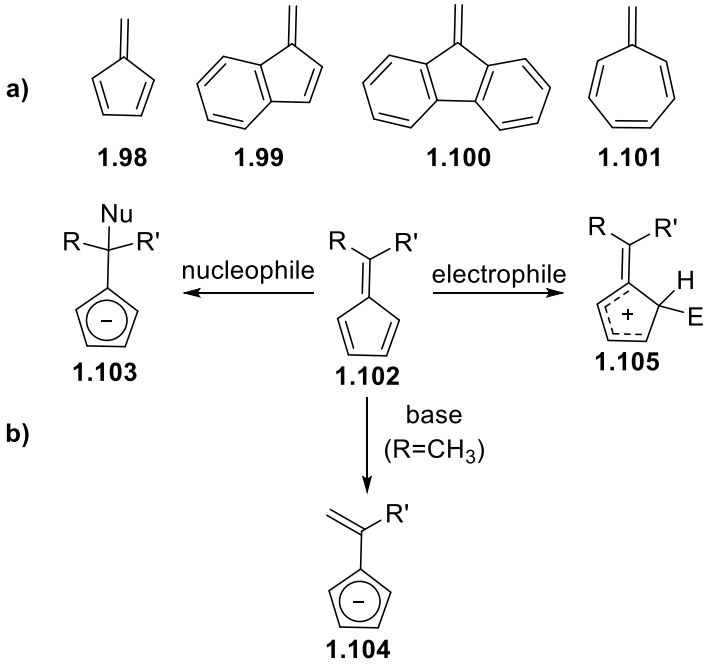

*Scheme 17: **a)** Examples of different types of fulvenes that have been synthesized; **b)** The different types of reactivity fulvenes are capable of.[55]*

Pentafulvene was first synthesized by Thiele in 1900, *via* a sodium ethoxide mediated condensation of CpH with acetone (Scheme 18a).[56] Since then, the methodology has been expanded but has not changed significantly. The work of Little and co-workers demonstrated the potential of pyrrolidine to catalyze this condensation, enabling a wider range of ketone and aldehyde derived pentafulvenes to be accessed (Scheme 18b).[57] This method has been used by other groups to access more functionalized pentafulvenes, for example Erden *et al* used pyrrolidine catalysis to access pentafulvenes bearing pendant halogens, alcohols and thioethers.[58] Ottosson and co-workers reported that the use of crystalline sodium cyclopenta-

1,3-dienide (**1.109**) afforded improved yields of some bulkier 6,6-disubsituted pentafulvene derivatives (Scheme 18c).[59] Other routes to pentafulvene derivatives exist, often involving multiple steps, for example the addition of a Grignard reagent to a ketone precursor and subsequent dehydration (often spontaneous in the presence of acid) (Scheme 18d).[60]

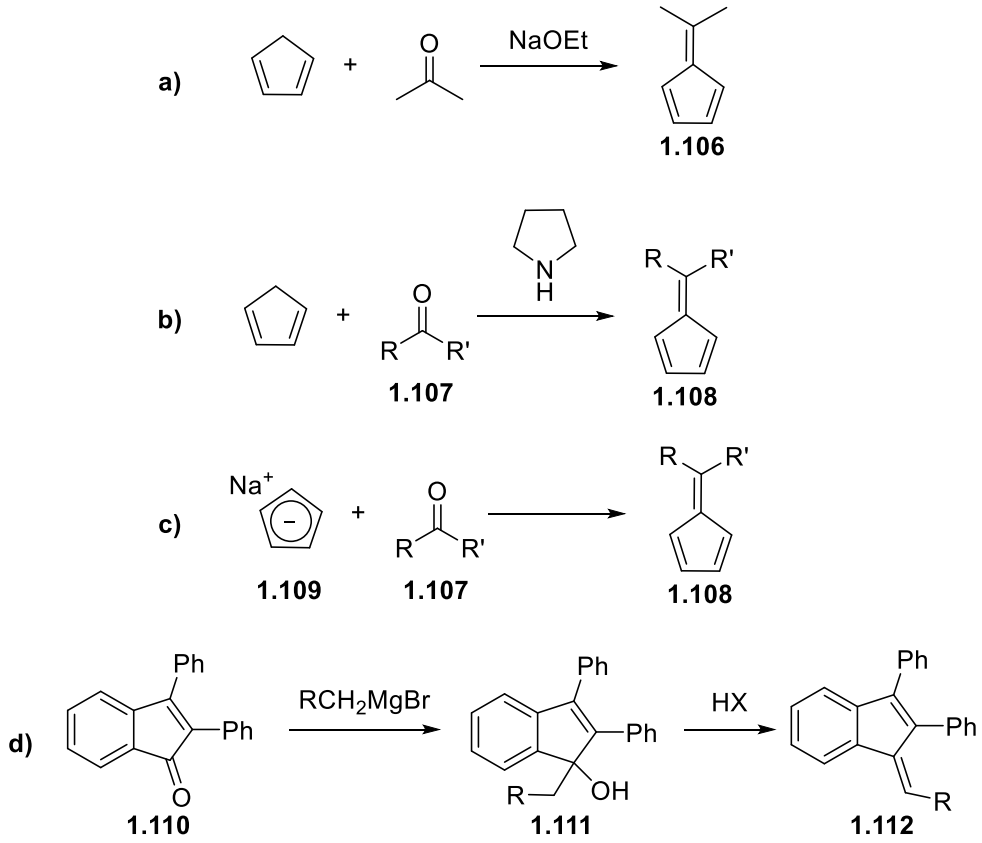

Scheme 18: Examples of the synthesis of pentafulvenes: ***a)*** *Thiele's original synthesis of pentafulvene;*[56] ***b)*** *Little's pyrrolidine catalyzed pentafulvene synthesis;*[57] ***c)*** *Ottosson's synthesis employing sodium cyclopenta-1,3-dienide (**1.109**);*[59] ***d)*** *Representative two-step synthesis of benzofulvene **1.112**.*[60]

Little's pyrrolidine catalyzed synthesis of pentafulvenes, reported in 1984, is another example of an organocatalytic reaction discovered before the field came into prominence. The use of sub-stoichiometric amounts of the organocatalyst was achieved by Erden *et al* more recently, who also observed a significant increase in reaction rate when using protic solvents (such as methanol:water mixtures) as well as a significant rate decrease when a tertiary amine is used rather than pyrrolidine.[61] These observations lend support to the suggestion that pyrrolidine is acting as an organocatalyst as well as a base.

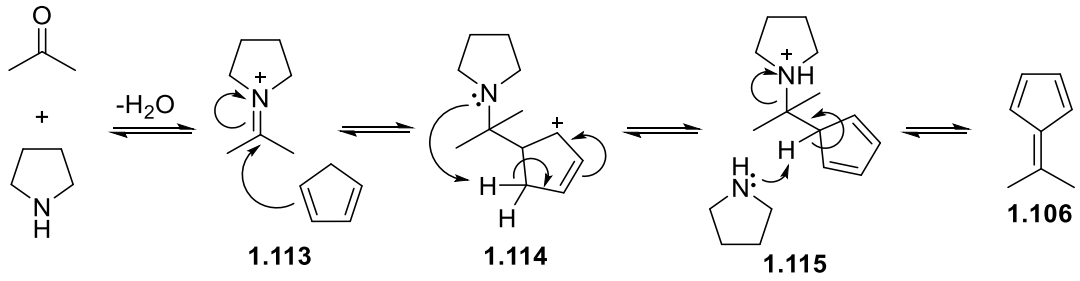

Scheme 19: Proposed mechanism for the pyrrolidine catalyzed synthesis of pentafulvenes.

As is the case when synthesizing some tetra-substituted olefins, obtaining high chemo, regio and stereoselectivity can often be problematic when working with bulky 6,6-disubstituted fulvenes.[60] The congested nature of the double bond can cause steric issues for approaching reagents, as well as the eclipsing interactions in the product potentially destabilizing both the product and transition states. Large enough substituents can cause twisting of the double bond and potentially distort the sp^2 centres.[62] Examples of 6,6-disubsituted fulvenes occur less commonly than monosubstituted examples, potentially due to these effects.

One more synthesis of note is an extremely rare example of a pentafulvene bearing a pendant chiral group from Togni and co-workers. In this synthesis they started from optically pure amines obtained from the chiral pool: (*R*)-1-(phenylethyl)amine, (*R*)-(1-cyclohexylethyl)amine and (-) or (+)-ephedrine. Following *N*-formylation, *N*/*O*-methylation and condensation with CpH, a small library of 6-monosubstituted pentafulvenes was synthesized (Scheme 20). Although affording only a limited number of examples, this did provide a very rare example of pentafulvenes bearing pendant chiral groups, which proved useful as intermediates in the synthesis of chiral ferrocenyl ligands.[63]

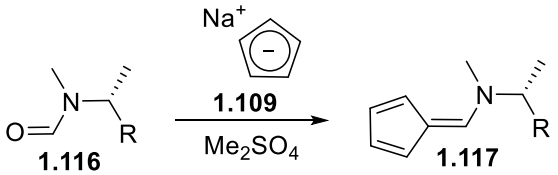

Scheme 20: An example of Togni's synthesis of pentafulvenes bearing a chiral pendant group.[63]

1.1.5 Uses of Fulvenes

Fulvenes show a variety of diverse reactivities due to their interesting electronic properties. Commonly, fulvenes are used in cycloaddition reactions (often to generate complex polycyclic frameworks) and as an intermediate in the synthesis of substituted Cp derivatives.[64] The reactivity of fulvenes is, however, not limited to these common uses.[55] Adam *et al.* demonstrated that pentafulvenes could be epoxidized by DMDO selectively at their more electron rich endocyclic double bonds. They also showed that by controlling the reaction conditions (temperature, reaction time and equivalents of DMDO), the selectivity between mono-epoxidized **1.118**, bis-epoxidized **1.119** and cyclopentenone **1.120** derived products could be controlled (Scheme 21a).[65] It has also been demonstrated that, using mild Lewis-acidic conditions, hydroarylation of pentafulvenes with indole derivatives can also be achieved regioselectively (Scheme 21b).[66]

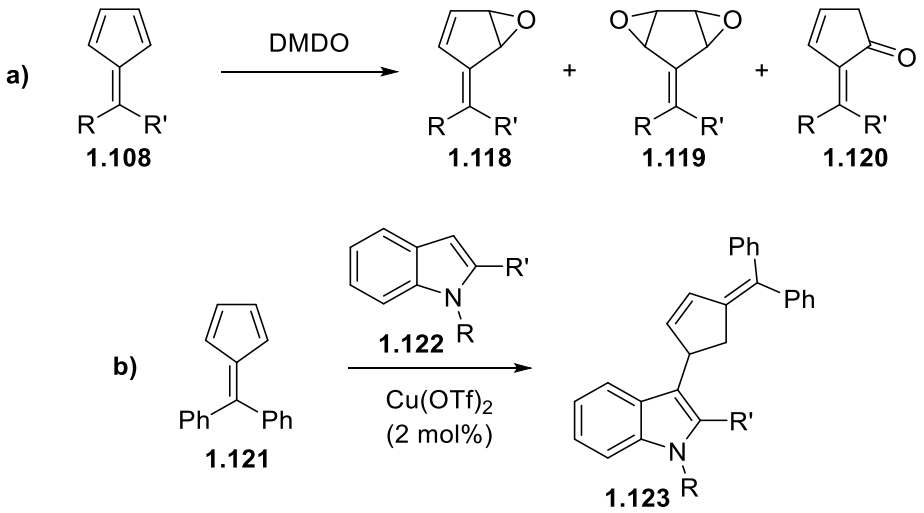

*Scheme 21: **a)** Epoxidation of pentafulvenes using DMDO;[65] **b)** Lewis-acid catalyzed hydroarylation of 6,6-diphenyl-pentafulvene.[66]*

Fulvenes are capable of taking part in a wide range of cycloaddition reactions, acting as either a 2π or 6π component depending on the electronics of the reaction partner.[55] This reactivity has been used in the generation of complex polycyclic scaffolds, for example in the [6+2] cycloaddition between *in situ* generated 4-amino-pentafulvenes (from cyclopentenone **1.124** and chiral amine catalyst **1.126**) and 3-olefinic-7-azaoxindole **1.125** (Scheme 22a).[67] It has also been used in the generation of libraries of chirally substituted Cp ligands, useful in the synthesis of organometallic catalysts capable of catalyzing asymmetric transformations, for example the (6+3) cycloaddition between pentafulvene **1.108** and imino esters **1.129**. In this example, the

use of BIPHEP derived ligand **1.131** afforded *exo* product **1.132** whereas the use of ferrocenyl ligand **1.130** results in *endo* product **1.133** (Scheme 22b).[68]

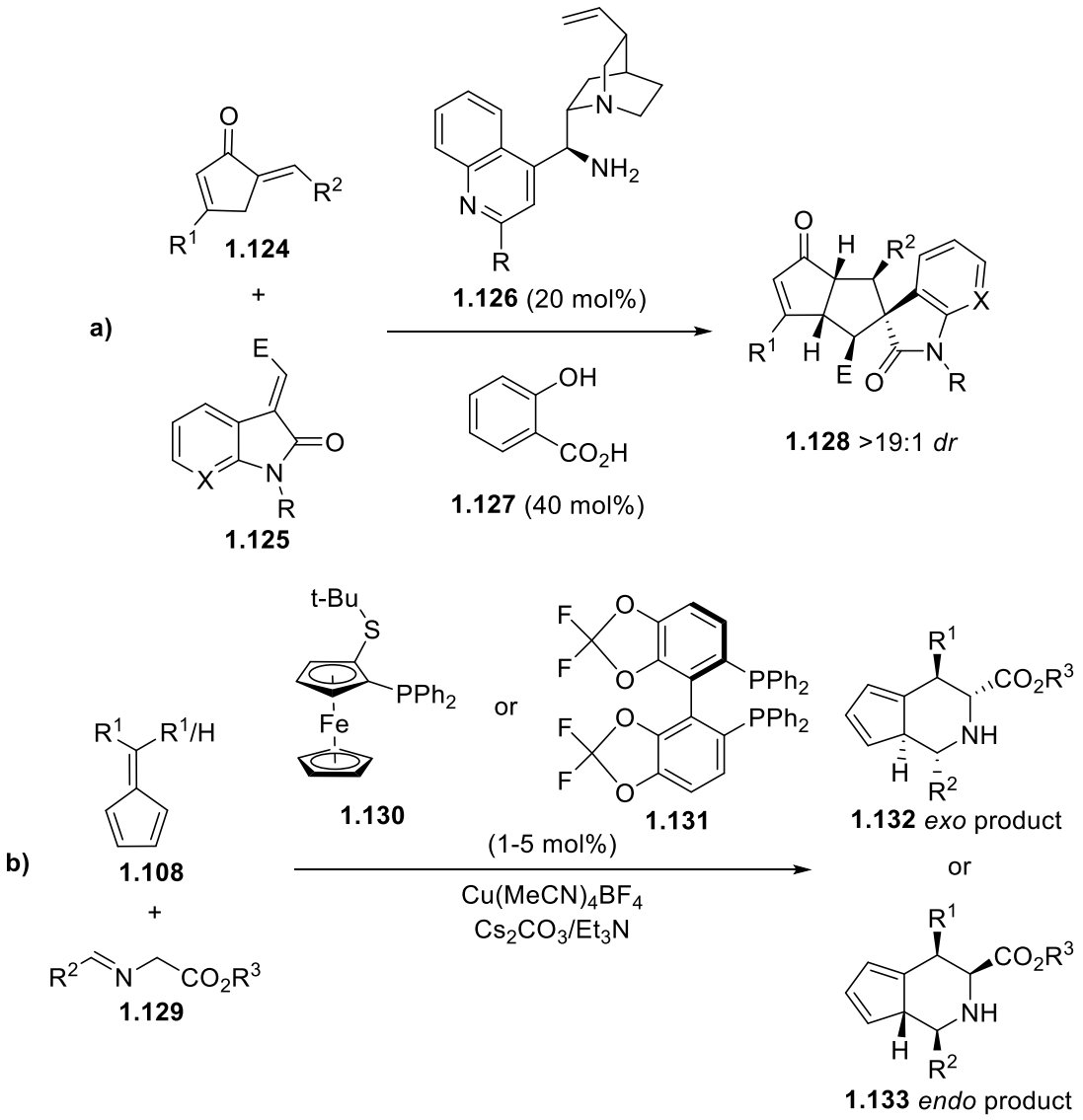

Scheme 22: Examples of cycloaddition reactions involving fulvenes: ***a)*** *[6+2] Cycloaddition catalyzed by chiral amine* ***1.126****;*[67] *[6+3] Cycloaddition with switchable selectivity depending on ligand choice.*[68]

The [6+3] cycloaddition described above demonstrates the utility of pentafulvenes as a source of substituted CpHs, which is perhaps the most common use of pentafulvenes. This is more commonly achieved *via* the addition of an organometallic reagent (often an organolithium) to the pentafulvene's electrophilic C-6, after which the resulting lithium-cyclopenta-1,3-dienide will often be directly *trans*-metallated onto a transition metal. Examples of this can be seen from the groups of Tacke[69][70] (Scheme 23a) and Woodward (Scheme 23b).[71][72] Alternatively, pentafulvenes can be directly reductively metallated onto a transition metal, for example by

pre-reducing titanium(IV) to titanium(II) which in turn reduces two equivalents of fulvene **1.139** to form *ansa*-metallocene **1.140** (Scheme 23c).[73]

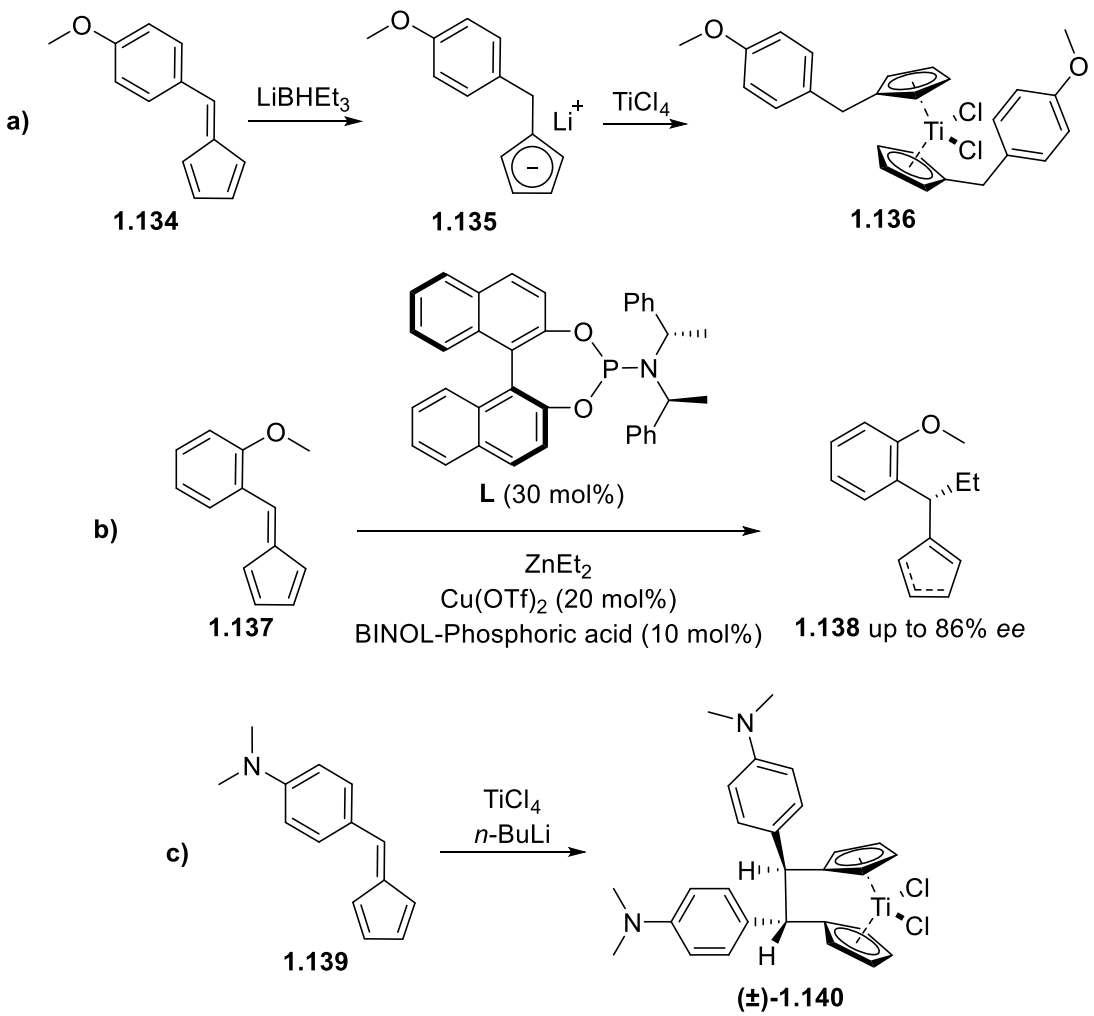

Scheme 23: Examples of pentafulvenes as sources of Cps: ***a)*** *Tacke and co-workers using Superhydride® to reduce pentafulvene* ***1.134*** *before trans-metallating onto titanium;*[70] ***b)*** *Woodward and co-workers using diethyl zinc to reduce fulvene* ***1.137*** *in a stereoselective manner;*[71] ***c)*** *Tacke and co-workers generating titanium dichloride in situ which reduces two equivalents of pentafulvene* ***1.139*** *to form ansa-titanocene* ***1.140****.*[73]

The example, shown above, from the Woodward group (Scheme 23b) demonstrates a route to a chirally substituted Cp in just two steps from commercial 2-methoxy-benzaldehyde. Other potential routes to chirally substituted Cp derivatives are limited, and often require either chiral pool starting materials[74] (which give little possibility for modification) or a lengthy synthetic sequence[75] (but enabling more structural modification). Early examples focussed on the use of chiral pool starting materials, rapidly synthesized in 2-4 steps, and include: neomenthyl derived **1.141**,[76] menthyl derived **1.142**[77] and camphor derived **1.143** (Figure 3).[78]

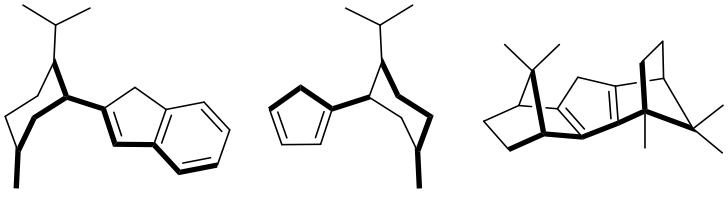

1.141 **1.142** **1.143**

Figure 3: Examples of chiral pool derived CpHs.[76][77][78]

More recent examples are the BINOL derived **1.145**, first synthesized in the group of Halterman[79] but popularized by Cramer and co-workers; who provided a route enabling more structural diversification, by functionalizing in the 3-position of both naphthyl groups.[80] This route requires three or more steps beginning from non-commercial **1.144** (Scheme 24a). Another recent example is the chiral spiro CpH **1.147** which is synthesized in five or more steps starting from dicarboxylic acid **1.146** (Scheme 24b).[81]

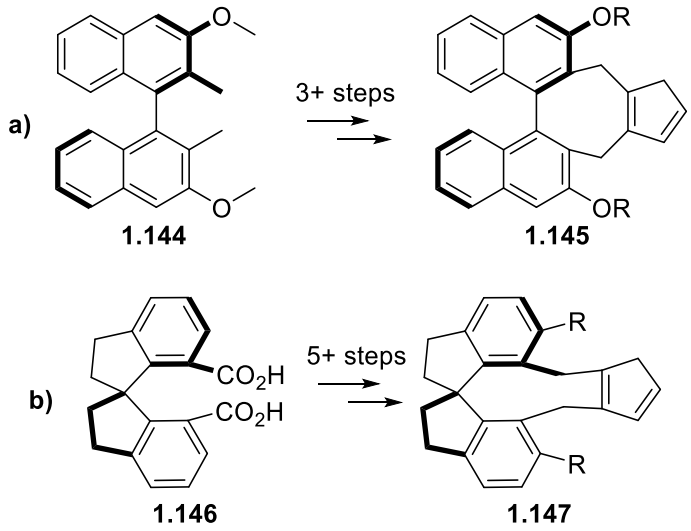

*Scheme 24: Recent examples of chiral substituted CpH synthesis: **a)** Cramer and co-workers synthesis of BINOL derived **1.145**;[80] **b)** You and co-workers synthesis of chiral-spiro CpH **1.147**.[81]*

The chirally substituted CpHs shown in Figure 3 and Scheme 24 were all synthesized as precursors for metal complexes useful in asymmetric synthesis – for example Cramer's BINOL derived **1.145**, once complexed with $[Rh(C_2H_4)_2Cl]_2$, showed high activity and stereoselectivity in the *ortho* allylation of aromatic amides with allenes (Scheme 25a).[80] One widely used asymmetric transformation catalyzed by a chiral cyclopentadienyl complex is Negishi's ZACA reaction. Using zirconium catalyst **1.153**, this reaction involves the stereoselective addition of an organoaluminium reagent across an alkene. This reaction is widely used due to its reliability, high yields and often excellent enantioselectivities (Scheme 25b).[82][83]

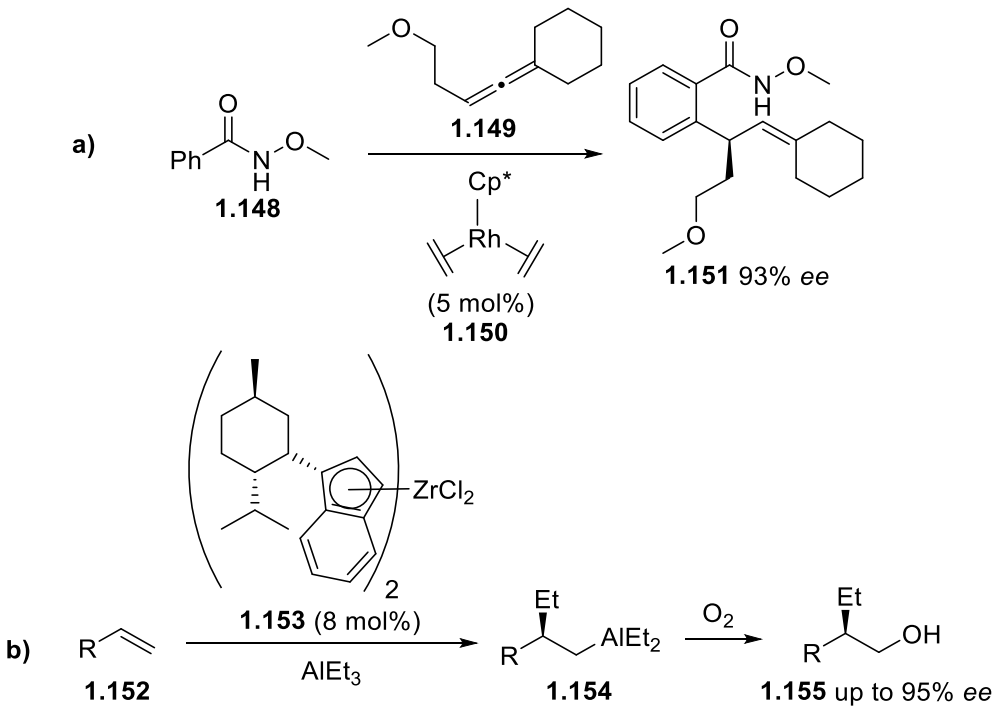

Scheme 25: Examples of the catalytic activity of chiral cyclopentadienyl metal complexes: ***a)*** *Cramer's ortho allylation of aromatic amide* ***1.148*** *using rhodium complex* ***1.150*** *where Cp* is a derivative of* ***1.145****;*[80] ***b)*** *Representative example of the ZACA reaction.*[82][83]

Another important use of chiral substituted CpHs is the potential utility of titanocene dichlorides as anti-cancer agents. Since the report of titanocene dichloride possessing anti-cancer properties in 1979 (reaching phase II clinical trials), a wide range of organotitanium compounds have been biologically evaluated.[84][85] It has been demonstrated that substitution of the Cp ligands improved the titanocene's cytotoxicity. Furthermore, chirally substituted Cps improve it even further. Woodward *et al* demonstrated that enantiopure (*S,S*)-**1.159** shows greater anti-cancer activity than the opposite enantiomer and the racemic sample (showing comparable cytotoxicity to *cis*platin) and greatly enhanced anti-cancer activity compared to unsubstituted or *ansa*-bridged titanocene dichlorides (Figure 4).[86]

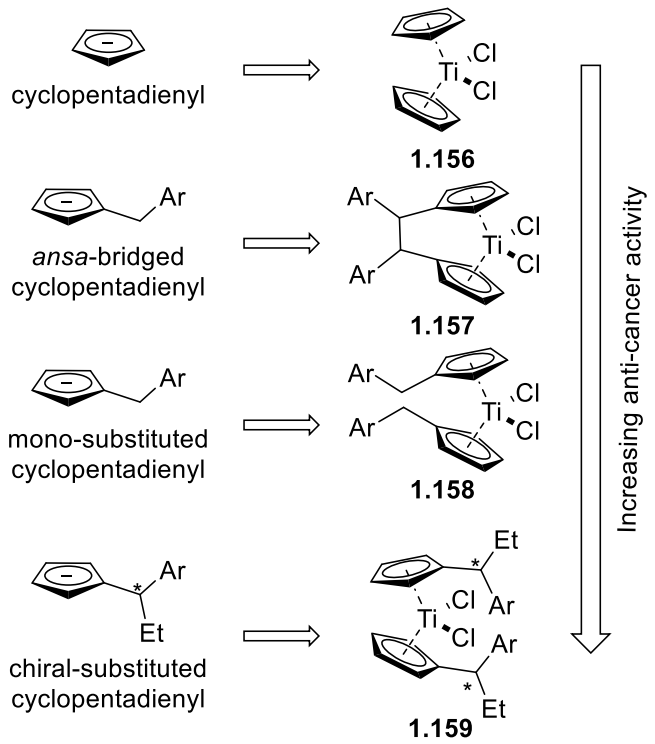

Figure 4: Relative anti-cancer activity of different types of titanocenes.[86]

1.1.6 Aims and Objectives

The first aim of this project was to explore the reactivity of 2-acetyl-benzaldehyde (**1.160a**) using organocatalytic methodology. The reaction between **1.160a** and CpH, catalyzed by pyrrolidine, unexpectedly afforded **(±)-1.162a** rather than the predicted **1.161** (Scheme 26). It was then envisaged that an asymmetric version of this reaction could be achieved using a chiral pyrrolidine derivative. Enantioenriched **1.162a** could then prove useful as an intermediate in the synthesis of chirally substituted CpH derivatives.[87] Alkylation of the hydroxyl group of **1.162a**, followed by reduction of the pentafulvene's exocyclic carbon-carbon double bond afforded a range CpH derivatives as single enantiomers and single diastereomers. The last aim of this project was to use these CpH derivatives as an intermediate in the synthesis of chiral titanocenes or zirconocenes.

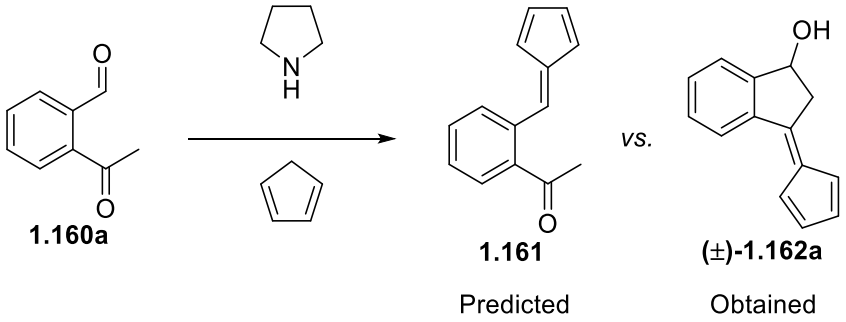

Scheme 26: Predicted vs. actual reactivity of 2-acetyl-benzaldehyde.

1.2 Results and Discussion

1.2.1 Discovery and Initial Optimization of Pentafulvene Synthesis

In an attempt to synthesize pentafulvene **1.161**, 2-acetyl-benzaldehyde was reacted with CpH using pyrrolidine catalysis, in the manner previously used within the Woodward group. This reaction did not afford the predicted product but rather novel pentafulvene **(±)-1.162a** (Scheme 27), which was confirmed *via* x-ray crystallography (Figure 5).[†]

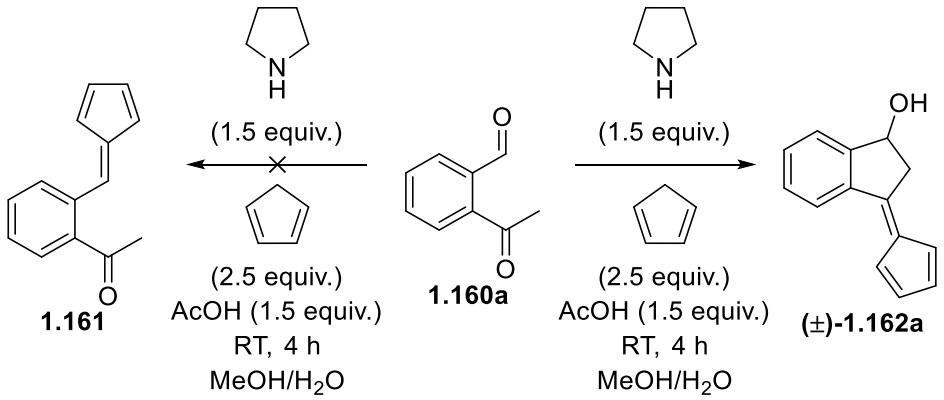

*Scheme 27: Attempted synthesis of pentafulvene **1.161,** affording previously unknown pentafulvene **(±)-1.162a** instead.*

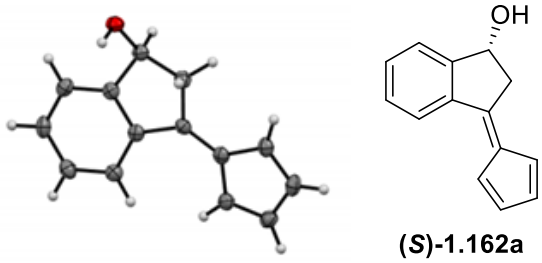

*Figure 5: Crystal structure of (S)-3-(cyclopenta-2,4-dien-1-ylidene)-2,3-dihydro-1H-inden-1-ol (**(S)-1.162a**).*

Perhaps more interesting still, the crystal submitted to x-ray crystallography was found to be a single enantiomer (this was later confirmed by chiral HPLC). Submission of a second crystal afforded the same result, a single enantiomer of pentafulvene **1.162a**. Although no chiral components were added to the reaction and the bulk product was found to be racemic (by chiral HPLC), each isolated crystal proved to be a single, unpredictable enantiomer. From this it was concluded that pentafulvene **1.162a** crystallizes as a conglomerate, in the manner of the

[†] I should like to thank Dr Melchior Cini again for his discovery of the novel reactivity of 2-acetyl-benzaldehyde and CpH, under pyrrolidine catalysis.

classical tartrate crystals of Pasteur.[88][89] This crystal formation is driven by a strongly stereodirecting helical hydrogen bonding array, seen in its crystal packing (Figure 6), that favors the assembly of homochiral molecules into crystals.

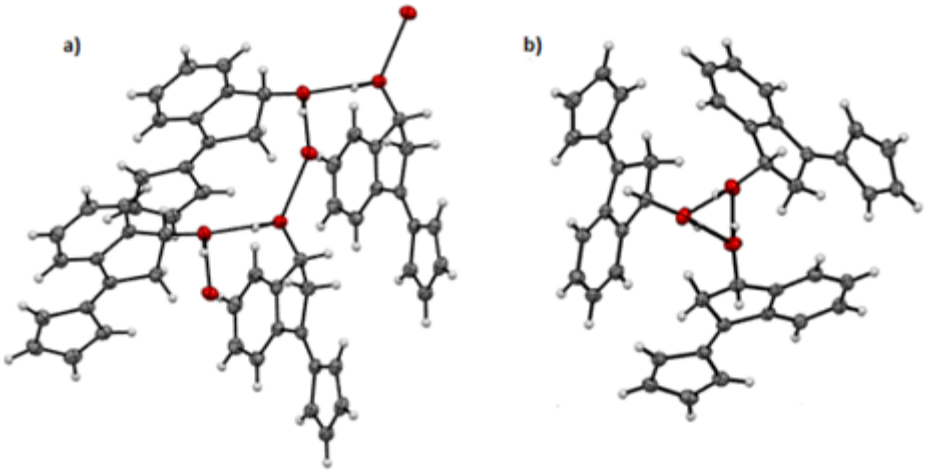

*Figure 6: Representation of the packing of crystals of **(S)-1.162a**.[87] a) View perpendicular to the c axis; b) View down the c axis.*

Whilst this crystallization occurs unpredictably from racemic **1.162a**, it was hypothesized that if a scalemic sample of **1.162a** could be prepared then, through recrystallization, it could be significantly enantioenriched further. An initial attempt was then made to create an asymmetric version of the pyrrolidine catalyzed reaction seen in Scheme 27, the results of which can be seen in Table 1.[‡] No conversion was observed with Jørgensen catalyst derivatives $\mathbf{L_f}$ and $\mathbf{L_h}$, MacMillan catalyst derivatives $\mathbf{L_c}$ and $\mathbf{L_d}$ or with C_2-symmetric $\mathbf{L_b}$. Use of chiral phosphoric acid $\mathbf{A_1}$ with pyrrolidine also afforded no conversion. Limited conversion, but no enantioselectivity, was observed with (*S*)-proline as the catalyst. This result was improved by using (*S*)-2-pyrrolidinemethanol ($\mathbf{L_e}$), affording an excellent conversion and moderate enantioselectivity, with DMF proving the best solvent. Of these initial trials, the best result was obtained using (*S*)-1-(2-pyrrolidinylmethyl)pyrrolidine ($\mathbf{L_g}$) giving a good yield and enantioselectivity (71%, 72% *ee*).

[‡] I should like to thank Dr Marc Magre again for his contributions to the early screening of potential chiral catalysts in the reaction between 2-acetyl-benzaldehyde and CpH.

Solvent	Amine[a]	Acid[b]	Temp. (˚C)	Time (h)	Yield (%)	*ee (%)*
DMSO	$\mathbf{L_a}$	-	25	24	28[c]	2
DMF	$\mathbf{L_a}$	-	25	24	<5[c]	n.d.[d]
MeCN	$\mathbf{L_e}$	AcOH	25	24	36[c]	52
DMSO	$\mathbf{L_e}$	AcOH	25	24	70[c]	54
DMF	$\mathbf{L_e}$	AcOH	25	24	90[c]	58
DMF	$\mathbf{L_g}$	AcOH	25	2	71	72
DMF	$\mathbf{L_b}$	AcOH	25	24	<5[c]	n.d.[d]
DMF	$\mathbf{L_f}$	AcOH	25	24	<5[c]	n.d.[d]
DMF	$\mathbf{L_h}$	AcOH	25	24	<5[c]	n.d.[d]
MeCN	$\mathbf{L_c}$	HCl	25	24	<5[c]	n.d.[d]
MeCN	$\mathbf{L_d}$	TFAH	25	24	<5[c]	n.d.[d]
DMF	Pyrrolidine	$\mathbf{A_1}$	25	24	<5[c]	n.d.[d]
MeCN/H_2O	$\mathbf{L_g}$	AcOH	25	4	<5	n.d.[d]

*Table 1: Results of the early trials toward an asymmetric synthesis of pentafulvene **1.162a**. [a]0.38 equiv. of amine; [b]0.38 equiv. of acid; [c]NMR conversion with no internal standard present; [d]not determined.*

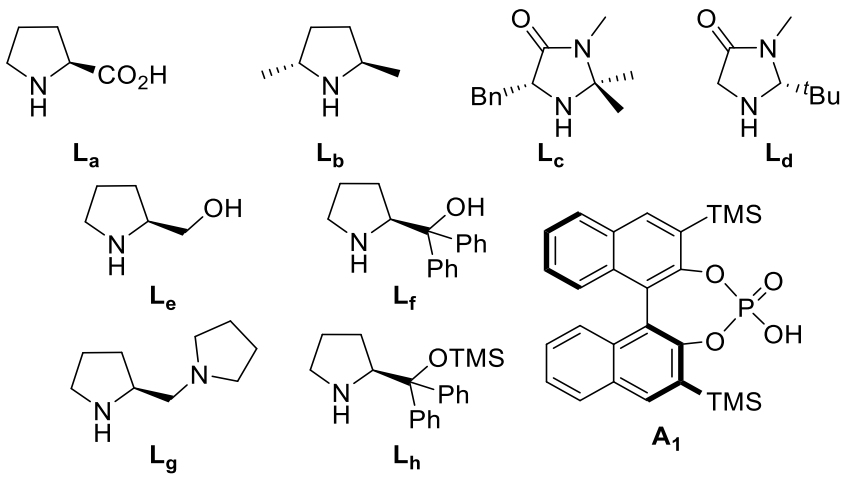

Figure 7: Structures of the chiral catalysts used in the initial asymmetric reaction trials (Table 1).

1.2.2 Synthesis of Proline Derived Organocatalysts

From the preliminary results, $\mathbf{L_g}$ was clearly the best performing catalyst for the asymmetric synthesis of pentafulvene **1.162a**. Although $\mathbf{L_g}$ is commercially available, it is relatively expensive (*ca*. £114.50 per gram[§]), meaning that it was preferable to synthesize. Such syntheses also provided the opportunity for further modification of the catalyst's structure, enabling further optimization of the reaction, and the ability to make the unnatural (*R*)-proline derived catalyst.

Numerous routes exist in the literature towards the synthesis of $\mathbf{L_g}$, each with their own advantages and disadvantages. These routes are summarized in Scheme 28 and Scheme 29. Initially it was proposed that diversification of (*S*)-proline could be achieved through the protection of the nitrogen with Cbz and subsequent amide coupling, *via* the method of Chowdhury and Ghosh.[90] This could be followed by a concurrent Cbz-deprotection and amide reduction by lithium aluminium hydride. However, this method required the use of super-stoichiometric quantities of an amide-coupling reagent (in this case the carbodiimide DIC). The urea by-product of this reaction proved extremely difficult to separate from the product, making purification impossible. This issue could have been avoided by using the alternative carbodiimide EDC, whose urea by-product is water soluble and can therefore be removed during workup, but this would have been prohibitively expensive on large scales.

[§] Obtained from https://www.sigmaaldrich.com/catalog/product/aldrich/324450?lang=en&region=GB on 12/8/18.

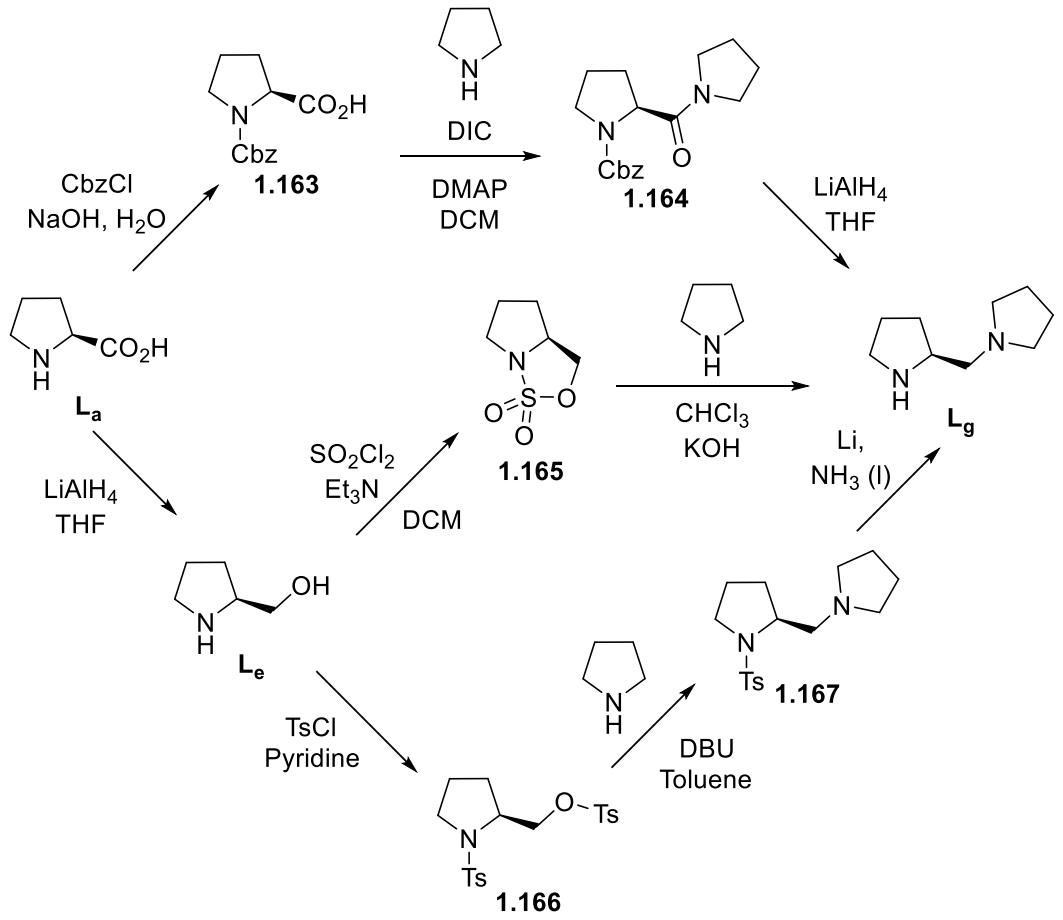

Scheme 28: Summary of the alternative potential routes towards $\mathbf{L_g}$.

The other potential routes all proceed *via* the common intermediate (*S*)-2-pyrrolidinemethanol ($\mathbf{L_e}$), which could be prepared on decagram scales, in quantitative yield, *via* the reduction of (*S*)-proline with lithium aluminium hydride. This reaction proved very sensitive to the quality of the lithium aluminium hydride used, meaning that it could only be used when freshly opened. Using previously opened lithium aluminium hydride resulted in intractable mixtures of products that proved difficult and time consuming to separate.

The route of Hendrie and Leonard[91] involved the bis-tosylation of $\mathbf{L_e}$, followed by a nucleophilic substitution with pyrrolidine and subsequent deprotection. The issue with this route arose in the challenging final deprotection, usually requiring forcing acidic conditions which would have been incompatible with $\mathbf{L_g}$, potentially eroding its chirality. Alternatively, a dissolving metal reduction (lithium metal in liquid ammonia) facilitated the deprotection. A more straightforward alternative to this reaction can be achieved using magnesium in methanol, *via* the method of Nyasse *et al*.[92] Although safer and easier to perform, this reaction suffered in

yield due to the difficult purification from the 4-toluenesulfonic acid derived by-products (formed by the further reduction of the removed toluenesulfonyl group).

An alternative synthetic route, adapted from the method of Carreras *et al*,[93] proceeded *via* the reaction of $\mathbf{L_e}$ with sulfuryl chloride to form cyclic sulfamate **1.165**. Whilst attractive due to the fewer steps required and the relatively clean subsequent hydrolysis of the sulfonate group from nitrogen, this pathway suffered due to the very low yield obtained in the synthesis of sulfamate **1.165** (potentially due to unwanted intermolecular side reactions).

Having discarded alternatives described in Scheme 28, the route shown in Scheme 29 was selected as the preferred option. Boc protection of $\mathbf{L_e}$ before tosylation at oxygen meant that, following the nucleophilic substitution with pyrrolidine, the final deprotection was relatively straightforward (requiring only TFAH at room temperature). Intermediate **1.169** proved unstable at room temperature for extended periods of time, spontaneously forming cyclic carbamate **1.171** (Figure 8), so had to be stored at -20 ˚C. Although requiring more steps than the alternative, each step was practically simple and high yielding. All steps could be telescoped, with the entire route requiring no purification except for one distillation at the end, resulting in an overall yield of 53% over five steps.

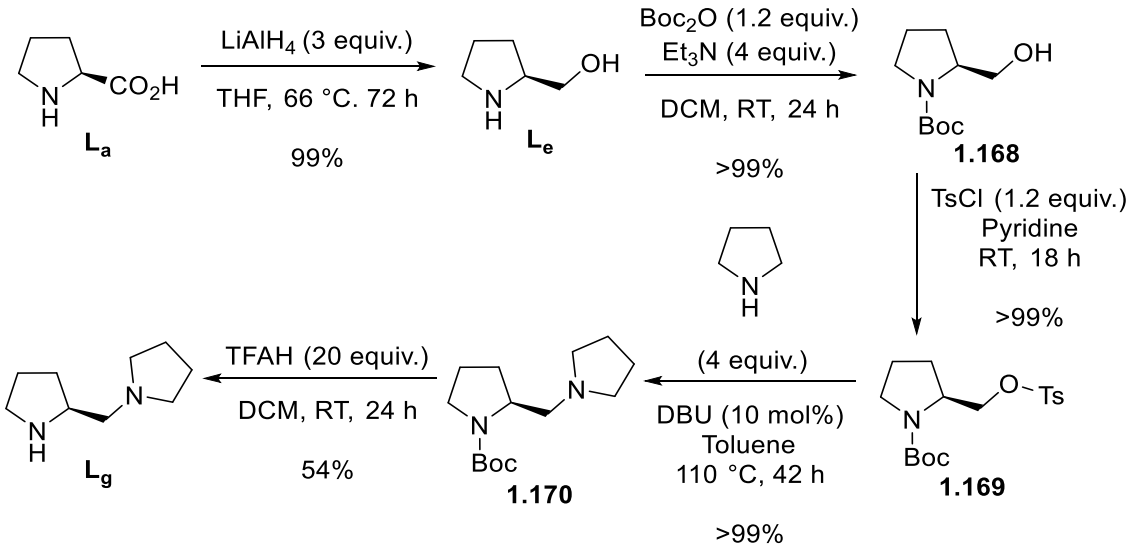

Scheme 29: Optimized route towards catalyst $\mathbf{L_g}$.

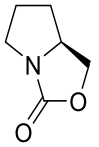

1.171

*Figure 8: Decomposition product of **1.169**.*

The route described in Scheme 29 also proved suitable for the synthesis of the opposite enantiomer and enabled some structural diversification of the catalyst. **(*R*)-L$_g$** was obtained in 4 steps, in similar yield, starting from commercially available **(*R*)-L$_e$** (Scheme 30).

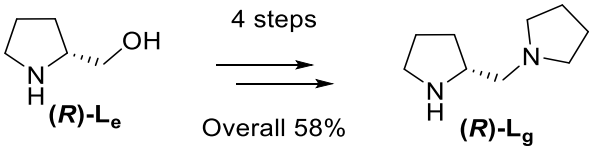

*Scheme 30: Synthesis of opposite handed catalyst **(R)-L$_g$**.*

Some important changes to the catalyst structure could also be tested, by the modification of this route (Scheme 31). The use of piperidine, rather than pyrrolidine, enabled the examination of steric effects of the pendant group without altering its electronic properties. Installation of an aryl ether moiety, by using 2-napthol as a nucleophile, enabled the importance of the lone pair donor ability of the pendant group to be examined. The oxygen lone pair of an aryl ether is much less electron donating than the tertiary amine present in **L$_g$**. Earlier attempts to install an aryl ether directly from 2-pyrrolidinemethanol, by Elliott and co-worker's Mitsunobu reaction,[94] only afforded low yields and intractable mixtures of products.

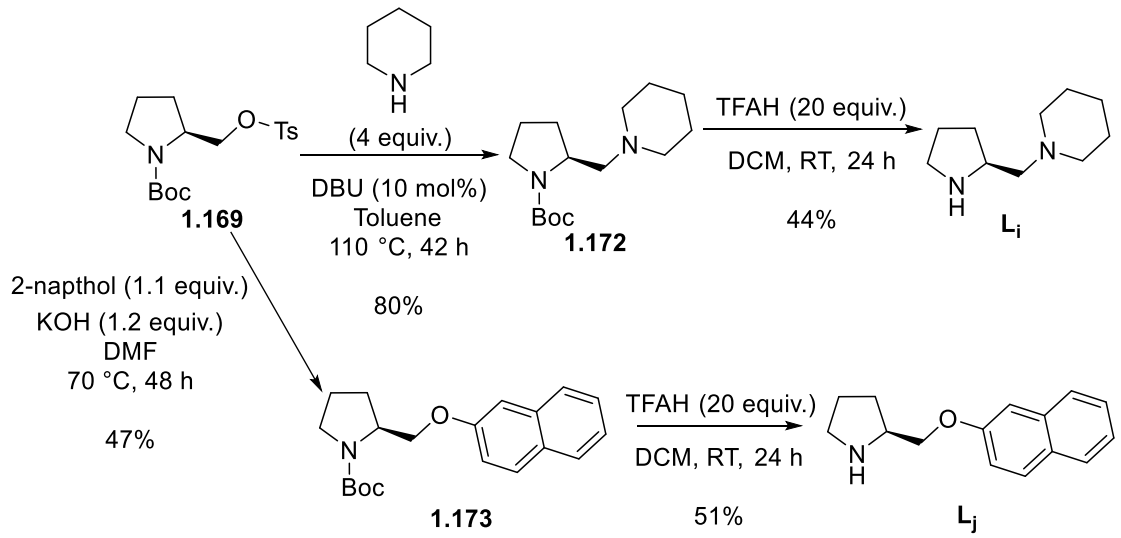

Scheme 31: Structural diversification of the catalyst, achieved by exchanging the pyrrolidine nucleophile for alternatives.

1.2.3 Synthesis of 2-Acetyl-benzaldehyde and its Derivatives

Initially, 2-acetyl-benzaldehyde was synthesized *via* the straightforward route shown in Scheme 32. Benzyl alcohol was *ortho* lithiated before quenching with acetaldehyde to yield diol **1.175a**, which was then oxidized using a Swern oxidation. This route afforded 2-acetyl-benzaldehyde on a multi-gram scale, in a time efficient manner and in a good overall yield (53% over two steps). This route was then applied to other benzyl alcohol derivatives but proved to be limited in scope. Only 4-substituted benzyl alcohols, bearing non-directing and non-acidic functional groups (**1.174b** and **1.174c**), were tolerated. This was due to the forcing conditions required to achieve the *ortho* lithiation and potential regioselectivity issues when using 3-substituted substrates. Derivatives of 2-acetyl-benzaldehyde presented a challenge to work with synthetically as they are self-reactive at room temperature, decomposing during workup/purification if left for any length of time as the neat compounds (the decomposition is slower in solution). Once the compounds had been purified, as swiftly as possible, they proved relatively stable when stored at -20 ˚C. For this reason, although 2-acetyl-benzaldehyde is commercially available, it was synthesized rather than purchased.

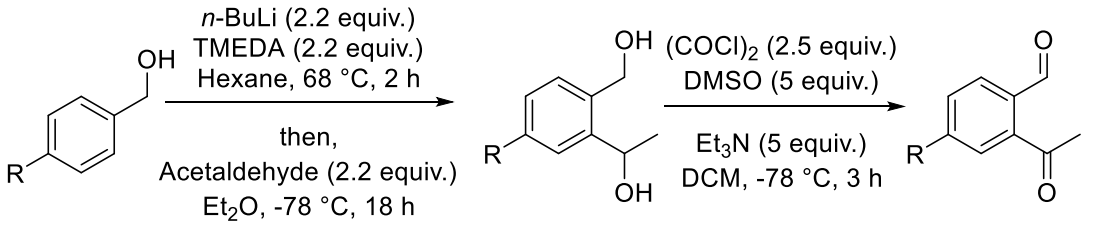

*Scheme 32: Synthesis of 2-acetyl-benzaldehydes **1.160a**, **1.160b** and **1.160c** in two steps, starting from the corresponding benzyl alcohol derivative.*

Modifying the procedure described in Scheme 32 was attempted in order to expand the potential range of **1.160** derivatives available. Using 2-phenyl-ethanol as a substrate was trialled, in which the ethyl alcohol group would act as the directing group rather than the methyl alcohol seen in previous benzyl alcohol derivatives (Scheme 33a). Unfortunately, the ethyl alcohol proved to be ineffective as a directing group, resulting in no conversion. Alternatively, modifying the aldehyde used in quenching lithiated benzyl alcohol, using propionaldehyde rather than acetaldehyde, proved successful. Diol **1.178** was obtained in good yield and the subsequent oxidation also behaved reasonably well (Scheme 33b).

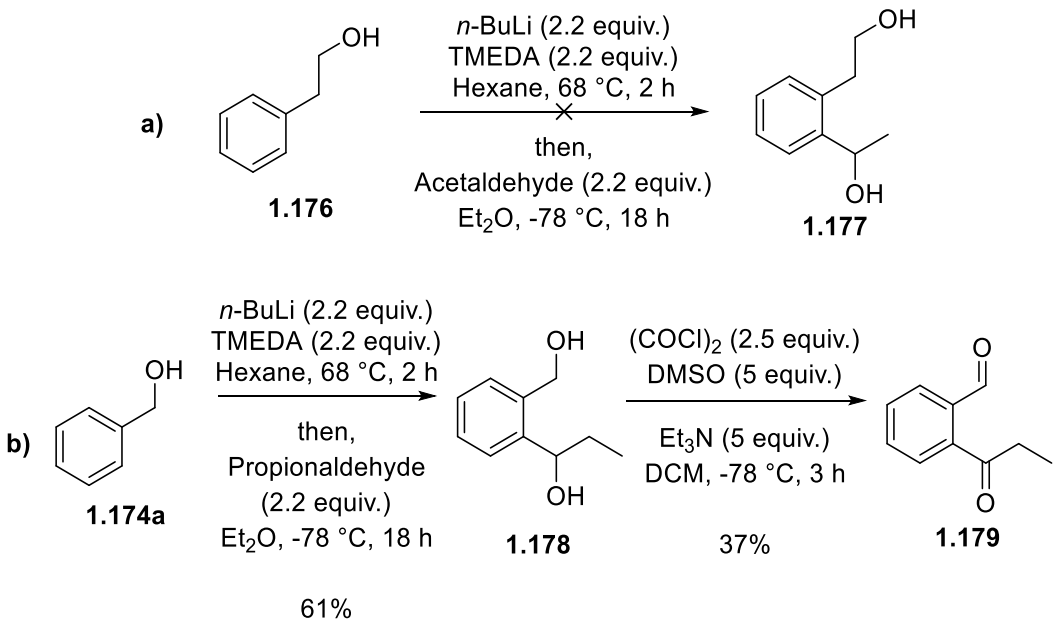

*Scheme 33: Further application of the synthetic route shown in Scheme 32: **a)** Attempted use of 2-phenylethanol as a substrate for ortho lithiation; **b)** Quenching ortho lithiated benzyl alcohol with propionaldehyde and subsequent oxidation.*

A challenging synthetic target was presented by 2-acetyl-3-fluoro-benzaldehyde. This could provide useful information about electronic effects in the synthesis of pentafulvene **1.162**. The original route proved unsuitable, as *ortho* lithiation adjacent to a fluorine atom at high temperatures can result in the elimination of lithium fluoride and generation of a reactive benzyne species. Because of this, the route shown in Scheme 34 was employed, adapted from the work of Freskos *et al*.[95] The acetal functionality in **1.181** proved to be a better directing group for lithiation than the original methyl alcohol moiety or an O-MOM group. This enabled milder lithiation conditions to be employed, using *s*-BuLi at -78 ˚C. Quenching the resulting organolithium species with acetaldehyde, followed by a Swern oxidation, resulted in a mixture of acetal-**1.184** and hemiacetal-**1.183** (which tautomerize rapidly at room temperature). Both compounds, when deprotected using the solid-supported acid Amberlyst®-15, afford the desired product **1.185**, rendering their separation unnecessary.

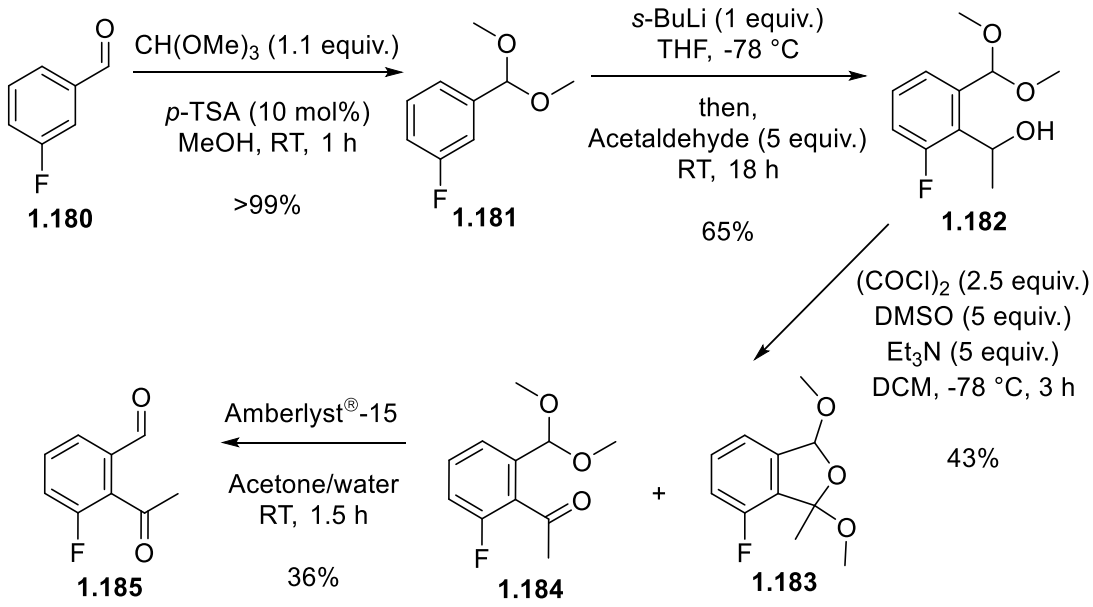

Scheme 34: Synthesis of 2-acetyl-3-fluoro-benzaldehyde.

One aim of this project was to generate a library of compounds, which requires the ability to make a wide variety of derivatives of pentafulvene **1.162**. Both routes shown previously are quite limited in substrate scope, meaning that another alternative route was required to achieve this aim. The route of Phan and co-workers[96] (Scheme 35) involved the *ortho* formylation of a range of phenol derivatives, followed by condensation with acetic acid hydrazide (synthesized from the reaction of hydrazine monohydrate with ethyl acetate).[97] The resulting hydrazide **1.189** then underwent the unusual lead(IV) acetate mediated rearrangement, which replaces a phenolic hydroxyl group with an acyl group.

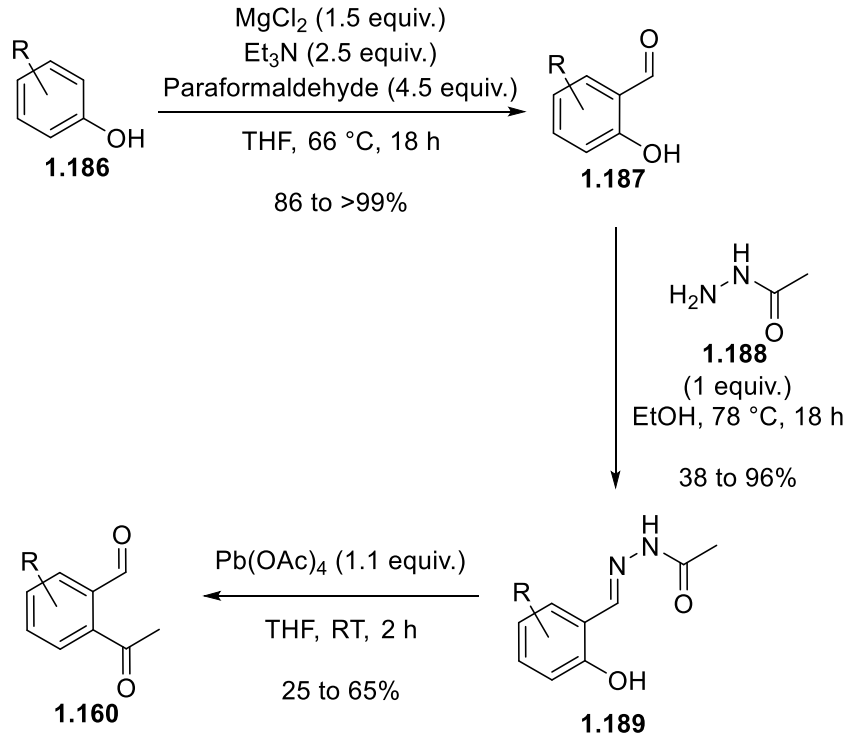

Scheme 35: Alternative synthetic route towards 2-acetyl-benzaldehyde derivatives requiring more steps, but with greater functional group tolerance.

The mechanism of this rearrangement was investigated in a publication from Katritzky and Harris.[98] They conclude, from a mixture of mass spectroscopic and ^{18}O labelling experiments, that this rearrangement likely proceeds *via* the mechanism shown in Scheme 36. Treatment of benzoyl-^{18}O-hydrazide with lead(IV) acetate lead to incorporation of the ^{18}O at the acetyl position of **1.196** (confirmed by mass spectroscopy). This would not be the case in the alternative potential mechanism proposed by the authors, where the acyl group from the hydrazide is simply transferred to the phenol's *ipso* carbon.

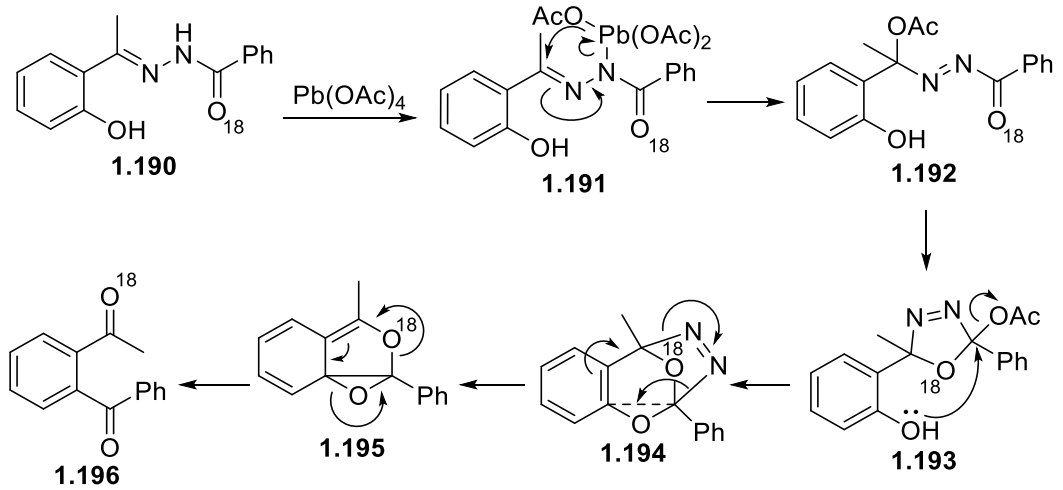

*Scheme 36: Proposed mechanism of lead(IV) acetate mediated rearrangement of hydrazide **1.190** to form acetyl-benzaldehyde derivative **1.196**.[98]*

This route proved useful for the synthesis of numerous 2-acetyl-benzaldehyde derivatives, shown in Figure 9. Electron rich derivatives, halogens and functionalization at three different positions were all tolerated well. The yields of each step for these derivatives are summarized in Table 2. In general, the yields of the first two steps are excellent; with only 4-fluoro and 4-chloro-phenol showing lower conversion in the *ortho* formylation step. The final step is lower yielding than the previous two due to a combination of the instability of the 2-acetyl-benzaldehyde products, discussed earlier, and as a result of the telescoping of the first two steps without purification (all impurities from the three steps are removed in the final purification).

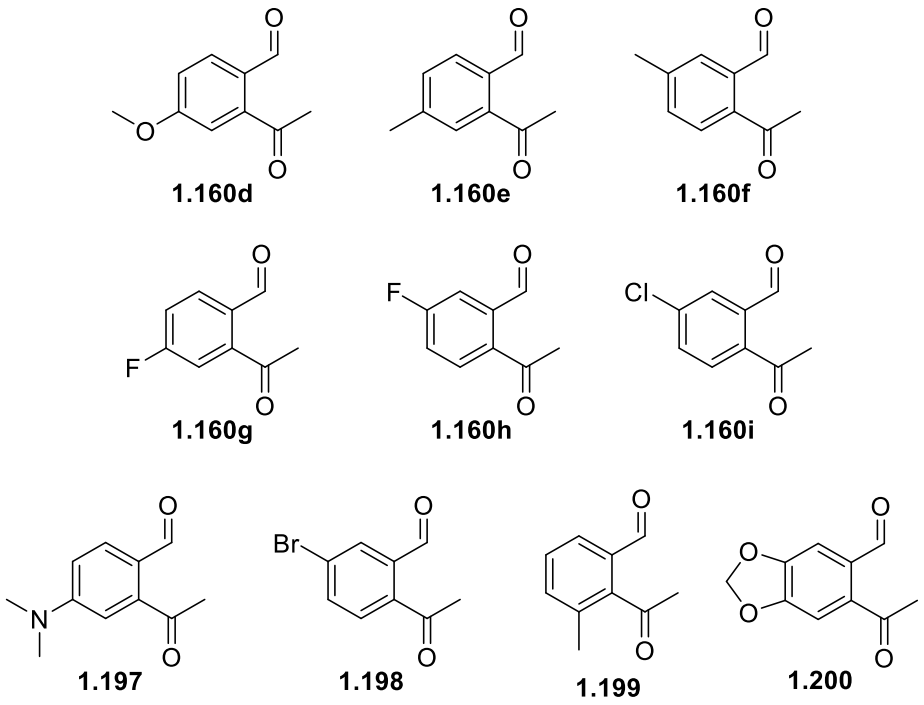

Figure 9: The derivatives of 2-acetyl-benzaldehyde accessed via the route described in Scheme 35.

2-Acetyl-benzaldehyde	Step 1 Yield (%)	Step 2 Yield (%)	Step 3 Yield (%)
1.160d	>99	88	56
1.160e	>99	96	47
1.160f	>99	96	25
1.160g	>99	91	60
1.160h	86[a]	38	49
1.160i	>99[a]	57	65
1.197	54[b]	80	27
1.198	97	>99	34
1.199	>99	73	31
1.200	>99	93	13

Table 2: Yields of each step towards the synthesis of the 2-acetyl-benzaldehyde derivatives shown in Figure 9. [a]obtained as an approximately 1:1 mixture of product:starting material, which was used directly in the next step and then purified; [b]obtained as the hydrochloride salt.

1.2.4 Further Optimization and Synthesis of Pentafulvene Derivatives

With a large stock of both the catalyst $\mathbf{L_g}$ and 2-acetyl-benzaldehyde prepared, further optimization could then be undertaken to improve upon the previous results. The results of which are summarized in Table 3. Reducing the equivalents of acetic acid used improved the enantioselectivity considerably, up to the maximum of 88% observed with 0.13 equiv. of acetic acid. Changing the acid used, to a variety of other acids with similar pK_a values, could not improve it any further. Using the methyl ether of 2-pyrrolidinemethanol ($\mathbf{L_k}$) gave a small improvement compared to unmodified 2-pyrrolidinemethanol but was much less selective than the bis-amine catalyst $\mathbf{L_g}$. Modification of $\mathbf{L_g}$ to possess a six-membered ring on its pendant group ($\mathbf{L_i}$) afforded a slightly reduced level of both enantio and regioselectivity, with greater amounts of by-products present, whereas modification with an aryl ether containing pendant group ($\mathbf{L_j}$) gave no conversion at all. Slight alterations of the reaction temperature and time resulted in a moderate increase in yield but had no effect on enantioselectivity. From this it could be concluded that the H-bond donor properties of the catalyst's pendant group may play an important role in determining the reaction outcome.

Amine[a]	Acid (Equiv.)	Temp. (˚C)	Time (h)	Yield (%)	*ee (%)*
$\mathbf{L_g}$	AcOH (0.38)	28	4	58	70
$\mathbf{L_g}$	AcOH (0.26)	22	2	76	78
$\mathbf{L_g}$	AcOH (0.13)	22	2	64	88
$\mathbf{L_g}$	AcOH (0.06)	22	2	69	80
$\mathbf{L_g}$	AcOH (0.13)	10	16	67	90
$\mathbf{L_g}$	AcOH (0.13)	5	42	54	84
$\mathbf{L_g}$	AcOH (0.13)	0	48	54[a]	88
$\mathbf{L_g}$	AcOH (0.13)	15	6	78	88
$\mathbf{L_k}$	AcOH (0.13)	22	24	69	60
$\mathbf{L_i}$	AcOH (0.13)	22	2	71	82
$\mathbf{L_j}$	AcOH (0.13)	22	4	<5	n.d.[b]
$\mathbf{L_g}$	$\mathbf{A_2}$ (0.13)	25	4	48	86
$\mathbf{L_g}$	$\mathbf{A_3}$ (0.13)	25	4	65	76
$\mathbf{L_g}$	$\mathbf{A_4}$ (0.13)	25	4	84	84
$\mathbf{L_g}$	$\mathbf{A_5}$ (0.13)	25	4	70	84

*Table 3: Results of the second round of optimization of the synthesis of pentafulvene **1.162a**. Each reaction was performed in DMF. [a]Product obtained as a 2:1 mixture with the starting material; [b]not determined.*

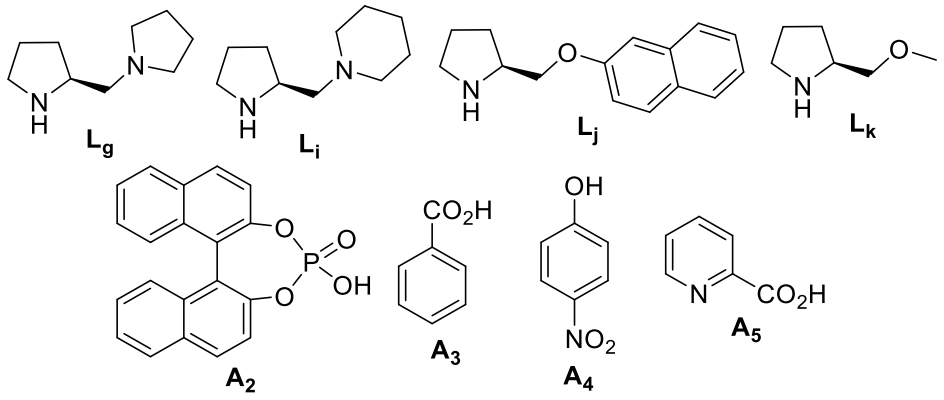

*Figure 10: Structures of the chiral catalysts and acid co-additives used in the second round of optimization of the synthesis of pentafulvene **1.162a**.*

Following the second round of optimization, the finalized reaction conditions (shown in Scheme 37) were obtained. Affording an initial *er* of 94:6 which, as predicted, was then improved *via* recrystallization to give the final product as effectively one enantiomer (*er* >99:1). The absolute regiochemistry and stereochemistry of the product, shown in Scheme 37, were confirmed *via*

X-ray crystallography of pentafulvene **1.162d** (Figure 11); which was obtained from the reaction between 2-acetyl-4-methoxy-benzaldehyde and CpH under the optimized conditions.

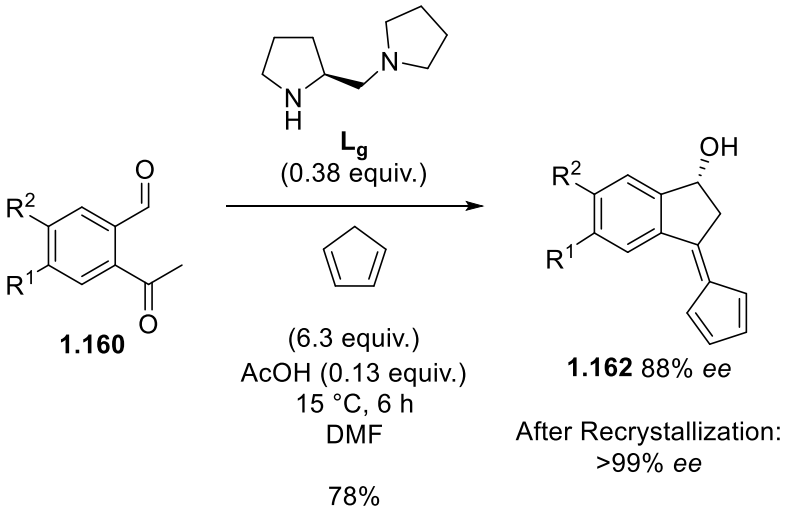

*Scheme 37: Optimized synthesis of pentafulvene **1.162a** (where R^1=R^2=H).*

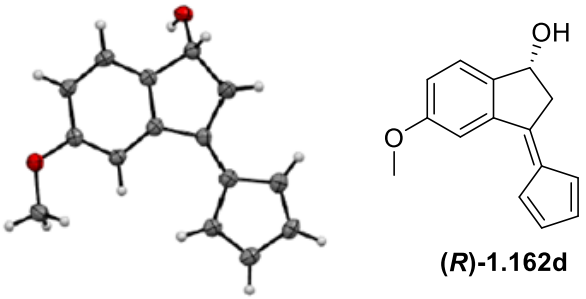

Figure 11: Crystal structure of (R)-3-(cyclopenta-2,4-dien-1-ylidene)-5-methoxy-2,3-dihydro-1H-inden-1-ol, the compound used to determine absolute regiochemistry and stereochemistry of the product.

The optimized reaction conditions were then applied to the range of 2-acetyl-benzaldehyde derivatives already synthesized (see Figure 9), the results of which are summarized in Table 4. Alkyl, aryl, halogens and methoxy substituents were tolerated well. Substitution in the 5-position of the pentafulvene products (modifying the R^1 group as described in Scheme 37) was less tolerated due to steric factors. The enantioselectivity decreased as R^1 increased in size, with the *tert*-butyl group giving the lowest *ee* of 64%. This sensitivity was not observed when altering the substituent in the 6-position (R^2). One observation worth noting was that the inclusion of an alkyl group at either position (either methyl or *tert*-butyl) inhibited the crystallization of the pentafulvene product and prevented the remarkable enantio-enrichment observed with all other derivatives. The opposite handed catalyst appeared to give comparable results with the trialled substrates, affording similar *ee* values and slightly reduced yields (potentially due to the small scale the reactions were performed on).

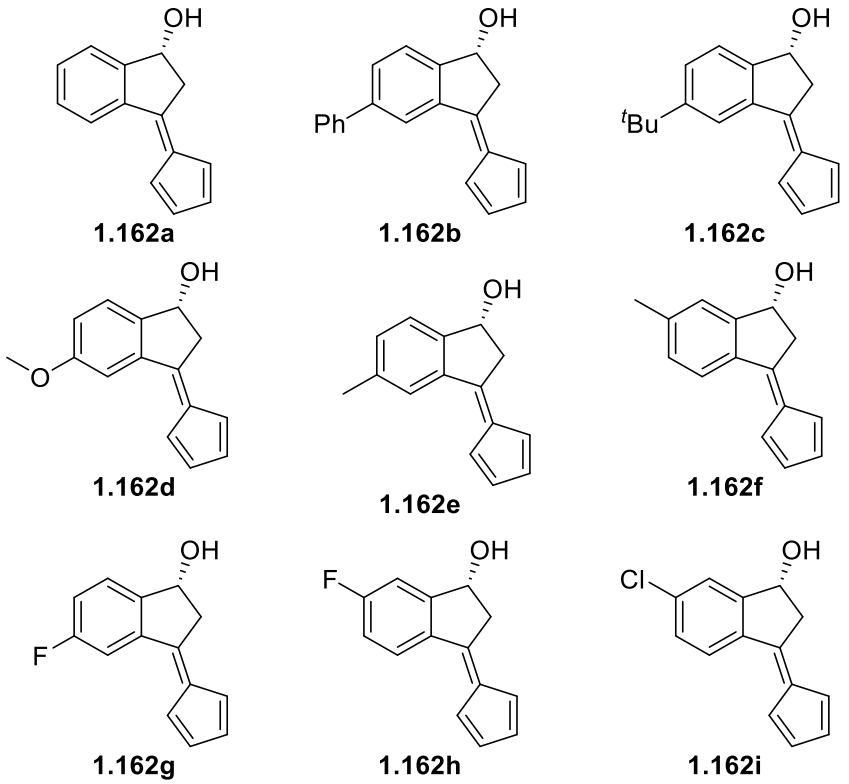

Figure 12: Pentafulvene derivatives accessed via the optimized reaction shown in Scheme 37.

Compound	Temp (˚C)	Time (h)	Yield (%)[b]	Initial *ee*	Recrystallized *ee*
1.162a	15	6	78	88	>99
(*S*)-1.162a[a]	15	6	65	88	96
1.162b	15	4.5	53	76	>99
1.162c	22	2.5	91	64	-[c]
1.162d	15	5	54	82	>99
1.162e	15	6	72	82	-[c]
1.162f	15	6	67	78	-[c]
1.162g	25	4.5	39	84	>99
1.162h	25	3	52	76	>99
(*S*)-1.162h[a]	25	3	39	80	>99
1.162i	25	3	38	82	98
(*S*)-1.162i[a]	25	2.5	30	78	98

*Table 4: Results of the synthesis of various derivatives of pentafulvene **1.162**. All reactions were carried out under the optimized conditions, only varying the specified time and temperature. [a]Synthesized using **(R)-L_g**; [b]isolated yields; [c]ee not improved by recrystallization.*

Figure 13 contains a summary of the pentafulvene derivatives which were not successfully synthesized. Functionalization at the 4-position of the pentafulvene with a methyl group was not tolerated (showing no conversion), likely due to steric factors, which is unsurprising when the decrease of enantioselectivity with increasing steric bulk in the 5-position is considered. The inclusion of a fluorine atom in the 4-position also resulted in no observed conversion, despite the minimal steric bulk increase from a hydrogen atom, likely due to the strong electron withdrawing effect of an *ortho* fluoro group. Inclusion of a bromine atom in the 5-position did not inhibit conversion but appeared to result in a destabilized product, as only polymeric material was observed after the reaction. The extremely electron rich substrates **1.202** and **1.205** appeared to convert slowly but the products were also destabilized, resulting in competition between the reactions forming the pentafulvene product and their decomposition, leading to no usable product being obtained. Using 2-propionyl-benzaldehyde, in an attempt to synthesize **1.208**, also resulted in no conversion being observed which is likely due to steric factors again.

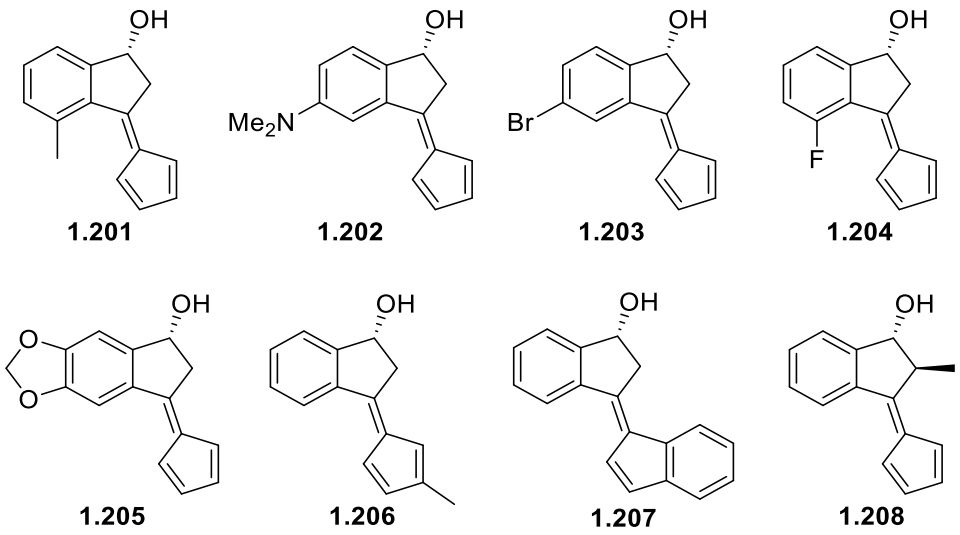

*Figure 13: Derivatives of pentafulvene **1.162** that were not successfully synthesized.*

Altering the CpH component of the reaction was also, unfortunately, not tolerated. Use of methyl-CpH (to form **1.206**) or indene (to form **1.207**) showed a slow rate of conversion which was in competition with product decomposition, resulting in no usable quantity of the desired product being obtained. This is potentially due to the decreased acidity of methyl-CpH (pK_a not reported, but addition of a methyl group is shown to increase the pK_a of indene by 1.7-2.4 units) and indene (pK_a 20.1 in DMSO) compared to CpH (pK_a 18.0 in DMSO), which may affect their relative nucleophilicity.[99] It was also investigated whether a non-CpH derived nucleophile could

participate in this reaction (Scheme 38). Diethyl malonate (**1.3**) was selected due to the similarity of its pK_a with CpH (14.2 in DMSO)[**] but it instead underwent a knoevanagel condensation with the aldehyde moiety.

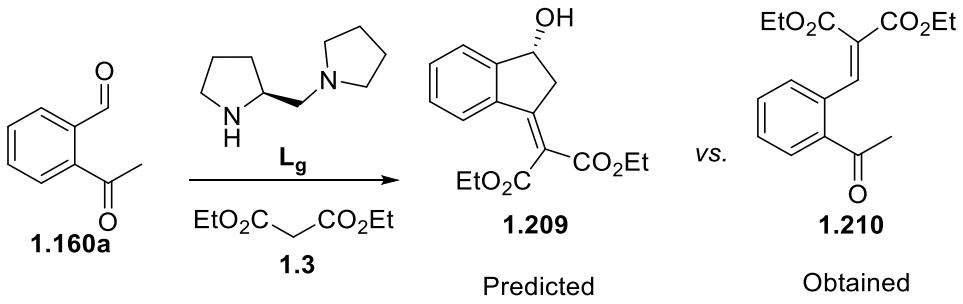

*Scheme 38: Predicted vs. actual reactivity, under the optimized reaction conditions, where CpH had been replaced by diethyl malonate (**1.3**)*

1.2.5 Mechanistic Investigations

In the optimized system previously mentioned, pentafulvene **1.162a** is not the sole product obtained. Pentafulvene **1.161** and indanol derivative **1.211** are both also observed, in less than 20 and 10% yields respectively (Scheme 39).

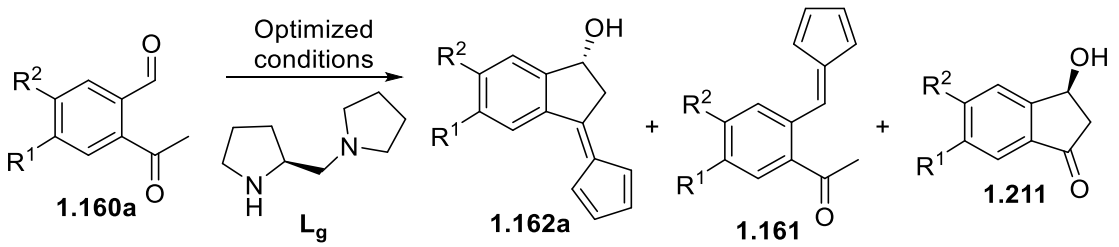

Scheme 39: All observed products from the optimized reaction between 2-acetyl-benzaldehyde and CpH.

Indanol **1.211** is the product of an aldol condensation, known to be catalyzed by proline derivatives under similar conditions.[100] Altering the reaction conditions, by removing the CpH, enabled **1.211** to be obtained in a 55% isolated yield (Scheme 40). This enabled interrogation of the first proposed mechanism; in which the first step is formation of indanol **1.211** followed by the amine catalyzed condensation of the ketone moiety with CpH (Scheme 41). As indanol **1.211** was proposed as an intermediate in this reaction, resubmitting it to the reaction conditions (this time with the CpH present) should result in conversion to the desired pentafulvene product.

[**] pK_a values also available from the Evans pK_a table (page 5 of link includes all references for the values): http://evans.rc.fas.harvard.edu/pdf/evans_pKa_table.pdf

But resubmission afforded none of the desired product. Additionally, the absolute stereochemistry of indanol **1.211** was elucidated, *via* literature chiral HPLC conditions,[101] to be (*S*) with an *ee* of *ca.* 70% - the opposite configuration to that of pentafulvene **1.162a**.

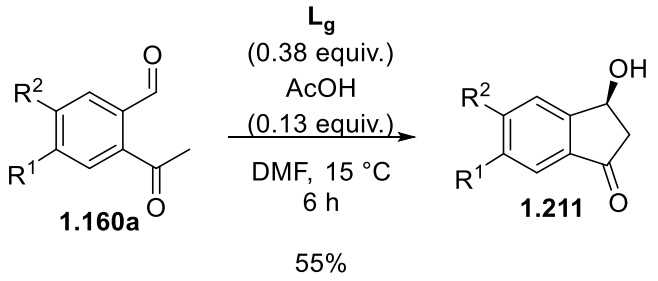

*Scheme 40: Modified reaction to maximize yield of indanol **1.211**.*

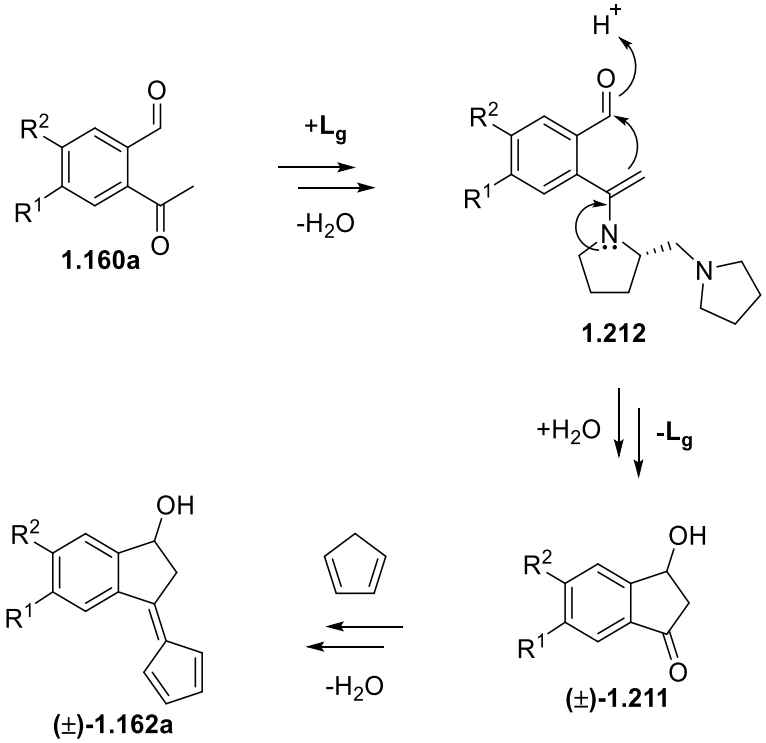

*Scheme 41: First mechanistic proposal involving an Aldol reaction to form **1.211**, via **1.212**, followed by condensation of CpH with indanol **1.211**.*

Pentafulvene **1.161** is the originally predicted product of the pyrrolidine catalyzed condensation between CpH and the aldehyde moiety of 2-acetyl-benzaldehyde. Altering the reaction conditions, by reducing the temperature to 0 ˚C and increasing the reaction duration to two days, increased the isolated yield of **1.161** to 45% (Scheme 42). This enabled interrogation of the second proposed mechanism, in which an initial condensation of CpH with the aldehyde moiety is followed by an enamine-mediated cyclization that sets the stereochemistry. Finally, a

1,3-hydride shift before hydrolysis of the amine catalyst would afford pentafulvene **1.162a** (Scheme 43). Resubmission of the proposed intermediate **1.161** should then result in conversion to the product but again, no conversion was observed. Additionally, the predicted regiochemistry of this mechanism would not agree with that which was observed in the products (confirmed by the X-ray crystal shown in Figure 11 and additional two-dimensional NMR studies).

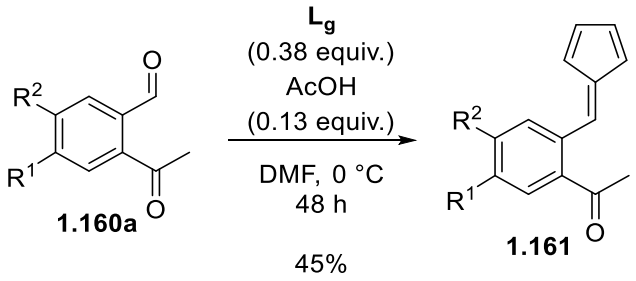

*Scheme 42: Modified reaction conditions to maximize yield of pentafulvene **1.161**.*

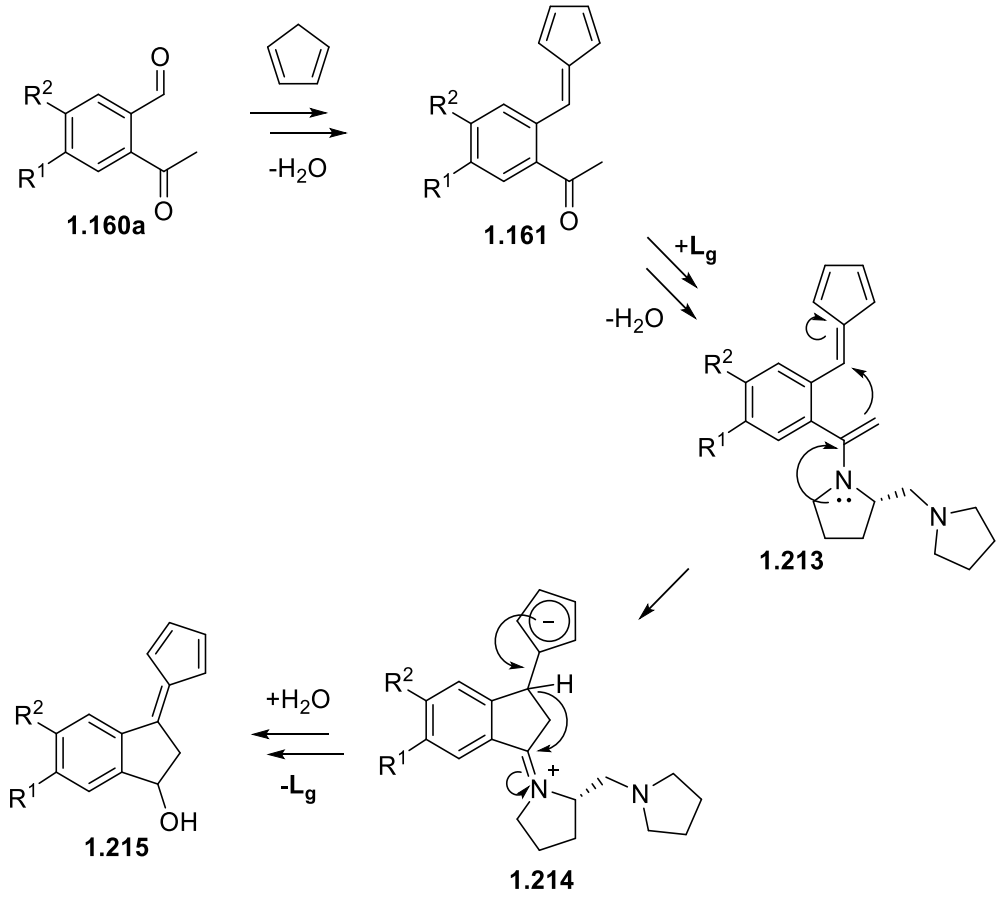

*Scheme 43: Second mechanistic proposal involving condensation of CpH with the aldehyde of 2-acetyl-benzaldehyde to form **1.161** before cyclization of **1.213**. The resulting CpH derivative **1.214** would undergo a 1,3-hydride shift and subsequent hydrolysis of the catalyst to afford pentafulvene **1.215**.*

Having excluded the previous two mechanistic proposals, only one potential remained. In this, CpH undergoes a condensation reaction with the ketone moiety of 2-acetylbenzaldehyde to form pentafulvene **1.216**. Iminium ion facilitated cyclization of the resulting pentafulvene stabilized carbanion (pK_a *ca.* 22.1 in DMSO)[102] would follow. This carbanion would be directed to attack on the bottom face (*Si* face) of the iminium ion due to a blocking group effect of the pendant methylpyrrolidine arm of the catalyst. Hydrolysis of the amine, proceeding with stereoinversion, would then follow to afford pentafulvene **1.162a** with the correct regiochemistry and stereochemistry (Scheme 44). The hydrolysis of the catalyst would likely proceed *via* an S_N1 type process. Literature precedent for the inversion of a stereocentre in an S_N1 process exists in Ingold's original publications, where it was observed that large leaving groups strongly favour inversion outcomes.[103][104] Furthermore, hydrolysis of secondary amines is known to proceed *via* S_N1 type processes.[105] Additional stabilization of the leaving group, *via* protonation, from the lone pair of the pendant pyrrolidine moiety may also account for the improved performance of catalyst $\mathbf{L_g}$, relative to the others trialled. Isolation or observation of the intermediates in this mechanistic proposal was unfortunately not possible but it remains the only potential route that accounts for all experimental results.

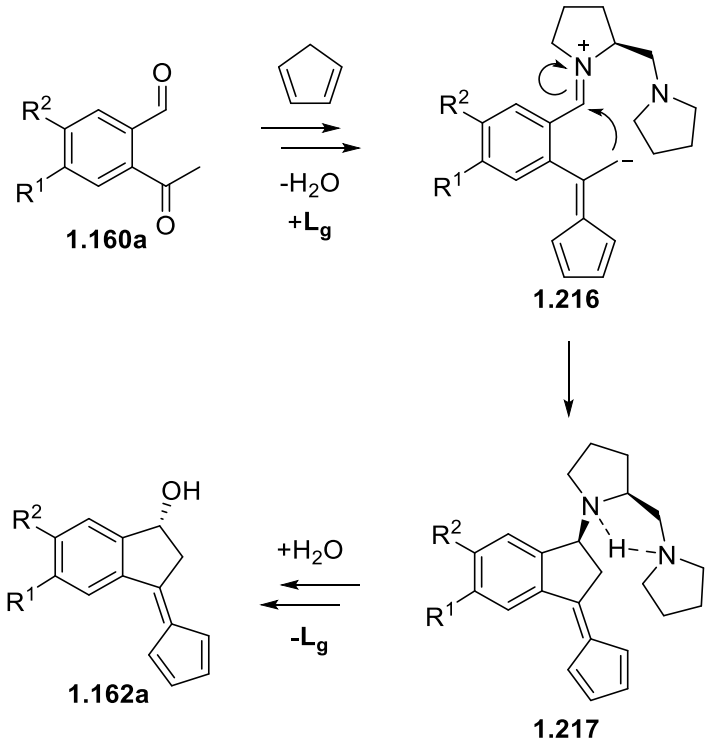

*Scheme 44: Accepted mechanistic proposal in which condensation of CpH with the ketone moiety of 2-acetyl-benzaldhyde is followed by cyclization of pentafulvene stabilized carbanion **1.216**. Subsequent hydrolysis of the catalyst by a stereoinverting S_N1 type process affords pentafulvene **1.162a**.*

1.2.6 Synthesis and Application of Chirally Substituted Cyclopenta-1,3-dienes (CpHs)

Initial studies towards the synthesis of chirally substituted CpH derivatives, from the previously obtained pentafulvenes, focussed on applying the widely used method of Tacke and co-workers.[70][71][106] This method involves the addition of an organometallic reagent to form a pentafulvenyl anion. In Tacke's case Super-Hydride® (lithium triethylborohydride), was used to form a lithium cyclopentadienide. This can then be either directly transmetallated onto a metal or worked up to afford the CpH-H derivative. Initial studies using commercial Super-Hydride® as supplied (1 M in THF) proved unsuccessful. However, in the manner of Tacke, if the solvent of the Super-Hydride® was removed *in vacuo* and the residue redissolved in diethyl ether, full conversion of pentafulvene **1.162g** to CpH **1.218** was observed (following an aqueous workup) (Scheme 45). As pentafulvene **1.162g** possesses an unprotected hydroxyl group a higher loading of Super-Hydride® was used, as one equivalent would deprotonate the alcohol. Encouragingly, this reduction proved to be diastereoselective, with the hydride adding to the top face (*Re face*) of the pentafulvene exocyclic double bond (forcing the CpH moiety to the same face as the hydroxyl group). This stereochemistry was confirmed by ^{1}H-^{1}H NOESY studies and meant that the hydroxyl group was acting as a face blocking group. Therefore, if its steric profile could be increased then the diastereoselectivity should also increase. Hydrogenation of CpH **1.218** to form the corresponding cyclopentane derivative also demonstrated that the two sets of peaks observed in the ^{1}H, ^{13}C and ^{19}F NMR spectra were the result of the α and β tautomers (from the rapid [1,3]-hydride shifts, occurring at room temperature, of the CpH moiety).

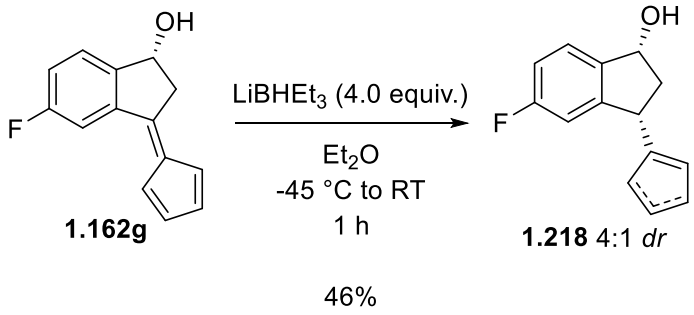

*Scheme 45: Reduction of pentafulvene **1.162g** to CpH **1.218** using the method of Tacke and co-workers.[70]*

Early attempts at modification of pentafulvene **1.162a** proved unsuccessful (Scheme 46). Traditionally the alkylation of a secondary alcohol with methyl iodide or benzyl bromide is achieved through deprotonation of the alcohol, often with sodium hydride. This was not

possible with pentafulvene **1.162a** as deprotonation of the hydroxyl group, at a range of temperatures, resulted in the formation of a self-reactive alkoxide which would polymerize extremely rapidly. Unfortunately, without prior deprotonation of the hydroxyl group, no reaction was observed between **1.162a** and methyl iodide, benzyl bromide or trimethyloxonium tetrafluoroborate. Electrophiles that do not require prior deprotonation, such as toluene sulfonyl chloride or chloro-diphenylphosphine, were then trialled. Both of these showed full consumption of the starting material, but the products proved to be too unstable to isolate.

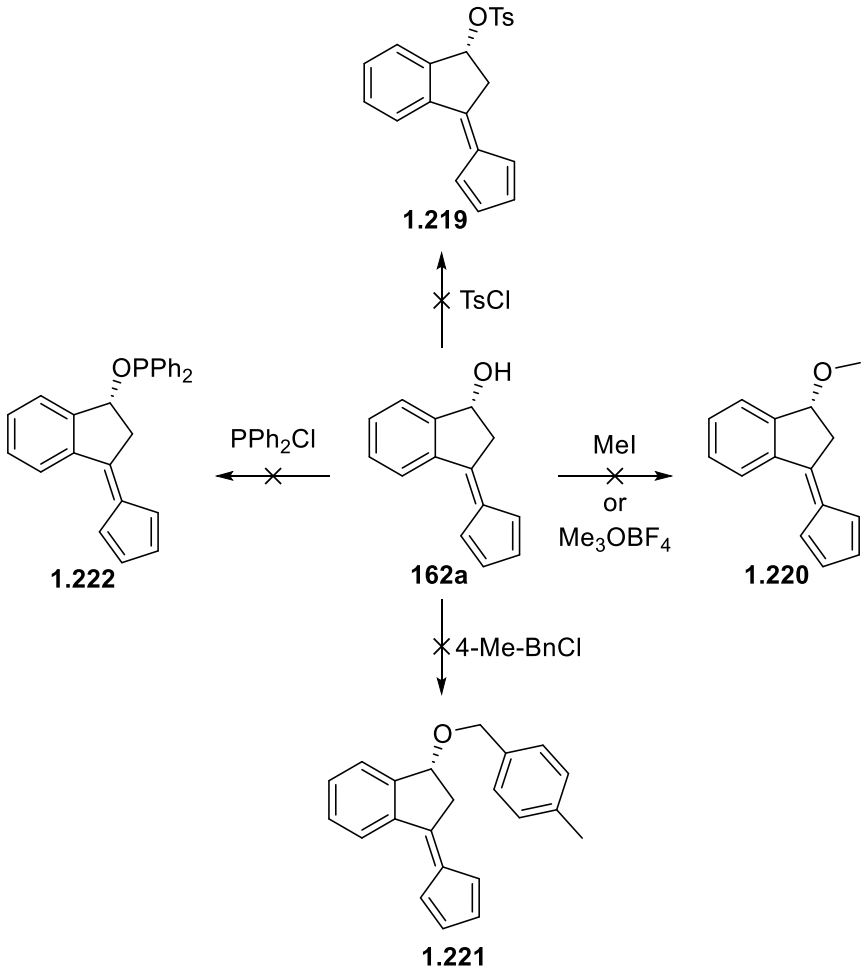

*Scheme 46: Unsuccessful attempts at the modification of pentafulvene **1.162a**'s hydroxyl group.*

Continuing to trial electrophiles that did not require prior deprotonation, success was had using chloro-alkyl ethers and silyl chlorides. MOM-chloride (Scheme 47a) and SEM chloride (Scheme 47b) both afforded good yields when reacted overnight with two equivalents of Hünig's base at room temperature. TES-chloride (Scheme 47c) and TBS-chloride (Scheme 47d) also performed well when using pyridine as the solvent and heating for a short time, although the TBS-chloride was lower yielding due to the higher temperature required. Pyridine dramatically increases the

reactivity of silyl chlorides due to the formation of charged silyl-pyridinium intermediates that are extremely reactive towards nucleophiles.

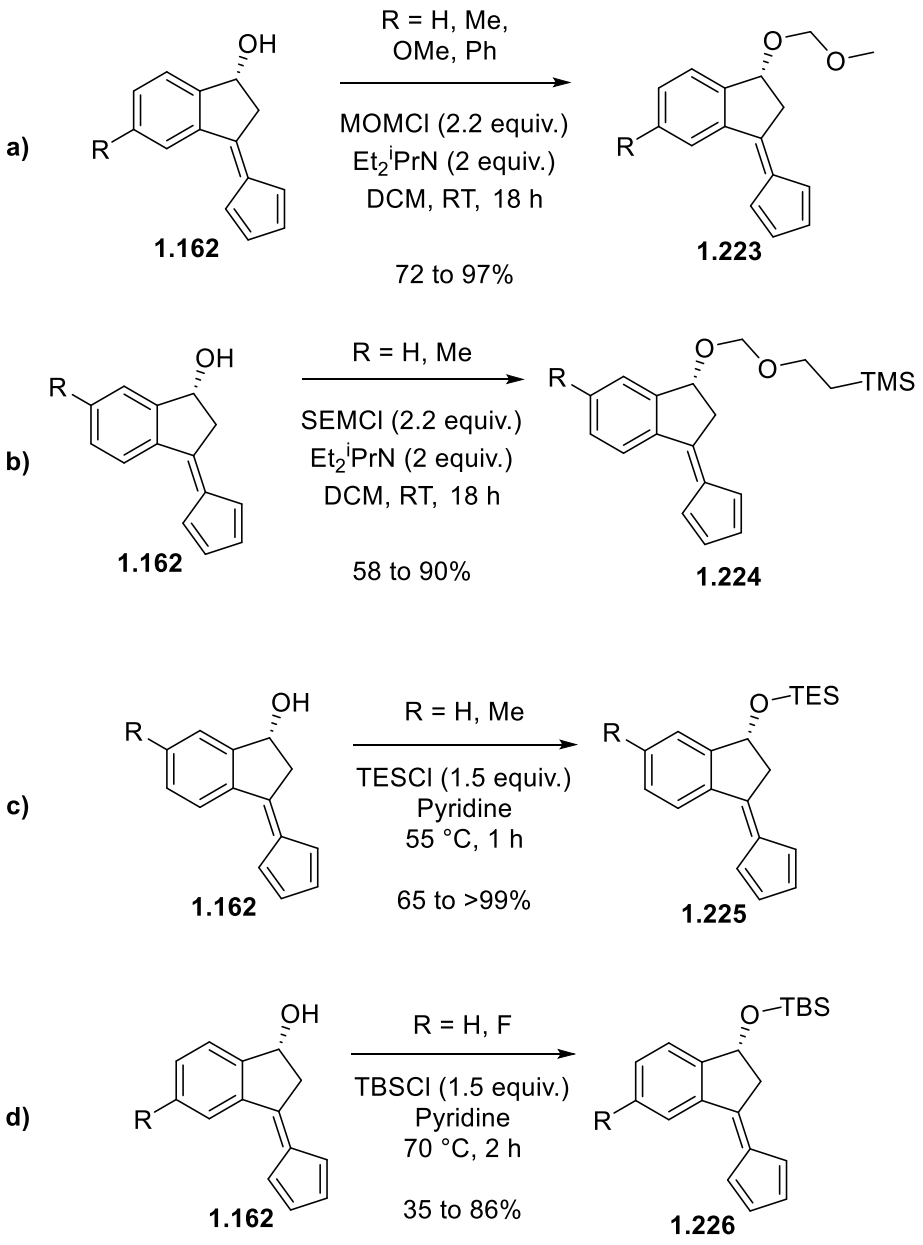

*Scheme 47: Successful modification of a range of **1.162** derivatives using: **a)** MOM-chloride; **b)** SEM-chloride; **c)** TES-chloride; **d)** TBS-chloride.*

After successfully modifying a range of pentafulvenes, the method described in Scheme 45 was then applied (Scheme 48). As predicted, the increase in steric bulk of the alcohol improved the selectivity of the reaction (Table 5), with the smaller MOM group giving a >16:1 diastereoselectivity and all other larger groups giving only one detectable diastereomer of product by NMR (>99:1 *dr*).

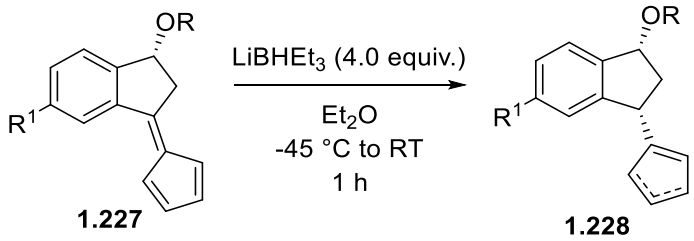

Scheme 48: Reduction of the modified pentafulvene derivatives, shown in Scheme 47, with Super-Hydride®.

R	R^1	Yield (%)	*dr*
MOM	H	77	>16:1
MOM	Ph	51	>16:1
TES	H	74	>99:1
TBS	H	23	>99:1
SEM	H	74	>99:1

Table 5: Results of the reduction described in Scheme 48.

Though complexation of these CpH derivatives was attempted, with both titanium and zirconium, the results were inconclusive. Some evidence for the desired targets was observed with ESI-MS but NMR spectroscopy showed a complex mixture of products which had a high degree of variability between runs.

1.3 Conclusions

A practically straightforward and rapid route to a range of chiral CpH derivatives has been developed, affording them often as single enantiomers and diastereomers in 2-3 steps.

A facile, scalable organocatalytic reaction, affording chirally substituted pentafulvene derivatives, was developed. This used commercial or easily generated starting materials, and catalysts, and could synthesize a range of different pentafulvene derivatives. These could be recrystallized to a single enantiomer, in most cases, and then functionalized further at the hydroxyl group. Reduction of these pentafulvenes, with Super-Hydride®, afforded a range of CpH derivatives as single enantiomers and diastereomers.

Further work is required towards the development of metal complexes containing these CpH derivatives, as early studies proved unreliable and often provided intractable material whose purification and characterization proved challenging. Development of a reliable complexation reaction and improvement of their purification is still required in order to synthesize chiral metal-CpH complexes whose catalytic or biological activity could then be elucidated.

1.4 Experimental

1.4.1 General Experimental

Reactions involving air or moisture sensitive reagents were carried out under argon atmospheres using flame-dried Schlenk apparatus. All temperatures refer to the temperature of the thermostated cooling/heating baths used (±2 °C). All solvents were dried over 4 Å molecular sieves prior to use. The amount of residual water present in the THF and diethyl ether was quantified, using a CA-200 moisture meter, and found to be below 11.0 ppm. Solutions of *n*BuLi (1.6 M in hexanes) were purchased from Sigma-Aldrich and titrated using the Gilman double titration prior to use. Solutions of $LiBEt_3H$ (1.0 M in THF) were purchased from Sigma-Aldrich and used as described. All solid reagents, oxalyl chloride, DBU, TFA, TESCl and acetic acid were used as supplied. All other liquid reagents were dried over 4 Å molecular sieves prior to use. Thin layer chromatography was performed on foil-backed plates coated with Merck Silica gel 60 F254. The plates were developed using ultraviolet light and basic aqueous potassium permanganate. Liquid chromatography was performed using forced flow (flash column) with the solvent system indicated. The stationary phase used was silica gel 60 (220-240 mesh) supplied by Fluorochem. Infrared spectra were recorded on a Bruker Alpha platinum-ATR (if neat) or Transmission (if in solution). Nuclear magnetic resonance spectra were recorded on a Bruker DPX-400 (400.2 MHz), Bruker DPX-300 (300.1 MHz), Bruker AV(III)400 (400.1 MHz), Bruker AV400 (400.1 MHz), Bruker Ascend™ 400 (400.1 MHz) or Bruker Ascend™ 500 (500.1 MHz) spectrometers at ambient temperature (unless otherwise stated). Chemical shifts are quoted in parts per million (ppm) and were referenced to residual solvent peaks using values provided by the MestReNova processing software. Coupling constants (*J*) are quoted in Hertz. Couplings are written using the following abbreviations: br (broad), s (singlet), d (doublet), t (triplet), q (quartet), m (multiplet) and app (apparent). Carbon NMR multiplicities and connectivities were assigned using DEPT and the relevant 2D NMR experiments. Mass spectrometry was performed using a VG Micromass AutoSpec spectrometer (EI) or Bruker MicroTOF (ESI) as noted. Theoretical HRMS molecular weights were taken from the spectrometer output file, for HRMS analyses deviations from expected values (σ) are given in ppm. The specific rotation $[\alpha]_D^t$ was measured using an ADP440 polarimeter or an Anton-Paar MC P100. Melting points were measured on a Gallenkampf melting point apparatus. High performance liquid chromatography spectra were recorded on a Varian ProStar or a Thermo Scientific UltiMate3000 with a UV detector at 254 nm.

1.4.2 Preparation of Catalyst L_g

***(2S)*-2-Pyrrolidinemethanol (L_e)**

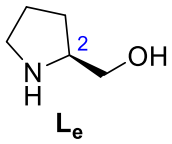

L_e

THF (130 mL) was slowly added to lithium aluminium hydride (10.0 g, 264 mmol) at 0 °C, to form a suspension to which (*L*)-proline (10.1 g, 87.7 mmol) was added over 30 minutes. The resulting mixture was heated to reflux for 72 hours, after which it was cooled to 0 °C and quenched – **CARE! Exotherm** - *via* dropwise addition of water (10 mL) over the course of an hour. This was then followed by the further careful addition of aqueous sodium hydroxide (10% w/v, 10 mL) and water (30 mL). The resulting mixture was filtered to remove the copious aluminium oxide formed, washing with dichloromethane, and the solvent removed *in vacuo* to give the product as a pale yellow oil in 99% yield (8.79 g, 86.9 mmol). **^{1}H NMR** (400.2 MHz, $CDCl_3$): δ_H 3.51 (dd, 1H, *J* = 8.8, 3.2 Hz, C*H*$_a$CH$_b$OH), 3.35-3.25 (m, 2H, CH$_a$C*H*$_b$OH + C*H*NH), 2.98-2.82 (m, 2H, C*H*$_2$NH), 2.52-2.38 (m, 2H, O*H*/N*H*), 1.85-1.65 (m, 3H, C*H*$_2$CH$_2$), 1.46-1.38 (m, 1H, CH$_2$C*H*$_2$). Data are in agreement with reported properties for **L_e**.[107]

(2*S*)-1,1-Dimethylethyl ester-2-(hydroxymethyl)-1-pyrrolidinecarboxylic acid (1.168)

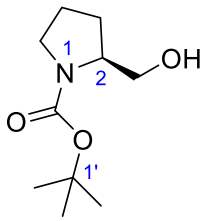

1.168

To a solution of **L_e** (4.00 g, 39.5 mmol) and triethylamine (21.8 mL, 156 mmol) in dichloromethane (250 mL) was added di-*tert*-butyl dicarbonate (10.4 g, 47.7 mmol). The resulting mixture was stirred at RT, open to air, for 24 hours before being quenched by the addition of water (250 mL) with stirring for 30 minutes. The aqueous layer was extracted with dichloromethane (3 × 100 mL), dried over anhydrous sodium sulfate and the solvent removed *in vacuo* to give the crude product, as a pale yellow oil, in quantitative yield which was used without further purification (8.25 g, 41.0 mmol). **R_f** (1:1 ethyl acetate:pentane): 0.37; **^{1}H NMR** (400.2 MHz, $CDCl_3$): δ_H 4.72 (app d, 1H, *J* = 7.7 Hz, O*H*), 3.96 (app d, 1H, *J* = 6.0 Hz, C*H*N), 3.68-3.55 (m, 2H, C*H*$_2$OH), 3.45 (ddd, *J* = 10.8, 6.7, 6.6 Hz 1H, C*H*$_a$H$_b$N), 3.30 (ddd, *J* = 10.6, 6.7, 6.6 Hz, 1H, CH$_a$*H*$_b$N), 2.05-1.96 (m, 1H, C*H*$_2$CH$_2$), 1.85-1.73 (m, 2H, C*H*$_2$CH$_2$), 1.58-1.50 (m, 1H, C*H*$_2$CH$_2$), 1.47 (s, 9H, C(C*H*$_3$)$_3$). Data are in agreement with reported properties for **1.168**.[108]

(2*S*)-1,1-Dimethylethyl ester-2-[[[(4-methylphenyl)sulfonyl]oxy]methyl]-1-pyrrolidinecarboxylic acid (1.169)

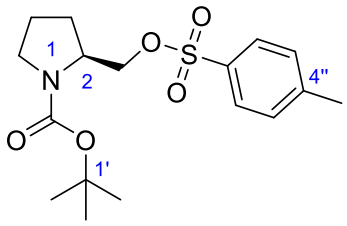

1.169

To a solution of crude **1.168** (5.80 g, 28.8 mmol) in pyridine (18 mL) was added a solution of 4-toluenesulfonyl chloride (6.2 g, 32.5 mmol) in pyridine (18 mL) portionwise over 15 minutes at 0 °C. The resulting solution was stirred at 0 °C for another hour before being allowed to warm to RT and stirred for a further 18 hours. The reaction was monitored *via* TLC, once complete, the solvent was removed *in vacuo* and the reaction redissolved in ethyl acetate (150 mL). This was then washed with HCl (100 mL, 0.5 M), saturated sodium hydrogen carbonate (100 mL) and water (100 mL) before being dried over anhydrous sodium sulfate and the solvent removed *in vacuo* to give the crude product in quantitative yield, as a yellow oil, which was identified *via* ^{1}H NMR and used without further purification (10.9 g, 30.7 mmol). $\mathbf{R_f}$ (1:1 ethyl acetate:pentane): 0.71; **^{1}H NMR** (400.2 MHz, $CDCl_3$): δ_H 7.77 (d, *J* = 8.1 Hz, 2H, Ar*H*), 7.30 (br s, 2H, Ar*H*), 4.15-4.05 (m, 2H, CH_2O), 3.93 (br s, 1H, C*H*N), 3.38-3.22 (m, 2H, CH_2N), 2.44 (s, 3H, CH_3), 1.98-1.74 (m, 4H, CH_2CH_2), 1.43-1.33 (m, 9H, C(CH_3)$_3$). Data are in agreement with reported properties for **1.169**.[109]

(2*S*)-1,1-Dimethylethyl ester-2-(1-pyrrolidinylmethyl)-1-pyrrolidinecarboxylic acid (1.170)

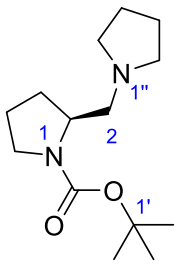

1.170

A solution of crude **1.169** (10.9 g, 30.7 mmol), pyrrolidine (10.1 mL, 123 mol) and DBU (0.46 mL, 3.08 mmol) in toluene (120 mL) was heated at reflux for 42 hours. After removal of all solvents *in vacuo*, the mixture was redissolved in ethyl acetate (100 mL), washed with water (3 × 50 mL), dried over anhydrous sodium sulfate and the solvent removed *in vacuo* to give the crude product, as a light brown solid, in quantitative yield which was identified *via* ^{1}H NMR and used without further purification (8.01 g, 31.5 mmol). **^{1}H NMR** (400.2 MHz, $CDCl_3$): δ_H 4.00-3.77 (m, 1H, C*H*N or CH_aH$_b$N), 3.37-3.27 (m, 2H, C*H*N or CH_2N), 2.65-2.40 (m, 6H, CH_2N), 2.00-1.65 (m, 8H, CH_2CH$_2$), 1.46 (s, 9H, C(CH_3)$_3$). Data are in agreement with reported properties for **1.170**.[110]

***(2S)*-1-(Pyrrolidin-2-ylmethyl)pyrrolidine (L_g)**

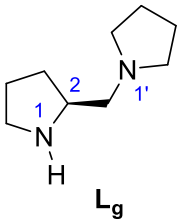

L_g

To a solution of crude **1.170** (8.01 g, 31.5 mmol) in dichloromethane (136 mL) was added TFA (48 mL, 627 mmol) **(CARE! – Corrosive)**. The resulting solution was stirred at RT, open to air, for 24 hours before removal of all solvents *in vacuo* to yield the product as the corresponding TFA salt. This was then dissolved in sodium hydroxide (4 M, 200 mL) and stirred for 30 mins before extraction with diethyl ether (3 × 200 mL). This was then dried over anhydrous sodium sulfate before removal of the solvent *in vacuo* to give the crude product which was purified by Kügelrohr distillation (2 mbar, 1.5 mmHg, 75 °C) to afford the product as a colorless oil in 54% yield (2.64 g, 17.1 mmol). **B.p.**: 75 °C (2 mbar, 1.5 mmHg) [lit 84 °C (5 mmHg)]; **^{1}H NMR** (400.2 MHz, $CDCl_3$): δ_H 3.16 (ddd, *J* = 8.6, 7.2, 5.2 Hz, 1H, C*H*N), 2.93 (ddd, *J* = 10.2, 7.2, 5.9 Hz, 1H, CH_aH$_b$N), 2.80 (ddd, 1H, *J* = 10.2, 7.2, 7.2 Hz, CH$_a$*H*$_b$N), 2.56-2.28 (m, 7H, CH_2*N* and N*H*), 1.84 (dddd, *J* = 12.4, 8.9, 7.2, 5.4 Hz, 1H, CH$_a$*H*$_b$CH$_2$), 1.81-1.63 (m, 6H, CH_2CH$_2$), 1.29 (dddd, *J* = 12.4, 8.8, 6.9, 6.9 Hz, 1H, CH_aH$_b$CH$_2$); **^{13}C NMR** (100.05 MHz, $CDCl_3$): δ_C 62.2 (CH_2), 57.5 (CH), 54.7 (CH_2), 46.2 (CH_2), 30.2 (CH_2), 25.1 (CH_2), 23.5 (CH_2); **ν_{max}** ($CHCl_3$): 3633, 3350, 3319, 3016, 2966, 2878, 2797, 2504, 1461, 1264, 1238, 909 cm^{-1}; **MS** (ESI+): *m/z* 155 $[M+H]^+$; **HRMS** found 155.1549 $C_9H_{19}N_2^+$ requires 155.1543 (|σ| = 3.9 ppm) ; **$[\alpha]_D^{23}$**: +10.0 (*c* = 1.00 in $CHCl_3$) [lit +8.2 (*c* = 2.38 in EtOH)]. Data are in agreement with reported properties for **L_g**.[111]

***(2R)*-1-(Pyrrolidin-2-ylmethyl)pyrrolidine ((*R*)-L_g)**

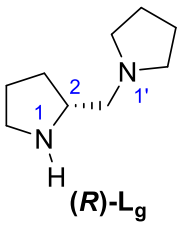

(*R*)-L_g

(*R*)-L_g was synthesized in the same manner as its opposite enantiomer from (2*R*)-2-pyrrolidinemethanol (1.00 g, 9.89 mmol) in 4 steps to afford the product as a colorless oil in 58% yield (887 mg, 5.75 mmol). **$[\alpha]_D^{20}$**: -10.0 (*c* = 1.00 in $CHCl_3$). All other data are in agreement with its opposite enantiomer.

1.4.3 Preparation of 2-Acetyl-benzaldehyde Derivatives 1.160a-i

1-(2-(Hydroxymethyl)phenyl)ethan-1-ol (1.175a)

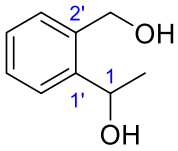

1.175a

TMEDA (9.8 mL, 64.0 mmol) was added dropwise to *n*BuLi (1.6 M in hexane, 40.0 mL, 64.0 mmol) at RT and the resulting yellow solution was stirred for 5 minutes. Benzyl alcohol (2.9 mL, 27.9 mmol) was then added dropwise, at RT, before heating the resulting brown mixture at reflux for 3 hours or until all gas evolution ceased. After cooling the resulting brown suspension to -78 °C, a solution of acetaldehyde (3.6 mL, 64.4 mmol) in diethyl ether (20 mL) was cooled to -78 °C and added dropwise to the lithiated benzyl alcohol. The reaction quickly changed to a pale yellow color and was allowed to warm to RT before being stirred overnight. The resulting orange reaction mixture was quenched *via* the addition of water (60 mL) before being extracted with ethyl acetate (2 x 50 mL), dried over anhydrous magnesium sulfate and the solvents removed *in vacuo* to yield the crude product as an orange oil. The crude product was purified *via* flash column chromatography (eluent: 1:1 ethyl acetate:pentane) to give the product as a yellow oil which crystallized slowly to give a yellow solid in 65% yield (2.90 g, 19.1 mmol). **M.p.**: 64-66 °C [lit[i] 64-66 °C]; $\mathbf{R_f}$ (ethyl acetate): 0.70; **^{1}H NMR** (400.2 MHz, $CDCl_3$): δ_H 7.46 (d, *J* = 7.6 Hz, 1H, Ar*H*), 7.36-7.26 (m, 3H, Ar*H*), 5.15 (q, *J* = 6.5 Hz, 1H, C*H*OH), 4.79 (d, *J* = 12.1 Hz, 1H, CH_aH$_b$), 4.62 (d, *J* = 12.1 Hz, 1H, CH_aH$_b$), 3.08 (m, 2H, 2 × O*H*), 1.57 (d, *J* = 6.5 Hz, 3H, CH_3); **^{13}C NMR** (100.05 MHz, $CDCl_3$): δ_C 143.4 (C), 138.1 (C), 130.0 (CH), 128.7 (CH), 128.0 (CH), 126.0 (CH), 67.2 (CH), 63.9 (CH_2), 23.0 (CH_3); $\boldsymbol{\nu_{max}}$ (neat): 3331, 2974, 1453, 1371, 1213, 1119, 1078, 1006, 896, 763 cm^{-1}; **MS** (ESI+): *m/z* 175 [M+Na]$^+$; **HRMS** found 175.0724 $C_9H_{12}O_2Na^+$ requires 175.0730 (|σ| = 3.4 ppm). Data are in agreement with reported properties for **1.175a**.[112]

1-(4-Hydroxymethyl)-[1,1'-biphenyl]-3-yl)ethan-1-ol (1.175b)

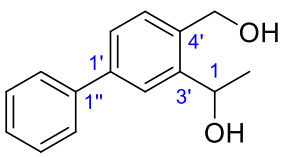

1.175b

TMEDA (9.8 mL, 65.3 mmol) was added dropwise to *n*BuLi (1.6 M in hexane, 43.8 mL, 70.1 mmol) at RT and the resulting yellow solution was stirred for 5 minutes. 4-Biphenylmethanol (5.47 g, 29.7 mmol) was then added portionwise, at RT, before heating the resulting dark purple mixture at reflux for 3 hours or until all gas evolution ceased. After cooling the resulting dark purple suspension to -78 °C, a solution of acetaldehyde (3.7 mL, 66.2 mmol) in diethyl ether (20 mL) was cooled to -78 °C and added dropwise to the lithiated benzyl alcohol. The reaction quickly changed to a pale yellow color and was allowed to warm to RT before being stirred overnight. The resulting orange reaction mixture was quenched *via* the addition of water (50 mL) before being extracted with ethyl acetate (2 x 50 mL), dried over anhydrous magnesium

sulfate and the solvents removed *in vacuo* to yield the crude product as a red oil. The crude product was purified *via* flash column chromatography (eluent: 1:1 ethyl acetate:pentane) to give the product as a yellow oil which crystallized slowly to give an orange solid in 51% yield (3.46 g, 15.2 mmol). **R_f** (1:1 ethyl acetate:pentane): 0.26; **^{1}H NMR** (400.2 MHz, $CDCl_3$): δ_H 7.71 (d, *J* = 1.9 Hz, 1H, Ar*H*), 7.59 (m, 2H, Ar*H*), 7.52-7.26 (m, 5H, Ar*H*), 5.26 (q, *J* = 6.5 Hz, 1H, C*H*OH), 4.87 (d, *J* = 12.1 Hz, 1H, C$H_a$$H_b$OH), 4.74 (d, *J* = 12.1 Hz, 1H, C$H_a$$H_b$), 2.78 (br s, 1H, O*H*), 2.70 (br s, 1H, O*H*), 1.65 (d, *J* = 6.5 Hz, 3H, CH_3); **^{13}C NMR** (100.05 MHz, $CDCl_3$): δ_C 143.9 (C), 141.6 (C), 140.9 (C), 137.1 (C), 130.5 (CH), 128.9 (CH), 127.5 (CH), 127.2 (CH), 126.6 (CH), 124.9 (CH), 67.4 (CH), 63.7 (CH_2), 23.2 (CH_3); **ν_{max}** (neat): 3329, 3058, 3030, 2972, 2926, 2249, 1667, 1600, 1566, 1485, 1450, 1104, 1022, 941, 852, 760, 698 cm^{-1}; **MS** (ESI+): *m/z* 251 $[M+Na]^+$; **HRMS** found 251.1042 $C_{15}H_{16}O_2Na^+$ requires 251.1043 (|σ| = 0.4 ppm).

1-(5-(1,1-Dimethylethyl)-2-(hydroxymethyl)phenyl)ethan-1-ol (1.175c)

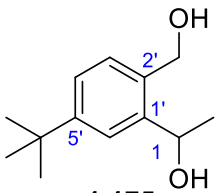

1.175c

TMEDA (9.8 mL, 65.3 mmol) was added dropwise to *n*BuLi (1.6 M in hexane, 43.8 mL, 70.1 mmol) at RT and the resulting yellow solution was stirred for 5 minutes. 4-*tert*-Butylbenzyl alcohol (5.3 mL, 29.9 mmol) was then added dropwise, at RT, before heating the resulting dark red mixture at reflux for 2 hours or until all gas evolution ceased. After cooling the resulting dark orange suspension to -78 °C, a solution of acetaldehyde (3.7 mL, 66.2 mmol) in diethyl ether (20 mL) was cooled to -78 °C and added dropwise to the lithiated benzyl alcohol. The reaction quickly changed to a pale yellow color and was allowed to warm to RT before being stirred overnight. The resulting orange reaction mixture was quenched *via* the addition of water (60 mL) before being extracted with ethyl acetate (2 x 50 mL), dried over anhydrous magnesium sulfate and the solvents removed *in vacuo* to yield the crude product as an orange oil. The crude product was purified *via* flash column chromatography (eluent: 1:1 ethyl acetate:pentane) to give the product as an orange oil in 55% yield (3.37 g, 16.2 mmol). **R_f** (1:1 pentane:ethyl acetate): 0.26; **^{1}H NMR** (400.2 MHz, $CDCl_3$): δ_H 7.51 (d, *J* = 2.0 Hz, 1H, Ar*H*), 7.30 (dd, *J* = 8.0, 2.0 Hz, 1H, Ar*H*), 7.24 (br s, 1H, Ar*H*), 5.18 (q, *J* = 6.5 Hz, 1H, C*H*OH), 4.77 (d, *J* = 12.0 Hz, 1H, C$H_a$$H_b$OH), 4.65 (d, *J* = 12.0 Hz, 1H, CH$_a$$H_b$OH), 2.91-2.76 (m, 2H, 2 × O*H*), 1.60 (d, *J* = 6.5 Hz, 3H, CH_3), 1.33 (s, 9H, C(CH_3)$_3$); **^{13}C NMR** (100.05 MHz, $CDCl_3$): δ_C 151.7 (C), 143.0 (C), 135.2 (C), 129.9 (CH), 124.9 (CH), 123.0 (CH), 67.8 (CH), 63.7 (CH_2), 34.9 (C), 31.5 (CH_3), 23.2 (CH_3); **ν_{max}** (neat): 3316, 2964, 2904, 2869, 1613, 1461, 1409, 1363, 1112, 1077, 1011, 919, 871, 836 cm^{-1}; **MS** (ESI+): *m/z* 231 $[M+Na]^+$; **HRMS** found 231.1366 $C_{13}H_{20}O_2Na^+$ requires 231.1356 (|σ| = 4.3 ppm).

2-Acetyl-benzaldehyde (1.160a)

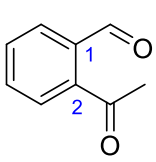

1.160a

A solution of oxalyl chloride (3.1 mL, 36.1 mmol) in dichloromethane (56 mL) was cooled to -78 °C before the dropwise addition of a solution of DMSO (5.2 mL, 73.2 mmol) in dichloromethane (8.5 mL). The resulting mixture was stirred at this temperature for 45 minutes before the addition of a solution of diol **1.175a** (2.25 g, 14.8 mmol) in dichloromethane (20 mL). The resulting mixture was stirred at this temperature for 90 minutes before the addition of triethylamine (9.8 mL, 70.3 mmol). The reaction was then allowed to slowly warm to RT and stirred for 30 minutes before quenching *via* the addition of HCl (1 M, 50 mL). The reaction was extracted with dichloromethane (50 mL), washed with water (50 mL), dried over anhydrous magnesium sulfate and the solvent removed *in vacuo* to yield the crude product as a brown oil. The crude product was purified *via* flash column chromatography (eluent: 5:1 pentane:ethyl acetate) to give the product as a yellow oil in 82% yield (1.81 g, 12.2 mmol). NOTE: The product is unstable at RT and will darken in color if left. If stored at -20 °C, product should be usable for up to 4 weeks and should solidify to a low melting pale brown solid. $\mathbf{R_f}$ (3:2 ethyl acetate:pentane): 0.76; **^{1}H NMR** (400.2 MHz, $CDCl_3$): δ_H 10.20 (s, 1H, *H*CO), 7.85-7.61 (m, 4H, Ar*H*), 2.63 (s, 3H, C*H*$_3$); **^{13}C NMR** (100.05 MHz, $CDCl_3$): δ_C 201.1 (C=O), 192.3 (C=O), 140.6 (C), 136.3 (C), 133.1 (CH), 131.9 (CH), 129.7 (CH), 128.6 (CH), 28.9 (CH_3); $\boldsymbol{\nu_{max}}$ (neat): 3068, 2861, 2750, 1761, 1694, 1594, 1573, 1359, 1262, 1197, 767, 642 cm^{-1}; **MS** (ESI+): *m/z* 171 $[M+Na]^+$; **HRMS** found 171.0424 $C_9H_8O_2Na^+$ requires 171.0417 ($|\sigma|$ = 4.1 ppm). Data are in agreement with reported properties of **1.160a**.[96]

2-Acetyl-4-phenyl-benzaldehyde (1.160b)

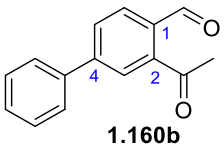

1.160b

A solution of oxalyl chloride (1.4 mL, 16.3 mmol) in dichloromethane (26 mL) was cooled to -78 °C before the dropwise addition of a solution of DMSO (2.4 mL, 33.8 mmol) in dichloromethane (4.3 mL). The resulting mixture was stirred at this temperature for 45 minutes before the addition of a solution of diol **1.175b** (1.50 g, 6.58 mmol) in dichloromethane (9 mL). The resulting mixture was stirred at this temperature for 90 minutes before the addition of triethylamine (4.6 mL, 33.0 mmol). The reaction was then allowed to slowly warm to RT and stirred for 30 minutes before quenching *via* the addition of HCl (1 M, 40 mL). The reaction was extracted with dichloromethane (50 mL), washed with water (50 mL), dried over anhydrous magnesium sulfate and the solvent removed *in vacuo* to yield the crude product as a brown oil. The crude product was purified *via* flash column chromatography (eluent: 4:1 pentane:ethyl acetate) to give the product as an orange oil in 62% yield (0.91 g, 4.06 mmol). NOTE: The product is unstable at RT

and will darken in color if left. If stored at -20 °C, product should be usable for up to 4 weeks and should solidify to a low melting pale brown solid. **R_f** (1:1 ethyl acetate:pentane): 0.85; **^{1}H NMR** (400.2 MHz, $CDCl_3$): δ_H 10.25 (s, 1H, *H*CO), 7.98 (dd, *J* = 7.9, 0.7 Hz, 1H, Ar*H*), 7.87-7.81 (m, 2H, Ar*H*), 7.65-7.60 (m, 2H, Ar*H*), 7.54-7.43 (m, 3H, Ar*H*), 2.70 (3H, s, CH_3); **^{13}C NMR** (100.05 MHz, $CDCl_3$): δ_C 201.5 (C=O), 191.8 (C=O), 146.4 (C), 141.8 (C), 139.1 (C), 134.4 (C), 130.8 (CH), 130.1 (CH), 129.3 (CH), 129.0 (CH), 127.5 (CH), 127.1 (CH), 29.4 (CH_3); **ν_{max}** (neat): 3061, 3033, 2921, 2854, 1759, 1688, 1599, 1357, 1306, 1274, 1239, 1204, 761, 696 cm^{-1}; **MS** (ESI+): *m/z* 247 $[M+Na]^+$; **HRMS** found 247.0728 $C_{15}H_{12}O_2Na^+$ requires 247.0730 (|σ| = 0.8 ppm).

2-Acetyl-4-(1,1-dimethylethyl)-benzaldehyde (1.160c)

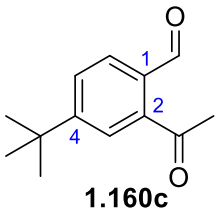

1.160c

A solution of oxalyl chloride (1.6 mL, 18.7 mmol) in dichloromethane (28 mL) was cooled to -78 °C before the dropwise addition of a solution of DMSO (2.6 mL, 36.6 mmol) in dichloromethane (4.3 mL). The resulting mixture was stirred at this temperature for 45 minutes before the addition of a solution of diol **1.175c** (1.50 g, 7.20 mmol) in dichloromethane (10 mL). The resulting mixture was stirred at this temperature for 90 minutes before the addition of triethylamine (4.9 mL, 35.1 mmol). The reaction was then allowed to slowly warm to RT and stirred for 30 minutes before quenching *via* the addition of HCl (1 M, 40 mL). The reaction was extracted with dichloromethane (50 mL), washed with water (50 mL), dried over anhydrous magnesium sulfate and the solvent removed *in vacuo* to yield the crude product as a brown oil. The crude product was purified *via* flash column chromatography (eluent: 5:1 pentane:ethyl acetate) to give the product as an yellow oil in 80% yield (1.18 g, 5.78 mmol). NOTE: The product is unstable at RT and will darken in color if left. If stored at -20 °C, product should be usable for up to 4 weeks and should solidify to a low melting pale brown solid. **R_f** (1:1 pentane:ethyl acetate): 0.94; **^{1}H NMR** (400.2 MHz, $CDCl_3$): δ_H 10.16 (s, 1H, C*H*O), 7.84-7.82 (m, 1H, Ar*H*), 7.67-7.61 (m, 2H, Ar*H*), 2.63 (s, 3H, CH_3), 1.37 (s, 9H, C(CH_3)$_3$); **^{13}C NMR** (100.05 MHz, $CDCl_3$): δ_C 202.2 (C=O), 191.9 (C=O), 157.5 (C), 141.4 (C), 133.2 (C), 130.0 (CH), 128.6 (CH), 125.2 (CH), 35.5 (C), 31.1 (CH_3), 29.5 (CH_3); **ν_{max}** (neat): 2964, 2908, 2870, 1688, 1599, 1562, 1362, 1276, 1240, 1212, 1112, 883, 825, 774 cm^{-1}; **MS** (ESI+): *m/z* 227 $[M+Na]^+$; **HRMS** found 227.1052 $C_{13}H_{16}O_2Na^+$ requires 227.1043 (|σ| = 4.0 ppm).

Acetic acid hydrazide (1.188)

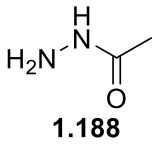

1.188

A solution of hydrazine monohydrate (4.4 mL, 90.7 mmol) and ethyl acetate (10.0 mL, 102 mmol) in ethanol (20 mL) was heated at reflux for 24 hours. Once cooled, the solvents were removed *in vacuo* and the resulting oil was resuspended in hexane which was once more removed *in vacuo* to give the product as a colorless solid in 83% yield (5.60 g, 75.6 mmol). **^{1}H NMR** (300.1 MHz, $CDCl_3$): δ_H 7.33 (br s, 1H, N*H*), 3.90 (br s, 2H, NH_2), 1.94 (s, 3H, CH_3). Data are in agreement with reported properties of **1.188**.[97]

General Procedure A: *ortho*-Formylation of Phenols

Anhydrous magnesium chloride (1.5 equiv.) was dried further by heating under vacuum (2 mbar) until free-flowing. To this was added THF, *m*-cresol (1 equiv.), triethylamine (2.5 equiv.) and paraformaldehyde (4.5 equiv.). The mixture was heated to reflux for 18 hours – **CARE! Carcinogenic chloroalkyl ether by-products may be formed, use an efficient hood!** – after which the reaction was quenched *via* the slow addition of HCl (2M, 50 mL). The reaction was extracted with ethyl acetate (2 x 50 mL), dried over anhydrous sodium sulfate and the solvent removed *in vacuo* to yield the crude product which could be used without further purification.

2-Hydroxy-4-methoxy-benzaldehyde (1.187a)

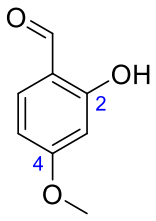

1.187a

Synthesized according to **General Procedure A** using anhydrous magnesium chloride (2.86 g, 30.0 mmol), THF (80 mL), 3-methoxyphenol (2.2 mL, 20.0 mmol), triethylamine (10.6 mL, 76.0 mmol) and paraformaldehyde (4.20 g, 140.0 mmol) to afford the crude product as a pale brown solid in a quantitative yield (3.20 g, 21.0 mmol) which was identified *via* ^{1}H NMR and used without further purification. **R_f** (6:1 pentane:ethyl acetate): 0.69; **^{1}H NMR** (300.1 MHz, $CDCl_3$): δ_H 11.48 (s, 1H, O*H*), 9.72 (s, 1H, C*H*O), 7.43 (d, 1H, *J* = 8.7 Hz, Ar*H*), 6.54 (dd, 1H, *J* = 8.7, 2.3 Hz, Ar*H*), 6.43 (d, 1H, *J* = 2.3 Hz, Ar*H*), 3.86 (s, 3H, CH_3). Data are in agreement with reported properties of **1.187a**.[96]

2-Hydroxy-4-methyl-benzaldehyde (1.187b)

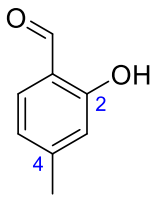

1.187b

Synthesized according to **General Procedure A** using anhydrous magnesium chloride (2.86 g, 30.0 mmol), THF (80 mL), *m*-cresol (2.1 mL, 20.0 mmol), triethylamine (10.6 mL, 76.0 mmol) and paraformaldehyde (4.20 g, 140.0 mmol) to afford the crude product as a pale pink solid in a quantitative yield (2.81 g, 20.6 mmol) which was identified *via* ^{1}H NMR and used without further purification. $\mathbf{R_f}$ (8:1 pentane:ethyl acetate): 0.83; **^{1}H NMR** (400.2 MHz, $CDCl_3$): δ_H 11.08 (s, 1H, O*H*), 9.81 (s, 1H, C*H*O), 7.42 (d, 1H, *J* = 7.9 Hz, Ar*H*), 6.85-6.77 (m, 2H, Ar*H*), 2.38 (s, 3H, CH_3). Data are in agreement with reported properties of **1.187b**.[96]

2-Hydroxy-5-methyl-benzaldehyde (1.187c)

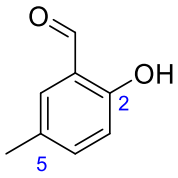

1.187c

Synthesized according to **General Procedure A** using anhydrous magnesium chloride (2.86 g, 30.0 mmol), THF (80 mL), *p*-cresol (2.16 g, 20.0 mmol), triethylamine (10.6 mL, 76.0 mmol) and paraformaldehyde (4.20 g, 140.0 mmol) to afford the crude product as a yellow oil in a quantitative yield (3.02 g, 22.2 mmol) which was identified *via* ^{1}H NMR and used without further purification. $\mathbf{R_f}$ (5:1 pentane:ethyl acetate): 0.95; **^{1}H NMR** (400.2 MHz, $CDCl_3$): δ_H 10.83 (s, 1H, O*H*), 9.85 (s, 1H, C*H*O), 7.36-7.32 (m, 2H, Ar*H*), 6.90 (d, 1H, *J* = 9.1 Hz, Ar*H*), 2.34 (s, 3H, CH_3). Data are in agreement with reported properties of **1.187c**.[96]

4-Fluoro-2-hydroxy-benzaldehyde (1.187d)

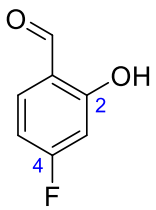

1.187d

Synthesized according to **General Procedure A** using anhydrous magnesium chloride (2.86 g, 30.0 mmol), THF (80 mL), 3-fluorophenol (1.8 mL, 19.9 mmol), triethylamine (10.6 mL, 76.0 mmol) and paraformaldehyde (4.20 g, 140.0 mmol) to afford the crude product as a pale pink oil in a quantitative yield (3.25 g, 23.2 mmol) which was identified *via* ^{1}H NMR and used without further purification. $\mathbf{R_f}$ (8:1 pentane:ethyl acetate): 0.87; **^{1}H NMR** (400.1 MHz, $CDCl_3$): δ_H 11.36 (s, 1H, O*H*), 9.83 (s, 1H, C*H*O), 7.56 (dd, 1H, *J* = 8.6, 6.3 Hz, Ar*H*), 6.75-6.66 (m, 2H, Ar*H*). Data are in agreement with reported properties for **1.187d**.[113]

5-Fluoro-2-hydroxy-benzaldehyde (1.187e)

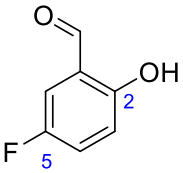

1.187e

Synthesized according to **General Procedure A** using anhydrous magnesium chloride (2.86 g, 30.0 mmol), THF (80 mL), 4-fluorophenol (2.24 g, 20.0 mmol), triethylamine (10.6 mL, 76.0 mmol) and paraformaldehyde (4.20 g, 140.0 mmol) to afford the crude product as a pale pink oil, and as an approximately 1:1 mixture of starting material and product, in 86% yield (2.40 g, 17.1 mmol) which was identified *via* ^{1}H NMR and used without further purification. $\mathbf{R_f}$ (9:1 pentane:ethyl acetate): 1.00; **^{1}H NMR** (400.1 MHz, $CDCl_3$): δ_H 10.78 (s, 1H, O*H*), 9.86 (d, 1H, *J* = 0.6 Hz, C*H*O), 7.00-6.90 (m, 2H, Ar*H*), 6.79-6.75 (m, 1H, Ar*H*). Data are in agreement with reported properties for **1.187e**.[113]

5-Chloro-2-hydroxy-benzaldehyde (1.187f)

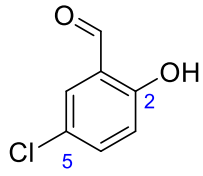

1.187f

Synthesized according to **General Procedure A** using anhydrous magnesium chloride (2.86 g, 30.0 mmol), THF (80 mL), 4-chlorophenol (2.56 g, 20.3 mmol), triethylamine (10.6 mL, 76.0 mmol) and paraformaldehyde (4.20 g, 140.0 mmol) to afford the crude product as a pale brown oil, and as an approximately 1:1 mixture of starting material and product, in a quantitative yield (3.69 g, 23.6 mmol) which was identified *via* ^{1}H NMR and used without further purification. $\mathbf{R_f}$ (9:1 pentane:ethyl acetate): 0.68; **^{1}H NMR** (400.1 MHz, $CDCl_3$): δ_H 10.92 (s, 1H, O*H*), 9.85 (d, 1H, *J* = 0.6 Hz, C*H*O), 7.54 (d, 1H, *J* = 2.6 Hz, Ar*H*), 7.48 (dd, 1H, *J* = 8.9, 2.6 Hz, Ar*H*), 6.97 (dd, 1H, *J* = 8.9, 0.6 Hz, Ar*H*). Data are in agreement with reported properties for **1.187f**.[113]

General Procedure B: **Synthesis of Hydrazides**

A mixture of *o*-formyl-phenol (1 equiv.) and acetic acid hydrazide (1 equiv.) in ethanol was heated to reflux for 18 hours. After cooling, the solvent was removed *in vacuo* to yield the crude product which was washed with diethyl ether and then used without further purification.

(2*E*)-2-[(2-Hydroxy-4-methoxyphenyl)methylene]-acetic acid hydrazide (1.189a)

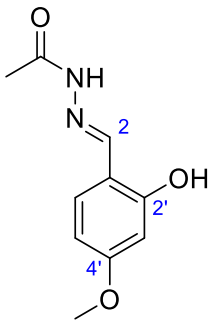

1.189a

Synthesized according to **General Procedure B** using phenol **1.187a** (3.20 g, 21.0 mmol) and **1.188** (1.56 g, 21.1 mmol) in ethanol (100 mL) to afford the crude product as a pale yellow solid in 88% yield (3.86 g, 18.5 mmol) which was identified *via* ^{1}H NMR and used without further purification. $\mathbf{R_f}$ (ethyl acetate): 0.50; **^{1}H NMR** (400.2 MHz, d_6-DMSO): δ_H 11.49 + 11.09 (2 × s, 1H, O*H*), 11.47 + 10.30 (2 × s, 1H, N*H*), 8.22 + 8.14 (2 × s, 1H, NC*H*), 7.47 + 7.35 (2 × d, 1H, *J* = 8.5 Hz, Ar*H*), 6.51-6.41 (m, 2H, Ar*H*), 3.73 + 3.72 (2 × s, 3H, OCH_3), 2.12 + 1.93 (2 × s, 3H, $COCH_3$). Data are in agreement with reported properties for **1.189a**.[96]

(2*E*)-2-[(2-Hydroxy-4-methylphenyl)methylene]-acetic acid hydrazide (1.189b)

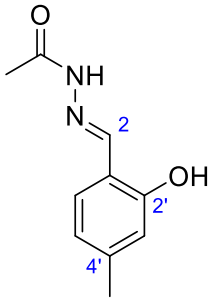

1.189b

Synthesized according to **General Procedure B** using phenol **1.187b** (3.02 g, 22.2 mmol) and **1.188** (1.64 g, 22.1 mmol) in ethanol (100 mL) to afford the crude product as a colorless solid in 96% yield (4.09 g, 21.3 mmol) which was identified *via* ^{1}H NMR and used without further purification. $\mathbf{R_f}$ (ethyl acetate): 0.64; **^{1}H NMR** (400.2 MHz, d_6-DMSO): δ_H 10.56 + 10.07 (2 × s, 1H, O*H*), 10.18 + 10.16 (2 × s, 1H, N*H*), 8.27 + 8.21 (2 × s, 1H, NC*H*), 7.47 + 7.35 (2 × d, 1H, *J* = 7.7 Hz, Ar*H*), 6.72-6.67 (m, 2H, Ar*H*), 2.26 + 2.24 (2 × s, 3H, $ArCH_3$), 2.15 + 1.96 (2 × s, 3H, $COCH_3$). Data are in agreement with reported properties for **1.189b**.[96]

(2*E*)-2-[(2-Hydroxy-5-methylphenyl)methylene]-acetic acid hydrazide (1.189c)

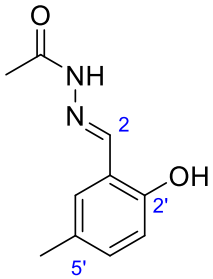

1.189c

Synthesized according to **General Procedure B** using phenol **1.187c** (3.02 g, 22.2 mmol) and **1.188** (1.64 g, 22.1 mmol) in ethanol (100 mL) to afford the crude product as a pale pink solid in 96% yield (4.09 g, 21.3 mmol) which was identified *via* ^{1}H NMR and used without further purification. $\mathbf{R_f}$ (ethyl acetate): 0.55; **^{1}H NMR** (500.1 MHz, d_6-DMSO): δ_H 11.58 + 11.19 (2 × s, 1H, O*H*), 10.91 + 9.89 (2 × s, 1H, N*H*), 8.27 + 8.22 (2 × s, 1H, NC*H*), 7.41 + 7.30 (2 × d, 1H, *J* = 2.3 Hz, Ar*H*), 7.08 + 7.03 (2 × dd, 1H, *J* = 8.3, 2.3 Hz, Ar*H*), 6.80 + 6.78 (2 × d, 1H, *J* = 8.3 Hz, Ar*H*), 2.23 + 2.21 (2 × s, 3H, $ArCH_3$), 2.17 + 1.96 (2 × s, 3H, $COCH_3$). Data are in agreement with reported properties of **1.189c**.[96]

(2*E*)-2-[(4-Fluoro-2-hydroxyphenyl)methylene]-acetic acid hydrazide (1.188d)

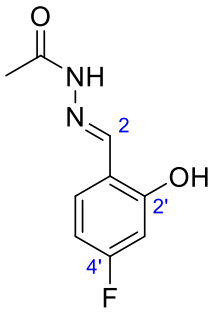

1.189d

Synthesized according to **General Procedure B** using phenol **1.187d** (3.26 g, 23.3 mmol) and **1.188** (1.70 g, 22.9 mmol) in ethanol (100 mL) to afford the crude product as a pale pink solid in 91% yield (4.10 g, 20.9 mmol) which was identified by ^{1}H NMR and used without further purification. $\mathbf{R_f}$ (ethyl acetate): 0.32; **^{1}H NMR** (400.1 MHz, d_6-DMSO): δ_H 11.60 + 11.20 (2 × s, 1H, O*H*), 8.30 + 8.20 (2 × s, 1H, NC*H*), 7.66 + 7.55 (2 × dd, 1H, *J* = 8.4, 7.0 Hz, Ar*H*), 6.77–6.66 (m, 2H, Ar*H*), 2.15 + 1.95 (2 × s, 3H, COCH_3).

(2*E*)-2-[(5-Fluoro-2-hydroxyphenyl)methylene]-acetic acid hydrazide (1.189e)

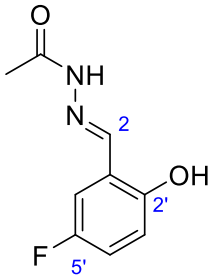

1.189e

Synthesized according to **General Procedure B** using phenol **1.187e** (2.49 g, 17.8 mmol) and **1.188** (878 mg, 11.9 mmol) in ethanol (53 mL) to afford the crude product as a pale yellow solid in 38% yield (1.34 g, 6.83 mmol) which was identified *via* ^{1}H NMR and used without further purification. $\mathbf{R_f}$ (ethyl acetate): 0.46; **^{1}H NMR** (400.1 MHz, d_6-DMSO): δ_H 11.66 + 11.28 (2 × br s, 1H, O*H*), 10.91 + 10.06 (2 × br s, 1H, N*H*), 8.31 + 8.23 (2 × d, 1H, *J* = 1.8 Hz, NC*H*), 7.39 (app ddd, 1H, *J* = 12.5, 9.5, 3.2 Hz, Ar*H*), 7.09 (app dddd, 1H, *J* = 19.3, 8.4, 8.4, 3.2 Hz, Ar*H*), 6.89 (app ddd, 1H, *J* = 9.0 Hz, 7.3 Hz, 4.7 Hz, Ar*H*), 2.18 + 1.96 (2 × s, 3H, COCH_3).

(2*E*)-2-[(5-Chloro-2-hydroxyphenyl)methylene]-acetic acid hydrazide (1.189f)

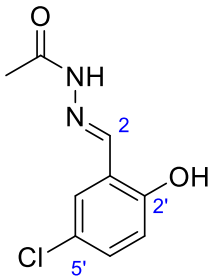

1.189f

Synthesized according to **General Procedure B** using phenol **1.187f** (1.84 g, 11.8 mmol) and **1.188** (873 mg, 11.8 mmol) in ethanol (50 mL) to afford the crude product as a pale yellow solid in 57% yield (1.43 g, 6.73 mmol) which was identified *via* ^{1}H NMR and used without further purification. $\mathbf{R_f}$ (ethyl acetate): 0.46; **^{1}H NMR** (500.1 MHz, d_6-DMSO): δ_H 11.68 + 11.29 (2 × s, 1H, O*H*), 11.19 + 10.35 (2 × br s, 1H, N*H*), 8.30 + 8.21 (2 × s, 1H, NC*H*), 7.63 + 7.61 (2 × d, 1H, *J* = 2.7 Hz, Ar*H*), 7.29 +7.25 (2 × dd, 1H, *J* = 8.7, 2.7 Hz, Ar*H*), 6.91 (2 × d, 1H, *J* = 8.7 Hz, Ar*H*), 2.18 + 1.96 (2 × s, 3H, COCH_3). Data is in agreement with reported properties of **1.189f**.[96]

General Procedure C: Synthesis of 2-Acetyl-benzaldehyde Derivatives

To lead (IV) acetate (1.1 equiv.) – supplied as a white solid (if the lead (IV) acetate used is not fresh, and has turned to a pale brown, the equivalents used of it can be increased to 1.3 for no

loss of yield. If it has turned to a dark brown/black, it can be recrystallized from hot glacial acetic acid) – was added THF followed by the portion wise addition of the hydrazide derivative (1 equiv.). After stirring at RT for 2 hours, after which the majority of effervescence has ceased, the reaction was filtered through Celite®. The crude material was then diluted into ethyl acetate (100 mL), washed with saturated sodium hydrogen carbonate (50 mL) and water (50 mL) and dried over anhydrous magnesium sulfate. After removal of the solvent *in vacuo*, the crude product was purified *via* flash column chromatography (eluent: 4:1 pentane:ethyl acetate) to yield the product.

2-Acetyl-4-methoxy-benzaldehyde (1.160d)

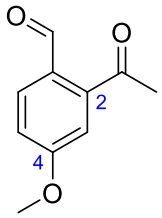

1.160d

Synthesized according to **General Procedure C** using lead (IV) acetate (3.10 g, 6.99 mmol), hydrazide **1.189a** (1.3 g, 6.24 mmol) and THF (31 mL) to give the product as a yellow solid in 56% yield (625 mg, 3.51 mmol). NOTE: The product is unstable at RT and will darken in color if left. If stored at -20 °C, product should be usable for up to 4 weeks. $\mathbf{R_f}$ (ethyl acetate): 0.86; **^{1}H NMR** (300.1 MHz, $CDCl_3$): δ_H 10.01 (s, 1H, C*H*O), 7.85 (dd, 1H, *J* = 8.4, 0.6 Hz, Ar*H*), 7.10-7.03 (m, 2H, Ar*H*), 3.88 (s, 3H, OCH_3), 2.56 (s, 3H, COCH_3); **^{13}C NMR** (75.025 MHz, $CDCl_3$): δ_C 202.5 (C=O), 190.9 (C=O), 164.1 (C), 144.3 (C), 133.6 (CH), 128.4 (C), 115.8 (CH), 114.5 (CH), 56.3 (CH_3), 30.1 (CH_3); $\boldsymbol{\nu_{max}}$ (neat): 3068, 2977, 2951, 2908, 2847, 1766, 1672, 1591, 1566, 1493, 1365, 1294, 1265, 1206, 1031, 957, 886, 804, 574 cm^{-1}; **MS** (ESI+): *m/z* 201 $[M+Na]^+$; **HRMS** found 201.0523 $C_{10}H_{10}O_3Na^+$ requires 201.0522 (|σ| = 0.5 ppm). Data are in agreement with reported properties of **1.160d**.[96]

2-Acetyl-4-methyl-benzaldehyde (1.160e)

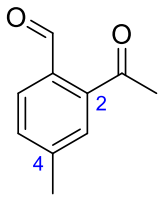

1.160e

Synthesized according to **General Procedure C** using lead (IV) acetate (2.20 g, 4.96 mmol), hydrazide **1.189b** (0.86 g, 4.47 mmol) and THF (22 mL) to give the product as a yellow oil in 47% yield (337 mg, 2.08 mmol). NOTE: The product is unstable at RT and will darken in color if left. If stored at -20 °C, product should be usable for up to 4 weeks and should solidify to a low melting yellow solid. $\mathbf{R_f}$ (ethyl acetate): 0.86; **^{1}H NMR** (400.2 MHz, $CDCl_3$): δ_H 10.16 (s, 1H, C*H*O), 7.80 (d, 1H, *J* = 7.8 Hz, Ar*H*), 7.44 (m, 2H, Ar*H*), 2.63 (s, 3H, CH_3), 2.48 (s, 3H, CH_3); **^{13}C NMR** (100.05 MHz, $CDCl_3$): δ_C 201.7 (C=O), 191.8 (CHO), 144.3 (C), 141.1 (C), 133.3 (C), 132.1 (CH), 130.1 (CH), 128.9 (CH), 29.1 (CH_3), 21.7 (CH_3); $\boldsymbol{\nu_{max}}$ (neat): 2923, 2863, 1765, 1682, 1601, 1567, 1424, 1358, 1267, 1210, 1184,

1131, 829, 796 cm^{-1}; **MS** (ESI+): *m/z* 185 $[M+Na]^+$; **HRMS** found 185.0572 $C_{10}H_{10}O_2Na^+$ requires 185.0573 (|σ| = 0.5 ppm). Data are in agreement with reported properties of **1.160e**.[96]

2-Acetyl-5-methyl-benzaldehyde (1.160f)

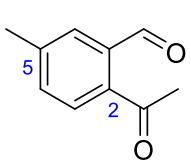

1.160f

Synthesized according to **General Procedure C** using lead (IV) acetate (2.30 g, 5.19 mmol), hydrazide **1.189c** (890 mg, 4.63 mmol) and THF (25 mL) to give the product as a yellow oil in 25% yield (187 mg, 1.15 mmol). NOTE: The product is unstable at RT and will darken in color if left. If stored at -20 °C, product should solidify to a low melting, pale brown solid and be usable for up to 4 weeks. $\mathbf{R_f}$ (4:1 pentane:ethyl acetate): 0.41; **^{1}H NMR** (400.1 MHz, $CDCl_3$): δ_H 10.26 (s, 1H, C*H*O), 7.70-7.65 (m, 2H, Ar*H*), 7.44 (ddd, 1H, *J* = 7.8, 1.9, 0.7 Hz, Ar*H*), 2.64 (s, 3H, CH_3), 2.46 (s, 3H, COCH_3); **^{13}C NMR** (100.025 MHz, $CDCl_3$): δ_C 200.3 (C=O), 192.9 (C=O), 143.2 (C), 137.7 (C), 137.0 (C), 133.4 (CH), 129.9 (CH), 129.2 (CH), 28.6 (CH_3), 21.6 (CH_3); $\mathbf{\nu_{max}}$ (neat): 2923, 2866, 1762, 1675, 1599, 1568, 1357, 1257, 1231, 1010, 824, 774 cm^{-1}; **MS** (ESI+): *m/z* 185 $[M+Na]^+$; **HRMS** found 185.0568 $C_{10}H_{10}O_2Na^+$ requires 185.0573 (|σ| = 2.7 ppm). Data are in agreement with reported properties of **1.160f**.[96]

2-Acetyl-4-fluoro-benzaldehyde (1.160g)

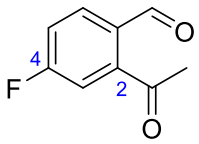

1.160g

Synthesized according to **General Procedure C** using lead (IV) acetate (2.89 g, 6.52 mmol), hydrazide **1.189d** (1.14 g, 5.81 mmol) and THF (29 mL) to give the product as a yellow solid in 60% yield (580 mg, 3.49 mmol). NOTE: The product is unstable at RT and will darken in color if left. If stored at -20 °C, product should be usable for up to 4 weeks. $\mathbf{R_f}$ (4:1 pentane:ethyl acetate): 0.58; **^{1}H NMR** (400.2 MHz, $CDCl_3$): δ_H 10.10 (s, 1H, C*H*O), 7.94 (dd, 1H, *J* = 8.5, 5.5 Hz, Ar*H*), 7.36-7.30 (m, 2H, Ar*H*), 2.61 (s, 3H, COCH_3); **^{13}C NMR** (100.05 MHz, $CDCl_3$): δ_C 200.0 (C=O), 190.5 (C=O), 165.2 (C, d, *J* = 258.1 Hz), 143.6 (C, d, *J* = 7.1 Hz), 133.0 (CH, d, *J* = 9.1 Hz), 132.1 (C, d, *J* = 3.1 Hz), 118.7 (CH, d, *J* = 21.9 Hz), 115.8 (CH, d, *J* = 23.4 Hz), 29.22 (CH_3); **^{19}F NMR** (376.5 MHz, $CDCl_3$): δ_F -102.86 (ddd, *J* = 8.2, 8.2, 5.5 Hz); $\mathbf{\nu_{max}}$ (neat): 3082, 2904, 1769, 1676, 1598, 1579, 1488, 1423, 1360, 1271, 1256, 1197, 968, 959, 914, 875, 842, 806, 731, 655, 574, 523, 475 cm^{-1}; **MS** (ESI+): *m/z* 189 $[M+Na]^+$; **HRMS** found 189.0326 $C_9H_7O_2FNa^+$ requires 189.0322 (|σ| = 2.1 ppm).

2-Acetyl-5-fluoro-benzaldehyde (1.160h)

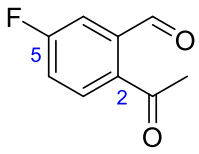

1.160h

Synthesized according to **General Procedure C** using lead (IV) acetate (3.34 g, 7.53 mmol), hydrazide **1.189e** (940 mg, 4.79 mmol) and THF (25 mL) to give the product as a yellow oil in 49% yield (390 mg, 2.35 mmol). NOTE: The product is unstable at RT and will darken in color if left. If stored at -20 °C, product should solidify to a low melting, pale yellow solid and be usable for up to 4 weeks. $\mathbf{R_f}$ (4:1 pentane:ethyl acetate): 0.40; **^{1}H NMR** (400.1 MHz, $CDCl_3$): δ_H 10.25 (s, 1H, C*H*O), 7.84 (dd, 1H, *J* = 8.6, 5.0 Hz, Ar*H*), 7.55 (dd, 1H, *J* = 8.6, 2.7 Hz, Ar*H*), 7.32 (ddd, 1H, *J* = 8.6, 7.4, 2.7 Hz, Ar*H*), 2.66 (s, 3H, COCH_3); **^{13}C NMR** (100.025 MHz, $CDCl_3$): δ_C 208.8 (C=O), 191.0 (C=O), 164.7 (C, d, *J* = 256.4 Hz), 140.0 (C, d, *J* = 6.9 Hz), 136.3 (C, d, *J* = 3.5 Hz), 131.8 (CH, d, *J* = 8.3 Hz), 119.5 (CH, d, *J* = 22.0 Hz), 116.3 (CH, d, *J* = 23.0 Hz), 28.5 (CH_3); **^{19}F NMR** (376.5 MHz, $CDCl_3$): δ_F -104.62 (dddd, *J* = 7.7, 7.7, 4.9, 2.4 Hz); $\boldsymbol{\nu_{max}}$ (neat): 3078, 2898, 1767, 1691, 1601, 1583, 1491, 1415, 1393, 1360, 1303, 1257, 1222, 1176, 1155, 1105, 1014, 977, 867, 832, 780, 597, 584, 536, 412 cm^{-1}; **MS** (ESI+): *m/z* 189 $[M+Na]^+$; **HRMS** found 189.0338 $C_9H_7O_2FNa^+$ requires 189.0322 (|σ| = 8.5 ppm).

2-Acetyl-5-chloro-benzaldehyde (1.160i)

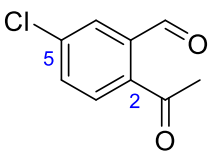

1.160i

Synthesized according to **General Procedure C** using lead (IV) acetate (3.11 g, 7.01 mmol), hydrazide **1.189f** (1.15 g, 5.41 mmol) and THF (25 mL) to give the product as a yellow oil in 65% yield (638 mg, 3.50 mmol). NOTE: The product is unstable at RT and will darken in color if left. If stored at -20 °C, product should solidify to a low melting, pale yellow solid and be usable for up to 4 weeks. $\mathbf{R_f}$ (4:1 pentane:ethyl acetate): 0.50; **^{1}H NMR** (500.1 MHz, $CDCl_3$): δ_H 10.21 (s, 1H, C*H*O), 7.83 (d, 1H, *J* = 2.2 Hz, Ar*H*), 7.73 (d, 1H, *J* = 8.3 Hz, Ar*H*), 7.61 (dd, 1H, *J* = 8.3, 2.2 Hz, Ar*H*), 2.65 (s, 3H, CH_3); **^{13}C NMR** (125.025 MHz, $CDCl_3$): δ_C 199.4 (C=O), 191.0 (C=O), 139.0 (C), 138.3 (C), 138.3 (C), 132.7 (CH), 130.4 (CH), 129.5 (CH), 28.6 (CH_3); $\boldsymbol{\nu_{max}}$ (neat): 3069, 2956, 2891, 1767, 1687, 1587, 1560, 1479, 1422, 1382, 1359, 1290, 1250, 1186, 1097, 1013, 963, 904, 887, 829, 761, 715, 656, 610, 594, 560, 503, 473, 433 cm^{-1}; **MS** (ESI+): *m/z* 185 $[M+Na]^+$; **HRMS** found 205.0026 $C_9H_7O_2ClNa^+$ requires 205.0027 (|σ| = 0.5 ppm). Data are in agreement with reported properties of **1.160i**.[96]

1.4.4 Synthesis of Pentafulvene Derivatives 1.162a-i

General Procedure D: Synthesis of Derivatives of Pentafulvene 1.162

The corresponding 2-acetyl-benzaldehyde (1 equiv.) derivative and cyclopentadiene (6.5 equiv.) – once freshly distilled, can be stored at -20 °C for up to 2 weeks – were dissolved in DMF at temperature T. Acetic acid (0.13 equiv.) was added followed by the dropwise addition of 1-(pyrrolidin-2-ylmethyl)pyrrolidine (0.38 equiv.). The reaction was stirred for 2-6 hours after which it was diluted into ethyl acetate (150 mL), washed with pH 7.4 phosphate buffer (3 × 50 mL) and the solvent removed *in vacuo*. The crude product was then purified *via* flash column chromatography (eluent: dichloromethane) to afford the product. The product can then be further purified *via* liquid-liquid diffusion (4:1 pentane:dichloromethane) or cold recrystallization from dimethoxyethane depending on the scale.

(*R*)-3-(Cyclopenta-2,4-dien-1-ylidene)-2,3-dihydro-1*H*-inden-1-ol (1.162a)

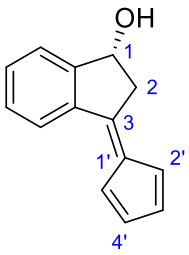

1.162a

Synthesized according to **General Procedure D** using 2-acetyl-benzaldehyde (200 mg, 78% purity, 1.05 mmol), cyclopentadiene (0.62 mL, 7.37 mmol), DMF (2.6 mL), acetic acid (7.7 µL, 0.134 mmol), *(2S)*-1-(pyrrolidin-2-ylmethyl)pyrrolidine (65 µL, 0.399 mmol) at 15 °C for 6 hours to afford the crude product as an orange solid in 78% yield (161 mg, 0.820 mmol) which was further purified to give the product as red needles (120 mg, 0.611 mmol, 75% recovery) and *er* >99:1. **M.p.**: 130-140 °C (darkens from this temperature); $\mathbf{R_f}$ (dichloromethane): 0.30; **^{1}H NMR** (400.2 MHz, $CDCl_3$): δ_H 7.96 (dd, *J* = 6.6, 1.9 Hz, 1H, Ar*H*), 7.58-7.55 (m, 1H, Ar*H*), 7.48-7.38 (m, 2H, Ar*H*), 6.92 (app ddd, *J* = 5.3, 1.7, 1.7 Hz, 1H, Cp*H*), 6.59-6.55 (m, 1H, Cp*H*), 6.53-6.49 (app t, *J* = 1.7 Hz, 2H, Cp*H*), 5.35 (ddd, *J* = 7.0, 7.0, 3.7 Hz, 1H, C*H*OH), 3.72 (dd, *J* = 17.5, 7.0 Hz, 1H, CH_aH_b), 3.09 (dd, *J* = 17.5, 7.0 Hz, 1H, CH$_a$*H*$_b$), 2.01 (d, *J* = 3.7 Hz, 1H, O*H*); **^{13}C NMR** (100.05 MHz, $CDCl_3$): δ_C 151.2 (C), 149.5 (C), 139.4 (C), 138.7 (C), 132.8 (CH), 131.1 (CH), 131.0 (CH), 129.4 (CH), 126.5 (CH), 125.4 (CH), 123.4 (CH), 120.0 (CH), 72.9 (CH), 44.0 (CH_2); $\boldsymbol{\nu_{max}}$ ($CHCl_3$): 3614, 3590, 3070, 3045, 3008, 2960, 2927, 2873, 1630, 1476, 1458, 1389, 1368, 1239, 1050, 1021, 997 cm^{-1}; **MS** (ESI+): *m/z* 197 $[M+H]^+$; **HRMS** found 197.0959 $C_{14}H_{13}O^+$ requires 197.0961 (|σ| = 1.0 ppm); **HPLC** (before crystallization): Chiralpak AD-H; mobile phase, hexane:2-propanol (4:1 v/v); flow rate, 0.5 mL.min^{-1}; retention times (*S*) enantiomer: 11.8 min (6.2%), (*R*) enantiomer: 14.2 min (93.8%), *er* 94:6; $\mathbf{[\alpha]_D^{23}}$: +68.0 (*er* >99:1, *c* = 0.50 in $CHCl_3$); **Anal**: Calcd. for $C_{14}H_{12}O$ C, 85.68%; H, 6.16%; found C, 85.20%; H, 6.47%.

(*S*)-3-(Cyclopenta-2,4-dien-1-ylidene)-2,3-dihydro-1*H*-inden-1-ol ((*S*)-1.162a)

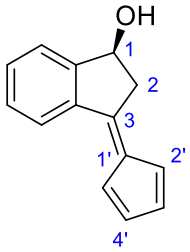

(*S*)-1.162a

Synthesized according to **General Procedure D** using 2-acetyl-benzaldehyde (300 mg, 78% purity, 1.58 mmol), cyclopentadiene (0.96 mL, 11.4 mmol), DMF (3.9 mL), acetic acid (11.6 µL, 0.202 mmol) and *(2R)*-1-(pyrrolidin-2-ylmethyl)pyrrolidine (98 µL, 0.602 mmol) at 15 °C for 6 hours to afford the crude product in 65% yield (202 mg, 1.03 mmol) which was further purified to the product as red needles (116 mg, 0.591 mmol, 57% recovery) and 98:2 *er*. **[α]$_D^{20}$**: -48.0 (98:2 *er*, *c* = 1.00 in $CHCl_3$). All other data are in agreement with its opposite enantiomer.

(*R*)-3-(Cyclopenta-2,4-dien-1-ylidene)-5-phenyl-2,3-dihydro-1*H*-inden-1-ol (1.162b)

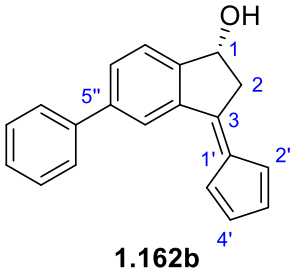

1.162b

Synthesized according to **General Procedure D** using 2-acetyl-4-phenyl-acetyl-benzaldehyde (312 mg, 78% purity, 1.09 mmol), cyclopentadiene (0.62 mL, 7.37 mmol), DMF (2.6 mL), acetic acid (7.7 µL, 0.134 mmol) and *(2S)*-1-(pyrrolidin-2-ylmethyl)pyrrolidine (65 µL, 0.399 mmol) at 15 °C for 4.5 hours to afford the crude product as an orange solid in 53% yield (157 mg, 0.576 mmol) which was further purified to give the product as orange needles (90.3 mg, 0.332 mmol, 58% recovery) and *er* >99:1. **M.p.**: 140-150 °C (darkening observed from this temperature); **R$_f$** (dichloromethane): 0.18; **^{1}H NMR** (300.1 MHz, $CDCl_3$): δ_H 8.12 (d, *J* = 1.6 Hz, 1H, Ar*H*), 7.71-7.57 (m, 4H, Ar*H*), 7.52-7.45 (m, 2H, Ar*H*), 7.41 (tt, 1H, *J* = 4.5, 1.3 Hz, Ar*H*), 6.98 (ddd, *J* = 5.3, 1.7, 1.7 Hz, 1H, Cp*H*), 6.60-6.57 (m, 1H, Cp*H*), 6.54-6.52 (m, 2H, Cp*H*), 5.39 (dd, *J* = 6.9, 3.8 Hz, 1H, C*H*OH), 3.74 (dd, *J* = 17.5, 6.9 Hz, 1H, CH_aH_b), 3.12 (dd, *J* = 17.5, 3.8 Hz, 1H, CH$_a$*H*$_b$), 2.03 (br s, 1H, O*H*); **^{13}C NMR** (75.03 MHz, $CDCl_3$): δ_C 150.2 (C), 149.2 (C), 142.8 (C), 140.8 (C), 140.0 (C), 138.9 (C), 132.9 (CH), 131.1 (CH), 130.4 (CH), 129.1 (CH), 127.9 (CH), 127.4 (CH), 125.6 (CH), 125.0 (CH), 123.4 (CH), 120.0 (CH), 72.7 (CH), 44.2 (CH_2); **ν_{max}** ($CHCl_3$): 3590, 3109, 3066, 3008, 2925, 1702, 1631, 1603, 1477, 1464, 1389, 1368, 1055, 1021, 1001, 910, 861, 840, 803, 790, 779 cm^{-1}; **MS** (FDMS+): *m/z* 193 [M-OC_5H_3]$^+$; **HPLC** (before crystallization): Chiralpak AD-H; mobile phase, hexane:2-propanol (4:1 v/v); flow rate, 0.5 mL.min^{-1}; retention times (*R*) enantiomer: 14.7 min (87.5%), (*S*) enantiomer : 25.9 min (12.5%), *er* 88:12; **[α]$_D^{23}$**: -12.8 (*er* >99:1, *c* = 0.47 in $CHCl_3$).

(*R*)-3-(Cyclopenta-2,4-dien-1-ylidene)-5-(1,1-dimethylethyl)-2,3-dihydro-1*H*-inden-1-ol (1.162c)

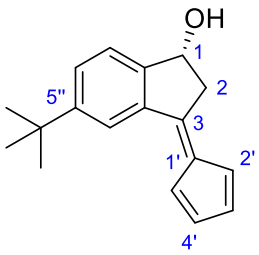

1.162c

Synthesized according to **General Procedure D** using 2-acetyl-4-(1,1-dimethylethyl)-benzaldehyde (450 mg, 78% purity, 1.72 mmol), cyclopentadiene (440 µL, 5.23 mmol), DMF (3.4 mL), acetic acid (10.0 µL, 0.175 mmol) and *(2S)*-1-(pyrrolidin-2-ylmethyl)pyrrolidine (85 µL, 0.527 mmol) at 22 °C for 2.5 hours to afford the product as an orange oil in 91% yield (396 mg, 1.57 mmol) and *er* 4.6:1. $\mathbf{R_f}$ (2:1 pentane:ethyl acetate): 0.59; **^{1}H NMR** (300.1 MHz, $CDCl_3$): 7.99 (s, 1H, Ar*H*), 7.56-7.46 (m, 2H, Ar*H*), 6.93 (ddd, *J* = 5.4, 1.7, 1.7 Hz, 1H, Cp*H*), 6.61-6.57 (m, 1H, Cp*H*), 6.54-6.49 (m, 2H, Cp*H*), 5.31 (ddd, *J* = 7.8, 7.8, 4.5 Hz, 1H, C*H*OH), 3.72 (dd, *J* = 17.5, 6.7 Hz, CH_aH_b), 3.09 (dd, *J* = 17.5, 3.7 Hz, 1H, CH_aH_b), 2.10 (d, 1H, *J* = 7.8 Hz, O*H*), 1.38 (s, 9H, $C(CH_3)_3$). **^{13}C NMR** (75.025 MHz, $CDCl_3$): δ_C 152.8 (C), 150.2 (C), 148.7 (C), 139.4 (C), 138.3 (C), 132.6 (CH), 130.7 (CH), 128.9 (CH), 124.9 (CH), 123.5 (CH), 123.1 (CH), 119.9 (CH), 72.7 (CH), 44.4 (CH_2), 35.1 (C), 31.5 (CH_3); $\boldsymbol{\nu_{max}}$ ($CHCl_3$): 3332, 2963, 2905, 2869, 1629, 1603, 1486, 1462, 1367, 1058, 1003, 909, 873, 760, 733, 622 cm^{-1}; **MS** (ESI-): *m/z* 233 $[M-H_3O]^-$; **HPLC**: Chiralpak AD-H; mobile phase, hexane:2-propanol (95:5 v/v); flow rate, $mL.min^{-1}$; retention times (*S*) enantiomer: 24.8 min (17.7%), (*R*) enantiomer: 27.7min (82.3%), *er* 82:18.

(*R*)-3-(Cyclopenta-2,4-dien-1-ylidene)-5-methoxy-2,3-dihydro-1*H*-inden-1-ol (1.162d)

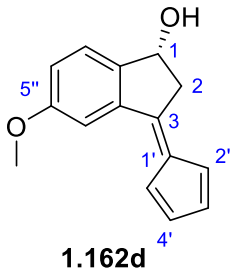

1.162d

Synthesized according to **General Procedure D** using 2-acetyl-4-methoxy-benzaldehyde (250 mg, 78% purity, 1.09 mmol), cyclopentadiene (0.64 mL, 7.61 mmol), DMF (2.7 mL), acetic acid (8.0 µL, 0.139 mmol) and *(2S)*-1-(pyrrolidin-2-ylmethyl)pyrrolidine (68 µL, 0.417 mmol) at 15 °C for 5 hours to afford the crude product as an orange solid in 54% yield (134 mg, 0.592 mmol) which was further purified to give the product as red needles (76.0 mg, 0.336 mmol, 57% recovery) and *er* >99:1. **M.p.** 180-190 °C (darkening observed from this temperature); $\mathbf{R_f}$ (dichloromethane): 0.41; **^{1}H NMR** (300.1 MHz, $CDCl_3$): δ_H 7.46 (d, 1H, *J* = 8.4 Hz, Ar*H*), 7.42 (d, 1H, *J* = 2.4 Hz, Ar*H*), 7.03 (dd, 1H, *J* = 8.4, 2.4 Hz, Ar*H*), 6.91 (ddd, 1H, *J* = 5.3, 1.7, 1.7 Hz, Cp*H*), 6.59-6.55 (m, 1H, Cp*H*), 6.53-6.48 (m, 2H, Cp*H*), 5.29 (ddd, 1H, *J* = 7.1, 6.9, 3.4 Hz, C*H*OH), 3.89 (s, 3H, OCH_3), 3.71 (dd, 1H, *J* = 17.6, 6.9 Hz, CH_aH_b), 3.09 (dd, 1H, *J* = 17.6, 3.4 Hz, CH_aH_b), 2.11 (d, 1H, *J* = 7.8 Hz, O*H*); **^{13}C NMR** (75.025 MHz, $CDCl_3$): δ_C 161.2 (C), 150.0 (C), 144.5 (C), 141.2 (C), 139.1 (C), 133.2 (CH), 131.4 (CH), 126.6 (CH), 123.9 (CH), 120.1 (CH), 119.0 (CH), 110.5 (CH), 72.8 (CH), 56.2 (CH_3), 44.9 (CH_2); $\boldsymbol{\nu_{max}}$ (neat): 3317, 2956, 2922, 2853, 2834,

1624, 1601, 1487, 1463, 1366, 1288, 1234, 1099, 1029, 759, 613 cm^{-1}; **MS** (ESI+): *m/z* 227 $[M+H]^+$; **HRMS** found 227.1069 $C_{15}H_{15}O_2^+$ requires 227.1067 (|σ| = 0.9 ppm); **HPLC** (before crystallization): Chiralpak AD-H; mobile phase, hexane:2-propanol (4:1 v/v); flow rate, mL.min^{-1}; retention times (*S*) enantiomer: 16.5 min (9.1%), (*R*) enantiomer: 17.7 min (90.9%), *er* 91:9; $[\alpha]_D^{23}$: +9.9 (*er* >99:1, *c* = 0.81 in $CHCl_3$); **Anal**: Calcd. for $C_{15}H_{14}O_2$ C, 79.62%; H, 6.24%; found C, 79.24%; H, 6.20%.

(*R*)-3-(Cyclopenta-2,4-dien-1-ylidene)-5-methyl-2,3-dihydro-1*H*-inden-1-ol (1.162e)

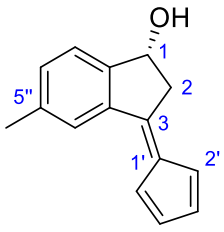

1.162e

Synthesized according to **General Procedure D** using 2-acetyl-4-methyl-benzaldehyde (120 mg, 78% purity, 0.577 mmol), cyclopentadiene (0.34 mL, 4.05 mmol), DMF (1.5 mL), acetic acid (4.2 µL, 0.0736 mmol) and *(2S)*-1-(pyrrolidin-2-ylmethyl)pyrrolidine (36 µL, 0.232 mmol) at 15 °C for 6 hours to afford the product as an orange solid in 72% yield (87.6 mg, 0.417 mmol) and 91:9 *er*. **M.p.** 160-170 °C (darkening observed from this temperature); $\mathbf{R_f}$ (dichloromethane): 0.29; **^{1}H NMR** (400.2 MHz, $CDCl_3$): δ_H 7.77 (d, 1H, *J* = 1.4 Hz, Ar*H*), 7.44 (d, 1H, *J* = 7.8 Hz, Ar*H*), 7.28-7.26 (m, 1H, Ar*H*), 6.94 (ddd, 1H, *J* = 5.3, 1.7, 1.7 Hz, Cp*H*), 6.59-6.55 (m, 1H, Cp*H*), 6.52-6.48 (m, 2H, Cp*H*), 5.31 (ddd, 1H, *J* = 7.3, 6.9, 3.7 Hz, C*H*OH), 3.71 (dd, 1H, *J* = 17.5, 6.9 Hz, C$H_a$$H_b$), 3.08 (dd, 1H, *J* = 17.5, 3.7 Hz, CH$_a$$H_b$), 2.43 (s, 3H, CH_3), 1.92 (d, 1H, *J* = 7.3 Hz, O*H*); **^{13}C NMR** (100.05 MHz, $CDCl_3$): δ_C 150.7 (C), 148.7 (C), 139.6 (C), 139.4 (C), 138.5 (C), 132.6 (CH), 132.3 (CH), 130.9 (CH), 126.8 (CH), 125.1 (CH), 123.4 (CH), 120.0 (CH), 72.7 (CH), 44.3 (CH_2), 21.7 (CH_3); $\boldsymbol{\nu_{max}}$ (neat): 3178, 3122, 3062, 2979, 2917, 2855, 1625, 1602, 1488, 1460, 1367, 1326, 1290, 1064, 1008, 761 cm^{-1}; **MS** (ESI-): *m/z* 191 $[M-H_3O]^-$; **HRMS** found 191.0870 $C_{15}H_{11}^-$ requires 191.0866 (|σ| = 2.1 ppm); **HPLC**: Chiralpak AD-H; mobile phase, hexane:2-propanol (4:1 v/v); flow rate, 0.5 mL.min^{-1}; retention times (*S*) enantiomer: 11.4 min (9.0%), (*R*) enantiomer: 13.8 min (91.0%), *er* 91:9; $[\alpha]_D^{20}$: +16.0 (*er* 91:9, *c* = 0.50 in $CHCl_3$).

(*R*)-3-(Cyclopenta-2,4-dien-1-ylidene)-6-methyl-2,3-dihydro-1*H*-inden-1-ol (1.162f)

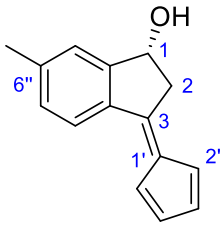

1.162f

Synthesized according to **General Procedure D** using 2-acetyl-5-methyl-benzaldehyde (120 mg, 78% purity, 0.577 mmol), cyclopentadiene (0.21 mL, 2.50 mmol), DMF (0.9 mL), acetic acid (2.6 µL, 0.0454 mmol) and *(2S)*-1-(pyrrolidin-2-ylmethyl)pyrrolidine (21.8 µL, 0.134 mmol) at 15 °C for 6 hours to afford the product as an orange solid in 67% yield (81.0 mg, 0.385 mmol) and 89:11 *er*. **M.p.** 85-95 °C (darkening observed from this temperature); $\mathbf{R_f}$ (dichloromethane): 0.35; **^{1}H NMR** (400.1 MHz, $CDCl_3$): δ_H 7.85 (d, 1H, *J* = 8.1

Hz, Ar*H*), 7.35 (br s, 1H, Ar*H*), 7.21 (br d, 1H, *J* = 8.0 Hz, ArH), 6.91 (ddd, 1H, *J* = 5.3, 1.8, 1.8 Hz, Cp*H*), 6.57-6.54 (m, 1H, Cp*H*), 6.51-6.48 (m, 2H, Cp*H*), 5.28 (br s, 1H, C*H*OH), 3.69 (dd, 1H, *J* = 17.6, 6.8 Hz, CH_aH_b), 3.06 (dd, 1H, *J* = 17.6, 3.8 Hz, CH$_a$$H_b$), 2.43 (s, 3H, CH_3), 2.12 (br s, 1H, O*H*); **^{13}C NMR** (100.025 MHz, $CDCl_3$): δ_C 149.8 (C), 141.9 (C), 137.8 (C), 136.8 (C), 132.2 (CH), 131.6 (C), 130.6 (CH), 130.5 (CH), 126.3 (CH), 125.8 (CH), 123.3 (CH), 119.9 (CH), 72.8 (CH), 44.1 (CH_2), 21.9 (CH_3); **ν_{max}** (neat): 3322, 3062, 2917, 2858, 1628, 1603, 1485, 1457, 1367, 1325, 1116, 1058, 1012, 999, 821, 758, 631 cm^{-1}; **MS** (ESI+): *m/z* 211 $[M+H]^+$; **HRMS** found 211.1114 $C_{15}H_{15}O^+$ requires 211.1117 (|σ| = 1.4 ppm); **HPLC**: Chiralpak AD-H; mobile phase, hexane:2-propanol (4:1 v/v); flow rate, 0.5 mL.min^{-1}; retention times (*S*) enantiomer: 11.9 min (11.1%), (*R*) enantiomer: 14.9 min (88.9%), *er* 89:11; **$[\alpha]_D^{20}$**: +32.0 (*er* 89:11, *c* = 1.00 in $CHCl_3$).

(*R*)-3-(Cyclopenta-2,4-dien-1-ylidene)-5-fluoro-2,3-dihydro-1*H*-inden-1-ol (1.162g)

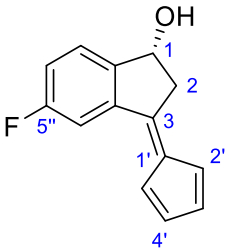

1.162g

Synthesized according to **General Procedure D** using 2-acetyl-4-fluoro-benzaldehyde (442 mg, 78% purity, 2.07 mmol), cyclopentadiene (1.1 mL, 13.1 mmol), DMF (4.8 mL), acetic acid (15.1 µL, 0.264 mmol) and *(2S)*-1-(pyrrolidin-2-ylmethyl)pyrrolidine (129 µL, 0.791 mmol) at 25 °C for 4.5 hours to afford the crude product as an orange solid in 39% yield (171 mg, 0.798 mmol) which was further purified to give the product as red needles (106 mg, 0.495 mmol, 62% recovery) and *er* >99:1. **M.p.** 190-200 °C (darkening observed from this temperature); **R_f** (dichloromethane): 0.25; **^{1}H NMR** (400.2 MHz, $CDCl_3$): δ_H 7.58 (dd, 1H, *J* = 9.4, 2.4 Hz, Ar*H*), 7.51 (dd, 1H, *J* = 8.5, 5.2 Hz, Ar*H*), 7.14 (ddd, 1H, *J* = 8.5, 8.5, 2.4 Hz Ar*H*), 6.83 (ddd, 1H, *J* = 5.4, 2.1, 1.3 Hz, Cp*H*), 6.60-6.55 (m, 1H, Cp*H*), 6.54-6.46 (m, 2H, Cp*H*), 5.31 (ddd, 1H, *J* = 7.5, 7.1, 3.7 Hz, C*H*OH), 3.73 (dd, 1H, *J* = 17.6, 7.1 Hz, CH_aH_b), 3.11 (dd, 1H, *J* = 17.6, 3.7 Hz, CH$_a$$H_b$), 1.97 (d, 1H, *J* = 7.5 Hz, O*H*); **^{13}C NMR** (100.05 MHz, $CDCl_3$): δ_C 163.3 (C, d, *J* = 246.6 Hz), 147.8 (C, d, *J* = 3.4 Hz), 146.8 (C, d, *J* = 2.7 Hz), 141.3 (C, d, *J* = 8.8 Hz), 139.6 (C), 133.5 (CH), 131.7 (CH), 126.8 (CH, d, *J* = 9.0 Hz), 123.4 (CH), 119.8 (CH), 118.5 (CH, d, *J* = 23.5 Hz), 112.6 (CH, d, *J* = 23.5 Hz), 72.3 (CH), 44.4 (CH_2); **^{19}F NMR** (376.5 MHz, $CDCl_3$): δ_F -112.35 (ddd, *J* = 9.0, 9.0, 5.2 Hz); **ν_{max}** (neat): 3186, 3118, 3096, 2969, 2927, 1625, 1604, 1585, 1484, 1474, 1461, 1365, 1280, 1230, 1093, 1065, 1002, 879, 869, 799, 765, 646, 609 cm^{-1}; **MS** (ESI+): *m/z* 215 $[M+H]^+$; **HRMS** found 215.0865 $C_{14}H_{12}OF^+$ requires 215.0865 (|σ| < 0.1 ppm); **HPLC** (before crystallization): Chiralpak AD-H; mobile phase, hexane:2-propanol (4:1 v/v); flow rate, mL.min^{-1}; retention times (*S*) enantiomer: 11.2 min (7.9%), (*R*) enantiomer: 12.6 min (92.1%), *er* 92:8; **$[\alpha]_D^{20}$**: +48.0 (*er* >99:1, *c* = 1.00 in $CHCl_3$); **Anal**: Calcd. for $C_{14}H_{11}OF$ C, 78.49%; H, 5.18%; found C, 78.64%; H, 4.91%.

(*R*)-3-(Cyclopenta-2,4-dien-1-ylidene)-6-fluoro-2,3-dihydro-1*H*-inden-1-ol (1.162h)

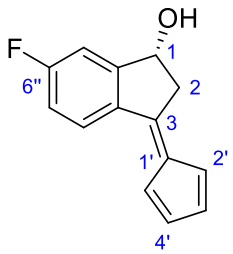

1.162h

Synthesized according to **General Procedure D** using 2-acetyl-5-fluoro-benzaldehyde (248 mg, 78% purity, 1.16 mmol), cyclopentadiene (0.62 mL, 7.37 mmol), DMF (2.7 mL), acetic acid (8.5 µL, 0.135 mmol) and *(2S)*-1-(pyrrolidin-2-ylmethyl)pyrrolidine (72.5 µL, 0.445 mmol) at 25 °C for 3 hours to afford the crude product as an orange solid in 52% yield (130 mg, 0.607 mmol) which was further purified to give the product as red needles(56 mg, 0.261 mmol, 43% recovery) and *er* >99:1. **M.p.** 120-130 °C (darkening observed from this temperature); $\mathbf{R_f}$ (dichloromethane): 0.35; **^{1}H NMR** (400.1 MHz, $CDCl_3$): δ_H 7.91 (dd, 1H, *J* = 8.7, 5.0 Hz, Ar*H*), 7.22 (dd, 1H, *J* = 8.1, 2.7 Hz, Ar*H*), 7.11 (ddd, 1H, *J* = 8.7, 8.7, 2.6 Hz Ar*H*), 6.83 (ddd, 1H, *J* = 5.3, 2.1, 1.4 Hz, Cp*H*), 6.59-6.55 (m, 1H, Cp*H*), 6.51-6.46 (m, 2H, Cp*H*), 5.30 (ddd, 1H, *J* = 7.3, 7.1, 4.1 Hz, C*H*OH), 3.73 (dd, 1H, *J* = 17.5, 7.1 Hz, CH_aH$_b$), 3.08 (dd, 1H, *J* = 17.5, 4.1 Hz, CH$_a$$H_b$), 2.14 (d, 1H, *J* = 7.8 Hz, O*H*); **^{13}C NMR** (100.025 MHz, $CDCl_3$): δ_C 164.7 (C, d, *J* = 253.1 Hz), 153.7 (C, d, *J* = 8.0 Hz), 147.9 (C), 138.1 (C), 135.5 (C), 133.0 (CH), 131.0 (CH), 128.1 (CH, d, *J* = 9.0 Hz), 123.3 (CH), 119.7 (CH), 117.3 (CH, d, *J* = 23.1 Hz), 112.3 (CH, d, *J* = 22.1 Hz), 72.7 (CH, d, *J* = 2.3 Hz), 44.3 (CH_2); **^{19}F NMR** (376.5 MHz, $CDCl_3$): δ_F -108.07 (ddd, *J* = 8.5, 8.5, 5.0 Hz); $\boldsymbol{\nu_{max}}$ (neat): 3201, 3104, 3080, 2966, 2928, 1627, 1601, 1480, 1433, 1365, 1325, 1290, 1264, 1246, 1196, 1165, 1142, 1103, 1061, 1010, 997, 883, 873, 825, 759, 634, 517, 480 cm^{-1}; **MS** (GCEIMS+): *m/z* 214 $[M]^+$; **HRMS** found 214.0796 $C_{14}H_{11}OF^+$ requires 214.0788 (|σ| = 3.7 ppm); **HPLC** (before crystallization): Chiralpak AD-H; mobile phase, hexane:2-propanol (4:1 v/v); flow rate, 0.5 mL.min^{-1}; retention times (*S*) enantiomer: 10.9 min (12.0%), (*R*) enantiomer: 13.5 min (88.0%), *er* 88:12; $\mathbf{[\alpha]_D^{20}}$: +72.0 (*er* >99:1, *c* = 1.00 in $CHCl_3$); **Anal**: Calcd. for $C_{14}H_{11}OF$ C, 78.49%; H, 5.18%; found C, 78.11%; H, 4.81%.

(*S*)-3-(Cyclopenta-2,4-dien-1-ylidene)-6-fluoro-2,3-dihydro-1*H*-inden-1-ol ((*S*)-1.162h)

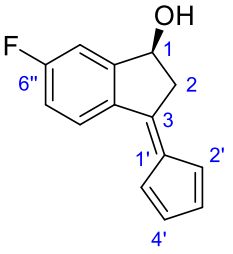

(*S*)-1.162h

Synthesized according to **General Procedure D** using 2-acetyl-5-fluoro-benzaldehyde (210 mg, 78% purity, 0.990 mmol), cyclopentadiene (0.53 mL, 6.30 mmol), DMF (2.4 mL), acetic acid (7.0 µL, 0.122 mmol) and *(2R)*-1-(pyrrolidin-2-ylmethyl)pyrrolidine (98 µL, 0.374 mmol) at 25 °C for 3 hours to afford the crude product in 39% yield (82.2 mg, 0.384 mmol) which was further purified to the product as red needles (37.0 mg, 0.173 mmol, 45% recovery) and *er* >99:1 $\mathbf{[\alpha]_D^{20}}$: -76.0 (*er* >99:1 *c* = 1.00 in $CHCl_3$). All other data are in agreement with its opposite enantiomer.

(*R*)-6-Chloro-3-(cyclopenta-2,4-dien-1-ylidene)-2,3-dihydro-1*H*-inden-1-ol (1.162i)

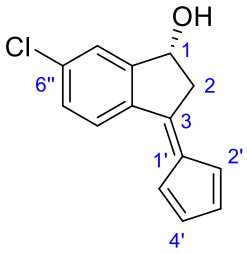

1.162i

Synthesized according to **General Procedure D** using 2-acetyl-5-chloro-benzaldehyde (484 mg, 78% purity, 2.07 mmol), cyclopentadiene (1.1 mL, 13.1 mmol), DMF (4.8 mL), acetic acid (15.1 µL, 0.264 mmol) and *(2S)*-1-(pyrrolidin-2-ylmethyl)pyrrolidine (129 µL, 0.791 mmol) at 25 °C for 3 hours to afford the crude product as an orange solid in 38% yield (181 mg, 0.785 mmol) which was then further purified to give the product as red needles (93.3 mg, 0.404 mmol, 52% recovery) and *er* 99:1. **M.p.** 135-145 °C (darkening observed from this temperature); **R_f** (dichloromethane): 0.53; **^{1}H NMR** (400.1 MHz, $CDCl_3$): δ_H 7.85 (d, 1H, *J* = 8.5 Hz, Ar*H*), 7.53 (m, 1H, Ar*H*), 7.37 (ddd, 1H, *J* = 8.5, 2.0, 0.7 ArH), 6.83 (ddd, 1H, *J* = 5.4, 2.1, 1.3 Hz, Cp*H*), 6.57 (dddd, 1H, *J* = 5.4, 2.2, 1.5, 0.7 Hz, Cp*H*), 6.59-6.45 (m, 2H, Cp*H*), 5.31 (br s, 1H, C*H*OH), 3.72 (dd, 1H, *J* = 17.5, 6.7 Hz, C$H_a$$H_b$), 3.09 (dd, 1H, *J* = 17.5, 3.9 Hz, CH$_a$$H_b$), 2.10 (br s, 1H, O*H*); **^{13}C NMR** (100.025 MHz, $CDCl_3$): δ_C 152.7 (C), 147.7 (C), 139.0 (C), 137.9 (C), 137.1 (C), 133.2 (CH), 131.4 (CH), 129.9 (CH), 127.4 (CH), 125.7 (CH), 123.4 (CH), 119.7 (CH), 77.6 (CH), 44.1 (CH_2); **ν_{max}** (neat): 3271, 3067, 2985, 2964, 2897, 1627, 1590, 1474, 1417, 1366, 1321, 1301, 1269, 1216, 1187, 1076, 1054, 997, 901, 881, 856, 824, 806, 757, 720, 614 cm^{-1}; **MS** (GCEIMS+): *m/z* 230 $[M]^+$; **HRMS** found 230.0493 $C_{14}H_{11}OCl^+$ requires 230.0493 ($|\sigma|$ < 0.1 ppm); **HPLC**: Chiralpak AD-H; mobile phase, hexane:2-propanol (4:1 v/v); flow rate, 0.5 mL.min^{-1}; retention times (*S*) enantiomer: 11.1 min (8.9%), (*R*) enantiomer: 14.5 min (91.1%), *er* 91:11; **$[\alpha]_D^{20}$**: +52.0 (*er* 99:1, *c* = 1.00 in $CHCl_3$); **Anal**: Calcd. for $C_{14}H_{11}OCl$ C, 72.89%; H, 4.81%; found C, 72.52%; H, 4.60%.

(*S*)-6-Chloro-3-(cyclopenta-2,4-dien-1-ylidene)-2,3-dihydro-1*H*-inden-1-ol ((*S*)-1.162i)

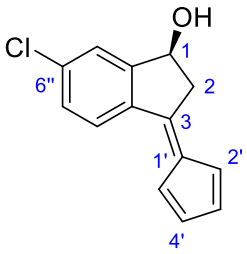

(*S*)-1.162i

Synthesized according to **General Procedure D** using 2-acetyl-5-chloro-benzaldehyde (183 mg, 78% purity, 0.782 mmol), cyclopentadiene (0.42 mL, 4.99 mmol), DMF (1.9 mL), acetic acid (5.5 µL, 0.0874 mmol) and *(2R)*-1-(pyrrolidin-2-ylmethyl)pyrrolidine (48 µL, 0.294 mmol) at 25 °C for 2.5 hours to afford the crude product in 30% yield (54.7 mg, 0.237 mmol) which was further purified to the product as red needles (26.7 mg, 0.116 mmol, 49% recovery) and *er* 99:1; **$[\alpha]_D^{20}$**: -52.0 (*er* 99:1, *c* = 1.00 in $CHCl_3$). All other data are in agreement with its opposite enantiomer.

1.4.5 Functionalization of Pentafulvene 1.162 Derivatives

General Procedure E: Methyl Ether Protection of 1.162 Derivatives

Chloromethyl methyl ether derivative (1.0-2.2 equiv.) – **CARE! Highly carcinogenic and toxic, take appropriate precautions throughout the course of the reaction** - was added to a solution of fulvene (1.0 equiv.) and *N,N*-diisopropylethylamine (2.0 equiv.) in dichloromethane and the resulting red solution was stirred at RT for 20 hours. Once complete, the reaction was quenched *via* the addition of water and extracted with dichloromethane. Removal of solvents *in vacuo* gave the crude product which was purified *via* flash column chromatography (eluent: dichloromethane) affording the product.

(*R*)-1-(Cyclopenta-2,4-diene-1-ylidene)-3-(methoxymethoxy)-2,3-dihydro-1*H*-indene (1.223a)

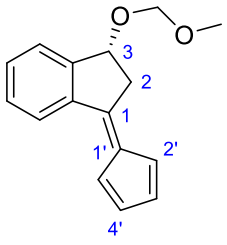

1.223a

Synthesized according to **General Procedure E** using chloromethyl methyl ether (150 µL, 1.97 mmol), fulvene **1.162a** (160 mg, 0.815 mmol), *N,N*-diisopropylethylamine (300 µL, 1.72 mmol) and dichloromethane (11.0 mL) to afford the product as a red oil in 85% yield (167 mg, 0.695 mmol). **R_f** (dichloromethane): 0.74; **^{1}H NMR** (400.2 MHz, $CDCl_3$): δ_H 7.99-7.95 (m, 1H, Ar*H*), 7.56-7.51 (m, 1H, Ar*H*), 7.46-7.37 (m, 2H, Ar*H*), 6.93 (ddd, 1H, *J* = 5.3, 2.1, 1.4 Hz, Cp*H*), 6.58-6.55 (m, 1H, Cp*H*), 6.54-6.49 (m, 2H, Cp*H*), 5.24 (dd, 1H, *J* = 6.7, 3.8 Hz, C*H*O), 4.87 (s, 2H, OCH_2O), 3.68 (dd, 1H, *J* = 17.3, 6.7 Hz, CH_aH$_b$ *anti* to OR), 3.49 (s, 3H, OCH_3), 3.20 (dd, 1H, *J* = 17.3, 3.8 Hz, CH$_a$$H_b$ *syn* to OR); **^{13}C NMR** (100.05 MHz, $CDCl_3$): δ_C 149.8 (C), 149.3 (C), 139.7 (C), 138.6 (C), 132.6 (CH), 130.8 (CH), 130.8 (CH), 129.4 (CH), 126.4 (CH), 125.8 (CH), 123.3 (CH), 120.0 (CH), 96.3 (CH_2), 77.8 (CH), 55.8 (CH_3), 41.6 (CH_2); **ν_{max}** (neat): 3268, 3065, 2959, 2933, 2875, 2821, 1628, 1597, 1427, 1367, 1151, 1028, 919, 760, 671, 574, 540 cm^{-1}; **HRMS** found 241.1228 $C_{16}H_{17}O_2^+$ requires 241.1223 (|σ| = 2.1 ppm); **$[\alpha]_D^{23}$**: +40.0 (*er* > 99:1, *c* = 1.00 in $CHCl_3$).

(*S*)-1-(Cyclopenta-2,4-diene-1-ylidene)-3-(methoxymethoxy)-2,3-dihydro-1*H*-indene ((*S*)-1.223a)

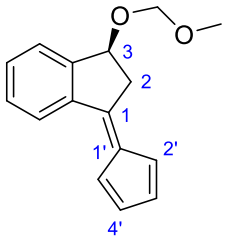

(*S*)-1.223a

Synthesized according to **General Procedure E** using chloromethyl methyl ether (100 µL, 1.32 mmol), fulvene **(*S*)-1.162a** (116 mg, 0.591 mmol), *N,N*-diisopropylethylamine (220 µL, 1.29 mmol) and dichloromethane (8 mL) to afford the product as a red oil in 72% yield (102 mg, 0.424 mmol). $[\alpha]_D^{20}$: -32.0 (98:2 *er*, *c* = 1.00 in $CHCl_3$). All other data are in agreement with its opposite enantiomer.

(*R*)-3-(Cyclopenta-2,4-diene-1-ylidene)-1-(methoxymethoxy)-5-phenyl-2,3-dihydro-1*H*-indene (1.223b)

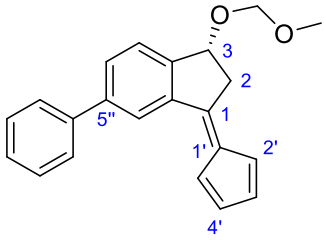

1.223b

Synthesized according to **General Procedure E** using chloromethyl methyl ether (80 µL, 1.05 mmol), fulvene **1.162b** (126 mg, 0.462 mmol), *N,N*-diisopropylethylamine (170 µL, 0.976 mmol) and dichloromethane (4 mL) to afford the product as a red oil in 73% yield (106 mg, 0.335 mmol). $\mathbf{R_f}$ (dichloromethane): 0.56; **^{1}H NMR** (400.1 MHz, $CDCl_3$): δ_H 8.17 (d, 1H, *J* = 1.5 Hz, Ar*H*), 7.70-7.60 (m, 4H, Ar*H*), 7.53-7.48 (m, 2H, Ar*H*), 7.43 (dd, 1H, *J* = 6.4, 1.2 Hz, Ar*H*), 7.01 (ddd, 1H, *J* = 5.4, 1.6, 1.6 Hz, Cp*H*), 6.62-6.58 (m, 1H, Cp*H*), 6.58-6.52 (m, 2H, Cp*H*), 5.30 (dd, 1H, *J* = 6.6, 3.7 Hz, C*H*O), 4.92 (s, 2H, OCH_2O), 3.75 (dd, 1H, *J* = 17.3, 6.6 Hz, CH_aCH$_b$ *anti* to OR), 3.53 (s, 3H, OCH_3), 3.28 (dd, 1H, *J* = 17.3, 3.7 Hz, CH$_a$CH_b *syn* to OR); **^{13}C NMR** (100.025 MHz, $CDCl_3$): δ_C 149.5 (C), 148.2 (C), 142.8 (C), 140.8 (C), 140.3 (C), 138.7 (C), 132.7 (CH), 130.9 (CH), 130.1 (CH), 129.0 (CH), 127.7 (CH), 127.4 (CH), 126.1 (CH), 125.0 (CH), 123.3 (CH), 120.0 (CH), 96.3 (CH_2), 77.5 (CH), 55.8 (CH_3), 41.9 (CH_2); $\boldsymbol{\nu_{max}}$ (neat): 3062, 3032, 2928, 2884, 2845, 2821, 1627, 1602, 1476, 1462, 1451, 1366, 1146, 1036, 912, 759, 730, 697 cm^{-1}; **HRMS** found 317.1534 $C_{22}H_{21}O_2^+$ requires 317.1536 (|σ| = 0.6 ppm); $[\alpha]_D^{20}$: -20.0 (*er* >99:1, *c* = 1.00 in $CHCl_3$).

(*R*)-3-(Cyclopenta-2,4-diene-1-ylidene)-1-(methoxymethoxy)-5-methoxy-2,3-dihydro-1*H*-indene (1.223c)

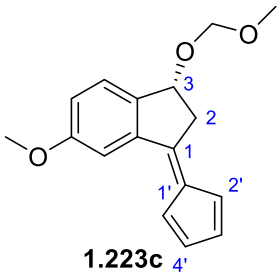

1.223c

Synthesized according to **General Procedure E** using chloromethyl methyl ether (40 µL, 0.527 mmol), fulvene **1.162d** (44 mg, 0.194 mmol), *N,N*-diisopropylethylamine (70 µL, 0.402 mmol) and dichloromethane (1.6 mL) to afford the product as a red oil in 97% yield (51 mg, 0.189 mmol). $\mathbf{R_f}$ (dichloromethane): 0.65; **^{1}H NMR** (400.1 MHz, $CDCl_3$): δ_H 7.46-7.40 (m, 2H, Ar*H*), 7.01 (dd, 1H, *J* = 8.5, 2.4 Hz, Ar*H*), 6.91 (ddd, 1H, *J* = 5.3, 1.9, 1.9 Hz, Cp*H*), 6.59-6.55 (m, 1H, Cp*H*), 6.54-6.48 (m, 2H, Cp*H*), 5.18 (dd, 1H, *J* = 6.5, 3.3 Hz, C*H*O), 4.84 (s, 2H, OCH_2O), 3.88 (s, 3H, OCH_3), 3.67 (dd, 1H, *J* = 17.3, 6.5 Hz, CH_aH$_b$ *anti* to OR), 3.47 (s, 3H, OCH_3), 3.21 (dd, 1H, *J* = 17.4, 3.3 Hz, CH$_a$$H_b$ *syn* to OR); **^{13}C NMR** (100.025 MHz, $CDCl_3$): δ_C 160.7 (C), 150.0 (C), 142.1 (C), 141.1 (C), 138.5 (C), 132.7 (CH), 130.8 (CH), 126.7 (CH), 123.5 (CH), 119.7 (CH), 118.4 (CH), 110.0 (CH), 96.2 (CH_2), 77.4 (CH), 55.8 (CH_3), 55.7 (CH_3), 42.1 (CH_2); $\boldsymbol{\nu_{max}}$ (neat): 2995, 2940, 2888, 2835, 1627, 1603, 1489, 1466, 1367, 1291, 1236, 1147, 1095, 1039, 760 cm^{-1}; **HRMS** found 293.1150 $C_{17}H_{18}O_3Na^+$ requires 293.1148 (|σ| = 0.7 ppm); $\mathbf{[\alpha]_D^{20}}$: -12.0 (*er* > 99:1, *c* = 1.00 in $CHCl_3$) .

(*R*)-3-(Cyclopenta-2,4-diene-1-ylidene)-1-(methoxymethoxy)-5-methyl-2,3-dihydro-1*H*-indene (1.223d)

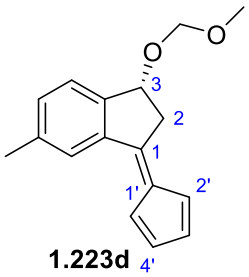

1.223d

Synthesized according to **General Procedure E** using chloromethyl methyl ether (50 µL, 0.658 mmol), fulvene **1.162e** (54 mg, 0.257 mmol), *N,N*-diisopropylethylamine (100 µL, 0.574 mmol) and dichloromethane (2.3 mL) to afford the product as a red oil in 87% yield (57 mg, 0.224 mmol). $\mathbf{R_f}$ (dichloromethane): 0.65; **^{1}H NMR** (400.1 MHz, $CDCl_3$): δ_H 7.78 (d, 1H, *J* = 1.6 Hz, Ar*H*), 7.42 (d, 1H, *J* = 7.7 Hz, Ar*H*), 7.28-7.22 (m, 1H, Ar*H*), 6.96 (ddd, 1H, *J* = 5.3, 2.0, 1.4 Hz, Cp*H*), 6.59-6.54 (m, 1H, Cp*H*), 6.55-6.48 (m, 2H, Cp*H*), 5.20 (dd, 1H, *J* = 6.6, 3.6 Hz, C*H*O), 4.86 (s, 2H, OCH_2O), 3.66 (dd, 1H, *J* = 17.3, 6.6 Hz, CH_aH$_b$ *anti* to OR), 3.48 (s, 3H, OCH_3), 3.20 (dd, 1H, *J* = 17.43 3.6 Hz, CH$_a$$H_b$ *syn* to OR), 2.44 (s, 3H, CH_3); **^{13}C NMR** (100.025 MHz, $CDCl_3$): δ_C 150.1 (C), 146.8 (C), 139.9 (C), 139.3 (C), 138.4 (C), 132.4 (CH), 132.1 (CH), 130.7 (CH), 126.8 (CH), 125.6 (CH), 123.4 (CH), 120.1 (CH), 96.2 (CH_2), 77.6 (CH), 55.8 (CH_3), 41.9 (CH_2), 21.8 (CH_3); $\boldsymbol{\nu_{max}}$ (neat): 2926, 2884, 2820, 1627, 1604, 1462, 1366, 1145, 1094, 1011, 989, 916, 758 cm^{-1}; **HRMS** found 277.1196 $C_{17}H_{18}O_2Na^+$ requires 277.1199 (|σ| = 1.1 ppm); $\mathbf{[\alpha]_D^{20}}$: +12.0 (91:9 *er*, *c* = 1.00 in $CHCl_3$).

(*R*)-1-(Cyclopenta-2,4-diene-1-ylidene)-3-(2-(trimethylsilyl)ethoxymethoxy)-2,3-dihydro-1*H*-indene (1.224a)

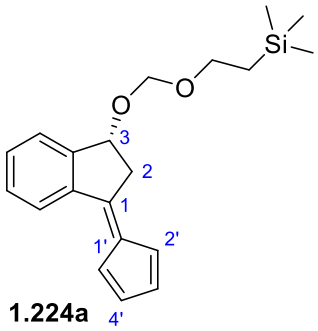

1.224a

Synthesized according to **General Procedure E** using 2-(trimethylsilyl)ethoxymethyl chloride (154 µL, 0.870 mmol), fulvene **1.162a** (154 mg, 0.785 mmol), *N,N*-diisopropylethylamine (270 µL, 1.55 mmol) and dichloromethane (6.4 mL) to afford the product as a red oil in 90% yield (230mg, 0.704 mmol) containing *ca.* 0.2 equiv. of 2-(trimethylsilyl)ethoxymethyl alcohol. $\mathbf{R_f}$ (dichloromethane): 0.89; **^{1}H NMR** (400.1 MHz, $CDCl_3$): δ_H 7.99-7.95 (m, 1H, Ar*H*), 7.54-7.50 (m, 1H, Ar*H*), 7.45-7.38 (m, 2H, Ar*H*), 6.93 (ddd, 1H, *J* = 5.3, 1.8, 1.8 Hz, Cp*H*), 6.58-6.55 (m, 1H, Cp*H*), 6.53-6.49 (m, 2H, Cp*H*), 5.26 (dd, 1H, *J* = 6.6, 3.7 Hz, C*H*O), 4.91 (s, 2H, OCH_2O), 3.77-3.58 (m, 3H, CH_2O + CH_aCH$_b$ *anti* to OR), 3.19 (dd, 1H, *J* = 17.2, 3.7 Hz, CH$_a$$H_b$ *syn* to OR), 1.05-0.98 (m, 2H, CH_2Si), 0.05 (s, 9H, Si(CH_3)$_3$); **^{13}C NMR** (100.025 MHz, $CDCl_3$): δ_C 150.0 (C), 149.5 (C), 139.7 (C), 138.6 (C), 132.6 (CH), 130.9 (CH), 130.8 (CH), 129.4 (CH), 126.5 (CH), 125.9 (CH), 123.4 (CH), 120.1 (CH), 94.6 (CH_2), 77.6 (CH), 65.7 (CH_2), 41.7 (CH_2), 18.3 (CH_2), -1.2 (CH_3); $\mathbf{\nu_{max}}$ (neat): 3067, 2952, 2923, 2891, 1629, 1476, 1457, 1367, 1248, 1192, 1153, 1096, 1055, 1036, 937, 921, 858, 835, 762, 736, 694, 631 cm^{-1}; **HRMS** found 349.1600 $C_{20}H_{26}O_2NaSi^+$ requires 349.1594 (|σ| = 1.7 ppm); $\mathbf{[\alpha]_D^{20}}$: +28.0 (*er* >99:1, *c* = 1.00 in $CHCl_3$).

(*R*)-1-(Cyclopenta-2,4-diene-1-ylidene)-6-methyl-3-(2-(trimethylsilyl)ethoxymethoxy)-2,3-dihydro-1*H*-indene (1.224b)

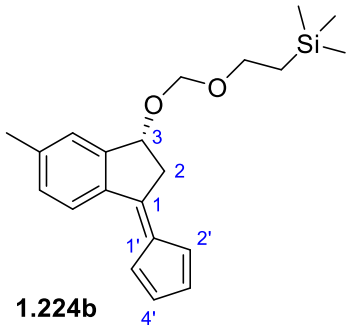

1.224b

Synthesized according to **General Procedure E** using 2-(trimethylsilyl)ethoxymethyl chloride (120 µL, 0.678 mmol), fulvene **1.162f** (120 mg, 0.571 mmol), *N,N*-diisopropylethylamine (210 µL, 1.21 mmol) and dichloromethane (5.0 mL) to afford the product as a red oil in 58% yield (113mg, 0.332 mmol) containing *ca.* 0.2 equiv. of 2-(trimethylsilyl)ethoxymethyl alcohol. $\mathbf{R_f}$ (dichloromethane): 0.79; **^{1}H NMR** (400.1 MHz, $CDCl_3$): δ_H 7.87 (d, 1H, *J* = 8.1 Hz, Ar*H*), 7.34 (d, 1H, *J* = 1.1 Hz, Ar*H*), 7.23 (dd, 1H, *J* = 8.1, 1.1 Hz, Ar*H*), 6.93 (ddd, 1H, *J* = 5.3, 2.1, 1.4 Hz, Cp*H*), 6.57-6.54 (m, 1H, Cp*H*), 6.54-6.49 (m, 2H, Cp*H*), 5.23 (dd, 1H, *J* = 6.6, 3.7 Hz, C*H*O), 4.92 (d, 2H, *J* = 1.4 Hz, OCH_2O), 3.79-3.72 (m, 2H, CH_2O), 3.68 (dd, 1H, *J* = 17.3, 6.6 Hz, CH_aCH$_b$ *anti* to OR), 3.19 (dd, 1H, *J* = 17.3, 3.7 Hz, CH$_a$$H_b$ *syn* to OR), 2.43 (s, 3H, CH_3), 1.06-1.02 (m, 2H, CH_2Si), 0.07 (s, 9H, Si(CH_3)$_3$); **^{13}C NMR** (100.025 MHz, $CDCl_3$): δ_C 150.2 (C), 149.9 (C), 141.6 (C), 137.7 (C), 137.1 (C), 132.1 (CH),

130.6 (CH), 130.4 (CH), 126.3 (CH), 126.2 (CH), 123.2 (CH), 119.9 (CH), 94.6 (CH_2), 77.5 (CH), 66.6 (CH_2), 41.8 (CH_2), 21.8 (CH_3), 18.3 (CH_2), -1.3 (CH_3); ν_{max} (neat): 2951, 2921, 2891, 1629, 1604, 1486, 1459, 1367, 1325, 1247, 1191, 1147, 1097, 1030, 931, 919, 857, 823, 757, 693, 628 cm^{-1}; **HRMS** found 341.1932 $C_{21}H_{29}O_2Si^+$ requires 341.1931 (|σ| = 0.3 ppm); $[\alpha]_D^{20}$: +20.0 (89:11 *er*, *c* = 1.00 in $CHCl_3$).

General Procedure F: Silyl Ether Protection of Fulvenes

R_3SiCl (1.5 equiv.) was added to a solution of fulvene (1 equiv.) in pyridine and the resulting solution heated to temperature T for 1-2 hours. After cooling, the reaction was quenched with water and then extracted with dichloromethane. The crude product was purified *via* flash column chromatography (eluent: 2:1 pentane:dichloromethane) to afford the product (sometimes containing *ca*. 10-20% of the corresponding disiloxane).

(*R*)-((3-(Cyclopenta-2,4-diene-1-ylidene)-2,3-dihydro-1*H*-inden-yl)oxy)triethylsilane (1.225a)

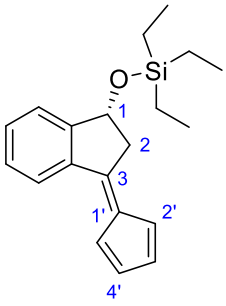

1.225a

Synthesized according to **General Procedure F** using fulvene **1.162a** (98 mg, 0.499 mmol), TESCl (126 µL, 0.751 mmol) and pyridine (1 mL) at 55 °C for 1 h to afford the product as a red oil in quantitative yield (178 mg, 0.573 mmol). $\mathbf{R_f}$ (dichloromethane): 0.90; **^{1}H NMR** (300.1 MHz, $CDCl_3$): δ_H 7.92 (dd, 1H, *J* = 7.1, 1.4 Hz, Ar*H*), 7.52-7.34 (m, 3H, Ar*H*), 6.92 (dd, 1H, *J* = 5.3, 1.7 Hz, Cp*H*), 6.59-6.54 (m, 1H, Cp*H*), 6.54-6.50 (m, 2H, Cp*H*), 5.34 (dd, 1H, *J* = 6.8, 4.8 Hz, C*H*O), 3.67 (dd, 1H, *J* = 16.6, 6.8 Hz, CH_aH$_b$ *anti* to OR), 3.06 (dd, 1H, *J* = 16.6, 4.8 Hz, CH$_a$$H_b$ *syn* to OR), 1.06 (t, 9H, *J* = 7.8 Hz, 3 × CH_3), 0.75 (q, 6H, *J* = 7.8 Hz, 3 × CH_2); **^{13}C NMR** (75.025 MHz, $CDCl_3$): δ_C 152.5 (C), 150.4 (C), 139.4 (C), 138.6 (C), 132.8 (CH), 131.4 (CH), 131.1 (CH), 129.3 (CH), 126.8 (CH), 125.5 (CH), 123.7 (CH), 120.6 (CH), 73.4 (CH), 45.4 (CH_2), 7.4 (CH_3), 5.6 (CH_2); ν_{max} (neat): 3065, 2953, 2909, 2874, 1627, 1598, 1474, 1456, 1413, 1366, 1236, 1226, 1114, 1076, 1001, 835, 729, 632 cm^{-1}; **HRMS** found 311.1826 $C_{20}H_{27}OSi^+$ requires 311.1826 (|σ| < 0.1 ppm); $[\alpha]_D^{20}$: +62.0 (*er* >99:1, *c* = 1.00 in $CHCl_3$).

(*R*)-((3-(Cyclopenta-2,4-diene-1-ylidene)-6-methyl-2,3-dihydro-1*H*-inden-yl)oxy)triethylsilane (1.225b)

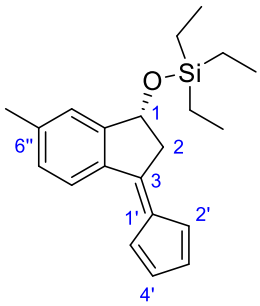

1.225b

Synthesized according to **General Procedure F** using fulvene **1.162f** (81 mg, 0.385 mmol), TESCl (101 µL, 0.602 mmol) and pyridine (1 mL) at 55 °C for 1 h to afford the product as a red oil in 65% yield (81 mg, 0.250 mmol). $\mathbf{R_f}$ (dichloromethane): 0.95; **^{1}H NMR** (400.1 MHz, $CDCl_3$): δ_H 7.84 (d, 1H, *J* = 8.0 Hz, Ar*H*), 7.28 (obscured by solvent, 1H, Ar*H*), 7.19 (d, 1H, *J* = 8.1 Hz, Ar*H*), 6.93 (ddd, 1H, *J* = 5.3, 2.1, 1.4 Hz, Cp*H*), 6.57-6.47 (m, 3H, Cp*H*), 5.33 (dd, 1H, *J* = 6.8, 4.8 Hz, C*H*O), 3.69 (dd, 1H, *J* = 16.7, 6.8 Hz, CH_aH$_b$ *anti* to OR), 3.07 (dd, 1H, *J* = 16.7, 4.8 Hz, CH$_a$$H_b$ *syn* to OR), 2.45 (s, 3H, CH_3), 1.08 (t, 9H, *J* = 7.9 Hz, 3 × CH_3), 0.77 (app qd, 6H, *J* = 7.8, 0.8 Hz, 3 × CH_2); **^{13}C NMR** (100.025 MHz, $CDCl_3$): δ_C 152.3 (C), 150.1 (C), 141.6 (C), 137.2 (C), 136.3 (C), 131.8 (CH), 130.1 (CH), 130.0 (CH), 126.1 (CH), 125.4 (CH), 123.0 (CH), 120.0 (CH), 72.7 (CH), 44.9 (CH_2), 21.8 (CH_3), 6.4 (CH_3), 5.0 (CH_2); $\boldsymbol{\nu_{max}}$ (neat): 3105, 3064, 3026, 2955, 2910, 2876, 1630, 1606, 1485, 1459, 1415, 1367, 1324, 1239, 1124, 1080, 1003, 838, 802, 756, 746, 726, 631 cm^{-1}; **HRMS** found 325.1977 $C_{21}H_{29}OSi^+$ requires 325.1982 (|σ| = 1.5 ppm); $\mathbf{[\alpha]_D^{20}}$: +60.0 (*er* = 89:11, *c* = 1.00 in $CHCl_3$).

(*R*)-((3-(Cyclopenta-2,4-diene-1-ylidene)-2,3-dihydro-1*H*-inden-yl)oxy)-(1,1-dimethyl(ethyl))-dimethylsilane (1.226a)

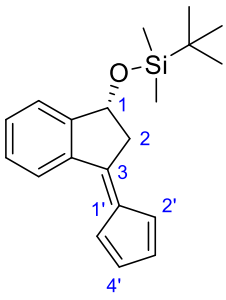

1.226a

Synthesized according to **General Procedure F** using fulvene **1.162a** (90 mg, 0.459 mmol), TBDMSCl (130 mg, 0.863 mmol) and pyridine (2 mL) at 70 °C for 2 h to afford the product as a red oil in 86% yield (122 mg, 0.393 mmol) containing *ca*. 1 equiv. of the corresponding disiloxane. $\mathbf{R_f}$ (dichloromethane): 0.89; **^{1}H NMR** (300.1 MHz, $CDCl_3$): δ_H 7.93 (d, 1H, *J* = 7.6 Hz, Ar*H*), 7.48-7.34 (m, 3H, Ar*H*), 6.92 (ddd, 1H, *J* = 5.3, 1.7, 1.7 Hz, Cp*H*), 6.57 (d, 1H, *J* = 5.3 Hz, Cp*H*), 6.55-6.48 (m, 2H, Cp*H*), 5.34 (dd, 1H, *J* = 6.7, 5.0 Hz, C*H*O), 3.67 (dd, 1H, *J* = 16.6, 6.7 Hz, CH_aH$_b$ *anti* to OR), 3.05 (dd, 1H, *J* = 16.6, 5.0 Hz, CH$_a$$H_b$ *syn* to OR), 0.98 (s, 9H, 3 × CH_3), 0.23 (s, 3H, CH_3), 0.20 (s, 3H, CH_3); **^{13}C NMR** (75.025 MHz, $CDCl_3$): δ_C 151.9 (C), 149.6 (C), 138.6 (C), 137.9 (C), 132.1 (CH), 130.6 (CH), 130.4 (CH), 128.5 (CH), 126.6 (CH), 124.8 (CH), 122.9 (CH), 119.9 (CH), 73.0 (CH), 44.5 (CH_2), 25.7 (CH_3), 18.1 (C), -4.5 (CH_3), -4.7 (CH_3); $\boldsymbol{\nu_{max}}$ (neat): 3066, 2955, 2929, 2886, 2856, 1629, 1473, 1462, 1389, 1255, 1116, 1079, 864, 840, 777, 761 cm^{-1}; **HRMS** found 311.1828 $C_{20}H_{27}OSi^+$ requires 311.1826 (|σ| = 0.6 ppm); $\mathbf{[\alpha]_D^{20}}$: +480.0 (*er* >99:1, *c* = 0.10 in $CHCl_3$).

(*R*)-((3-(Cyclopenta-2,4-diene-1-ylidene)-5-fluoro-2,3-dihydro-1*H*-inden-yl)oxy)-(1,1-dimethyl(ethyl))-dimethylsilane (1.226b)

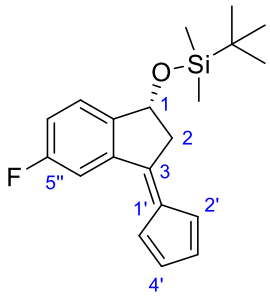

1.226b

Synthesized according to **General Procedure F** using fulvene **1.162g** (37 mg, 0.173 mmol), TBDMSCl (51 mg, 0.338 mmol) and pyridine (1 mL) at 70 °C for 2 h to afford the product as a red oil in 35% yield (20 mg, 0.0609 mmol). $\mathbf{R_f}$ (dichloromethane): 0.95; **^{1}H NMR** (500.1 MHz, $CDCl_3$): δ_H 7.55 (dd, 1H, *J* = 9.4, 2.4 Hz, Ar*H*), 7.39 (dd, 1H, *J* = 8.6, 5.2 Hz, Ar*H*) 7.12 (ddd, 1H, *J* = 8.6, 8.6, 2.4 Hz, Ar*H*), 6.82 (ddd, 1H, *J* = 5.4, 2.0, 1.3 Hz, Cp*H*), 6.58-6.56 (m, 1H, Cp*H*), 6.53-6.47 (m, 2H, Cp*H*), 5.29 (dddd, 1H, *J* = 6.4, 4.8, C*H*O), 3.66 (dd, 1H, *J* = 16.7, 6.4 Hz, CH_aH_b *anti* to OR), 3.05 (dd, 1H, *J* = 16.7, 4.8 Hz, CH$_a$*H*$_b$ *syn* to OR), 0.97 (s, 9H, 3 × CH_3), 0.21 (s, 3H, CH_3), 0.19 (s, 3H, CH_3); **^{13}C NMR** (125.025 MHz, $CDCl_3$): δ_C 163.3 (C, d, *J* = 245.9 Hz), 148.2 (C, d, *J* = 3.5 Hz), 147.7 (C, d, *J* = 1.4 Hz), 140.7 (C, d, *J* = 9.0 Hz), 139.0 (C), 133.1 (CH), 131.4 (CH), 126.4 (CH, d, *J* = 9.1 Hz), 123.3 (CH), 119.8 (CH), 118.3 (CH, d, *J* = 23.4 Hz), 112.4 (CH, d, *J* = 23.5 Hz), 73.0 (CH), 44.5 (CH_2), 25.7 (CH_3), 18.1 (C), -4.5 (CH_3), -4.7 (CH_3); **^{19}F NMR** (376.5 MHz, $CDCl_3$): δ_F -113.50 (ddd, *J* = 9.1, 9.0, 5.1 Hz); $\boldsymbol{\nu_{max}}$ (neat): 3114, 3069, 2955, 2927, 2884, 2856, 1630, 1482, 1465, 1367, 1322, 1279, 1254, 1103, 1080, 852, 836, 789, 775, 756, 727 cm^{-1}; **HRMS** found 329.1726 $C_{20}H_{26}OFSi^+$ requires 329.1731 (|σ| = 1.5 ppm); $\boldsymbol{[\alpha]_D^{20}}$: +48.0 (*er* >99:1, *c* = 0.10 in $CHCl_3$).

1.4.6 Reduction of Pentafulvene 1.162 Derivatives

General Procedure G: Synthesis of the Corresponding CpHs From Fulvene 1.162 Derivatives

A solution of Superhydride® (1M in THF, 2.0-4.0 equiv. (higher loadings are used on small scales)) had its solvent removed by heating at 90 °C under a vacuum of 2 mbar for 1 hour and was then redissolved in diethyl ether. The solution of superhydride® was added dropwise to a solution of protected fulvene (1.0 equiv.) in 2:1 THF:diethyl ether at -45 °C. The resulting mixture was allowed to warm to 0 °C over the course of an hour after which it was removed from the cold bath and allowed to warm to room temperature. The solvent was then removed *in vacuo*, before being redissolved in the minimum dichloromethane and loaded directly onto a silica column and purified *via* flash column chromatography – **CARE! The reaction will give off gas initially when loaded onto the silica, allow this to subside before applying pressure to the column** – to afford the product as a mixture of 2 tautomers.

(1*R*,3*R*)-1-(Cyclopenta-1,3-diene-1-yl)-3-(methoxymethoxy)-2,3-dihydro-1*H*-indene + (1*R*,3*R*)-1-(cyclopenta-1,4-diene-1-yl)-3-(methoxymethoxy)-2,3-dihydro-1*H*-indene (1.228a)

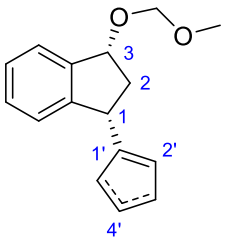

1.228a

Synthesized according to **General Procedure G** using fulvene **1.223a** (275 mg, 1.14 mmol) in THF/diethyl ether (6 mL/3 mL), Superhydride® (2.3 mL, 2.3 mmol) in diethyl ether (10 mL), purified *via* flash column chromatography (eluent: dichloromethane) to afford the product as a colorless oil in 77% yield (212 mg, 0.875 mmol) and >16:1 *d.r.* as a mixture of 2 tautomers. $\mathbf{R_f}$ (dichloromethane): 0.50; **^{1}H NMR** (400.1 MHz, $CDCl_3$): δ_H 7.45-7.41 (m, 2H, Ar*H*), 7.30-7.23 (m, 4H, Ar*H*), 7.11-7.07 (m, 2H, Ar*H*), 6.49-6.41 (m, 3H, Cp*H*), 6.39-6.37 (m, 1H, Cp*H*), 6.32 (app dq, 1H, *J* = 5.4, 1.5 Hz, Cp*H*), 6.22-6.20 (m, 1H, Cp*H*), 5.17 (dd, 1H, *J* = 7.0, 7.0 Hz, C*H*O), 5.14 (dd, 1H, *J* = 7.0, 7.0 Hz, C*H*O), 4.89 (d, 2H, *J* = 0.9 Hz, OCH_2O), 4.87 (d, 2H, *J* = 0.9 Hz, OCH_2O), 4.16 (dd, 1H, *J* = 8.2, 8.2 Hz, C*H*Cp), 4.10 (dd, 1H, *J* = 8.2, 8.2 Hz, C*H*Cp), 3.48 (s, 6H, OCH_3), 3.05-2.79 (m, 6H, CH_aCH$_b$ *anti* to OR and CH_2), 2.08-1.96 (m, 2H, CH$_a$CH_b *syn* to OR); **^{13}C NMR** (100.025 MHz, $CDCl_3$): δ_C 150.8 (C), 148.5 (C), 145.5 (C), 144.8 (C), 143.1 (C), 142.8 (C), 134.3 (CH), 133.1 (CH), 132.1 (CH), 131.8 (CH), 128.3 (CH), 128.3 (CH), 128.2 (CH), 127.4 (CH), 127.0 (2 × CH), 124.7 (CH), 124.7 (CH), 124.3 (CH), 124.3 (CH), 96.2 (CH_2), 96.2 (CH_2), 80.2 (CH), 80.1 (CH), 55.6 (2 × CH_3), 44.0 (CH), 43.0 (CH), 42.6 (CH_2), 41.4 (CH_2), 41.2 (CH_2), 40.8 (CH_2); $\boldsymbol{\nu_{max}}$ (neat): 3068, 3027, 2931, 2882, 2843, 2821, 1629, 1603, 1475, 1459, 1441, 1363, 1146, 1109, 1040, 916, 898, 752 cm^{-1}; **HRMS** found 265.1192 $C_{16}H_{18}O_2Na^+$ requires 265.1199 (|σ| = 2.6 ppm); $\mathbf{[\alpha]_D^{20}}$: -8.0 (*er* >99:1, *c* = 1.00 in $CHCl_3$).

(1*S*,3S)-1-(Cyclopenta-1,3-diene-1-yl)-3-(methoxymethoxy)-2,3-dihydro-1*H*-indene + (1*R*,3*R*)-1-(cyclopenta-1,4-diene-1-yl)-3-(methoxymethoxy)-2,3-dihydro-1*H*-indene ((*S*)-1.228a)

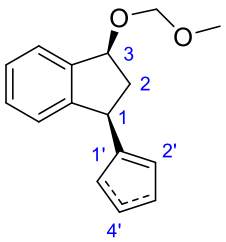

(*S*)-1.228a

Synthesized according to **General Procedure G**, except with an added quench of the crude reaction onto pH 7.4 phosphate buffer before adding to column, using fulvene **(*S*)-1.223a** (102 mg, 0.424 mmol) in THF/diethyl ether (3.0 mL/1.5 mL) and Superhydride® (1.7 mL, 1.7 mmol) in diethyl ether (4.3 mL), purified *via* flash column chromatography (eluent: 2:1 dichloromethane:pentane) to afford the product as a colorless oil in 22% yield (23.1 mg, 0.0953 mmol) and >16:1 *dr* as a mixture of 2 tautomers. **$[\alpha]_D^{20}$**: +24.0 (*er* 99:1, *c* = 1.00 in $CHCl_3$). All other data are in agreement with its opposite enantiomer.

(1*R*,3*R*)-1-(Cyclopenta-1,3-diene-1-yl)-3-(methoxymethoxy)-5-phenyl-2,3-dihydro-1*H*-indene + (1*R*,3*R*)-1-(cyclopenta-1,4-diene-1-yl)-3-(methoxymethoxy)-5-phenyl-2,3-dihydro-1*H*-indene (1.228b)

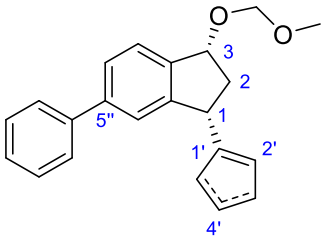

1.228b

Synthesized according to **General Procedure G**, except with an added quench of the crude reaction onto pH 7.4 phosphate buffer before adding to column, using fulvene **1.223b** (106 mg, 0.334 mmol) in THF/diethyl ether (1.8 mL/1mL) and Superhydride® (1.3 mL, 1.3 mmol) in diethyl ether (2.5 mL), purified *via* flash column chromatography (eluent: 2:1 dichloromethane:pentane) to afford the product as a colorless oil in 51% yield (54.3 mg, 0.171 mmol) and >16:1 *dr* as a mixture of 2 tautomers. **R_f** (2:1 dichloromethane:pentane): 0.23; **^{1}H NMR** (400.1 MHz, $CDCl_3$): δ_H 7.57-7.53 (m, 4H, Ar*H*), 7.52-7.49 (m, 4H, Ar*H*), 7.45-7.39 (m, 4H, Ar*H*), 7.35-7.29 (m, 4H, Ar*H*), 6.49-6.42 (m, 4H, Cp*H*), 6.33 (app dq, 1H, *J* = 5.4, 1.5 Hz, Cp*H*), 6.27-6.23 (m, 1H, Cp*H*), 5.22 (dd, 1H, *J* = 7.0, 7.0 Hz, C*H*O), 5.19 (dd, 1H, *J* = 6.9, 6.9 Hz, C*H*O), 4.91 (s, 2H, OCH_2O), 4.90 (s, 2H, OCH_2O) 4.23 (dd, 1H, *J* = 8.1, 8.1 Hz, C*H*Cp), 4.17 (dd, 1H, *J* = 8.2, 8.2 Hz, C*H*Cp), 3.50 (s, 6H, OCH_3), 3.11-2.83 (m, 6H, CH_aH$_b$ *anti* to OR and CH_2), 2.14-2.03 (m, 2H, CH_aCH_b *syn* to OR); **^{13}C NMR** (100.025 MHz, $CDCl_3$): δ_C 150.7 (C), 148.5 (C), 146.4 (C), 145.6 (C), 142.4 (C), 142.1 (C), 141.8 (C), 141.7 (C), 141.6 (C), 141.5 (C), 134.5 (CH), 133.2 (CH), 132.2 (CH), 132.0 (CH), 128.8 (CH), 128.8 (CH), 128.6 (CH), 127.7 (CH), 127.4 (CH), 127.4 (CH), 127.3 (CH), 127.3 (CH), 126.4 (CH), 124.8 (CH), 124.8 (CH), 123.7 (CH), 123.5 (CH), 96.4 (CH_2), 96.3 (CH_2), 80.2 (CH), 80.1 (CH), 55.7 (CH_3), 44.2 (CH), 43.2 (CH), 43.0 (CH_2), 41.8 (CH_2), 41.4 (CH_2), 41.0 (CH_2); **ν_{max}** (neat): 3059, 3030, 2926, 2884, 2854, 2821, 2778, 1600, 1572, 1479, 1449, 1409, 1213, 1146, 1110, 1095, 1042, 760, 587 cm^{-1};

HRMS found 341.1507 $C_{22}H_{22}O_2Na^+$ requires 341.1512 (|σ| = 1.5 ppm); **$[\alpha]_D^{20}$**: +36.0 (*er* >99:1, *c* = 1.00 in $CHCl_3$).

(((1*R*,3*R*)-3-Cyclopenta-1,3-dien-1-yl)-2,3-dihydro-1*H*-inden-1-yl)oxy)triethylsilane + (((1*R*,3*R*)-3-cyclopenta-1,4-dien-1-yl)-2,3-dihydro-1*H*-inden-1-yl)oxy)triethylsilane (1.228c)

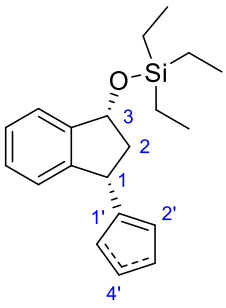

1.228c

Synthesized according to **General Procedure G** using fulvene **1.225a** (314 mg, 1.01 mmol) in THF/diethyl ether (7.0 mL/3.5 mL), Superhydride® (4.0 mL, 4.0 mmol) in diethyl ether (8.5 mL), purified *via* flash column chromatography (eluent: 8:1 pentane:dichloromethane) to afford the product as a colorless oil in 74% yield (235 mg, 0.752 mmol) and >99:1 *dr* as a mixture of 2 tautomers. **R_f** (1:4 dichloromethane:pentane): 0.52; **^{1}H NMR** (400.1 MHz, $CDCl_3$): δ_H 7.39-7.35 (m, 2H, Ar*H*), 7.29-7.16 (m, 4H, Ar*H*), 7.06-7.00 (m, 2H, Ar*H*), 6.48 (app dq, 1H, *J* = 5.3, 1.7 Hz, Cp*H*), 6.46-6.43 (m, 2H, Cp*H*), 6.42-6.40 (m, 1H, Cp*H*), 6.33 (app dq, 1H, *J* = 5.4, 1.5 Hz, Cp*H*), 6.25-6.20 (m, 1H, Cp*H*), 5.26 (app t, 1H, *J* = 8.0 Hz, C*H*O), 5.23 (app t, 1H, *J* = 8.0 Hz, C*H*O), 4.11 (dd, 1H, *J* = 10.4, 7.0 Hz, C*H*Cp), 4.05 (dd, 1H, *J* = 10.4, 7.0 Hz, C*H*Cp), 3.06-2.69 (m, 6H, CH_aH$_b$ *anti* to OR and CH_2), 2.00-1.89 (m, 2H, CH_aCH_b *syn* to OR), 1.05 (app t, 18H, *J* = 7.9 Hz, CH_2CH_3), 0.73 (app q, 12H, *J* = 7.9 Hz, CH_2CH_3); **^{13}C NMR** (100.025 MHz, $CDCl_3$): δ_C 150.5 (C), 148.3 (C), 145.8 (C), 145.5 (C), 145.0 (C), 144.2 (C), 134.3 (CH), 133.3 (CH), 133.3 (CH), 132.2 (CH), 132.0 (CH), 128.7 (CH), 127.8 (CH), 127.8 (CH), 127.7 (CH), 127.1 (CH), 124.5 (CH), 124.4 (CH), 123.8 (CH), 123.7 (CH), 75.0 (CH), 74.9 (CH), 46.2 (CH_2), 45.0 (CH_2), 43.6 (CH), 42.7 (CH), 41.4 (CH_2), 40.8 (CH_2), 7.04 (CH_3), 5.1 (CH_2); **ν_{max}** (neat): 2954, 2935, 2910, 2875, 1603, 1458, 1413, 1362, 1315, 1237, 1107, 1073, 1004, 983, 974, 898, 845, 830, 738, 679, 632, 611 cm^{-1}; **HRMS** found 335.1803 $C_{2o}H_{28}OSiNa^+$ requires 335.1802 (|σ| = 0.3 ppm); **$[\alpha]_D^{20}$**: -16.0 (*er* >99:1, *c* = 1.00 in $CHCl_3$).

(((1*R*,3*R*)-3-Cyclopenta-1,3-dien-1-yl)-2,3-dihydro-1*H*-inden-1-yl)oxy)-(1,1-dimethylethyl)-dimethylsilane + (((1*R*,3*R*)-3-cyclopenta-1,4-dien-1-yl)-2,3-dihydro-1*H*-inden-1-yl)oxy)-(1,1-dimethylethyl)dimethylsilane (1.228d)

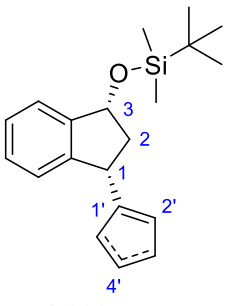

1.228d

Synthesized according to **General Procedure G** using fulvene **1.226a** (122 mg, 0.393 mmol, contains *ca*. 1 equiv. of the corresponding disiloxane) in THF/diethyl ether (2.8 mL/1.3 mL), Superhydride® (1.6 mL, 1.6 mmol) in diethyl ether (3.7 mL), purified *via* flash column chromatography (eluent: 8:1 pentane:dichloromethane) to afford the product as a colorless oil in 23% yield (28 mg, 0.0896 mmol) and >99:1 *dr* as a mixture of 2 tautomers.

$\mathbf{R_f}$ (1:8 dichloromethane:pentane): 0.29; **^{1}H NMR** (400.1 MHz, $CDCl_3$): δ_H 7.38-7.33 (m, 2H, Ar*H*), 7.28-7.19 (m, 4H, Ar*H*), 7.06-7.01 (m, 2H, Ar*H*), 6.48 (dddd, 1H, *J* = 5.3, 1.7, 1.7, 1.7 Hz, Cp*H*), 6.46-6.40 (m, 3H, Cp*H*), 6.33 (app dq, 1H, *J* = 5.2, 1.4 Hz Cp*H*), 6.25-6.22 (m, 1H, Cp*H*), 5.26 (dd, 1H, *J* = 8.0, 8.0 Hz, C*H*O), 5.23 (dd, 1H, *J* = 8.0, 8.0 Hz, C*H*O), 4.11 (dd, 1H, *J* = 10.2, 7.1 Hz, C*H*Cp), 4.05 (dd, 1H, *J* = 10.2, 7.1 Hz, C*H*Cp), 3.06-2.69 (m, 6H, CH_aH$_b$ *anti* to OR and CH_2), 2.00-1.88 (m, 2H, CH_aCH_b *syn* to OR), 0.98 (s, 18H, C(CH_3)$_3$), 0.22 (s, 6H, CH_3), 0.18 (s, 6H, CH_3); **^{13}C NMR** (100.025 MHz, $CDCl_3$): δ_C 150.5 (C), 148.3 (C), 145.9 (C), 145.6 (C), 144.9 (C), 144.2 (C), 134.3 (CH), 133.4 (CH), 132.2 (CH), 132.0 (CH), 128.7 (CH), 127.8 (CH), 127.8 (CH), 127.7 (CH), 127.0 (2 × CH), 124.5 (CH), 124.4 (CH), 123.8 (CH), 123.7 (CH), 75.4 (CH), 75.3 (CH), 46.1 (CH_2), 44.8 (CH_2), 43.6 (CH), 42.7 (CH), 41.4 (CH_2), 40.1 (CH_2), 26.1 (CH_3), 18.5 (C), -4.2 (CH_3), -4.4 (CH_3); $\mathbf{\nu_{max}}$ (neat): 3069, 3026, 2955, 2927, 2895, 2856, 1472, 1460, 1362, 1253, 1196, 1110, 1075, 867, 835, 774, 750, 736 cm^{-1}; **HRMS** found 181.1005 $C_{2o}H_{28}OSiNa^+$ requires 181.1012 (|σ| = 3.9 ppm); **$[\alpha]_D^{20}$**: -12.0 (*er* >99:1, *c* = 1.00 in $CHCl_3$).

(1*R*,3*R*)-1-(Cyclopenta-1,3-diene-1-yl)-3-(2-(trimethylsilyl)ethoxymethoxy)-2,3-dihydro-1*H*-indene + (1*R*,3*R*)-1-(cyclopenta-1,4-diene-1-yl)-3-(2-(trimethylsilyl)ethoxymethoxy)-2,3-dihydro-1*H*-indene (1.228e)

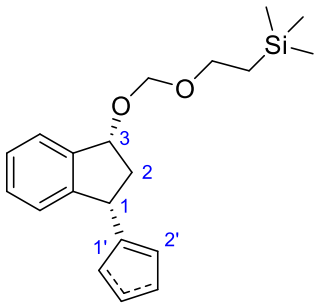

1.228e

Synthesized according to **General Procedure G** using fulvene **1.224a** (283 mg, 0.867 mmol) in THF/diethyl ether (6.0 mL/3.0 mL), Superhydride® (3.5 mL, 3.5 mmol) in diethyl ether (7.2 mL), purified *via* flash column chromatography (eluent: 2:1 pentane:dichloromethane) to afford the product as a colorless oil in 74% yield (237 mg, 0.721 mmol) and >99:1 *dr* as a mixture of 2 tautomers. $\mathbf{R_f}$ (1:2 dichloromethane:pentane): 0.36; **^{1}H NMR** (400.1 MHz, $CDCl_3$): δ_H 7.43-7.38 (m, 2H, Ar*H*), 7.27-7.23 (m, 4H, Ar*H*), 7.11-7.06 (m, 2H, Ar*H*), 6.46 (app dq, 1H, *J* = 5.1, 1.7 Hz, Cp*H*), 6.45-6.42 (m, 2H, Cp*H*), 6.40-6.36 (m, 1H, Cp*H*), 6.32 (app dq, 1H, *J* = 5.4, 1.5 Hz, Cp*H*), 6.22-6.19 (m, 1H, Cp*H*), 5.24-5.14 (m, 2H, C*H*O), 4.93-4.91 (m, 4H, OCH_2O), 4.16 (m, 2H, C*H*Cp), 3.81-3.68 (m, 4H, OCH_2), 3.05-2.78 (m, 6H, CH_aH$_b$ *anti* to OR and CH_2), 2.07-1.96 (m, 2H, CH_aCH_b *syn* to OR), 1.03-0.92 (m, 4H, CH_2Si), 0.05 (s, 9H, Si(CH_3)$_3$), 0.05 (s, 9H, Si(CH_3)$_3$); **^{13}C NMR** (100.025 MHz, $CDCl_3$): δ_C 150.9 (C), 148.6 (C), 145.6 (C), 144.9 (C), 143.4 (C), 143.1 (C), 134.4 (CH), 133.2 (CH), 132.2 (CH), 131.9 (CH), 128.4 (CH), 128.4 (CH), 128.3 (CH), 127.4 (CH), 127.1 (2 × CH), 124.8 (CH), 124.7 (CH), 124.4 (CH), 124.4 (CH), 94.4 (2 × CH_2), 80.0 (CH), 80.0 (CH), 65.3 (CH_2), 65.3 (2 × CH_2), 65.1 (CH_2), 44.1 (CH), 43.1 (CH), 42.6 (CH_2), 41.4 (CH_2), 41.3 (CH_2), 40.9 (CH_2), 18.3 (2 × CH_2), -1.3 (CH_3); $\mathbf{\nu_{max}}$ (neat): 2952, 2926, 2895, 2880, 2856,

1644, 1601, 1582, 1453, 1402, 1367, 1248, 1192, 1171, 1104, 1056, 1029, 937, 920, 897, 858, 832, 782, 754, 700, 679, 632, 613, 581, 563, 540, 515, 448 cm^{-1}; **HRMS** found 351.1752 $C_{20}H_{28}O_2SiNa^+$ requires 351.1751 (|σ| = 0.3 ppm); **$[\alpha]_D^{20}$**: -8.0 (*er* >99:1, *c* = 1.00 in $CHCl_3$).

(1*R*,3*R*)-1-(Cyclopenta-1,3-diene-1-yl)-3-(hydroxy)-5-fluoro-2,3-dihydro-1*H*-indene + (1*R*,3*R*)-1-(cyclopenta-1,4-diene-1-yl)-3-(hydroxy)-5-fluoro-2,3-dihydro-1*H*-indene (1.218)

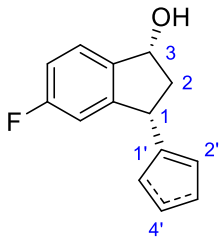

1.218

Synthesized according to **General Procedure G** using fulvene **1.162g** (76 mg, 0.356 mmol) in THF/diethyl ether (2.4 mL/1.2 mL), Superhydride® (1.7 mL, 1.7 mmol) in diethyl ether (2.9 mL), purified *via* flash column chromatography (eluent: dichloromethane) to afford the product as a pale yellow oil in 46% yield (35 mg, 0.163 mmol) and 4:1 *dr* as a mixture of 2 tautomers. **R_f** (dichloromethane): 0.30; **^{1}H NMR** (400.2 MHz, $CDCl_3$): δ_H 7.42-7.34 (m, 2H, Ar*H*), 7.01-6.91 (m, 2H, Ar*H*), 6.84-6.74 (m, 2H, Ar*H*), 6.50-6.40 (m, 3H, Cp*H*), 6.37-6.29 (m, 2H, Cp*H*), 6.17-6.09 (m, 1H, Cp*H*), 5.23-5.15 (m, 2H, C*H*O), 4.11 (dd, 1H, *J* = 8.0, 8.0 Hz, C*H*Cp), 4.05 (dd, 1H, *J* = 8.0, 8.0 Hz, C*H*Cp), 3.06-2.79 (m, 6H, CH_aH_b *anti* to OR and CH_2), 2.02-1.89 (m, 2H, CH_aCH_b *syn* to OR); **^{13}C NMR** (125.025 MHz, $CDCl_3$): δ_C 163.5 (2 × d, *J* = 245.3 Hz, 2 × C), 150.2 (C), 148.3 (C), 140.8 (d, *J* = 2.6 Hz, C), 140.5 (d, *J* = 2.6 Hz, C), 135.0 (CH), 132.9 (CH), 132.2 (CH), 132.2 (CH), 128.8 (CH), 127.7 (CH), 125.4 (2 × d, *J* = 9.5 Hz, 2 × CH), 114.5 (2 × d, *J* = 22.7 Hz, 2 × CH), 111.8 (2 × d, *J* = 22.2 Hz, 2 × CH), 74.7 (CH), 74.6 (CH), 45.5 (CH_2), 44.4 (CH_2), 43.8 (d, *J* = 1.9 Hz, CH), 42.9 (d, *J* = 2.6 Hz, CH), 41.4 (CH_2), 41.1 (CH_2); **^{19}F NMR** (376.5 MHz, $CDCl_3$): δ_F -114.37 (ddd, *J* = 9.0, 9.0, 5.1 Hz), -114.51 (ddd, *J* = 8.9, 8.9, 5.1 Hz); **ν_{max}** (neat): 3333, 3061, 2961, 2926, 2875, 2857, 1612, 1597, 1484, 1428, 1365, 1327, 1266, 1251, 1236, 1081, 1058, 978, 946, 927, 896, 870, 825, 811, 748, 679, 646, 621, 579, 453 cm^{-1}; **HRMS** found 215.0875 $C_{14}H_{12}OF^-$ requires 215.0878 (|σ| = 1.4 ppm); **$[\alpha]_D^{20}$**: -8.0 (*er* >99:1, *c* = 1.00 in $CHCl_3$).

2 Kinetic Analysis of Copper Catalyzed 1,4-Addition

2.1 Introduction

2.1.1 Introduction to 1,4-Addition

In chemistry, 1,4-addition (alternatively Michael or conjugate addition) typically occurs in reactions between nucleophiles and α,β-unsaturated carbonyl compounds. For example, when a nucleophile adds to α,β-enone **2.1**, there are two possible outcomes: either the 1,2-addition into the carbonyl (to form alcoholate **2.3**) or the 1,4-addition to the β-carbon (to form enolate **2.2**) (Scheme 49). The favoured addition mode is controlled by many factors but is predominantly determined by the nature of the nucleophile. Organometallic reagents derived from unstabilized carbanions (*e.g.* organolithiums, Grignard reagents – 'hard' nucleophiles) favor 1,2-addition,[114] whereas enolates or other stabilized carbanions (*e.g.* organocuprates - 'soft' nucleophiles) favor 1,4-addition.[115]

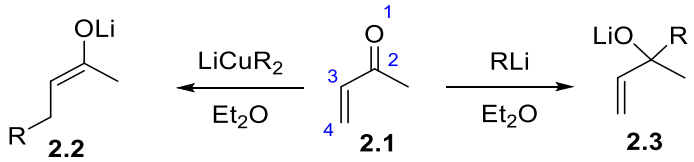

*Scheme 49: Alternative reactivities of enone **2.1**. In diethyl ether, organolithium species give 1,2-addition to afford alcoholate **2.3**; whereas with the addition of an organocopper reagent, 1,4-addition is favoured to afford enolate **2.2**.*

The 1,4-addition mode was first proposed by Arthur Michael in the 1880s. Building upon the observation of a cyclopropane derivative **2.7** formed in the reaction between diethyl-2,3-dibromo propionate (**2.4**) and sodium diethylmalonate (**2.6**), made earlier by Conrad and Guthzeit,[116] Michael theorized that a 1,4-addition was occurring (following an elimination of HBr to form **2.7**) after which an intramolecular cyclization could occur (Scheme 50a).[117] To test this hypothesis, he examined the reactivity of malonate derivatives (**1.3**) with α,β-unsaturated acid esters (**2.8**) and confirmed that the 1,4-additions could occur, under even mild conditions (Scheme 50b).[118]

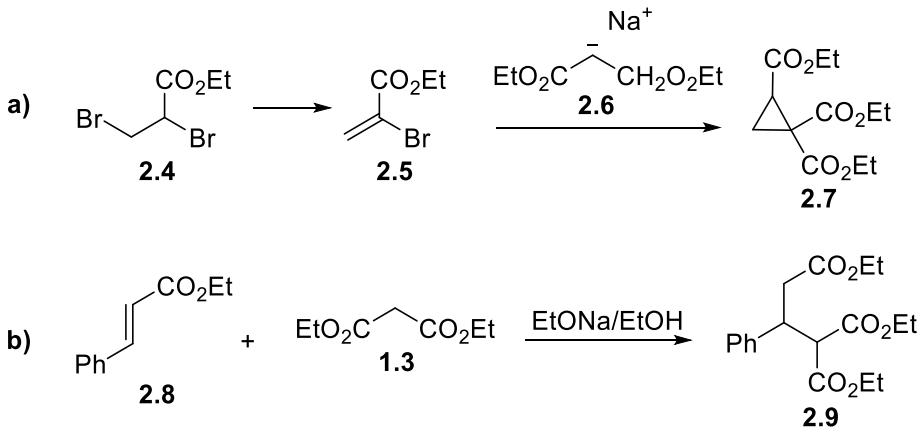

Scheme 50: Early reactions involved in the discovery of 1,4-addition:[117] ***a)*** *formation of cyclopropane* ***2.7****;*[116] ***b)*** *1,4-Addition of diethyl malonate (****1.3****) to ethyl cinnamate* ***2.8****.*[118]

Early attempts towards organometallic asymmetric 1,4-additions used a diastereoselective approach in which a chiral α,β-unsaturated compound was used as the substrate (of which **2.10** is an example - Scheme 51a). After addition, the original chiral auxiliary is removed to afford the enantioenriched 1,4-product.[119] In Scheme 51a, the required α,β-unsaturated ester (**2.10**) is prepared from a crotonic acid and 9-phenylmenthol (**2.12**). The alcohol unit acts as a chiral auxiliary within **2.10**, facilitating the diastereoselective 1,4-addition of an organo-copper reagent.[120] An alternative method towards achieving these asymmetric additions involved the use of stoichiometric, chiral, non-transferable ligands for the organometallic reagent. For example, Dieter and Tokles used (*S*)-proline derivatives as ligands to form chiral organo(hetero)cuprates, which afforded moderate to good enantioselectivities (Scheme 51b).[121]

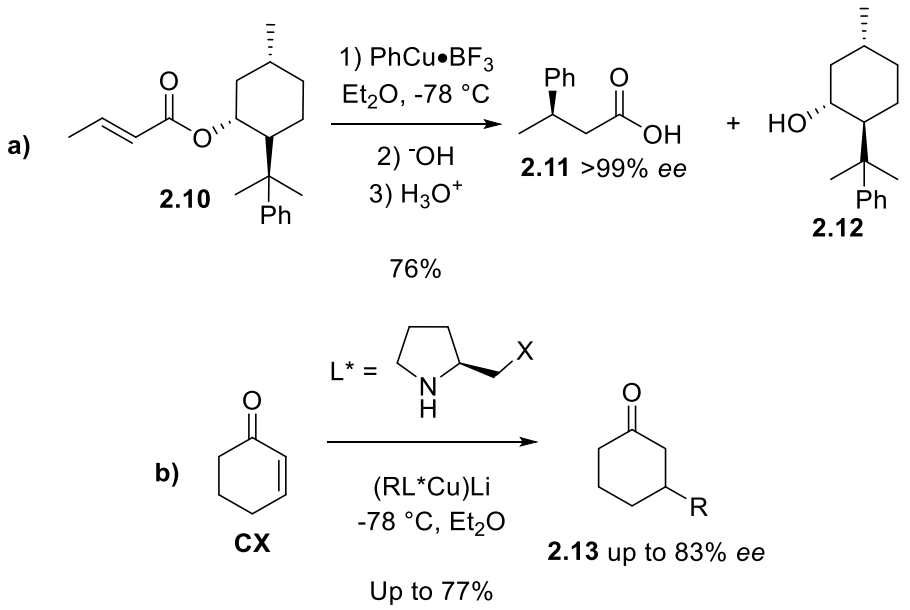

*Scheme 51: **a)** Example of a diastereoselective 1,4-addition which, following hydrolysis of the chiral alcohol, affords a product as a single enantiomer;*[120] ***b)** example of an organometallic asymmetric 1,4-addition using a stoichiometric chiral organo(hetero)cuprate (where X is a variable group on the side-chain of the ligand).*[121]

The first catalytic organometallic asymmetric 1,4-addition using a chiral copper/ligand system was published in 1988, by Lippard and co-workers.[122] This first example was soon followed up by a second publication in which the enantioselectivity had been improved (from 14.5% *ee*, up to 74% in some cases).[123] This improved system involved the addition of a Grignard reagent to **CX** (2-cyclohexen-1-one), using a catalytic system consisting of a copper source and ligand **2.14** (Scheme 52), and containing HMPA and a silyl chloride as additives.

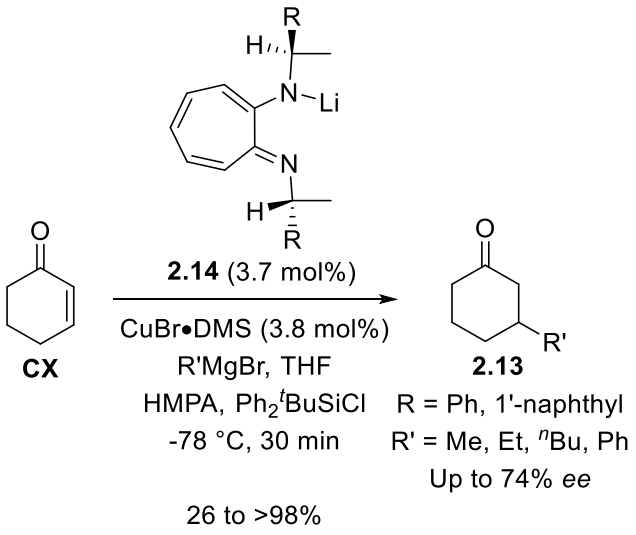

*Scheme 52: Early example of an enantioselective 1,4-addition catalyzed by a chiral catalyst consisting of a copper source and ligand **2.14**.*[123]

Since this early beginning, multitudinous examples of asymmetric 1,4 carbon-carbon bond forming reactions have been published, as evidenced by extensive reviews.[124][125][126][127] Copper catalyzed asymmetric conjugate additions (ACAs) of organometallic reagents have become a 'go to' method for enantioselective carbon-carbon bond formation; due to their reliability, high yields, high enantioselectivities and their low catalyst/ligand loading requirements.[128] By careful tuning of the reaction conditions (solvent, copper source, ligand and organometallic reagent can all be varied with large effects on the reaction outcomes), extremely efficient and well-performing reactions can be obtained.[126] An enormous range of different ligands have been developed in an effort to optimize a variety of ACAs. Examples of some of the major classes of ligand are shown in Figure 14, and include but are not limited to: bisphosphines,[129] aryl-thiolates,[125] hydroxyphosphines,[130] NHCs[131] and SimplePhos ligands.[132]

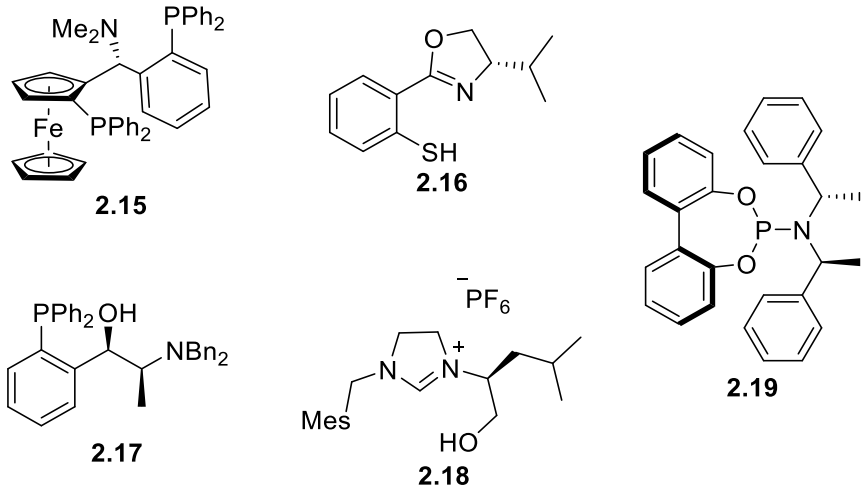

Figure 14: Summary of some of the different classes of chiral ligands used in ACA reactions.

2.1.2 Contemporary Mechanistic Understanding

The currently accepted consensus for the mechanism of the 1,4-addition to enones, catalyzed by $RCuL_n$ like species, is shown in Scheme 53. Typically, formation of the active Cu(I) species **2.20**, is achieved by reduction of a Cu(II) pre-catalyst. The active copper(I) complex then forms a π-complex with the enone (**2.21**), in the presence of stabilizing ligands. The Cu(I) π-complex can undergo an oxidative addition, to form a Cu(III) σ-complex (**2.22**) (related structures to which have been observed and isolated),[133] these in turn can reductively eliminate product **2.23** and regenerate the active Cu(I) catalyst.[134] This reductive elimination is widely considered the rate and stereo-determining step, as supported by the theoretical studies of Nakamura and

co-workers.[135][136] It is believed that π-acceptor behaviour in ancillary ligands (in particular cyanide and phosphine ligands) leads to significant rate acceleration as the Cu^{III} intermediate (or Cu^{III} transition state) is destabilized.[124]

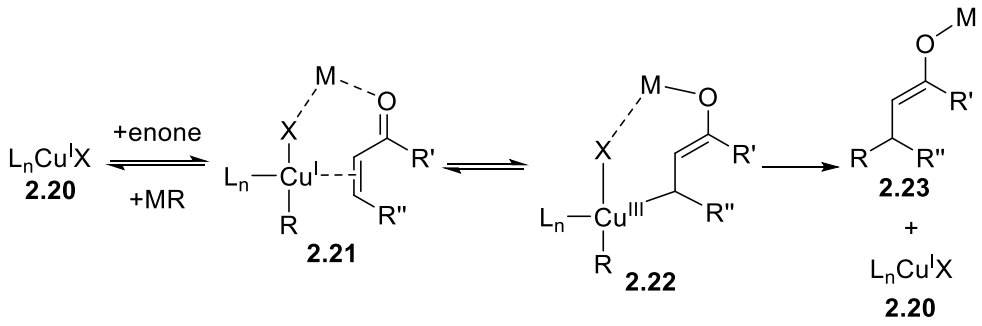

Scheme 53: Summary of the consensus mechanistic understanding of copper catalyzed 1,4-addition.[128]

An alternative to the mechanism described in Scheme 53 can also be considered (see Scheme 54).[124] In this proposal a syn-carbocupration could occur (**2.21** to **2.24**) rather than an oxidative insertion step (**2.21** to **2.22**). However, this carbocupration should be irreversible, as opposed to the reversible oxidative addition described previously. The *cis-trans* isomerization of some acyclic enones, within a conjugate addition reaction, has been observed in the groups of Feringa[137] and Alexakis,[138] among others. This isomerization is used to explain the fact that, in some cases, the same enantiomer of product is obtained regardless of the starting geometry of the enone substrate (see Scheme 55). Whilst the geometry of the starting material does not alter the configuration of the product, it can alter its *ee*. If the approach of the nucleophile to the same face was slower for the (*Z*)-3-nitrostyrene, the isomerization process could occur faster than the conjugate addition reaction. This could result in the lower observed enantioselectivity overall (affording 33% *ee* for the (*Z*)-enone). Both groups propose that this isomerization occurs due to the reversibility of the oxidative addition step described in Scheme 53, which would not be observed if the irreversible carbocupration pathway described in Scheme 54 was occurring. This proposal also requires the generated enolate to be configurationally stable. The configurational stability of zinc enolates and aluminium enolates have been reported within the groups of Alexakis[139] and Woodward[140] respectively. However, Woodward found that exchange between the two configurations of an enolacetate may be occurring following the quenching of a dimethylaluminium enolate with acetic anhydride.

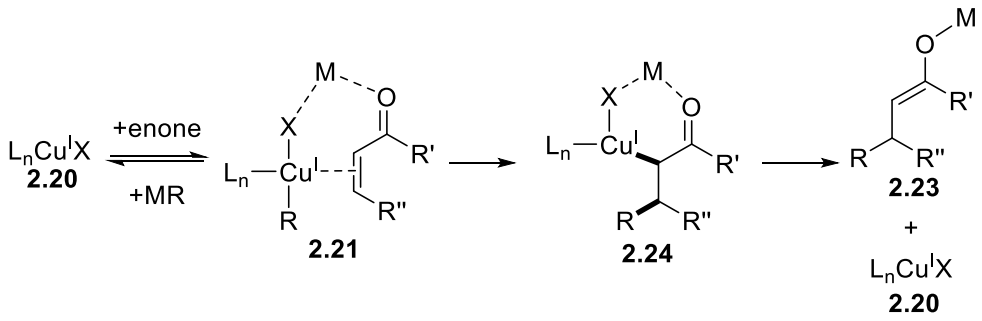

Scheme 54: Alternative mechanistic pathway involving a carbocupration step.[124]

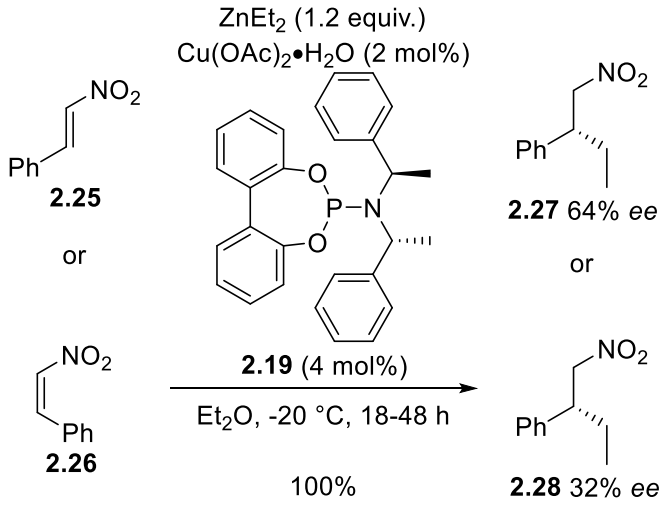

*Scheme 55: Experiment performed by Alexakis and co-workers, using two different isomers of 3-nitrostyrene (**2.25** and **2.26**) as the substrate for identical asymmetric conjugate addition reactions. The same configuration of product was obtained in both reactions.*[138]

Hard evidence supporting the structures of the key, rate-determining transition states, in the area of copper-catalyzed asymmetric 1,4-addition, is limited but has been attained indirectly. Feringa and co-workers have studied the mechanism of the enantioselective 1,4-addition of Grignard reagents to α,β-unsaturated carbonyl compounds.[137] First, it was established that the copper/ligand containing precursor exists in a solvent dependent equilibrium. Polar solvents (acetonitrile or methanol) favored a mononuclear species that is insoluble in ethereal solvents. However, less polar solvents commonly used in conjugate addition reactions (diethyl ether or dichloromethane) favored dinuclear species **2.29** (see Figure 15a). A solvent study was then performed which highlighted the importance of the Schlenk equilibrium on the reaction outcome. Diethyl ether has been shown to favor the solvent coordinated monoalkylmagnesium species (EtMgBr·Et_2O),[141] and afforded high regio- and enantioselectivity. THF has been shown to favor dialkyl and dibromo-magnesium species (MgR_2 and $MgBr_2$),[142] and resulted in a significant decrease in reactivity and selectivity. It was proposed that Mg^{2+} plays a dual role in a

conjugate addition reaction: to activate the enone through a Lewis acid effect and to associate with the copper complex *via* the bridging halide (which was also shown to be important to the reaction outcome). However, NMR studies performed also indicated a rapid conversion of dimeric **2.29** to mononuclear **2.30** (Figure 15b), upon the addition of the Grignard reagent, and assigned a signal at -0.31 ppm in the ^{1}H NMR spectrum to a Cu(I)-Me moiety.[143]

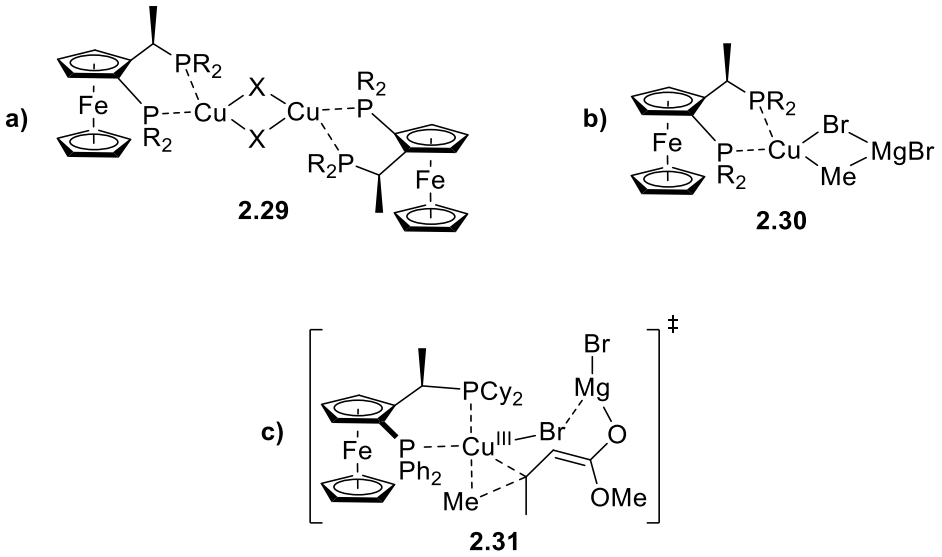

Figure 15: Structures of: ***a)*** *copper/ligand precursor in conjugate addition solvents;* ***b)*** *monomeric species, possessing a Cu-Me species, identified using NMR studies;* ***c)*** *transition state proposed by Feringa and co-workers.*[137]

As mentioned above, Feringa and co-workers also observed *cis*-*trans* isomerization of some enones (see Scheme 55). Although no conjugate addition reaction was observed between methyl magnesium bromide and a *cis* or *trans* cinnamate ester; when the *cis*-cinnamate ester was used, isomerization to the *trans*-enoate was observed. They also concluded that this was as a result of a rapid equilibrium between copper(I)-π complex **2.21** and copper(III)-σ complex **2.22**, prior to the rate-determining reductive elimination step. Finally, kinetic studies were performed. Fitting the reaction data to 2nd order kinetics, in enoate consumption, the reaction was found to have an order of 1.17 with respect to the concentration of dimeric complex **2.29** (or the monomer derived from it). It was also demonstrated that the reaction rate had a dependence on both the Grignard and the enoate substrate. Based upon the observations summarized above, Feringa and co-workers proposed transition state **2.31** (Figure 15c) for the catalysis rate determining step.[137]

Noyori and co-workers studied the addition of diethyl zinc to α,β-unsaturated ketones, catalyzed by copper(I) cyanide and *N*-benzylbenzenesulfonamide.[144] Investigating the kinetics of the reaction, 1st order dependencies were observed with respect to the concentrations of the catalyst (copper and ligand), diethyl zinc and the **CX** substrate. Based upon their kinetic data, in the absence of any supportive NMR studies, transition state **2.32** (Figure 16a) was proposed. Schrader and co-workers worked on a closely related system, with an added chiral ligand.[145] Performing kinetic studies, Schrader showed that the system demonstrated approximate 1st order kinetics with respect to the substrate, organozinc and ligands. Using this data, Schrader proposed transition state **2.33** (Figure 16b). This was a simple analogy of Noyori's previously described system, with an added chiral ligand. The second organozinc present in **2.33** was rationalised to be due to a rapid association of the cuprate with a second diethylzinc.[143]

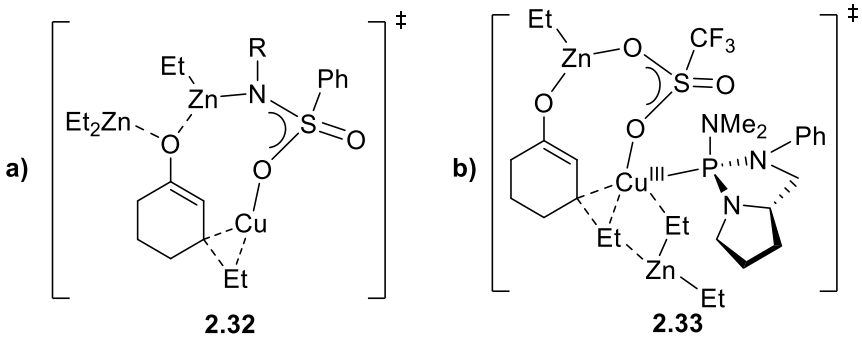

Figure 16: Transition states proposed by: ***a)*** *Noyori and co-workers (redrawn to highlight their similarity);*[144] ***b)*** *proposed by Schrader and co-workers.*[145]

Both of these studies unfortunately suffered from issues. Noyori identified the existence of an induction period, in which the active catalyst is still forming. This results in a sinusoidal shaped graph of conversion against time, due to initial the acceleration of product formation (similar to the kinetics of an autocatalytic reaction). This forced Noyori to discard a significant proportion of the collected data (the first half life). In Schrader's system, significant conversion had already occurred before the first aliquot was taken (up to 40% conversion). This resulted in the obtained data also missing a significant proportion of the early events in the reaction.

In a series of publications, Gschwind and co-workers performed intensive NMR studies on organocopper complexes of relevance to ACA reactions.[146][147][148][149] Initial studies focussed on identifying the structure of the precatalytic copper ligand complexes. Using ^{31}P and diffusion NMR studies of mixtures of copper(I) chloride and a phosphoramidite ligand, at different concentrations, two key structures were observed (Figure 17a). Up to a ligand:copper ratio of

1:1, trinuclear **2.34** is the only species present in solution. Above the ratio of 1:1 (dependant on temperature and solvent), the binuclear species **2.35** begins to appear. And at ratios of greater than 1.5:1, only binuclear **2.35** and free ligand are present.[147] Continuing these NMR studies confirmed that the previously discovered binuclear motif **2.35** is the basic structural motif for not just copper(I) chloride but several copper sources and ligands (with the possible exception of copper(I) bromide).[149][146] Binuclear **2.35** possesses a novel mixed trigonal/tetrahedral motif and may provide an explanation as to why conjugate addition optimization strategies enabled reduction of the ligand loading to 1.5 × [copper], but no lower.

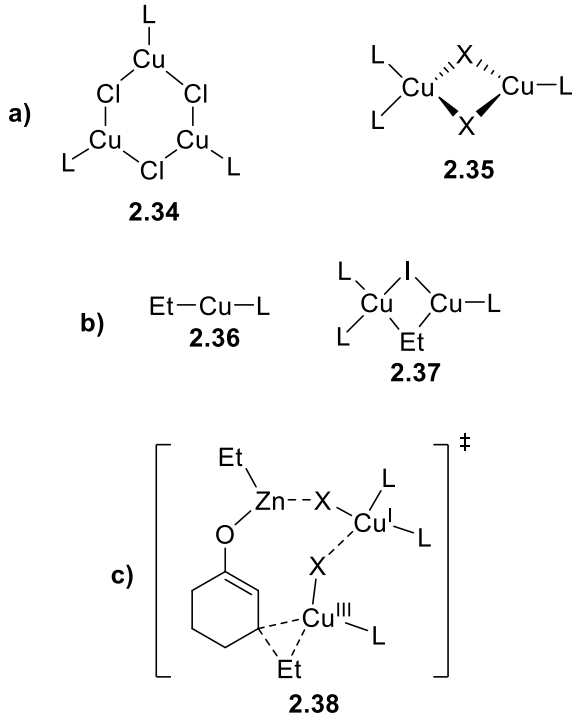

*Figure 17: Structures proposed by Gschwind: **a)** Proposed precatalyst formation and structure;[147] **b)** Transmetalation products;[148] **c)** transition state proposed by Gschwind and co-workers (where L = (R,S,S)-Feringa's ligand).*[149][148]

Gschwind and co-workers also used specialized ^{1}H-^{31}P HMBC NMR methods which enabled the observation of species below the usual ^{1}H or ^{31}P NMR detection limit. This was required to detect P-Cu-Et moieties – *ie* the transmetalation intermediates.[148] These occurred at very low concentrations, within a large mixture of numerous unidentifiable compounds. Experiments using copper(I) chloride, zinc iodide and varying quantities of diethylzinc identified the two predominant transmetalation intermediates (Figure 17b). One (**2.36**) possesses just one ligand and one ethyl group whereas the other (**2.37**) possessed the binuclear mixed trigonal/tetrahedral coordination of copper atoms with one ethyl and three ligands. Based upon

this observation of what was proposed to be the active transmetalation intermediate, Gschwind proposed transition state **2.38** (Figure 17c).

Computational approaches have also been taken to characterize the enone-π complexes, in the absence of direct experimental observation. DFT computational studies were carried out on the 1,4-addition of dimethyl zinc to dienone **2.39** (Scheme 56). The calculated activation energy for the 1,4-methylation of **2.39**, *via* transition state **2.41**, was 12.2 kcal/mol (11.7 kcal/mol was determined experimentally).[150] This appears to lend further support to the proposal of Gschwind and co-workers.[124]

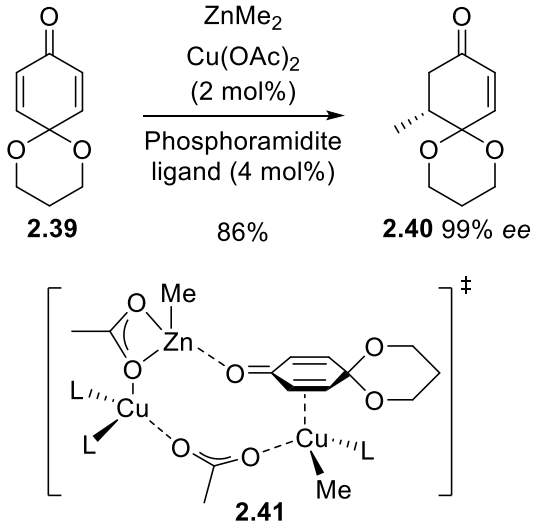

*Scheme 56: Transition state calculated for the 1,4-addition reaction between dienone **2.39** and dimethylzinc.*[150]

2.1.3 Aims and Objectives

For simplicity, in the mathematical equations and figures/schemes required throughout this chapter, the following abbreviations will be used for components of the model system (also listed in the abbreviations section): **A** (triethylaluminium); **Cu_a** (copper(II) acetate); **Cu_b** (Copper(I) tetrakis(acetonitrile) trifluoroacetate, trifluoroacetic acid adduct); **CX** (2-cyclohexen-1-one); **CX·A** (Lewis acid-base adduct with triethylaluminium); **CX·Zn** (Lewis acid-base adduct with diethylzinc); **E** (enolate product); **L** ((*R,S,S*)-Feringa's ligand); **P** ((*R*)-3-ethyl-cyclohexanone); **Zn** (diethylzinc).

The first aim of this project was to provide high-quality kinetic data, using a ReactIR to obtain a greater data density than previously obtainable using GC aliquot assays, which would help

elucidate the structure of the key transition state in the copper catalyzed 1,4-addition of triethylaluminium (using the model system shown in Scheme 57) to 2-cyclohexen-1-one.

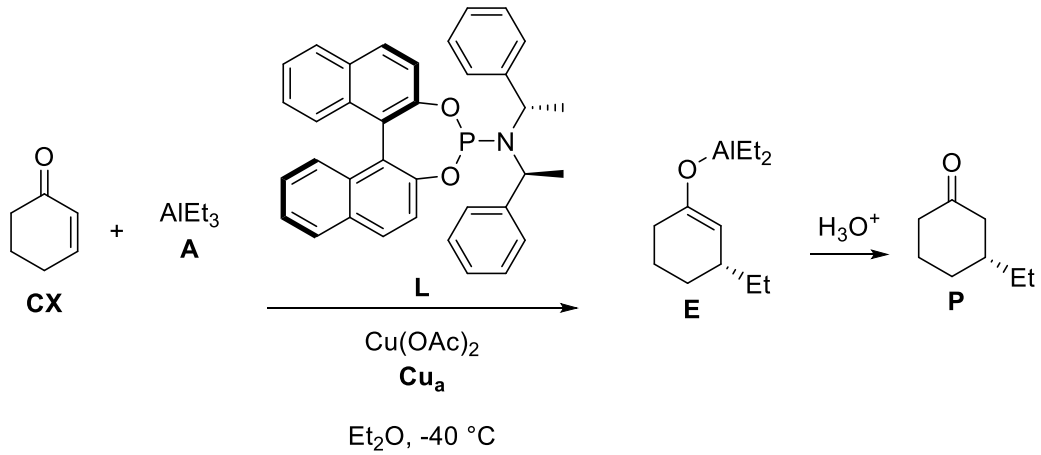

*Scheme 57: Model system used for kinetic studies of the 1,4-addition of **A** to **CX**.*

Furthermore, development of a novel copper(I) trifluoroacetate complex (**Cu_b**) was attempted, allowing further kinetic investigation of the more experimentally and theoretically challenging system shown in Scheme 58.

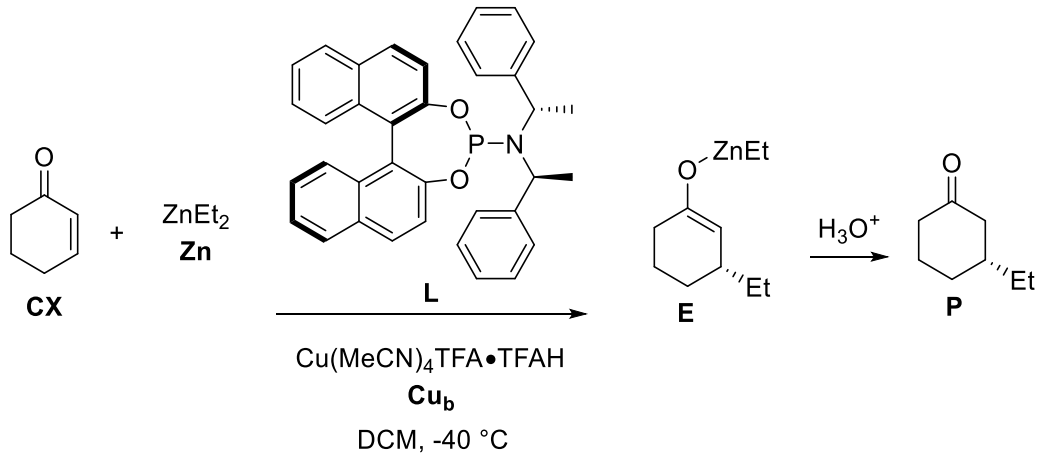

*Scheme 58: Model system used for kinetic studies of the 1,4-addition of **Zn** to **CX**.*

2.2 Results and Discussion

2.2.1 Kinetic Investigations Using Triethylaluminium

Mechanistic investigation of the ACA reactions of organoaluminium reagents was previously undertaken within the Woodward group.[††] These early studies relied upon the cryogenic GC sampling method of Krause, using the model system shown in Scheme 57.[151] This method involved taking aliquots of reactions, with liquid nitrogen cooled Pasteur pipettes, which were then quenched into acid immediately. The conversion and product *ee* in each aliquot could then be ascertained by GC analysis. This method unfortunately suffers due to its technical difficulty and the low data density that can be obtained.

By using this aliquot method to monitor conversion over the course of each reaction, non-linear least squares fitting of $[\mathbf{CX}]_{obs}$ to $[\mathbf{CX}]_{calc}=[\mathbf{CX}]_0\exp(-k_1t)$ enabled calculation of their rate constant (k_1) (Table 6; for further details, see experimental section). By varying only the concentration of ligand between runs and calculating each reaction's rate constant, a Ln-Ln plot could be generated (Figure 18). In this study, the natural logarithm of the rate constants were plotted against the natural logarithm of the concentrations of ligand. Usually, the gradient of the straight line generated gives the order in the varied component. In the case of Figure 18, two straight lines were generated. The first was from ligand acceleration, occurring at $[\mathbf{L}]/[\mathbf{Cu_a}]$ ratios between 0 to 3.5, which showed an order in ligand of 0.6. The second was from ligand deceleration, occurring at $[\mathbf{L}]/[\mathbf{Cu_a}]$ ratios greater than 3.5, which showed an order in ligand of -2.56. From this it can be observed that increasing the concentration of ligand (relative to copper) accelerates the ACA of **A** to **CX**, up to a point (where $[\mathbf{L}] = 3.5[\mathbf{Cu_a}]$). After this point, any additional ligand causes deceleration of the reaction.

An advantage of this method is that it enabled the measurement of the product *ee* as a function of time (each aliquot was analysed *via* chiral GC). It was observed that the product *ee* was lower in the initial stages of the reaction, only rising to observed final value (82%) after approximately 500 seconds (Figure 19). This suggests that there may be an induction period in the early stages of the reaction, in which the active catalytic species is forming.

[††] I should like to thank Dr. Darren Willcox again for his early studies into the ACA of organoaluminium reagents.

[L] (mM)	k_1 (s^{-1})
3.0	0.0021
4.5	0.0030
6.0	0.0034
9.0	0.0043
10.6	0.0028
13.6	0.0014
15.2	0.0011

Table 6: Early data from within the Woodward group, obtained via the cryogenic GC sampling method. Calculated k_1 values for varying concentrations of ligand. Across all experiments: $[\mathbf{Cu_a}] = 3.0$ mM; $[\mathbf{CX}]_0 = 303$ mM; $[\mathbf{A}]_0 = 364$ mM; performed in diethyl ether at -40 ˚C; k_1 values obtained the from non-linear least squares fitting $[\mathbf{CX}]_{obs}$ to $[\mathbf{CX}]_{calc}=[\mathbf{CX}]_0 exp(-k_1 t)$.

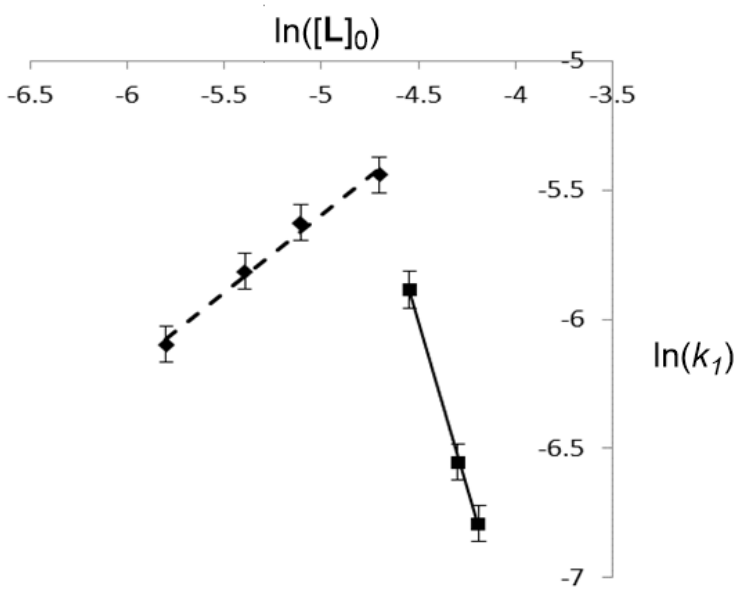

Figure 18: Ln-Ln plot generated from the data presented in Table 6. The order of the catalytic reaction shows both ligand acceleration (for $0<[\mathbf{L}]/[\mathbf{Cu_a}]<3.5$) and deceleration ($[\mathbf{L}]/[\mathbf{Cu_a}]>3.5$).[128]

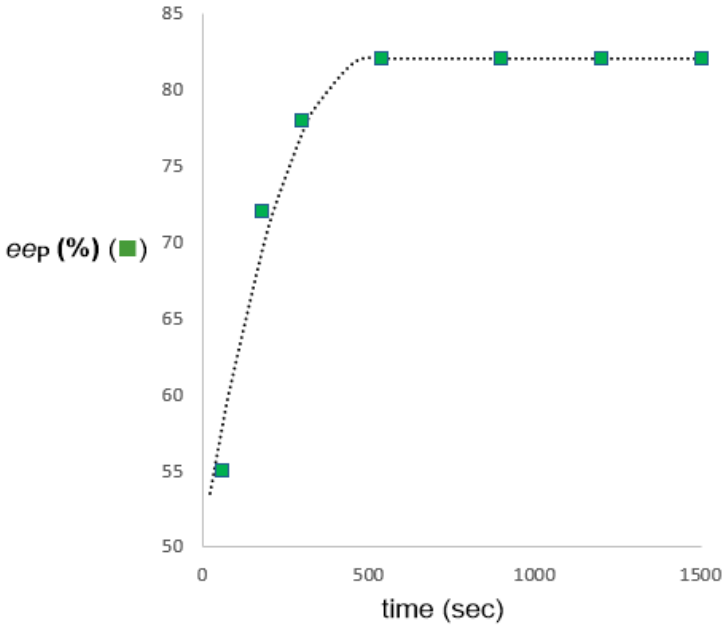

Figure 19: Variation of ee versus time, as monitored by chiral GC.[128]

As stated previously, one main disadvantage of this method is the low data density it provides. An alternative method of monitoring a reaction is the use of a ReactIR, which can generate an IR spectrum of a reaction up to every 10 seconds (*in situ* monitoring). Provided that the substrate/product of a reaction possesses an isolated IR signal that can be monitored (*i.e.* a signal that is not overlapping with any other signals), extremely high-density reaction monitoring data can be obtained *via* this method. Therefore, it was envisaged that a ReactIR could provide a complementary method of monitoring the ACA of triethylaluminium to 2-cyclohexen-1-one.

The carbonyl stretch of **CX** (ν 1676 cm^{-1} in diethyl ether) was initially selected as the stretch to be monitored. Spectra were recorded of the other reaction components and no detrimental signal overlaps were detected. However, mixing **CX** and **A** (1.2 equiv.), in diethyl ether at -40 ˚C, caused the formation of a bright yellow solution. Monitoring of the formation of this bright yellow solution showed the almost instantaneous consumption of the **CX** carbonyl IR stretch, as well as the concurrent formation of a new signal at 1630 cm^{-1}. Quenching of this solution and subsequent NMR analysis afforded quantitative recovery of the starting material. It was proposed that the formation of this new signal was due to the formation of a Lewis acid-base adduct (**CX·A**) between **CX** and **A** (Scheme 59). This proposal was investigated *via* the titration of **A** into a solution of **CX** (in *ca.* 0.1 equiv. aliquots). After each addition of **A**, the intensity of **CX**'s carbonyl stretch decreased and the intensity of the presumed carbonyl stretch of the

adduct increased (see Figure 20). From this titration, it was possible to fit a 1:1 binding isotherm (for further details, see experimental section) and calculate an association constant for the formation of adduct **CX·A**: *K = 12.0 M^{-1}*.

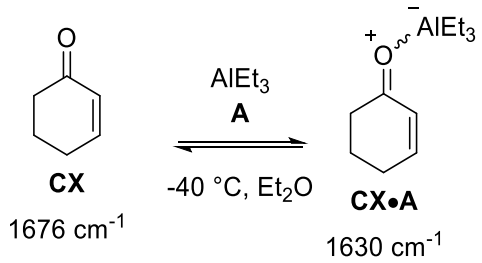

*Scheme 59: Proposed formation of the Lewis acid-base adduct **CX·A**.*

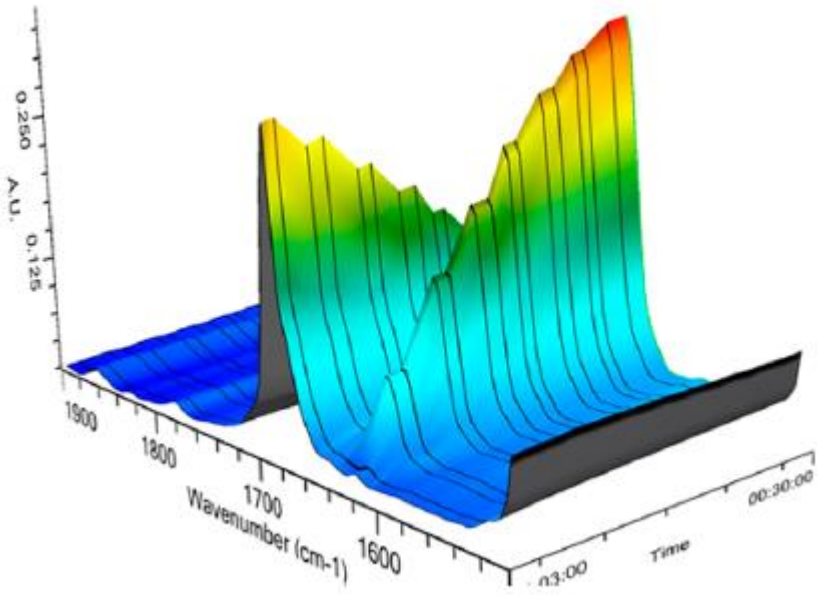

Figure 20: Results of the titration of triethylaluminium into a solution of 2-cyclohexen-1-one, obtained from the ReactIR.[128]

The rapid formation of adduct **CX·A** enabled the use of its carbonyl stretch (ν 1630 cm^{-1}) to monitor the ACA reaction of **A** to **CX** (Figure 21). Initial monitoring revealed a slower reaction rate in the first 300 seconds (Figure 22). Following the rapid formation of the adduct **CX·A**, an initially slow consumption of **CX·A** was observed. After 300 seconds, the consumption of **CX·A** (and the total **CX**) had accelerated and then followed first order behaviour. This supports the previously mentioned hypothesis that an induction period is present during the first 300 seconds of the reaction. During this time, formation of the active catalyst is occurring

simultaneously with substrate consumption. After the induction period, catalyst formation is complete and a single active species dominates catalysis.

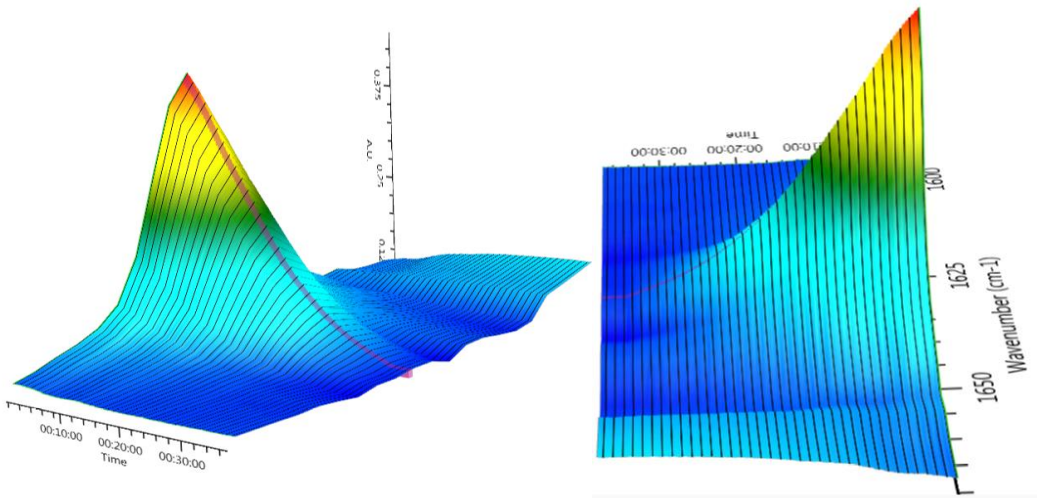

*Figure 21: Output from the ReactIR under standard reaction conditions, as seen from two different perspectives. Rapid formation followed by consumption of the signal at 1630 cm^{-1} (carbonyl stretch of **CX·A**) was monitored.*

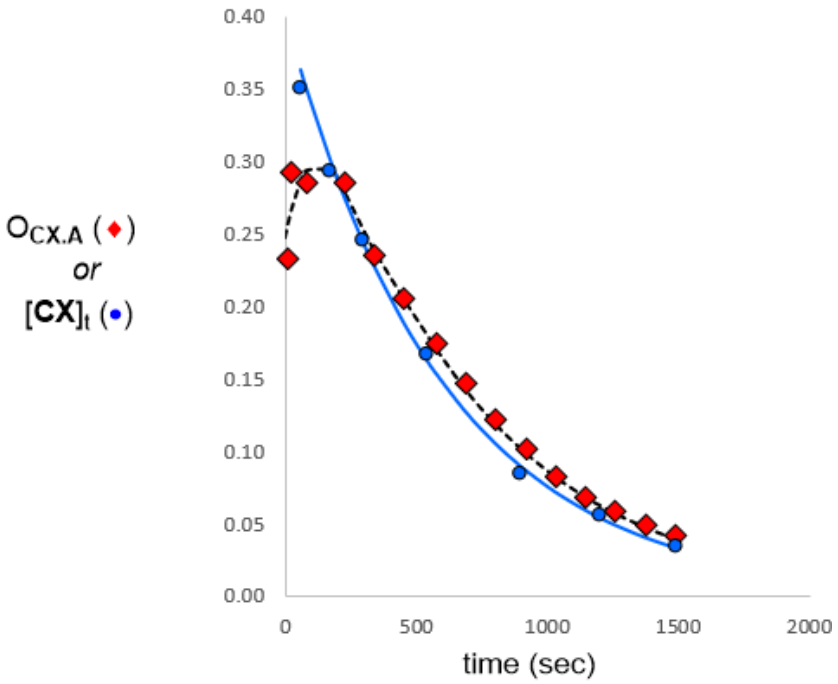

*Figure 22: Monitored absorption of adduct **CX·A** and calculated total **CX** as a function of time. Following the rapid formation of adduct **CX·A**, a slower induction period can be observed in the first 300 seconds. After this, first order consumption is observed.*[128]

In a manner similar to that described previously, but using the ReactIR, the rate constant (k_1) of a series of experiments were then determined. In these experiments, the concentration of one

reaction component was varied whilst the others were kept constant. Ln-Ln plots were then generated, in order to determine the order in each reaction component. Whilst the concentration of adduct **CX·A** added to each reaction could not be measured, it was calculated based upon the known values of $[\mathbf{A}]_0$ and $[\mathbf{CX}]_0$ and the previously calculated equilibrium constant (*K*) (for further details, see experimental section). The results of the experiments with varying $[\mathbf{CX{\cdot}A}]_0$ are summarized in Table 7 and the Ln-Ln plot generated shown in Figure 23. From these, it was deduced that the order in $[\mathbf{CX{\cdot}A}]_0$ is 1.

$[\mathbf{CX{\cdot}A}]_0$ (mM)	k_1 (s^{-1})
40.4	0.00024
124	0.000566
232	0.00194
300	0.001558

*Table 7: Calculated k_1 values for varying concentrations of adduct **CX·A**. Across all experiments: $[\mathbf{Cu_a}]_0$ = 3.1-3.6 mM; $[\mathbf{L}]_0$ = 4.8-5.2 mM; performed in diethyl ether at -40 ˚C; k_1 values obtained the from non-linear least squares fitting $[\mathbf{CX{\cdot}A}]_{obs}$ to $[\mathbf{CX{\cdot}A}]_{calc}=[\mathbf{CX{\cdot}A}]_0 exp(-k_1 t)$.*

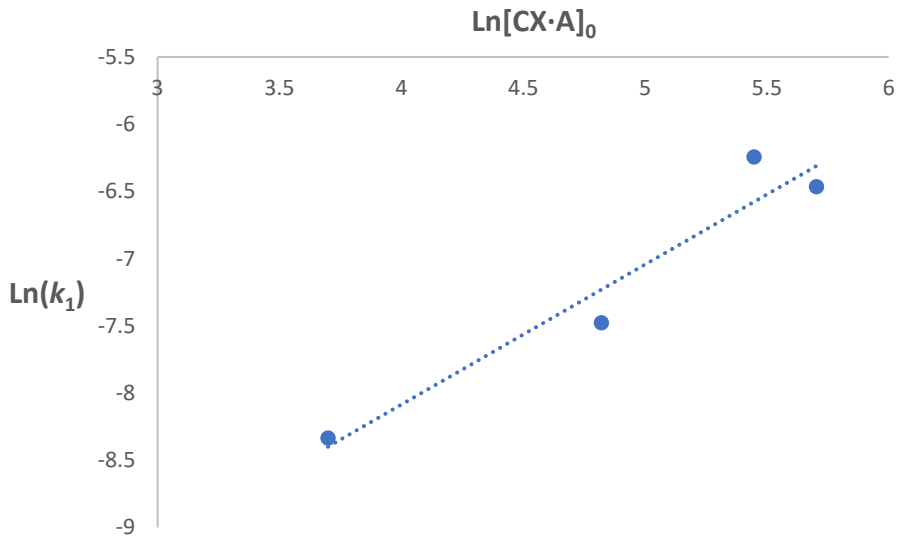

Figure 23: Ln-Ln plot generated from the data presented in Table 7, produced by varying $[\mathbf{CX{\cdot}A}]_0$. Repeated analyses gave a slope of 1.0 (±0.1).

The results of experiments with varying $[\mathbf{Cu_a}]_0$ are summarized in Table 8 and the Ln-Ln plot generated shown in Figure 24. Throughout these experiments the $[\mathbf{L}]_0/[\mathbf{Cu_a}]_0$ ratio was kept at

a constant 1.5, to prevent any changes in the copper-ligand association equilibrium affecting the reaction rate. From these experiments, it was deduced that the order of the reaction in $[\mathbf{Cu_a}]_0$ is 1.5.

$[\mathbf{Cu_a}]_0$ (mM)	k_1 (s^{-1})
1.1	0.000323
2	0.00049
3.8	0.001517
6.1	0.00433

Table 8: Calculated k_1 values for varying concentrations of $\mathbf{Cu_a}$. Across all experiments: $[\mathbf{CX{\cdot}A}]_0$ = 213-218 mM; $[\mathbf{L}]_0$ kept at 1.5 × $[\mathbf{Cu_a}]_0$; performed in diethyl ether at -40 ˚C; k_1 values obtained the from non-linear least squares fitting $[\mathbf{CX{\cdot}A}]_{obs}$ to $[\mathbf{CX{\cdot}A}]_{calc}=[\mathbf{CX{\cdot}A}]_0 exp(-k_1 t)$.

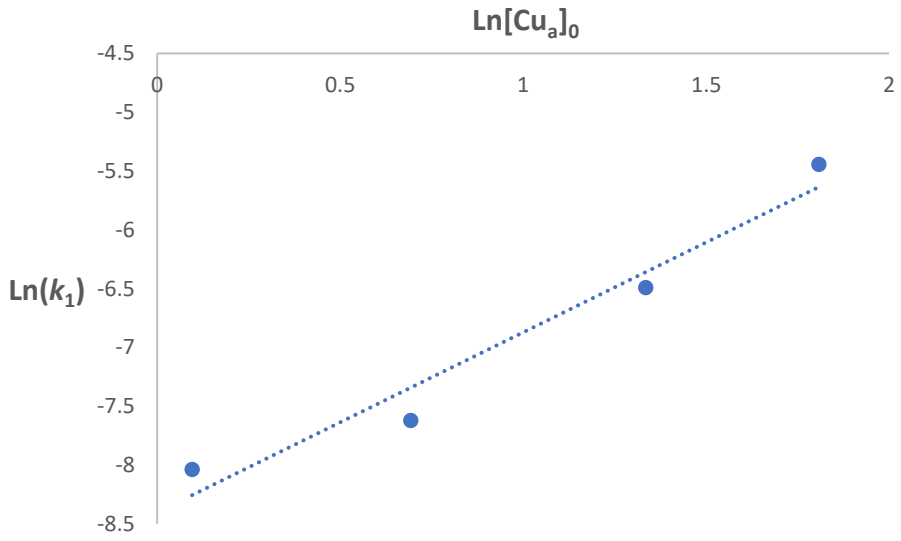

Figure 24: Ln-Ln plot generated from the data presented in Table 8, produced by varying $[\mathbf{Cu_a}]_0$. Repeated analyses gave a slope of 1.5 (±0.1).

Increasing the concentration of ligand, as already observed in the GC assay results, caused an initial acceleration in the reaction (up to $[\mathbf{L}]_0/[\mathbf{Cu_a}]_0$ = 3.5) before a secondary decelerating effect occurred at higher ligand concentrations. The greater data density obtained from the ReactIR method enabled the determination that the deceleration process fit better to a 0-order process rather than the 1st order seen previously. The results of these experiments are summarized in Table 9 (acceleration phase) and Table 10 (deceleration phase) and the corresponding Ln-Ln plots generated shown in Figure 25 (acceleration phase) and Figure 26 (deceleration phase).

From these experiments, averaged across several experiments including both ReactIR and GC data, it was deduced that the order of the reaction in $[\mathbf{L}]_0$ is 0.66 (acceleration) and -2.52 (deceleration).

$[\mathbf{L}]_0$ (mM)	k_1 (s^{-1})
1.7	0.000674
3.5	0.001066
5.5	0.001517
6.5	0.00194
11.7	0.00276

Table 9: Calculated k_1 values for varying concentrations of ligand up to $[\mathbf{L}]_0/[\mathbf{Cu_a}]_0 = 3.5$. Across all experiments: $[\mathbf{Cu_a}]_0 = 3.2\text{-}3.8$ mM; $[\mathbf{CX{\cdot}A}]_0 = 213\text{-}254$ mM; performed in diethyl ether at -40 ˚C; k_1 values obtained the from non-linear least squares fitting $[\mathbf{CX{\cdot}A}]_{obs}$ to $[\mathbf{CX{\cdot}A}]_{calc}=[\mathbf{CX{\cdot}A}]_0 exp(-k_1 t)$.

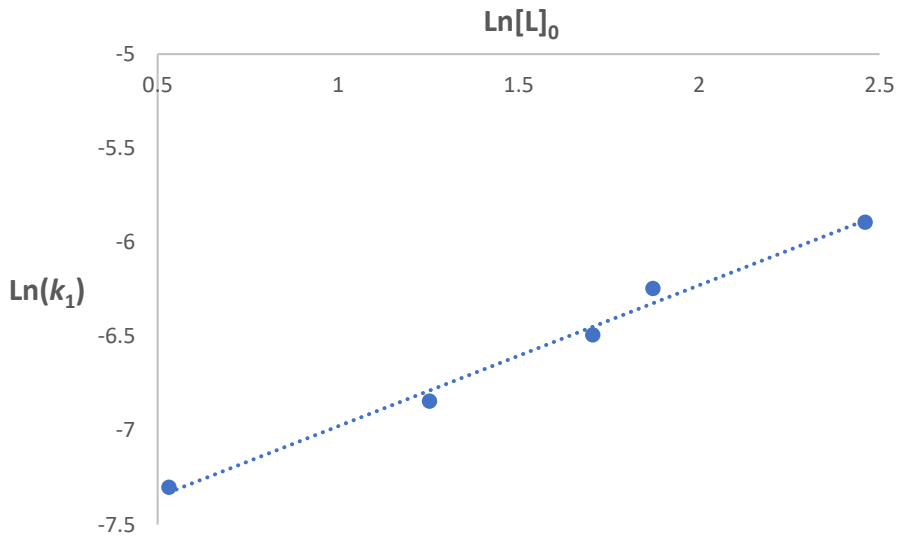

Figure 25: Ln-Ln plot generated from the data presented in Table 9, produced by varying $[\mathbf{L}]_0$. Analysis gave a slope of 0.74(5).

$[L]_0$ (mM)	k_0 ($M.s^{-1}$)
11.7	0.000456
13.6	0.000324
15.4	0.000235

Table 10: Calculated k_o values for varying concentrations of ligand greater than or equal to $[L]_0/[Cu_a]_0 = 3.5$. Across all experiments: $[Cu_a]_0 = 3.4$ mM; $[CX{\cdot}A]_0 = 220$-248 mM; performed in diethyl ether at -40 ˚C; k_0 values obtained the from non-linear least squares fitting $[CX{\cdot}A]_{obs}$ to $[CX{\cdot}A]_{calc}=[CX{\cdot}A]_0-k_0t$.

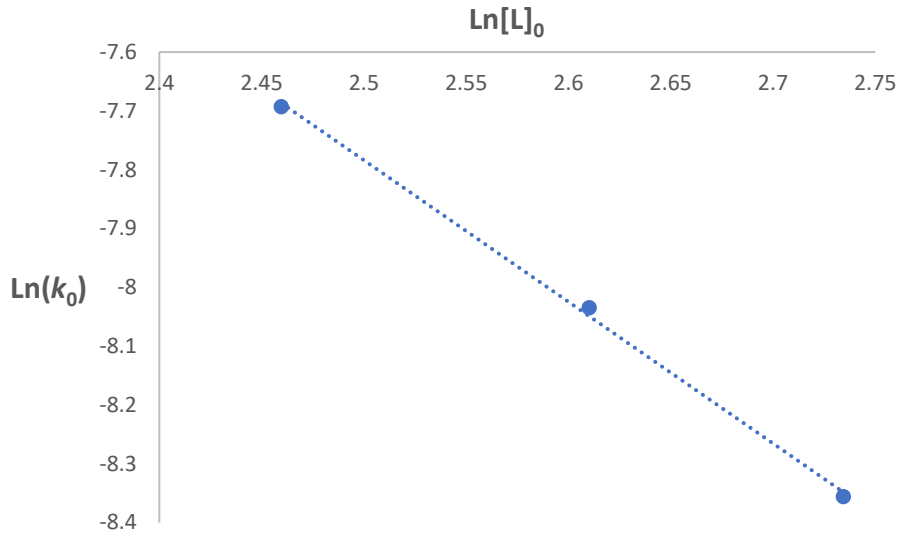

Figure 26: Ln-Ln plot generated from the data presented in Table 10, produced by varying $[L]_0$. Analysis gave a slope of -2.44(8).

The kinetic data are concordant with a rate law α $[\mathbf{CX{\cdot}A}]^1[\mathbf{Cu_a}]^{1.5}[\mathbf{L}]^{0.66}$. One simple transition state stoichiometry consistent with this rate law is: $[\mathbf{CX{\cdot}A}]_2[\mathbf{Cu_a}]_3[\mathbf{L}]_{1.33}$. This is inconsistent with the proposals described previously: Feringa *et* al proposed [**CX·M**][**Cu**][**L**] (Figure 15c – where **M** was a Grignard reagent); Noyori/Schrader *et al* proposed [**CX**][**M**]$_2$[**Cu**][**L**] (Figure 16 – where **M** was an organozinc); Gschwind *et al* proposed [**CX·M**][**Cu**]$_2$[**L**]$_3$ (Figure 17c – where **M** was an organozinc).

Based on the derived transition state stoichiometries, two simple potential transition states could be proposed: **2.42** or **2.43** (Figure 27). These both contain the correct stoichiometries of the reaction components, but **2.42** would be more consistent with the observation of an induction period. Reduction of the $\mathbf{Cu_a}$ is assumed to occur prior to the initiation of the reaction (by **A**), discounting it from causing the induction period. Also, redosing the experiment with a

second equivalent of **A** and **CX**, after completion of the reaction, instantaneously restarts catalysis with no observed second induction period. The recovered product also possesses a slightly higher *ee* than the product observed from the usual single dose experiments. This suggests the presence of **E** within the transition state, lending support to transition state **2.42** being the dominant active species.

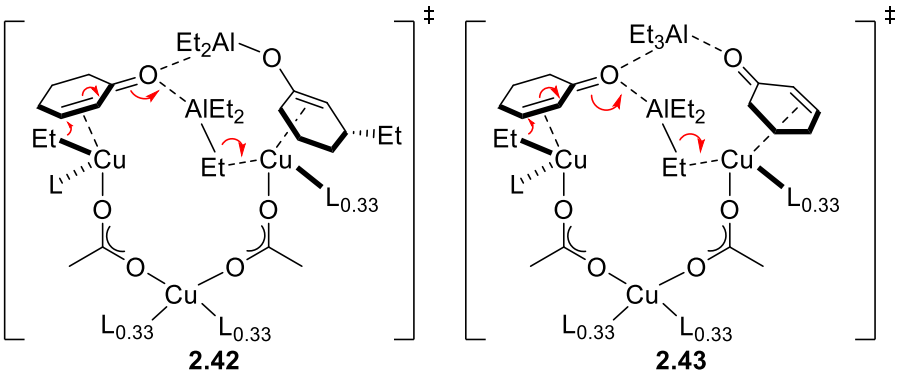

Figure 27: Two potential transition states that could be proposed based on the rate law obtained from kinetic investigations.[128]

A fractional rate order, as observed with the ligand in this system, can indicate an equilibrium occurring prior to the rate determining step. A complex mixture of equilibria could be occurring in the formation of the pre-catalyst (Figure 28), with the ligand exchanging with a variety of different copper(I) acetate aggregates. Whilst this cannot be ruled out based on this work, Gschwind's diffusion and ^{31}P NMR experiments demonstrated the formation of a single dominant pre-catalyst structure with bridging halides rather than acetates (**2.35** and **2.37**, see Scheme 17a and b).[146][148] Additionally, Schrader's ^{31}P NMR experiments found the ligand-copper equilibrium to be fast with a low activation barrier.[145]

From this work, an alternative proposal was made for the origin of the ligand's fractional rate order. This proposal first involves the formation of **2.48** upon the 'loading' of one ligand (Figure 29). This then possesses three potential sites for the second ligand to occupy (represented as a, b and c in **2.48**). If a random distribution of the ligand is assumed, then each of the three sites should have 0.33 ligands occupying them - *i.e.* a ligand occupies each site a third of the time (also shown in **2.42** in Figure 27). But, only in site a (which is proximal to the catalytic site) does the presence of a ligand have a strong effect on the reaction rate. Occupation in sites b or c would have a negligible effect on the reaction rate (as they are too far from the catalytic site).

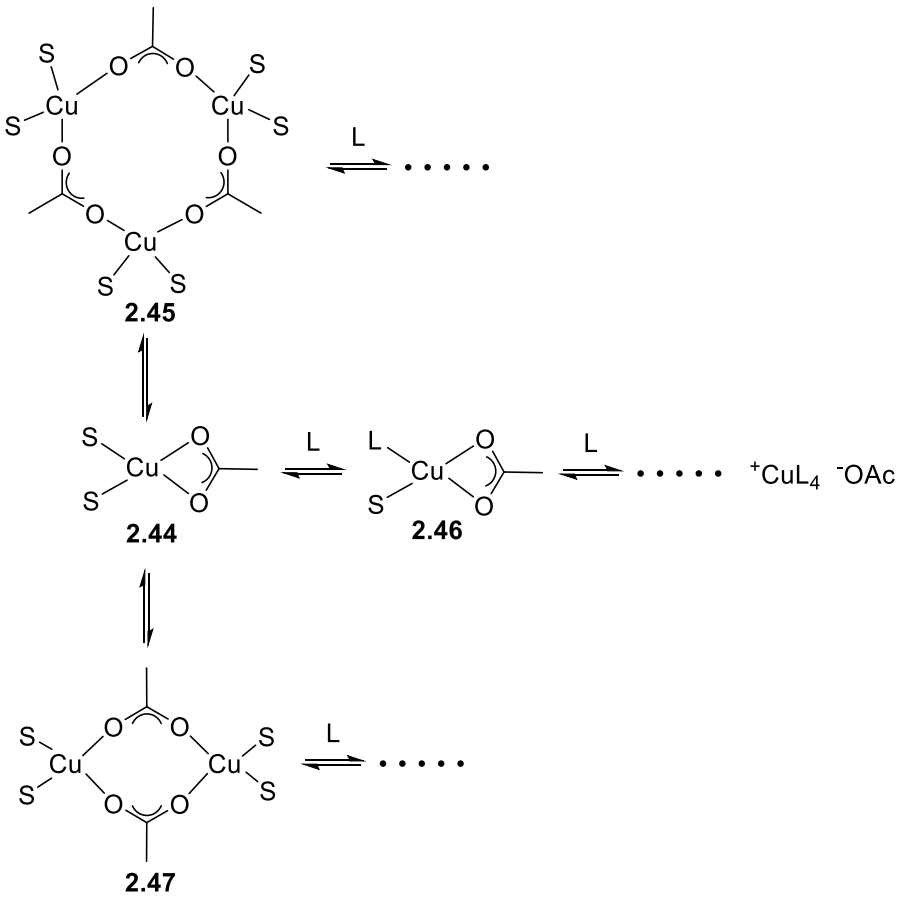

Figure 28: A sample of the complex mixture of equilibria that could exist within a mixture of copper(I) acetate and phosphine ligands in solution (where S indicates a solvent molecule). This involves equilibria between the exchanging solvent and ligand molecules as well as between monomeric, dimeric etc copper species.

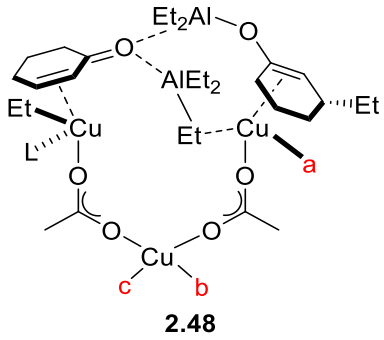

Figure 29: Describing the potential origin of the fractional order in ligand concentration.[128]

Based upon the observations described previously, the mechanism described in Scheme 60 was proposed for the ACA reaction of **A** and **CX**. This mechanism accounts for the observed induction period with the presence of **E** in the key transition state, as described previously. Each catalytic turnover releases a molecule of **E** and interconverts **2.49** and **2.50**, which reverses the roles of the two proximal copper atoms. When excess ligand is present, formation of the off-cycle non-

active **2.51** occurs (requiring up to 3 ligands). The unusual copper-(μ-Et)-copper motif proposed in **2.51** has been observed before, for a methyl group, *via* X-ray crystallography.[152] This therefore also accounts for the order of ligand inhibition observed ($\mathbf{L}^{-2.44}$).

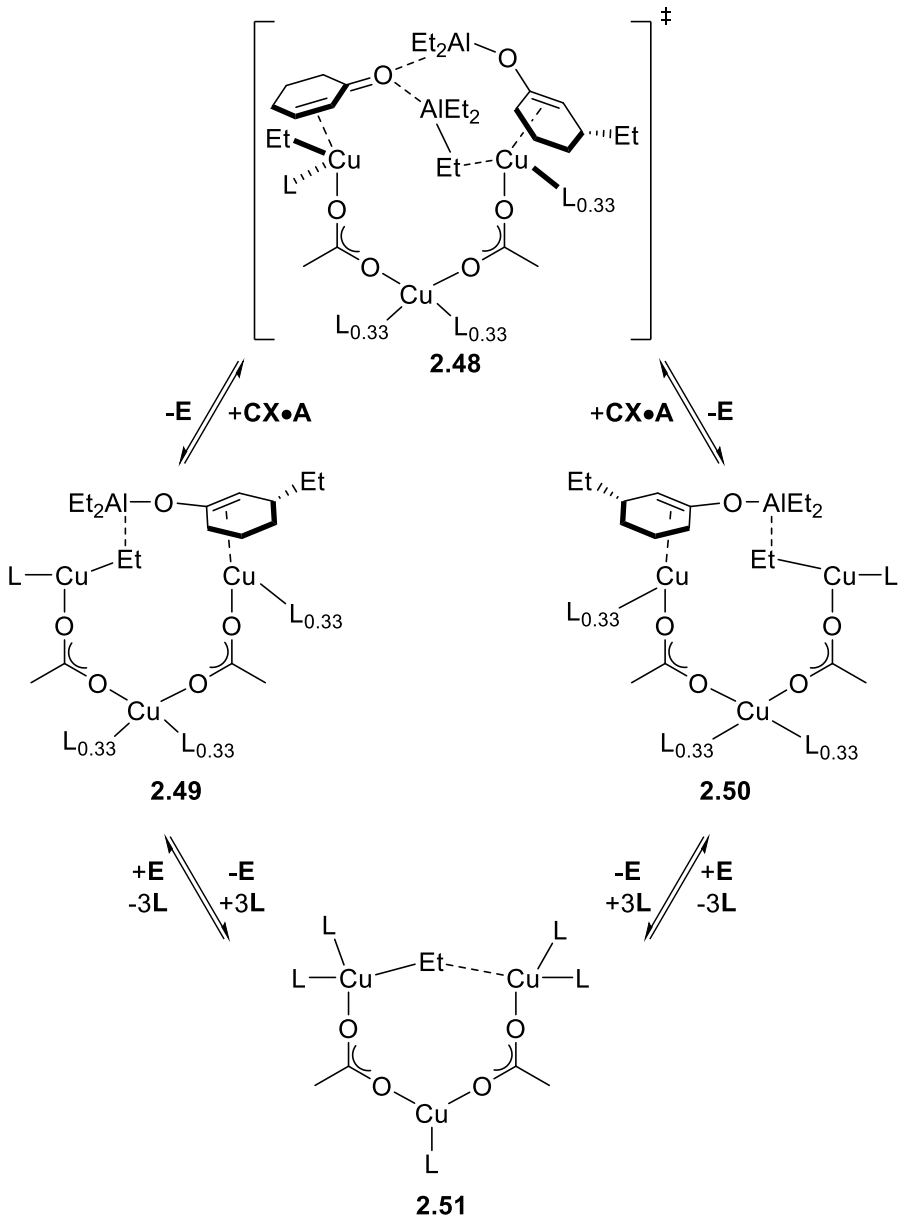

Scheme 60: Proposed mechanism for the ACA reaction of triethylaluminium and 2-cyclohexen-1-one.[128]

2.2.2 Synthesis and Application of a Novel Copper(I) Trifluoroacetate Complex

A search of the literature reveals very few examples of copper(I) trifluoroacetate complexes. Unligated copper(I) trifluoroacetate was reportedly synthesized by Petrukhina and co-workers, *via* vapor deposition.[153] In this publication, the authors comment on the extreme instability of copper(I) trifluoroacetate when not stabilized by additional ligands. A review of the complexes synthesized in the literature, summarized in Figure 30, demonstrates the usual requirement of multiple stabilizing and chelating ligands for a copper(I) trifluoroacetate complex to be isolable. Even these pseudo-stable complexes often require rigorously inert atmospheres to synthesize (usually requiring a glovebox).

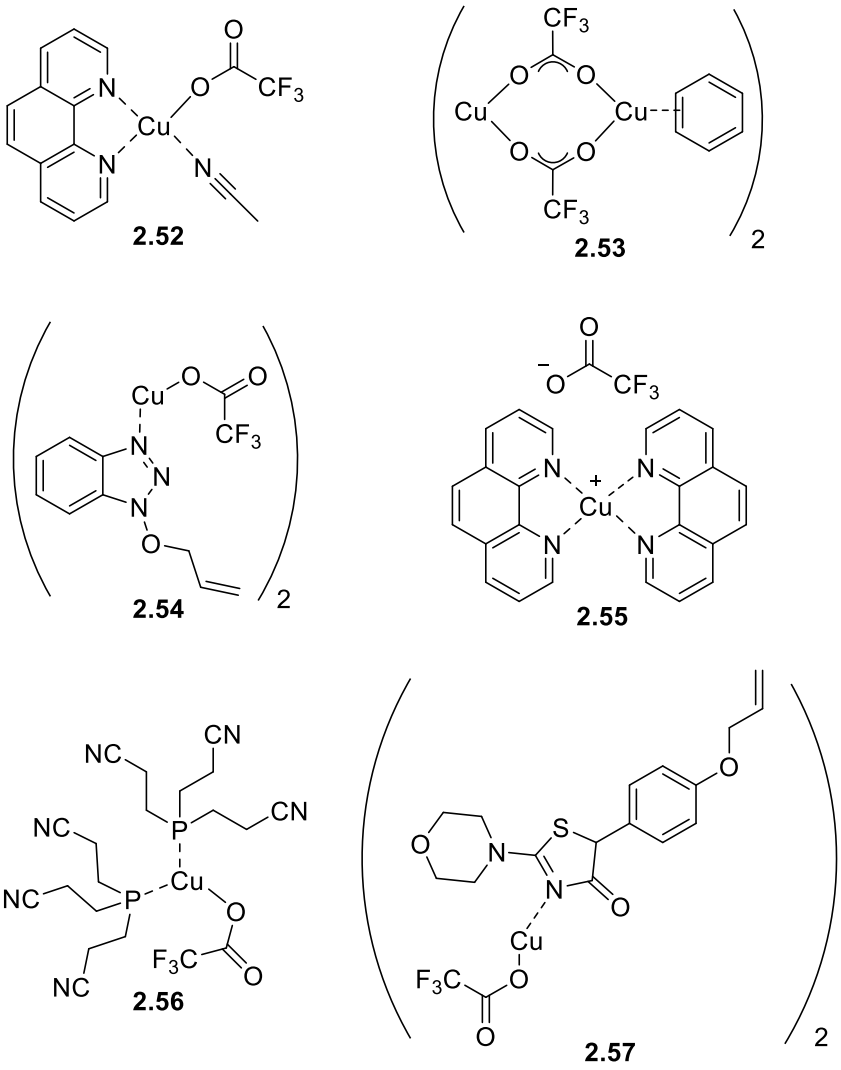

Figure 30: Examples of previously synthesized copper(I) trifluoroacetate complexes: ***2.52****,*[154] ***2.53****,*[155] ***2.54****,*[156] ***2.55****,*[157] ***2.56***[158] *and* ***2.57***.[159] *For clarity, additional chelating interactions have not been included.*

The instability of copper(I) complexes is not limited to the trifluoroacetate salt. The tendency of copper(I) complexes to disproportionate to the corresponding copper(II) complex and copper metal has been well documented and known since the beginning of the 20th century.[160] The rate of this disproportionation is controlled, in part, by the nature of the counter-ion, ligand and solvent.[161] The tendency of copper(I) species to increase their coordination number, especially when ligated with very electron withdrawing groups (such as trifluoroacetate), is the likely cause of their relative instability.[153] It is also likely the cause of why they tend to be extremely hygroscopic, as in the cases of copper(I) trifluoromethanesulfonate[162] and copper(I) acetate[163] (as well as copper(I) trifluoroacetate). The disproportionation of copper(I) salts is reversible and therefore provides a method for their synthesis, as well as being the cause of their decomposition. The solid-state reaction between copper metal and copper(II) acetate, at 220 ˚C under vacuum, is a reliable method for the synthesis of copper(I) acetate (Scheme 61a). This often provides a purer product than other methods, such as the reaction of copper(I) oxide and acetic acid-acetic anhydride, as it produces no by-products or partial hydrates/solvates (Scheme 61b).[163]

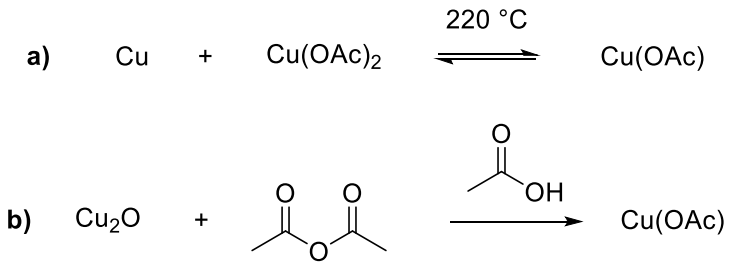

*Scheme 61: Common methods used to synthesize copper(I) acetate: **a)** solid-state reaction of copper metal and copper(II) acetate; **b)** reaction of copper(I) oxide with acetic acid-acetic anhydride.*

It was initially hypothesized that the synthesis of a copper(I) trifluoroacetate salt would be useful, for continuing studies on ACA, for two reasons: first, the addition of a fluorine containing group would give a new NMR active tag for *in situ* monitoring of an ACA reaction; and secondly it may provide a more active catalyst due to the destabilized nature of the copper. This proposition is supported by the work of Welker *et al* who compare the activation energy of two related copper-phosphoramidite catalyzed 1,4-additions.[150] The more Lewis acidic copper(II) trifluoromethanesulfonate containing complex (E_a = 6.7 kcal.mol^{-1}) shows a reduced activation energy when compared to copper(II) acetate (E_a = 12.2 kcal.mol^{-1}). Two initial attempts were made to synthesize the simplest previously known copper(I) trifluoroacetate complexes **2.52** and **2.53** *via* their published procedures.[154][155] The synthesis of copper(I)-phenanthroline-trifluoroacetate complex, of Weng and co-workers (Scheme 62a), involved a multi-step

synthetic sequence. First, copper(I) chloride was converted to copper(I) *tert*-butoxide (*via* salt metathesis); after which, the ligand and then the acid were added. Whilst the product was observed *via* MS and NMR, the purification of this complex proved to be non-trivial. The simpler procedure of Rodesiler and Amma (Scheme 62b), whilst more attractive due to its simplicity, unfortunately afforded no identifiable product.

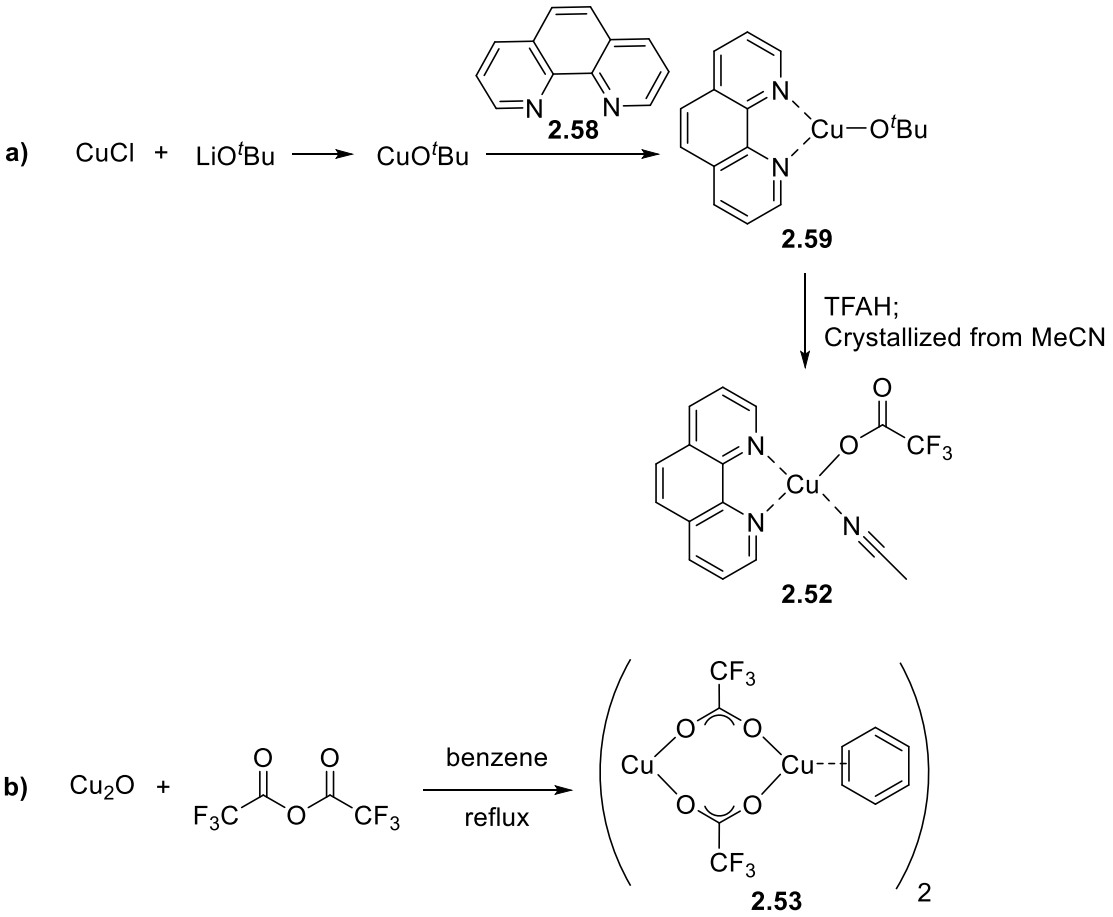

Scheme 62: Attempted syntheses of copper(I) trifluoroacetate complexes: ***a)*** *synthesis of* ***2.52*** *by the method of Weng and co-workers;*[154] ***b)*** *synthesis of* ***2.53*** *by the method of Rodesiler and Amma.*[155]

Copper(I) complexes possessing four acetonitrile ligands, with an acid salt counterion, have become extremely common. They are often practically very simple to synthesize, usually just requiring the addition of the corresponding acid to an acetonitrile suspension of copper(I) oxide. They are also relatively air stable for short periods, stable enough that they usually do not require a glovebox to use and many are commercially available.‡‡ Copper(I) tetrakisacetonitrile tetrafluoroborate,[164] hexafluorophosphate,[165] trifluoromethanesulfonate[166] and

‡‡ For example copper(I) tetrakisacetonitrile trifluoromethanesulfonate and hexafluorophosphate are available from https://www.sigmaaldrich.com/catalog/product/aldrich/685038?lang=en&region=GB and https://www.sigmaaldrich.com/catalog/product/aldrich/346276?lang=en&region=GB respectively.

perchlorate[167] are all known (to name only a small selection of the known salts). Furthermore, examples of these salts as catalysts in 1,4 conjugate additions are known, such as the use of copper(I) tetrakisacetonitrile tetrafluoroborate as shown in Scheme 63.

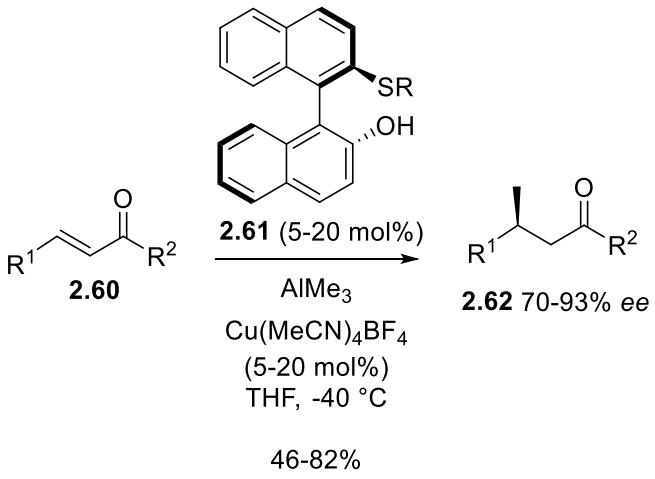

Scheme 63: Example of the use of copper(I) tetrakisacetonitrile tetrafluoroborate as a catalyst for the ACA of trimethylaluminium to linear enones.[168]

The addition of trifluoroacetic acid to a suspension of copper(I) oxide in acetonitrile, in the same manner to that commonly applied in the synthesis of related compounds, caused the rapid formation of a colorless, homogeneous solution (Scheme 64). In the related synthesis of copper(I) tetrakisacetonitrile tetrafluoroborate, chilling this solution to 0 ˚C causes the crystallization of the desired product as colorless plates. These plates can be easily collected by filtration in the open air. Unfortunately, the trifluoroacetate complex demonstrated a higher solubility in acetonitrile; meaning that no crystallization was observed upon chilling (even to -20 ˚C). Instead, the solvent and residual acid had to be removed *in vacuo* and replaced with a dichloromethane:diethyl ether mixture. Small, colorless needles of **Cu_b** were obtained from this solvent mixture. These crystals were able to be quickly weighed in the open air but begin to turn blue if left exposed to air for any extended period of time.

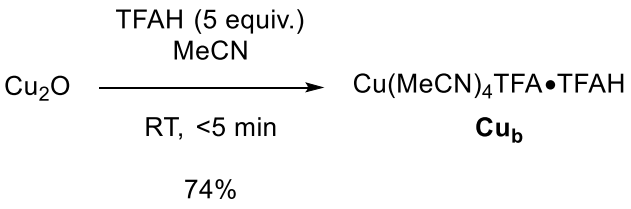

*Scheme 64: Formation of copper(I) tetrakisacetonitrile trifluoroacetate, trifluoroacetic acid adduct (**Cu_b**).*

The solvent system was altered to enable the direct crystallization of **Cu$_b$** from the reaction mixture (Scheme 65). However, this resulted in the formation of bright blue crystals. X-ray crystallographic analysis of these crystals (see Figure 31) identified the alternative product as a polymeric copper(II) trifluoroacetate chain with the repeating unit $[Cu_4TFA_{10}]^{2-}$. For every one of these repeating units, two copper(I) tetrakisacetonitrile cations are present. This product highlights the instability of copper(I) complexes towards disproportionation. The same complex can also be found in old samples of **Cu$_b$** that have been left in air.

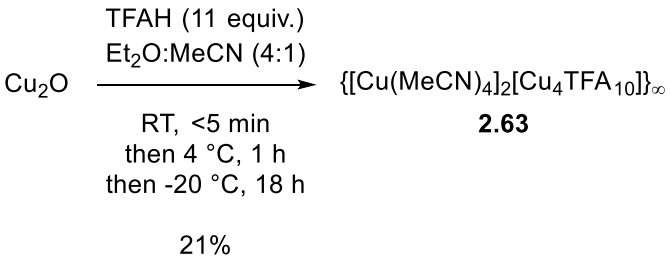

*Scheme 65: Modification of the conditions used to form **Cu$_b$** lead to the formation of polymeric structure **2.63**.*

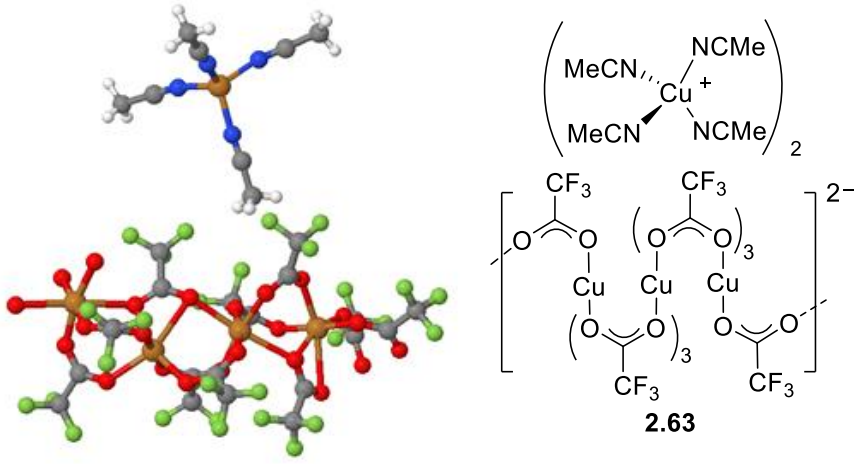

*Figure 31: Molecular structure of $\{[Cu(MeCN)_4]_2[Cu_4(TFA)_{10}]\}_\infty$ (**2.63**, as determined via x-ray crystallography) and its schematic representation. For clarity, only one of the equivalent $[Cu(MeCN)_4]^+$ cations is shown.*

As an additional piece of structural confirmation, as well as demonstrating the ability of **Cu$_b$** to act as a P-ligand ligated catalyst precursor, **Cu$_b$** was reacted with two equivalents of tricyclohexylphosphine (see Scheme 66). Other than a small amount of protonated tricyclohexylphosphine, quantitative conversion to complex **2.64** was observed. This reactivity agrees with that previously described for the corresponding tetrafluoroborate complex.[169]

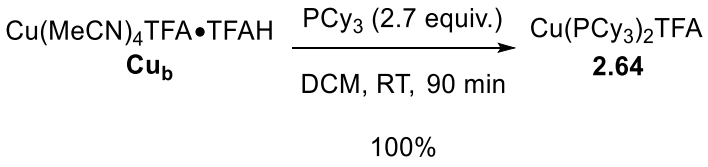

*Scheme 66: Quantitative formation of complex **2.64** observed, in the same manner as previously observed with copper(I) tetrakisacetonitrile tetrafluoroborate.[169]*

The competency of **Cu_b** as a catalyst precursor for asymmetric conjugate additions was then examined. Using the standard conditions, described in Scheme 67, the asymmetric conjugate additions of organozinc reagents, to a range of α,β-unsaturated carbonyl compounds, was examined (see Figure 32 for the compounds used and see Table 11 for the results of these trials). Preliminary investigations revealed that **Cu_b** was not a competent catalyst for the asymmetric conjugate addition of organoalanes (**A**). However, it proved to be an extremely efficient catalyst for use with organozinc reagents, providing rapid reactions and high enantioselectivities for both diethylzinc (**Zn**) and dimethylzinc. Reduced reaction rates were observed for chalcone and benzylideneacetone, due to the more hindered nature of the π* orbital, as is commonly observed. A reduction in stereoselectivity is also observed, as the literature predicts (68% *ee*[170] and 76%[138] *ee* are two of the highest results reported with diethylzinc in the literature), when non-cyclic, aliphatic 3-nonen-2-one was used.

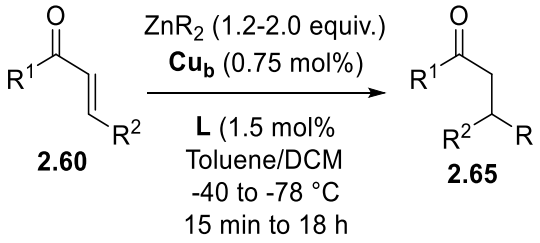

Scheme 67: General conditions for the asymmetric conjugate addition reactions described in Table 11.

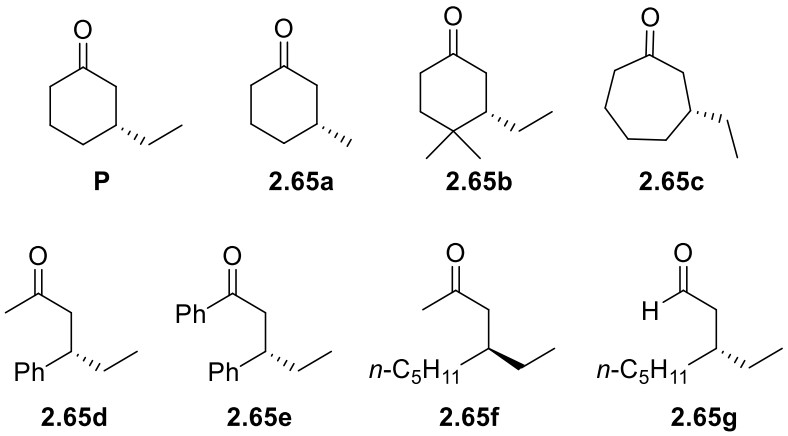

*Figure 32: Derivatives of **2.65** synthesized via the conditions described in Scheme 67.*

Derivative	Temperature (˚C)	Time	Yield (%)	*er*
P	-40	18 min	88	98:2
2.65a	-40	18 h	46	>99:1
2.65b	-40	18 h	98	>99:1
2.65c	-78	2 h	40	95:5
2.65d	-40	4 h	76	96:4
2.65e	-40	4 h	90	96:4
2.65f	-40	4 h	65	79:21
2.65g	-30	15 min	39	58:42

*Table 11: Results of the synthesis of **2.65** derivatives via the conditions described in Scheme 67.*

Direct asymmetric conjugate additions to α,β-unsaturated aldehydes are rare due to the increased reactivity of the aldehyde vs. ketones. This often results in 1,2-addition being more favoured that 1,4-addition, as well as the dimerization of the enolate products with the aldehyde starting materials. Some copper/ligand systems have been developed to afford good levels of selectivity by the groups of Alexakis[171] and Córdova.[172] Alternatively, indirect methods have been developed within the groups of Feringa[173] (using chiral enol acetates as intermediates) and Tomioka[174] (using sulfonylaldimines as intermediates). In this work, reasonable 1,4 vs. 1,2-addition selectivity (>10:1) was obtained when synthesizing **2.65g** (but no enantioselectivity). This demonstrates the potential of $\mathbf{Cu_b}$ to catalyze 1,4-additions to α,β-unsaturated aldehydes, with some ligand optimization required to improve the enantioselectivity.

However, no conversion was observed at any temperature for β-substituted derivative **2.66** or for linear, aliphatic α,β-unsaturated ester **2.67**. These are often considered among the most challenging substrates for asymmetric conjugate additions, due to the extremely hindered π* orbital of **2.66** and the less electrophilic β-carbon of **2.67**. Modest conversion was observed for cinnamaldehyde (**2.68**) and lactone **2.69**, but they had poor chemoselectivity and were slow. 2-Cyclopenten-1-one (**2.70**) is known to be a challenging substrate, due to the highly reactive nature of its enolate product. This often results in polymerization side-reactions. Which was also observed in this work, with full consumption of the starting material but little/no isolable product.

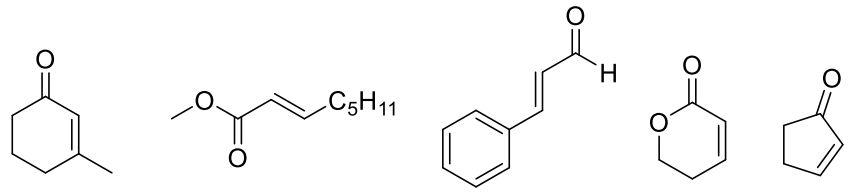

Figure 33: α,β-Unsaturated carbonyl derivatives that were not successfully used as substrates.

Comparison of the rate of the 1,4-addition of **Zn** and dimethylzinc to **CX**, catalyzed by $\mathbf{Cu_b}$, to the fastest examples in the literature showed that it performed as least as well as the other most efficient systems. The addition of **Zn** occurred within two hours, at -78 ˚C, with low catalyst loadings (0.8 mol% of $\mathbf{Cu_b}$ and 1.5 mol% **L**). The addition of dimethylzinc occurs within 18 hours, at -40 ˚C, with the same low catalyst loading. For comparison, the 9 other most efficient systems are shown in Table 12 (for **Zn**) and Table 13 (for dimethylzinc).

Temp (˚C)	Time (h)	Cu, L (mol%)	Yield (%)	*ee* (%)	Ref.
-78	2	0.8, 1.5	>90[a]	96	This work
-80	24	1, 1	79	83	[175]
-78	5	2, 4	54	88	[176]
-78	16	4, 4	>99	88	[177]
-78	16	4, 4	91	50	[178]
-40	3	5, 11	>99	85	[179]
-40	4	1, 2	98	79	[180]
-40	24	1, 2.5	70	98	[181]
-35	3	1.2, 2.5	>99	89	[182]
-30	1	0.5, 1	95	96	[183]

*Table 12: The 10 most active known copper-catalyzed 1,4-additions of diethylzinc (**Zn**) to cyclohex-2-en-1-one (**CX**). [a] Conversion.*[§§]

Temp (˚C)	Time (h)	Cu, L (mol%)	Yield (%)	*ee* (%)	Ref.
-40	18	0.8, 1.5	>90[a]	98	This work
-40	24	1, 2.5	70	98	[181]
-40	24	1, 2.5	59	99	[184]
-30	3	3, 3.3	91	82	[185]
-30	12	1, 2.4	71	98	[186]
-30	12	2, 4	>99	93	[187]
-30	23	1, 2.4	n.d.	49	[188]
-20	12	2, 4	97	90	[189]
0	10	25, 25	63	80	[190]
0	48	10, 10	62	45	[174]

*Table 13: The 10 most active known copper-catalyzed 1,4-additions of dimethylzinc to cyclohex-2-en-1-one (**CX**). [a] Conversion.*[8]

[§§] I should like to thank Prof. Simon Woodward for compiling the data on the fastest 1,4-additions of diethylzinc and dimethylzinc to **CX**.

The initial investigations into the chemoselectivity of the 1,4-addition reaction of **Zn** to **CX** catalyzed by **Cu_b** found that another by-product was forming in the reaction (in an approximate ratio of 4:1 desired:undesired, as determined by proton NMR). This by-product was isolated *via* column chromatography, characterized and determined to be dimeric product **2.71** (see Scheme 68) as a mixture of two diastereomers (with a *dr* of 87:13). Similar dimerization reactions have been observed in 1,4-addition reactions to **CX**.[191] In subsequent reactions, the ratio of desired to undesired product was found to be highly variable. Alteration of the quench conditions - from addition of 1 M HCl and immediate warming to RT, to adding methanol and continuing to stir at the same temperature for 5 minutes before allowing to warm to RT – completely halted formation of by-product **2.71**. Alternatively, if half an equivalent of **P** was added to the reaction mixture, after the reaction had been allowed to run to completion, which was then stirred for a further ten minutes before quenching, then a greatly increased yield of **2.71** was observed. This led to the conclusion that **2.71** was forming during the quench, when the reaction temperature was increasing and both the enolate **E** and product **P** were present in the reaction mixture.

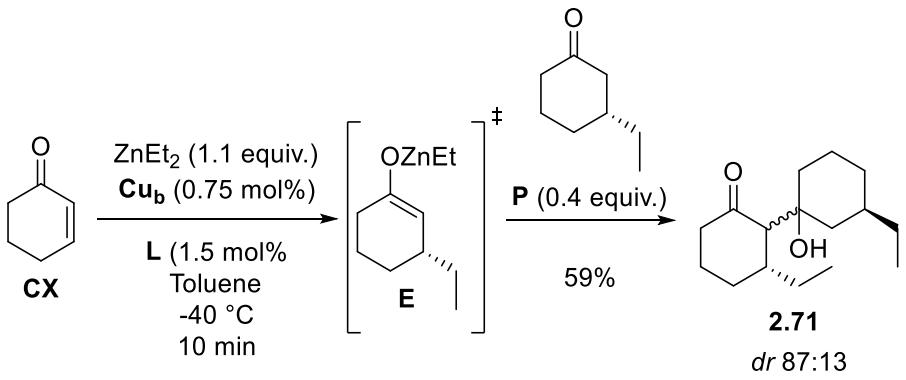

*Scheme 68: Aldol reaction between 1,4-addition product (**P**) and intermediate enolate (**E**).*

2.2.3 Kinetic Investigations Using Diethylzinc

To begin the kinetic investigation into the **Cu_b** catalyzed 1,4-addition of **Zn** to **CX**, identical conditions to those used in previous studies (with **Cu_a** and **A**, see Scheme 57) were employed. The results of this initial investigation are shown in Figure 34. It was observed that the reaction occurred at a remarkably rapid rate, with a half-life of less than 30 seconds. This was not conducive towards obtaining useful kinetic data, as the rate of addition was too rapid (not enough data was collectible in the reaction's time period).

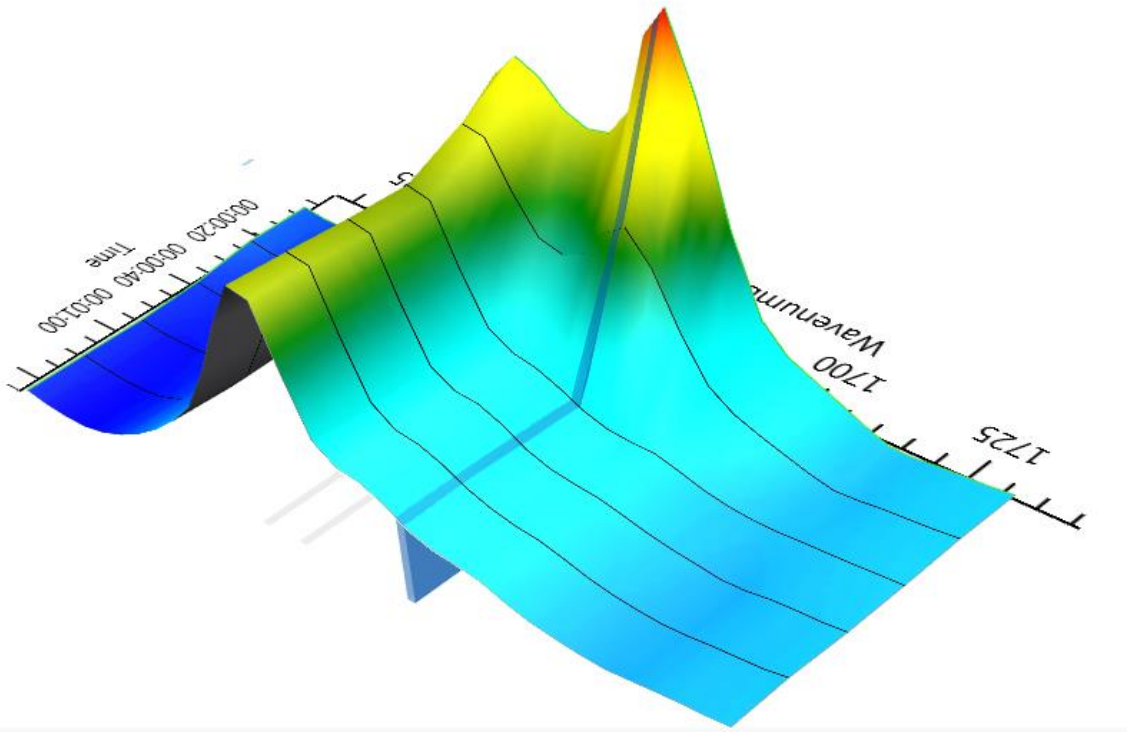

*Figure 34: ReactIR output of initial trial of the **Cu_b** catalyzed 1,4-addition of **Zn** to **CX**, at -40 ˚C.*

Cooling the reaction to -78 ˚C to reduce the reaction rate, a solvent screen was then performed to find more appropriate reaction conditions (the results of which are summarized in Table 14). The rate of reaction appears to increase, with decreasing donor number of the solvent used (except for with diethyl ether). The donor number is defined as the negative change in enthalpy for the interaction of the electron pair donor with antimony(V) chloride in a highly diluted dichloroethane solution.[192] The reduction in rate of reaction with increasing donor number is likely due to the increased stability of the organometallic species (stabilized by the Lewis acid-base interaction of the solvent and organometallic). However, both diethyl ether and toluene afford very rapid reaction times despite their very different donor numbers.

Solvent	Conversion at 45 min (%)	Donor Number (kcal.mol^{-1})
Diethyl ether	>98	19
Toluene	90	0.1
DCM	60	1.0
Ethyl acetate	40	17
THF	<5	20

*Table 14: Relative conversion of **CX** to **E** after 45 min, with **Zn** (1.2 equiv.), **Cu$_b$** (0.75 mol%), **L** (1.5 mol%), at -78 ˚C as determined by ^{1}H NMR spectroscopy. The donor number for each solvent is also included, as reported by Gutmann.*[192]

Portionwise titration of **Zn** into solutions of **CX** in diethyl ether or toluene results in the formation of a carbonyl stretch at *ca.* 1660 cm^{-1} and the consumption of another carbonyl stretch at *ca.* 1685 cm^{-1} which correspond to **CX·Zn** and **CX** respectively (see Figure 35). When dichloromethane was used as the solvent, the two stretches are not well separated, and a single broad signal was observed.

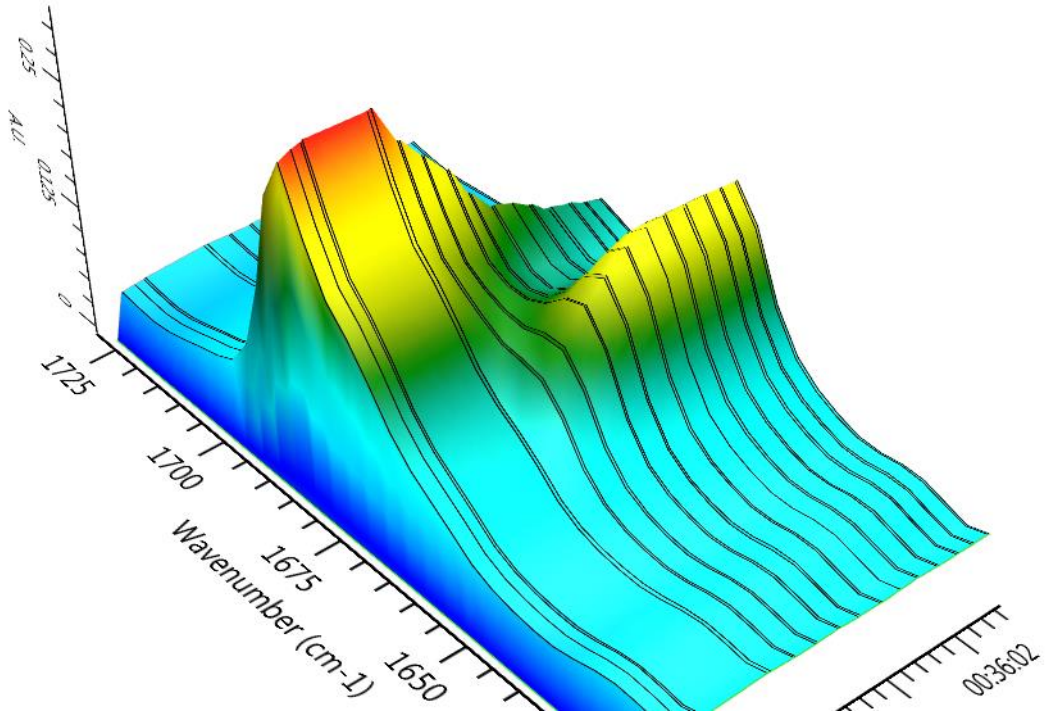

*Figure 35: ReactIR output from the titration of **Zn** into a solution of **CX** in diethyl ether at -40 ˚C.*

From these titrations, the equilibrium constant could be calculated for both diethyl ether and toluene (for further details, see experimental section). A complicating factor in this system, as opposed to the previous system (with **A**) is the potential for **Zn** and **CX** to bind in either a 1:1 (**2.72**) or 1:2 (**2.73**) manner (see Scheme 69). The results of these calculations are summarized in Table 15. In both solvents, the 1:1 adduct is the best fit, although it is not overly, significantly favoured. With either adduct, there is a correlation between equilibrium constant and the donor number of the solvent. The equilibrium constant is higher in toluene than in diethyl ether – *i.e.* higher in a solvent with a low donor number. Due to the potential for these adducts to undergo rapid exchange, and the similarity in quality of fit of the data for each adduct, accurate identification and quantification of the transmetalating species was unlikely. For this reason, dichloromethane was chosen as the solvent for further kinetic investigations. This enabled monitoring of the formation of **E** *via* its C-O stretch at 1145 cm^{-1} as well as providing an appropriate rate of reaction at -40 ˚C. This allowed direct monitoring of the reaction by multinuclear NMR as well as ReactIR.

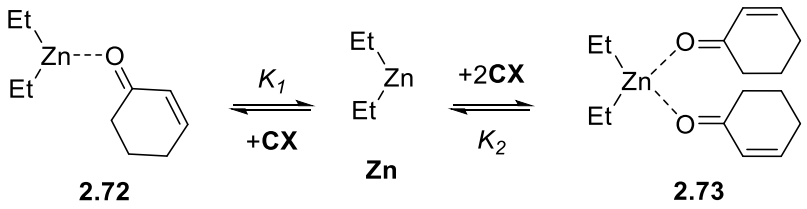

*Scheme 69: Potential Lewis acid-Lewis base adducts formed between **Zn** and **CX**.*

	Value (toluene)	**R^2 (toluene)**	**Value (diethyl ether)**	**R^2 (diethyl ether)**
K_1 (M^{-1})	4.5	0.99	0.69	>0.99
K_2 (M^{-2})	11	0.98	1.4	0.99

*Table 15: Equilibrium constants and qualities of fit calculated from the titrations of **Zn** into solutions of **CX**.*[193]

Using the model system described previously in Scheme 58, a reproducible *ee* of 96% was obtained (in a reaction time of *ca*. 700 s). However, when the rate constant was determined from the ReactIR data of duplicate runs (for further details of the determination of rate constants, see experimental section), it was shown to be poorly reproducible (see Figure 36). This apparently random variation (or at least unpredictable) in rate constant suggested the

presence of a slow, varying induction period. The variability of derived rate constants in related reactions was also observed in the work of Pfretzschner *et al*.[145]

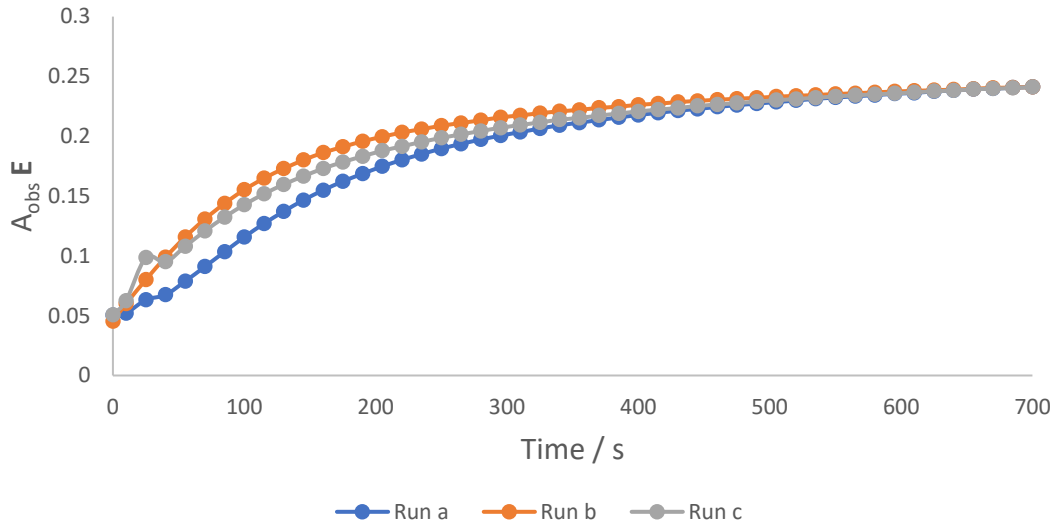

Figure 36: Duplicate runs of the first dose. Derived rate constants are: k_{1a} = 4.3 × 10^{-3} s^{-1}, k_{1b} = 8.4 × 10^{-3} s^{-1}, k_{1c} = 6.6 × 10^{-3} s^{-1}.[193]

A slow, varying induction period, lasting most of the initial reaction, was suspected to be causing this irreproducibility. To confirm this, multiple dose experiments were carried out. Addition of a second and third dose of **Zn** and **CX**, after completion of the previous dose, found that both doses afforded identical and reproducible rate constants (with correction for a change in concentration to allow for the dilution of the reaction). A summary of the triple dose experiment is shown in Figure 37 and an example output from the ReactIR is shown in Figure 38. Due to the high reproducibility observed from the 2nd and 3rd dose, a double-dose protocol was adopted for the subsequent reaction component order studies.

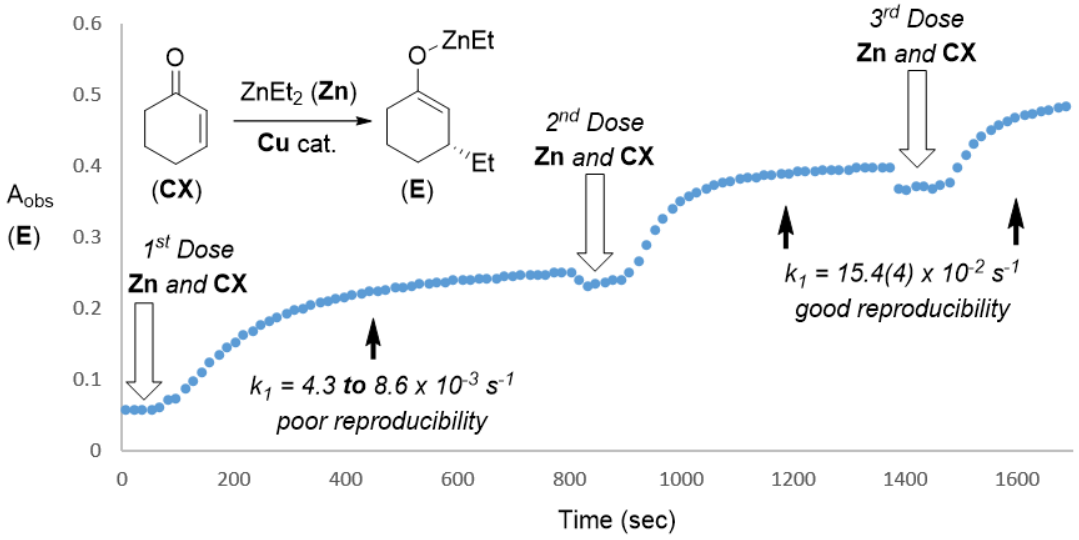

Figure 37: Summary of the triple dose experiment.[193]

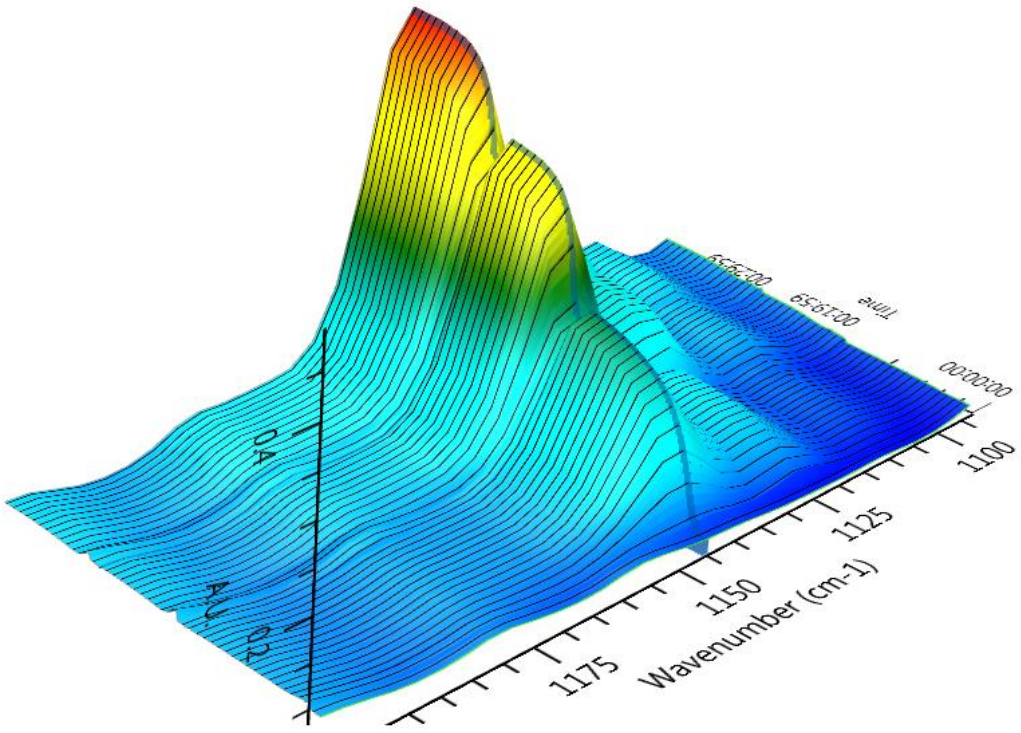

Figure 38: ReactIR output of the triple dose experiment.

In a similar manner to that described previously with the studies on **A**, the rate constant (k_1) of a series of experiments were then determined. The $\mathbf{Cu_b}$ catalyzed 1,4-addition of **Zn** to **CX** to form **E** strictly followed 1st order kinetics (with R^2 values consistently greater than 0.99). However, when $[\mathbf{L}]_0/[\mathbf{Cu_b}]_0$ ratios were below 0.8 or above 2.1 a lack of reaction homogeneity and strong reaction inhibition respectively prevent the attainment of accurate kinetic data. In

these experiments, as before, the concentration of one reaction component was varied whilst the others were kept constant. Ln-Ln plots were then generated, in order to determine the order in each reaction component. The results of the experiments in which the initial concentration of **Zn** was varied are summarized in Table 16 and the Ln-Ln plot generated from those results is shown in Figure 39. From the slope of the Ln-Ln plot, it was deduced that the order in $[\mathbf{Zn}]_0$ was 0.217(30).

$[\mathbf{Zn}]_0$ (mM)	k_1 (s^{-1})
76.2	0.0109
203	0.0127
347	0.0154

*Table 16: Calculated k_1 values for varying concentrations of **Zn**. Across all experiments: $[\mathbf{Cu_b}]_0$ = 1.7±0.1 mM; $[\mathbf{L}]_0$ = 3.4±0.4 mM; $[\mathbf{CX}]_0$ = 220±27 mM; performed in dichloromethane at -40 ˚C; k_1 values obtained the from non-linear least squares fitting $[\mathbf{E}]_{obs}$ to $[\mathbf{E}]_t=[\mathbf{E}]_{40}+\Delta[\mathbf{E}]_0(1-\exp(-k_1t))$.*

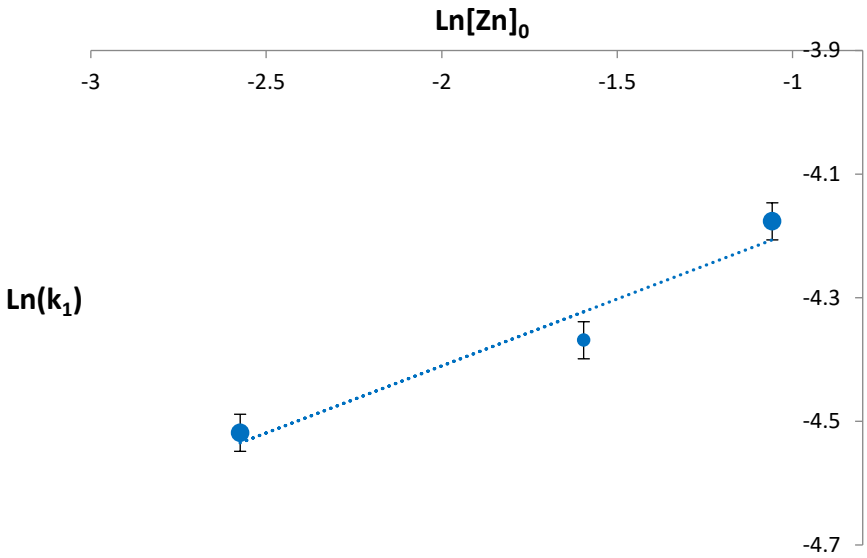

Figure 39: Ln-Ln plot generated from the data presented in Table 16, produced by varying $[\mathbf{Zn}]_0$. Analysis gave a slope of 0.217(30).

The results of the experiments in which the initial concentration of **CX** was varied are summarized in Table 17 and the Ln-Ln plot generated from those results is shown in Figure 40. From the slope of the Ln-Ln plot, it was deduced that the order in $[\mathbf{CX}]_0$ was 0.272(20).

$[CX]_0$ (mM)	k_1 (s^{-1})
72.3	0.0095
233	0.0129
275	0.0139

*Table 17: Calculated k_1 values for varying concentrations of **CX**. Across all experiments: $[\mathbf{Cu_b}]_0$ = 1.7±0.06 mM; $[\mathbf{L}]_0$ = 3.6±0.04 mM; $[\mathbf{Zn}]_0$ = 285±9 mM; performed in dichloromethane at -40 ˚C; k_1 values obtained the from non-linear least squares fitting $[\mathbf{E}]_{obs}$ to $[\mathbf{E}]_t=[\mathbf{E}]_{40}+\Delta[\mathbf{E}]_0(1-exp(-k_1t))$.*

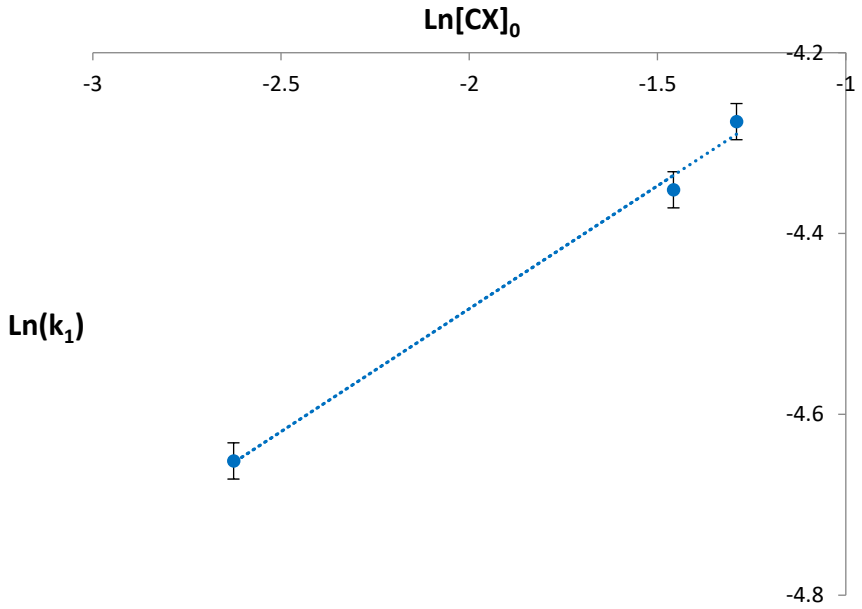

Figure 40: Ln-Ln plot generated from the data presented in Table 17, produced by varying $[\mathbf{CX}]_0$. Analysis gave a slope of 0.272(20).

The results of the experiments in which the initial concentration of $\mathbf{Cu_b}$ was varied are summarized in Table 18 and the Ln-Ln plot generated from those results is shown in Figure 41. From the slope of the Ln-Ln plot, it was deduced that the order in $[\mathbf{Cu_b}]_0$ was 0.123(4).

$[Cu_b]_0$ (mM)	k_1 (s^{-1})
0.87	0.0138
2.70	0.0170
3.61	0.0175

*Table 18: Calculated k_1 values for varying concentrations of **Cu_b**. Across all experiments: $[CX]_0$ = 235±2 mM; $[Zn]_0$ = 277±5 mM; fixed $[L]_0/[Cu_b]_0$ = 2.00±0.08 for $[Cu_b]$ 0.87-3.61 mM; performed in dichloromethane at -40 ˚C; k_1 values obtained the from non-linear least squares fitting $[E]_{obs}$ to $[E]_t=[E]_{40}+\Delta[E]_0(1-\exp(-k_1t))$.*

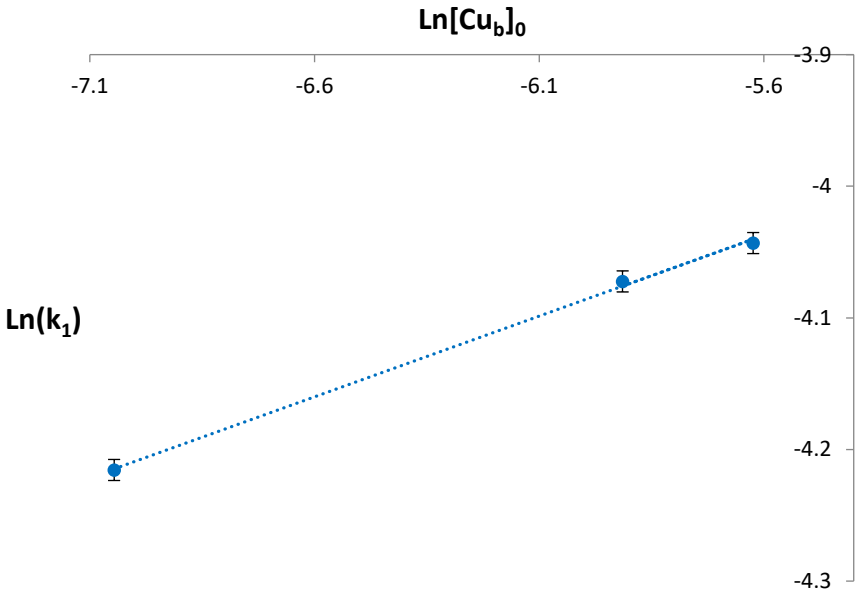

Figure 41: Ln-Ln plot generated from the data presented in Table 18, produced by varying $[Cu_b]_0$. Analysis gave a slope of 0.123(4).

The results of the experiments in which the initial concentration of **L** was varied are summarized in Table 19 and the Ln-Ln plot generated from those results is shown in Figure 42. From the slope of the Ln-Ln plot, it was deduced that the order in $[L]_0$ was 0.175(20).

$[L]_0$ (mM)	k_1 (s^{-1})
1.59	0.0120
2.40	0.0143
3.44	0.0154

*Table 19: Calculated k_1 values for varying concentrations of **L**. Across all experiments: $[Cu_b]_0$ = 1.75±0.08 mM; $[CX]_0$ = 231±5 mM; $[Zn]_0$ = 287±8 mM; performed in dichloromethane at -40 ˚C; k_1 values obtained the from non-linear least squares fitting $[E]_{obs}$ to $[E]_t=[E]_{40}+\Delta[E]_0(1-\exp(-k_1t))$.*

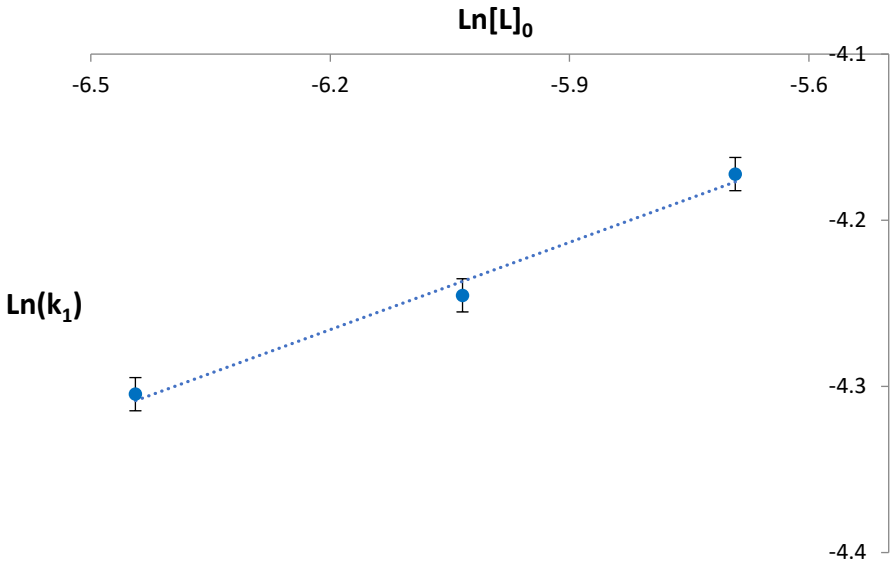

Figure 42: Ln-Ln plot generated from the data presented in Table 19, produced by varying $[L]_0$. Analysis gave a slope of 0.175(20).

The data described above are concordant with a rate law α $[\mathbf{Zn}]^{0.217}[\mathbf{CX}]^{0.272}[\mathbf{Cu_b}]^{0.123}[\mathbf{L}]^{0.175}$. One simple transition state stoichiometry consistent with this rate law is: $[\mathbf{Zn}]_{3.5}[\mathbf{CX}]_{4.4}[\mathbf{Cu_b}]_{2.0}[\mathbf{L}]_{2.9}$. A simple model consistent with this stoichiometry is shown in Scheme 70. In this model, catalysis proceeds through the two C_2-related structures **2.74**, which possess the stoichiometry $[\mathbf{Cu_b}]_2\mathbf{L}_3[\mathbf{CX}]_2[\mathbf{Zn}]_2$. The rate determining step is the asymmetric 1,4-addition driven by transmetalation of $\mathbf{Zn}[\mathbf{CX}]_2$. One simple structure for the transmetallated intermediate **2.75** (**2.74**+$\mathbf{ZnCX}_2$) is shown. The exact structure of this intermediate is still being sought computationally. This is in agreement with the proposal of Gschwind *et al* from their NMR studies of model systems[146][147][148][149] – who suggest an optimal copper:ligand ratio of 2:3. The presence of **E** in this species also explains the observed induction period.

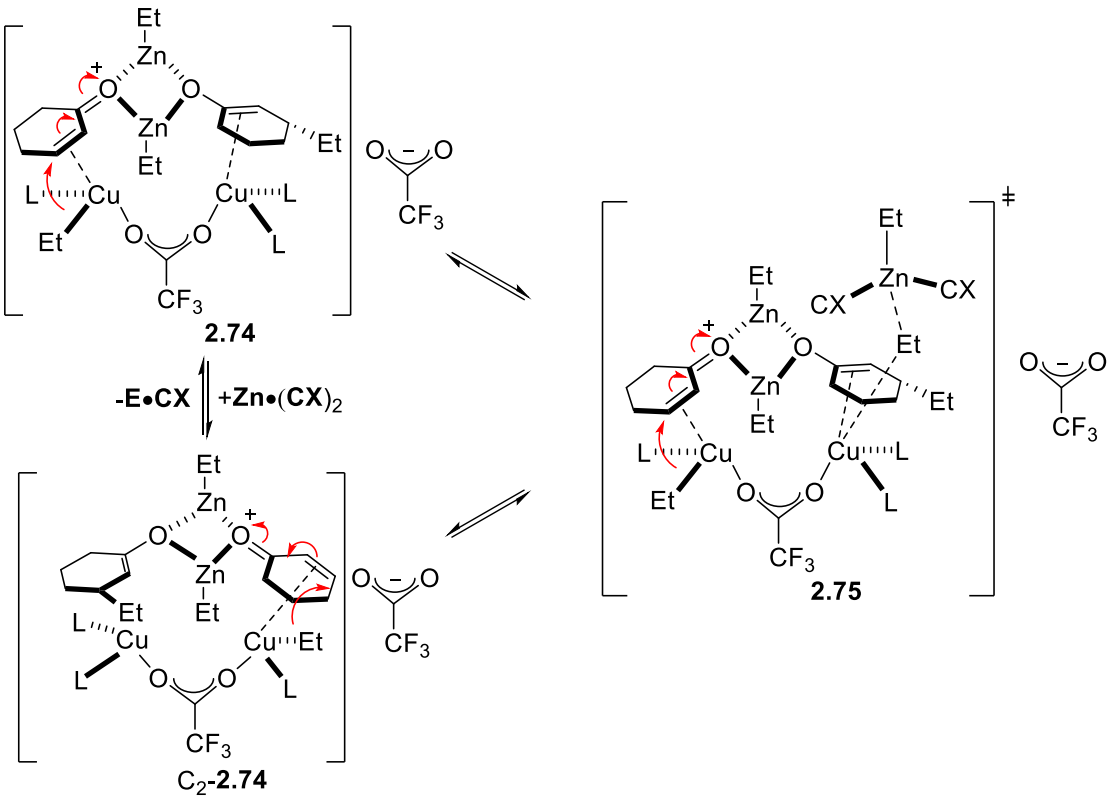

Scheme 70: Potential model consistent with the derived transition state stoichiometry.[193]

The other advantage of the model system used in these experiments, is that it enabled the use of multinuclear NMR to study the system under identical conditions to the ReactIR studies. The results of these studies are shown in Figure 43. A mixture of **L** and **Cu_b**, in dichloromethane at -40 ˚C, showed a broadened signal in both the ^{31}P and ^{19}F NMR spectra, indicating a rapid exchange of ligands is occurring. After the addition of **Zn**, a mixture of species is formed with three major components. By ^{31}P NMR, these components are δ_P 123.0, 123.8 and 124.8 ppm; which are at similar values to those of the species described, in a closely related system, by the group of Gschwind.[148] Following the addition of **CX**, there is a rapid collapse of the ^{31}P NMR signals as the reaction progresses. This collapse is not due to catalyst deactivation, as there is no corresponding decrease in reaction rate in the 2nd dose that would occur if catalyst deactivation was occurring. The emergence of a final, rapidly equilibrating catalyst is supported by the ^{19}F NMR spectra. Immediately after **Zn** addition, two major, sharp signals appear at δ_F -75.7 and -76 ppm. One corresponds to independently prepared zinc trifluoroacetate (-75.7 ppm), the other to trifluoroacetic acid (-76.1 ppm) within experimental error. After the addition of **CX**, these signals convert to a single new signal at -75.8 ppm which then collapses to a broadened signal as the reaction proceeds.

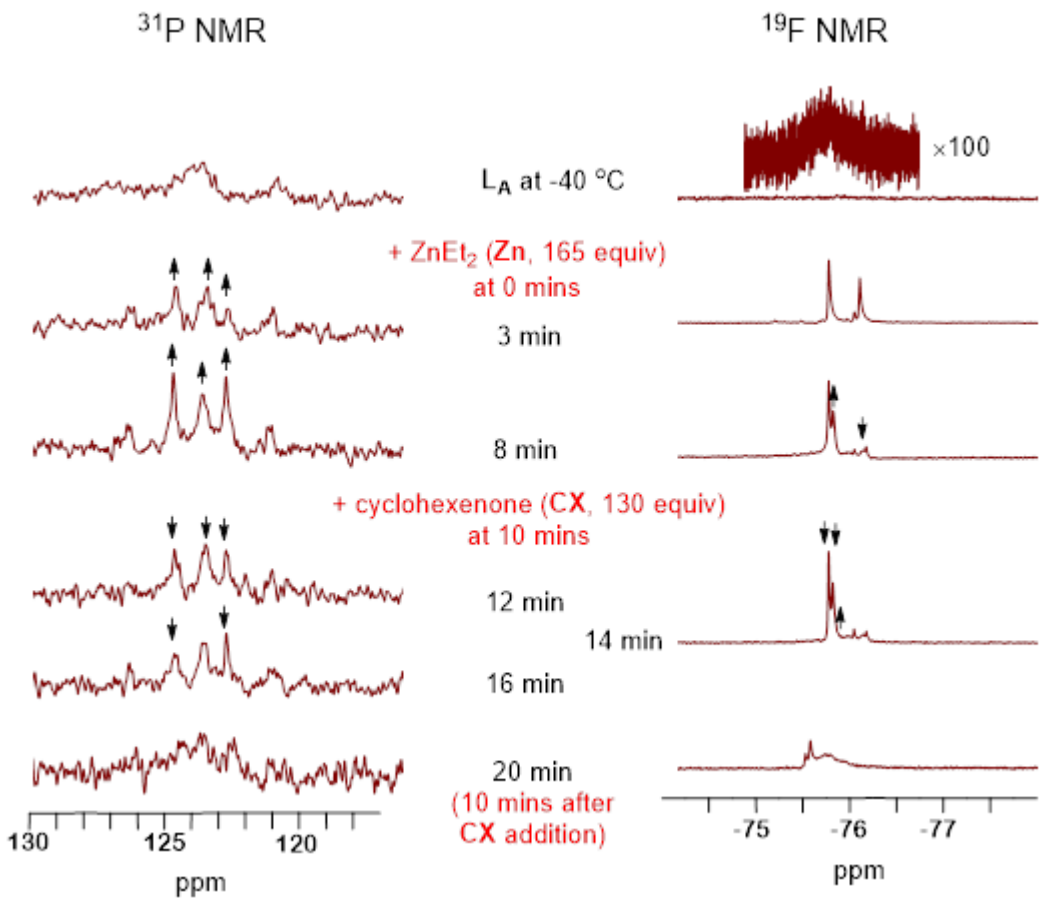

Figure 43: Phosphorus-31 and fluorine-19 NMR studies of catalyst genesis and reaction progress under identical conditions to the ReactIR studies already described. The arrows indicate signal intensity changes from spectrum to spectrum.[193]

2.3 Conclusions

Kinetic studies of the 1,4-addition of **A** to **CX**, catalyzed by $\mathbf{Cu_a}$ and **L**, using a ReactIR were performed. The results of this supported previously obtained GC aliquot studies. Using the kinetic data obtained, a transition state stoichiometry of $[\mathbf{CX{\cdot}A}]_2[\mathbf{Cu_a}]_3[\mathbf{L}]_{1.33}$ was proposed. This was not in agreement with previously proposed and published transition state stoichiometries for related systems.

A novel copper(I) trifluoroacetate complex ($\mathbf{Cu_b}$) was synthesized, which proved to be an extremely effective catalyst for the 1,4-addition of organozinc reagents to enones, affording extremely rapid reaction rates and comparable enantioselectivities to some of the best catalytic systems in the current literature.

This copper complex was used in further kinetic investigations into the 1,4-addition of **Zn** to **CX**, also using a ReactIR. Using the kinetic data obtained, a transition state stoichiometry of $[\mathbf{Zn}]_{3.5}[\mathbf{CX}]_{4.4}[\mathbf{Cu_b}]_{2.0}[\mathbf{L}]_{2.9}$. This was supported by the previously proposed transition state from the group of Gschwind. This complex also enabled further analysis of the model reaction system using multinuclear NMR.

2.4 Experimental

2.4.1 General Experimental

Diethyl ether and THF were distilled from sodium-benzophenone under argon; hexanes were dried over freshly cut clean sodium for >16 h and deoxygenated with argon. Other anhydrous deoxygenated solvents were taken from an Inert Technology's solvent tower, whose moisture contents were assessed to be <10 ppm using a CA-200 moisture meter. Feringa's (*R,S,S*)-phosphoramidite ligand (**L**) was prepared from fresh PCl_3, (*R*)-BINOL and (*S*)-*N*-((*S*)-1'-phenylethanyl)-1-phenylethan-1-amine by a literature method (preparation is described below).[194] Triethylaluminum (98% pure) was either commercial 2.0 M or 25% w/w, solutions in hexanes (originally Aldrich, now available from Alfa Aesar: Cat. No. 89054), corresponding to a molality of 2.19 $mmol.g^{-1}$. Alternatively, solutions were prepared from neat triethylaluminum (>98%, **CARE!** Pyrophoric) and hexane under argon to concentrations of 2.09-2.26 M (molalities of 2.47-2.67 $mmol.g^{-1}$). Diethylzinc solutions were prepared from neat diethylzinc (>98%, Sigma-Aldrich, **CARE!** Pyrophoric) and toluene under argon to concentrations of 1.95-2.21 M (molalities of 1.91-2.09 $mmol.g^{-1}$) The molarity/molalities of organometallics was determined *via* gas evolution on quench into wet THF using a gas manometer; identical results were attained when using Gilman-titration methods.[195] Triethylaluminum and diethylzinc solutions were stored in flame-dried glass Schlenk storage flasks, equipped with Teflon 'Young's taps' their concentrations/purities were stable for the two week period batches were used over. Septa/'Sure-seal' closures were avoided as they were found to favour solvent loss and alkoxide formation. Maintaining pure triethylaluminium and diethylzinc is critical to attaining high kinetic reproducibility. Anhydrous $Cu(OAc)_2$ (**Cu_a**, Aldrich 326755) was certified as analytically pure (>98%). Ligand **L** was purified from a CH_2Cl_2 solution by layering with pentane (under argon) to yield large, clear, colourless, pentagonal crystals that assayed by multinuclear NMR spectroscopy as >99% pure. Cyclohex-2-en-1-one (**CX**, Aldrich 92509) was distilled/dried (4Å molecular sieves) and assayed >98% pure by ^1H NMR or GC techniques. Accurate quantification of triethylaluminium (**A**) and diethylzinc (**Zn**) solutions were attained by pre- and post-weighing of the addition syringes used (to ±0.1 mg). Similar dual weighing of all other component delivery vials/syringes (**Cu_a**, **Cu_b**, **L**, **CX** and solvents) was used (±0.1 mg). Bath temperatures were controlled by a Huber TC50E cryostat and were accurate to ±0.5 °C at -40 °C. Aliquots from GC kinetic samples were analysed using a Bruker GC-430 using internal standards. ReactIR data were collected using a Mettler-Toledo ReactIR™ 15. Enantioselectivities were measured by chiral GC (on a Bruker GC-430) or HPLC (Thermo Ultimate 3000).

(11b*R*)-*N,N*-Bis((1*S*)-1-phenylethyl)dinaptho(2,1-*d*:1',2'-*f*)(1,3,2)dioxaphosphephin-4-amine (L)

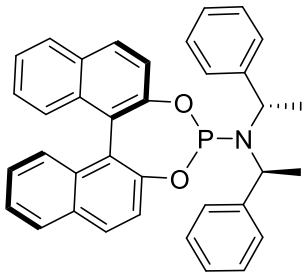

L

To a solution of phosphorus trichloride (0.95 mL, 1.49 g, 10.9 mmol) in dichloromethane (40.0 mL) at 0 °C, was added triethylamine (7.5 mL, 5.44 g, 53.8 mmol). The resulting pale yellow solution was stirred at the same temperature for 30 min before the addition of bis-((*S*)-1-phenylethyl)amine (2.4 mL, 2.37 g, 10.5 mmol). The resulting yellow suspension was warmed to RT and stirred for 3 hours. (*R*)-1,1'-Bi(2-naphthol) (3.1 g, 10.8 mmol) was then added portionwise, over 10 min, at 0 °C before warming to RT and stirring for 18 hours. The reaction was quenched *via* the addition of water (30 mL), extracted with dichloromethane (3 × 50 mL), dried over anhydrous magnesium sulfate and the solvent removed *in vacuo* to afford the crude product as a yellow foam. This was then rapidly filtered through a plug of silica, eluting with 3 × column volumes of dichloromethane, which after removal of the solvent gave a colorless foam. This was then crystallised *via* the layering of pentane (60 mL) over a solution of crude **L** in dichloromethane (15 mL) at 4 °C to afford **L** as colorless crystals in 73% yield (4.13 g, 7.65 mmol). **M.p.** 118-120 °C [lit[196] 106-110 °C]; **^{1}H NMR** (500.1 MHz, C_6D_6): δ_H 7.69 (dd, 2H, *J* = 7.8, 7.8 Hz, Ar*H*), 7.58 (d, 2H, *J* = 8.6 Hz, Ar*H*), 7.54 (d, 2H, *J* = 8.6 Hz, Ar*H*), 7.42 (d, 1H, *J* = 8.6 Hz, Ar*H*), 7.26 (d, 1H, *J* = 8.7 Hz, Ar*H*), 7.15-7.08 (m, 6H, Ar*H*), 7.07-7.01 (m, 4H, Ar*H*), 7.01-6.96 (m, 2H, Ar*H*), 6.93-6.85 (m, 2H, Ar*H*), 4.58 (br s, 2H, 2 × NC*H*Ph), 1.59 (d, 6H, *J* = 7.0 Hz, 2 × CH_3); **^{13}C NMR** (125.025 MHz, C_6D_6, some peaks obscured by solvent): δ_C 150.8, 150.8, 150.3, 143.3, 133.5, 133.3, 132.0, 131.0, 130.8, 129.8, 128.7, 128.5, 128.5, 128.4, 128.2, 128.1, 128.0, 127.7, 127.6, 127.0, 126.6, 126.5, 125.0, 124.9, 124.7, 124.7, 123.0, 122.8, 122.8, 122.6, 122.6, 52.7, 52.6, 22.2 (br); **^{31}P NMR** (202.5 MHz, C_6D_6): δ_P 145.98 (dd, *J* = 11.8, 11.8 Hz); **ν_{max}** (neat): 3055, 3033, 2998, 2973, 1591, 1506, 1496, 1463, 1429, 1390, 1375, 1328, 1231, 1204, 1134, 1070, 1050, 949, 925, 823, 800, 780, 750, 717, 684, 626, 609, 556, 481, 419 cm^{-1}; **HRMS** (ESI+) found 540.2090 $C_{36}H_{31}NO_2P^+$ $[M+H]^+$ requires 540.2087 (|σ| 0.6 ppm); **$[\alpha]_D^{25}$**: -410.0 (*er* >99:1, *c* = 0.79 in $CHCl_3$) [lit[194] +456.0 (*S,R,R*, *er* >99:1, *c* = 0.79, $CHCl_3$)]. Data are in agreement with reported properties of **L**.[194]

2.4.2 Kinetic Investigations Using Triethylaluminium

2.4.2.1 Formation of CX·A Adduct

Formation of CX·A Adduct Experimental Procedure

To a flame-dried, three necked flask under argon, cyclohex-2-en-1-one (**CX**, 0.9512 g 0.958 mL, 9.895 mmol) was dissolved in anaerobic, anhydrous diethyl ether (16.674 g, 23.385 mL) and stirred at -40 ^{o}C over 10 minutes. Data collection using the ReactIR was then started, in the range 1900-1500 cm^{-1}, using manual sampling corrected for initial minor experimental off-sets (typically ~0.02-0.04 absorbance units). Two scans were taken *ca.* 2 min apart to ensure thermodynamic equilibrium had been attained. This procedure was repeated after each addition of triethylaluminium (**A**, 2.09 M, 2.47 $mmol.g^{-1}$, 0.405 g, 1.00 mmol) on the derived bright yellow solutions. After 10 additions, data collection was halted and the reaction was quenched *via* the addition of HCl_{aq} (1 M, 10 mL) providing colourless **CX** recovered in quantitative yield. The volumes used were estimated from standard densities for **CX** (0.993 g mL^{-1}) and diethyl ether (0.713 g ml^{-1}), while that of 2.09 M triethylaluminium (**A**) solutions in diethyl ether was determined experimentally to be 0.81 $g.mL^{-1}$ in these titration runs. Reaction component volumes were assumed to be additive (*i.e.* partial molar volume/phase change effects were assumed minimal).

Formation of CX·A Adduct Data Analysis

Data were collected based on titration of known quantities of triethylaluminium (**A**) into a known cyclohex-2-en-1-one (**CX**) solution. The quantity of **CX** remaining was determined by the, off-set corrected, absorbance (O_{CX}) at 1676 cm^{-1} as [**CX**] = $\varepsilon_{CX} \times O_{CX}$ where ε_{CX} is the molar constant of the ReactIR instrument. Values of ε_{CX} can be both measured against standard solutions and thus fitted against the **CX**/**A** mixtures. Best fits were attained for a 1:1 complex formation whose derivation is shown in Figure 44.

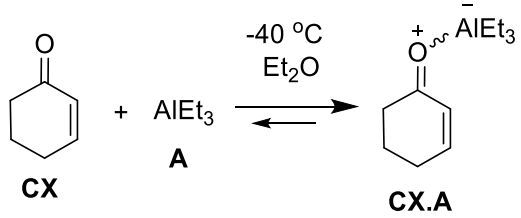

With equilibrium const:

$$K = \frac{[CX.A]}{[CX][A]} \quad (1)$$

Mass balance, all of CX and A species must total at any given moment:

$$[A_{TOT}] = [A] + [CX.A] \quad (2)$$

$$[CX_{TOT}] = [CX] + [CX.A] \quad (3)$$

Sub (2) and (3) into (1):

$$K = \frac{[CX.A]}{([CX_{TOT}] - [CX.A])([A_{TOT}] - [CX.A])} \quad (4)$$

...multiply out (4) and rearrange:

$$K[CX_{TOT}][A_{TOT}] - K[CX_{TOT}][CX.A] - K[CX.A][A_{TOT}] + K[CX.A]^2 = [CX.A] \quad (5)$$

$$K[CX.A]^2 - K[CX_{TOT}][CX.A] - K[CX.A][A_{TOT}] + K[CX_{TOT}][A_{TOT}] = [CX.A] \quad (6)$$

$$K[CX.A]^2 - K[CX_{TOT}][CX.A] - K[CX.A][A_{TOT}] - [CX.A] + K[CX_{TOT}][A_{TOT}] = 0 \quad (7)$$

$$K[CX.A]^2 + (- K[CX_{TOT}] - K[A_{TOT}] -1)[CX.A] + K[CX_{TOT}][A_{TOT}] = 0 \quad (8)$$

Eq (8) is just of standard quadratic form with known solution:

$$ax^2 + bx + c = 0 \quad \textit{with..} \quad x = \frac{-b \pm \sqrt{b^2 - 4ac}}{2a} \quad \text{where } x = [CX.A] \quad (9)$$

One of the solutions of (9) must have a 'real world' meaning, viz:

K, $\varepsilon_{CX.A}$ and [CX.A] must all be positive, where: $[CX.A] = \varepsilon_{CX.A} \times O_{CX.A}$
and $\varepsilon_{CX.A}$ is the molar constant for CA.A and $O_{CX.A}$ its absorbance

...so:

$a = K$
$b = (- K[CX_{TOT}] - K[A_{TOT}] -1)$
$c = K[CX_{TOT}][A_{TOT}]$

Thus, [CX] can be calculated through (10):

$$[CX] = [CX_{TOT}] - [CX.A] \quad (10)$$

as the total cyclohex-2-en-1-one CX_{TOT} can only be present as CX or CX.A

*Figure 44: Derivation of the predicted binding curve for **CX.A** formation from cyclohex-2-en-1-one (**CX**) and triethylaluminium (**A**) in diethyl ether at -40 °C.*

Duplicate runs gave *K* values of 12.1(9) and 11.8(7) which were averaged giving 12.0(9) corresponding to a binding energy of $\Delta G^{o}(-40\ ^{o}C)_{react}$ = -4.8±0.4 kJ mol^{-1} (-1.1±0.1 kcal mol^{-1}) (using $\Delta G^{o} = -RT\ln K$). As the absorbance is being used to precisely quantify the **CX** concentration great care was taken to eliminate minor off-sets in instrument backgrounds (in A_{obs}, ~0.03 which are common) before data analysis. Based on duplicate readings of 19 independent determinations at concentrations between 3-481 mM (at -40 ^{o}C) the average molar constants of **CX** and **CX.A** were determined to be: ε_{CX} = 0.565 M and $\varepsilon_{CX.A}$ = 0.697 M.

$[\mathbf{A}_{TOT}]$ (mM)	$[\mathbf{CX}_{TOT}]$ (mM)	$O_{\mathbf{CX.A}}$ (A_{obs})	$[\mathbf{CX.A}]_{calc}$ (mM)	$[\mathbf{A}_{TOT}]$ (mM)	$[\mathbf{CX}_{TOT}]$ (mM)	$O_{\mathbf{CX.A}}$ (A_{obs})	$[\mathbf{CX.A}]_{calc}$ (mM)
0.0	406.5	0.226	0.0	220.5	361.4	0.118	157.0
37.0	398.9	0.214	30.2	252.6	354.8	0.103	173.5
76.8	390.8	0.192	61.4	282.5	348.7	0.092	186.9
113.4	383.3	0.173	88.5	311.2	342.9	0.081	198.0
149.5	375.9	0.154	113.6	340.0	337.0	0.073	207.5
187.5	368.2	0.134	137.9				

*Table 20: Data from titration 1. $[\mathbf{A}_{TOT}]$ = 0-340 mM, $[\mathbf{CX}_{TOT}]$ = 406-337 mM (the **CX** concentration falls due to volume of **A** added), $O_{\mathbf{CX}}$ = the calculated absorbance for **CX**, vs. observed $O_{CX.A}$ and $[\mathbf{CX.A}]_{calc}$. A_{obs} corrected for instrument off-set. Non-linear least squares fitting of equation 8 (Figure 44) gave* K *= 12.1(9) M^{-1} [R^2 = >0.99].*

$[\mathbf{A}_{TOT}]$ (mM)	$[\mathbf{CX}_{TOT}]$ (mM)	$O_{\mathbf{CX.A}}$ (A_{obs})	$[\mathbf{CX.A}]_{calc}$ (mM)	$[\mathbf{A}_{TOT}]$ (mM)	$[\mathbf{CX}_{TOT}]$ (mM)	$O_{\mathbf{CX.A}}$ (A_{obs})	$[\mathbf{CX.A}]_{calc}$ (mM)
0.0	481.2	0.263	0.0	227.4	441.8	0.150	172.9
49.1	472.7	0.242	41.0	269.1	434.6	0.131	198.1
95.9	464.6	0.217	78.6	309.4	427.6	0.114	219.8
142.5	456.5	0.192	114.3	344.9	421.5	0.101	236.6
186.1	449.0	0.171	145.5				

*Table 21: Data from titration 2. $[\mathbf{A}_{TOT}]$ = 0-345 mM, $[\mathbf{CX}_{TOT}]$ = 481-449 mM (the **CX** concentration falls due to volume of **A** added), $O_{\mathbf{CX}}$ = the calculated absorbance for **CX**, vs. observed $O_{CX.A}$ and $[\mathbf{CX.A}]_{calc}$. A_{obs} corrected for instrument off-set. Non-linear least squares fitting of equation 8 (Figure 44) gave* K *= 11.8(7) M^{-1} [R^2 = >0.99].*

2.4.2.2 Measurement and Calculation of the Order in Each Reaction Component

General Experimental Procedure

To a flame-dried three necked flask under argon, (*R*,*S*,*S*)-phosphoramidite ligand **L** (79.8 mg, 148 µmol) and $Cu(OAc)_2$ (**Cu_a**, 17.6 mg, 97 µmol) were added to anhydrous anaerobic diethyl ether (16.507 g, 23.15 mL) and the mixture stirred at room temperature for 30 minutes. The solution was cooled to -40 °C for 10 minutes, after which time triethyl aluminium (**A**, 2.09 M in hexane, 2.47 mmol.g^{-1}, 4.928 g, 6.12 mL of solution, 12.17 mmol) was added to the mixture and stirred at this temperature for an additional 10 minutes at -40 °C. Experiments confirmed reproducible reduction to a homogeneous stable Cu^{I} precatalyst was attained by this procedure. At this timepoint, t_0, cyclohex-2-en-1-one (**CX**, 1.002 g, 1.01 mL, 10.44 mmol) was added and data collection using the ReactIR started. Calculated initial values: $[\mathbf{CX}]_0$ = 345 mM, $[\mathbf{A}]_0$ = 402 mM, $[\mathbf{Cu_a}]_0$ = 3.18 mM, $[\mathbf{L}]_0$ = 4.88 mM; $[\mathbf{L}]/[\mathbf{Cu_a}]$ = 1.54; total volume = 30.28 mL. Data ($O_{CX.A}$ in A_{obs} absorbance units) for the 1630 cm^{-1} carbonyl band of the **CX.A** adduct were collected until complete consumption of this IR band was observed, recording 1 scan every 10 seconds. Following completion, the reaction was quenched with HCl_{aq} (1 M, 10 mL), extracted with diethyl ether, washed with water, dried over anhydrous magnesium sulfate and the solvent removed *in vacuo* to provide (*R*)-3-ethylcyclohexanone **P** with identical properties to genuine independent samples [chiral GC range (Lipodex-A) of final product 82±2% *ee*]. The volumes used were estimated from standard densities for **CX** (0.993 g mL^{-1}) and diethyl ether (0.713 g ml^{-1}), while that of 2.09 M triethylaluminium (**A**) solutions in diethyl ether was determined experimentally to be 0.83 g mL^{-1} in the kinetic runs. Reaction component volumes were assumed to be additive (*i.e.* partial molar volume/phase change effects were assumed minimal). Similarly, the volumes of dissolved **Cu_a** and **L** were assumed to contribute negligibly (<0.5%) to the total volume of the system.

Data Analysis for CX·A adduct

Due to the high data density of the ReactIR technique genesis of the catalyst could clearly be detected in the behaviour of the **CX.A** absorbance at 1630 cm^{-1} up to *ca.* 300 sec. Thus, at fixed $[\mathbf{Cu_a}]$ (3.5 mM) and [**L**] (5 mM) the absorbance data for **CX.A** at 1630 cm^{-1} ($O_{\mathbf{CX.A}}$) were used from 305 or 395 sec (the latter for slightly slower catalyst genesis at lower **CX** concentrations) until the signal for the **CX·A** species was no longer apparent. A range of $[\mathbf{CX.A}]_0$ (300-40 mM) concentrations were investigated. Values of $[\mathbf{CX.A}]_t$ were attained via $[\mathbf{CX{\cdot}A}] = \varepsilon_{CX\cdot A} \times O_{CX\cdot A}$.

Values of [**CX.A**]$_t$ were fitted to [**CX.A**]$_t$ = [**CX.A**]$_0$exp(-k_1t) by non-linear least squares procedures. This approach has been described in detail by Billo.[197] In brief, for each data point the squared error is calculated: δ = {[**CX.A**]$_t$(obs) - [**CX.A**]$_t$(calc)]^2 and the total squared error over all data points summed = Σ(δ). Minimisation of Σ(δ) is attained by use of the solver function in Excel providing [**CX.A**]$_0$(calc) and k_1 directly. Based on the solver stat analysis approach of Billo the fit of the data by this approach is superior to traditional linearization of the [**CX.A**]$_t$ data *via* ln([**CX.A**]$_t$)/ln([**CX.A**]$_0$) plots. For the rate order plots in **CX.A** values of [**CX.A**]$_0$ were based on the added (accurately weighed) [**CX**]$_0$ and [**A**]$_0$ in each run via equation (9). The fitted [**CX.A**]$_0$ concentrations derived from the kinetic best fits were found to be rather sensitive to background A_{obs} offsets effects in the ReactIR set up and were thus not used. Fortunately, the value of [**CX.A**]$_0$ does not affect k_1 determination/accuracy as this is independent of $(A_{obs})_0$. The main error sources on the order **CX.A** data are, partly the experimental difficulty in systematically varying [**CX.A**] while keeping both the both the ratios [**A**]/[**CX**] and [**L**]/[**Cu$_a$**] constant in this sensitive system, and partly due to the higher molecularity of the transition state (first order behaviour of **CX.A** from [**Cu$_a$**$_3$**L**$_2$(**CX.A**)(**E**)]‡. Duplicated/reanalysed [**CX.A**]^c order runs gave values of c = 0.9-1.1. Based on this (and the vastly superior fit to first order of the primary data to all other trialled rate laws), first order behaviour in [**CX.A**] is clearly the dominant behaviour.

Data Analysis for Other Reaction Components

Identical procedural methods, to those described above, were used to study the behaviour of the rate of catalysis at -40 ˚C. For the order in **Cu$_a$**, the concentration of copper [**Cu$_a$**] was varied between 1-6 mM whilst under conditions providing nominally [**CX.A**]$_0$ = 220 mM and [**L**]/[**Cu$_a$**] = 1.5. The error bar on the order **Cu$_a$** data is due, in part, to the experimental difficulty in systematically varying [**Cu$_a$**] while keeping the ratio [**L**]/[**Cu$_a$**] and [**CX.A**] constant in this sensitive system. Separate [**Cu$_a$**]^a order analyses/duplicate runs gave values of a = 1.4-1.5. For the order in **L**, the concentration of ligand [**L**] was varied between 1.7-15.4 mM whilst under conditions providing nominally [**CX.A**]$_0$ = 230 mM and [**Cu**]$_0$ = 3.5 mM.

Primary Data

time (sec)	$O_{CX.A}$ (A_{obs})	time (sec)	$O_{CX.A}$ (A_{obs})	time (sec)	$O_{CX.A}$ (A_{obs})	time (sec)	$O_{CX.A}$ (A_{obs})	time (sec)	$O_{CX.A}$ (A_{obs})	time (sec)	$O_{CX.A}$ (A_{obs})
305	0.307	455	0.249	605	0.195	755	0.155	905	0.117	1055	0.096
315	0.301	465	0.243	615	0.194	765	0.152	915	0.116	1065	0.096
325	0.297	475	0.240	625	0.190	775	0.149	925	0.114	1074	0.094
335	0.293	485	0.234	635	0.188	784	0.146	934	0.112	1085	0.093
345	0.292	494	0.230	645	0.185	795	0.144	945	0.111	1095	0.093
354	0.288	505	0.226	655	0.186	805	0.141	955	0.109	1104	0.092
365	0.282	515	0.223	665	0.182	814	0.139	965	0.108	1115	0.092
375	0.278	524	0.221	675	0.179	825	0.136	975	0.106	1125	0.090
384	0.274	535	0.222	685	0.172	835	0.133	985	0.105	1135	0.090
395	0.268	545	0.215	695	0.169	845	0.131	994	0.103	1145	0.090
405	0.265	555	0.213	705	0.165	855	0.129	1005	0.102	1155	0.090
415	0.263	565	0.203	715	0.167	865	0.126	1014	0.101		
425	0.257	575	0.209	725	0.163	874	0.125	1025	0.100		
435	0.251	584	0.201	735	0.159	885	0.122	1035	0.098		
444	0.253	595	0.201	745	0.158	895	0.120	1045	0.097		

Table 22: $[\mathbf{Cu_a}] = 3.5$ mM, $[\mathbf{L}] = 5.0$ mM, $[\mathbf{CX}]_0 = 413$ mM, $[\mathbf{A}]_0 = 520$ mM; (data fitted from 305-1155 sec). A_{obs} uncorrected for experimental off-sets. Non-linear least squares fitting of $[\mathbf{CX.A}]_{obs} = O_{CX.A} \times \varepsilon_{\mathbf{CX.A}}$ to $[\mathbf{CX.A}]_{obs} = [\mathbf{CX.A}]_0 exp(-k_1 t)$ gave $k_1 = 1.558(8) \times 10^{-3}\ s^{-1}$ [$R^2 > 0.99$]. $\varepsilon_{\mathbf{CX.A}} = 0.697$ M was used; $[\mathbf{CX.A}]_{0,calc}$ (eq 8) 300 mM.

time (sec)	$O_{CX.A}$ (A_{obs})	time (sec)	$O_{CX.A}$ (A_{obs})	time (sec)	$O_{CX.A}$ (A_{obs})	time (sec)	$O_{CX.A}$ (A_{obs})	time (sec)	$O_{CX.A}$ (A_{obs})	time (sec)	$O_{CX.A}$ (A_{obs})
385	0.310	485	0.280	585	0.232	685	0.187	785	0.147	885	0.117
395	0.310	495	0.271	595	0.228	695	0.184	795	0.142	895	0.116
405	0.303	505	0.267	605	0.224	705	0.179	805	0.140	905	0.114
415	0.296	515	0.263	615	0.221	715	0.175	815	0.137	915	0.111
425	0.293	525	0.259	625	0.214	725	0.170	825	0.133	925	0.110
435	0.292	535	0.258	635	0.209	735	0.166	835	0.129		
445	0.289	545	0.249	645	0.205	745	0.160	845	0.126		
455	0.286	555	0.245	655	0.200	755	0.156	855	0.124		
465	0.282	565	0.244	665	0.195	765	0.154	865	0.122		
475	0.282	575	0.236	675	0.191	775	0.150	875	0.120		

Table 23: $[\mathbf{Cu_a}] = 3.2$ mM, $[\mathbf{L}] = 4.9$ mM, $[\mathbf{CX}]_0 = 345$ mM, $[\mathbf{A}]_0 = 402$ mM; (data fitted from 385-925 sec). A_{obs} uncorrected for experimental off-sets. Non-linear least squares fitting of $[\mathbf{CX.A}]_{obs} = O_{CX.A} \times \varepsilon_{\mathbf{CX.A}}$ to $[\mathbf{CX.A}]_{obs} = [\mathbf{CX.A}]_0 exp(-k_1 t)$ gave $k_1 = 1.94(3) \times 10^{-3}\ s^{-1}$ [$R^2 = 0.99$]. $\varepsilon_{\mathbf{CX.A}} = 0.697$ M was used; $[\mathbf{CX.A}]_{0,calc}$ (eq 8) 232 mM.

time (sec)	$O_{CX.A}$ (A_{obs})	time (sec)	$O_{CX.A}$ (A_{obs})	time (sec)	$O_{CX.A}$ (A_{obs})	time (sec)	$O_{CX.A}$ (A_{obs})	time (sec)	$O_{CX.A}$ (A_{obs})	time (sec)	$O_{CX.A}$ (A_{obs})
395	0.261	594	0.217	794	0.191	995	0.170	1195	0.154	1394	0.142
405	0.261	605	0.216	805	0.190	1005	0.169	1204	0.153	1404	0.142
415	0.256	614	0.214	815	0.189	1015	0.168	1215	0.151	1415	0.140
424	0.250	624	0.213	824	0.188	1025	0.167	1225	0.151	1424	0.140
435	0.248	635	0.211	835	0.187	1035	0.166	1234	0.151	1434	0.140
445	0.244	645	0.210	845	0.185	1045	0.165	1245	0.150	1445	0.139
455	0.242	655	0.209	854	0.184	1055	0.165	1255	0.150	1455	0.138
465	0.238	665	0.207	865	0.183	1065	0.163	1265	0.148	1465	0.139
474	0.236	675	0.206	875	0.182	1075	0.163	1275	0.148	1475	0.138
485	0.231	685	0.205	884	0.181	1085	0.162	1285	0.147	1485	0.138
495	0.231	695	0.204	895	0.180	1095	0.162	1295	0.147	1495	0.138
504	0.230	705	0.202	905	0.179	1105	0.160	1305	0.146	1505	0.137
515	0.228	715	0.201	915	0.178	1115	0.159	1314	0.146	1515	0.136
525	0.226	725	0.200	925	0.177	1125	0.159	1325	0.145	1524	0.136
534	0.225	735	0.198	934	0.176	1134	0.157	1335	0.145	1535	0.136
545	0.224	745	0.198	944	0.175	1144	0.157	1344	0.145	1545	0.136
555	0.222	754	0.195	955	0.174	1155	0.156	1355	0.143	1555	0.135
564	0.220	764	0.194	965	0.173	1164	0.155	1365	0.144	1565	0.135
575	0.219	775	0.193	975	0.172	1174	0.155	1375	0.142	1574	0.135
584	0.217	785	0.192	985	0.171	1185	0.153	1385	0.142		

Table 24: $[\mathbf{Cu_o}] = 3.6$ mM, $[\mathbf{L}] = 5.2$ mM, $[\mathbf{CX}]_0 = 202$ mM, $[\mathbf{A}]_0 = 255$ mM; (data fitted from 395-1574 sec). A_{obs} uncorrected for experimental off-sets. Non-linear least squares fitting of $[\mathbf{CX.A}]_{obs} = O_{CX.A} \times \varepsilon_{\mathbf{CX.A}}$ to $[\mathbf{CX.A}]_{obs} = [\mathbf{CX.A}]_0 exp(-k_1 t)$ gave $k_1 = 5.66(7) \times 10^{-4}\ s^{-1}$ [$R^2 = 0.98$]. $\varepsilon_{\mathbf{CX.A}} = 0.697$ M was used; $[\mathbf{CX.A}]_{0,calc}$ (eq 8) 124 mM.

time (sec)	$O_{CX.A}$ (A_{obs})	time (sec)	$O_{CX.A}$ (A_{obs})	time (sec)	$O_{CX.A}$ (A_{obs})	time (sec)	$O_{CX.A}$ (A_{obs})	time (sec)	$O_{CX.A}$ (A_{obs})	time (sec)	$O_{CX.A}$ (A_{obs})
304	0.089	455	0.085	604	0.081	755	0.078	904	0.076	1054	0.074
315	0.088	464	0.085	614	0.081	764	0.078	915	0.075	1064	0.073
324	0.088	474	0.085	624	0.081	775	0.078	924	0.075	1074	0.074
334	0.089	484	0.085	634	0.081	785	0.078	934	0.075	1085	0.074
344	0.088	494	0.084	645	0.080	794	0.077	944	0.074	1094	0.074
354	0.088	505	0.084	654	0.080	805	0.077	954	0.074	1104	0.073
364	0.087	515	0.084	664	0.080	815	0.078	964	0.074	1114	0.074
375	0.087	524	0.083	674	0.079	824	0.077	975	0.075	1124	0.074
384	0.086	535	0.083	684	0.080	835	0.077	984	0.074	1135	0.073
395	0.087	544	0.083	695	0.079	844	0.077	994	0.074	1144	0.073
404	0.087	555	0.083	705	0.079	855	0.076	1004	0.074	1154	0.073
414	0.087	565	0.083	714	0.079	865	0.076	1014	0.074	1164	0.074
424	0.086	574	0.082	725	0.078	874	0.076	1025	0.073	1174	0.074
434	0.086	585	0.082	734	0.079	885	0.076	1034	0.074		
444	0.085	594	0.082	744	0.079	894	0.075	1044	0.074		

*Table 25: [**Cu$_a$**] = 3.1 mM, [**L**] = 4.8 mM, [**CX**]$_0$ = 80 mM, [**A**]$_0$ = 125 mM; (data fitted from 395-1574 sec). A_{obs} uncorrected for experimental off-sets. Non-linear least squares fitting of [**CX.A**]$_{obs}$ = $O_{CX.A} \times \varepsilon_{CX.A}$ to [**CX.A**]$_{obs}$ = [**CX.A**]$_0$exp(-k_1t) gave k_1 = 2.40(4) × 10^{-4} s^{-1} [R^2 = 0.98]. $\varepsilon_{CX.A}$ = 0.697 M was used; [**CX.A**]$_{0,calc}$ (eq 8) 40.4 mM.*

time (sec)	$O_{CX.A}$ (A_{obs})	time (sec)	$O_{CX.A}$ (A_{obs})	time (sec)	$O_{CX.A}$ (A_{obs})	time (sec)	$O_{CX.A}$ (A_{obs})	time (sec)	$O_{CX.A}$ (A_{obs})	time (sec)	$O_{CX.A}$ (A_{obs})
1505	0.182	1685	0.171	1865	0.160	2045	0.148	2225	0.142	2405	0.136
1515	0.182	1695	0.171	1875	0.159	2055	0.149	2235	0.142	2415	0.136
1525	0.181	1705	0.170	1885	0.158	2065	0.149	2245	0.142	2425	0.135
1535	0.181	1715	0.169	1895	0.158	2075	0.149	2255	0.142	2435	0.136
1545	0.181	1725	0.171	1905	0.157	2085	0.148	2265	0.141	2445	0.136
1555	0.180	1735	0.167	1915	0.156	2095	0.148	2275	0.141	2455	0.135
1565	0.179	1745	0.167	1925	0.156	2105	0.148	2285	0.140	2465	0.135
1575	0.179	1755	0.167	1935	0.155	2115	0.147	2295	0.140	2475	0.134
1585	0.179	1765	0.166	1945	0.154	2125	0.146	2305	0.140	2485	0.134
1595	0.178	1775	0.165	1955	0.154	2135	0.146	2315	0.139	2495	0.134
1605	0.176	1785	0.164	1965	0.153	2145	0.145	2325	0.139	2505	0.133
1615	0.178	1795	0.164	1975	0.152	2155	0.145	2335	0.138	2515	0.133
1625	0.176	1805	0.163	1985	0.151	2165	0.145	2345	0.137	2525	0.134
1635	0.175	1815	0.163	1995	0.152	2175	0.144	2355	0.138	2535	0.134
1645	0.174	1825	0.163	2005	0.151	2185	0.144	2365	0.138	2545	0.133
1655	0.174	1835	0.162	2015	0.151	2195	0.143	2375	0.137	2555	0.132
1665	0.174	1845	0.161	2025	0.150	2205	0.143	2385	0.137		
1675	0.172	1855	0.160	2035	0.150	2215	0.143	2395	0.137		

*Table 26: [**Cu$_a$**] = 1.1 mM, [**L**] = 1.6 mM, [**CX**]$_0$ = 337 mM, [**A**]$_0$ = 397 mM; (data fitted from 1505-2555 sec). A_{obs} uncorrected for experimental off-sets. Non-linear least squares fitting of [**CX.A**]$_{obs}$ = $O_{CX.A} \times \varepsilon_{CX.A}$ to [**CX.A**]$_{obs}$ = [**CX.A**]$_0$exp(-k_1t) gave k_1 = 3.23(4) × 10^{-4} s^{-1} [R^2 = 0.98]. $\varepsilon_{CX.A}$ = 0.697 M was used; [**CX.A**]$_{0,calc}$ (eq 8) 226 mM.*

time (sec)	$O_{CX.A}$ (A_{obs})	time (sec)	$O_{CX.A}$ (A_{obs})	time (sec)	$O_{CX.A}$ (A_{obs})	time (sec)	$O_{CX.A}$ (A_{obs})	time (sec)	$O_{CX.A}$ (A_{obs})	time (sec)	$O_{CX.A}$ (A_{obs})
395	0.334	675	0.284	955	0.240	1235	0.207	1515	0.183	1795	0.168
405	0.332	685	0.283	965	0.240	1245	0.206	1525	0.183	1805	0.169
415	0.330	695	0.280	975	0.238	1255	0.205	1535	0.183	1815	0.168
425	0.328	705	0.279	985	0.237	1265	0.204	1545	0.182	1825	0.168
435	0.327	715	0.277	995	0.235	1275	0.204	1555	0.181	1835	0.167
445	0.324	725	0.276	1005	0.234	1285	0.203	1565	0.180	1845	0.166
455	0.324	735	0.274	1015	0.233	1295	0.200	1575	0.181	1855	0.166
465	0.321	745	0.272	1025	0.232	1305	0.200	1585	0.180	1865	0.166
475	0.320	755	0.271	1035	0.230	1315	0.199	1595	0.178	1875	0.165
485	0.318	765	0.270	1045	0.229	1325	0.198	1605	0.178	1885	0.165
495	0.316	775	0.267	1055	0.228	1335	0.198	1615	0.178	1895	0.165
505	0.314	785	0.266	1065	0.226	1345	0.197	1625	0.178	1905	0.165
515	0.312	795	0.265	1075	0.225	1355	0.196	1635	0.177	1915	0.164
525	0.310	805	0.264	1085	0.225	1365	0.195	1645	0.176	1925	0.164

535	0.308	815	0.262	1095	0.223	1375	0.194	1655	0.176	1935	0.163
545	0.307	825	0.260	1105	0.222	1385	0.193	1665	0.175	1945	0.163
555	0.304	835	0.259	1115	0.221	1395	0.192	1675	0.175	1955	0.163
565	0.303	845	0.257	1125	0.220	1405	0.192	1685	0.174	1965	0.163
575	0.300	855	0.255	1135	0.218	1415	0.191	1695	0.174	1975	0.162
585	0.300	865	0.255	1145	0.217	1425	0.190	1705	0.174	1985	0.162
595	0.298	875	0.253	1155	0.216	1435	0.189	1715	0.172	1995	0.162
605	0.296	885	0.251	1165	0.215	1445	0.189	1725	0.172	2005	0.162
615	0.294	895	0.250	1175	0.213	1455	0.187	1735	0.172	2015	0.161
625	0.292	905	0.248	1185	0.213	1465	0.187	1745	0.171	2025	0.162
635	0.290	915	0.247	1195	0.211	1475	0.186	1755	0.171	2035	0.161
645	0.289	925	0.245	1205	0.210	1485	0.186	1765	0.169		
655	0.288	935	0.244	1215	0.210	1495	0.185	1775	0.170		
665	0.286	945	0.242	1225	0.209	1505	0.185	1785	0.169		

*Table 27: [**Cu$_o$**] = 2.0 mM, [**L**] = 3.1 mM, [**CX**]$_0$ = 327 mM, [**A**]$_0$ = 381 mM; (data fitted from 395-2035 sec). A_{obs} uncorrected for experimental off-sets. Non-linear least squares fitting of [**CX.A**]$_{obs}$ = $O_{CX.A} \times \varepsilon_{CX.A}$ to [**CX.A**]$_{obs}$ = [**CX.A**]$_0$exp(-k_1t) gave k_1 = 4.90(5) × 10^{-4} s^{-1} [R^2 = 0.99]. $\varepsilon_{CX.A}$ = 0.697 M was used; [**CX.A**]$_{0,calc}$ (eq 8) 217 mM.*

time (sec)	$O_{CX.A}$ (A_{obs})	time (sec)	$O_{CX.A}$ (A_{obs})	time (sec)	$O_{CX.A}$ (A_{obs})	time (sec)	$O_{CX.A}$ (A_{obs})	time (sec)	$O_{CX.A}$ (A_{obs})	time (sec)	$O_{CX.A}$ (A_{obs})
395	0.220	605	0.166	814	0.119	1025	0.084	1235	0.059	1445	0.044
405	0.219	615	0.164	825	0.117	1035	0.082	1245	0.059	1455	0.043
415	0.214	625	0.162	835	0.116	1045	0.080	1255	0.058	1465	0.043
425	0.215	635	0.159	845	0.114	1055	0.079	1265	0.058	1474	0.043
435	0.209	645	0.156	855	0.112	1065	0.078	1274	0.056	1485	0.042
445	0.206	655	0.154	865	0.110	1075	0.077	1285	0.055	1495	0.041
455	0.205	665	0.153	874	0.107	1085	0.076	1295	0.054	1505	0.041
465	0.201	675	0.149	885	0.106	1095	0.074	1305	0.054	1515	0.041
475	0.201	685	0.147	895	0.104	1104	0.072	1315	0.053	1525	0.040
485	0.199	695	0.146	905	0.102	1115	0.072	1325	0.052	1535	0.040
495	0.195	704	0.143	915	0.100	1125	0.071	1335	0.051	1545	0.039
505	0.192	715	0.141	925	0.099	1135	0.070	1345	0.050	1555	0.039
515	0.190	725	0.138	934	0.097	1145	0.069	1355	0.050	1565	0.038
525	0.187	735	0.136	945	0.096	1155	0.067	1364	0.049	1575	0.037
535	0.185	745	0.134	955	0.094	1164	0.067	1375	0.049	1585	0.037
545	0.183	755	0.131	965	0.092	1175	0.065	1385	0.048	1595	0.038
555	0.181	764	0.129	975	0.090	1185	0.064	1395	0.047	1605	0.037
565	0.177	775	0.128	985	0.089	1195	0.063	1405	0.047		
575	0.175	785	0.125	995	0.088	1205	0.062	1414	0.046		
584	0.172	795	0.123	1005	0.087	1214	0.061	1425	0.045		
595	0.169	805	0.121	1015	0.085	1225	0.061	1435	0.045		

*Table 28: [**Cu$_o$**] = 3.8 mM, [**L**] = 5.5 mM, [**CX**]$_0$ = 321 mM, [**A**]$_0$ = 379 mM; (data fitted from 395-1605 sec). A_{obs} uncorrected for experimental off-sets. Non-linear least squares fitting of [**CX.A**]$_{obs}$ = $O_{CX.A} \times \varepsilon_{CX.A}$ to [**CX.A**]$_{obs}$ = [**CX.A**]$_0$exp(-k_1t) gave k_1 = 1.517(9) × 10^{-3} s^{-1} [R^2 = >0.99]. $\varepsilon_{CX.A}$ = 0.697 M was used; [**CX.A**]$_{0,calc}$ (eq 8) 213 mM.*

time (sec)	$O_{CX.A}$ (A_{obs})	time (sec)	$O_{CX.A}$ (A_{obs})	time (sec)	$O_{CX.A}$ (A_{obs})	time (sec)	$O_{CX.A}$ (A_{obs})	time (sec)	$O_{CX.A}$ (A_{obs})	time (sec)	$O_{CX.A}$ (A_{obs})
395	0.154	485	0.115	575	0.082	665	0.051	755	0.031	844	0.016
405	0.147	495	0.111	585	0.076	675	0.049	765	0.029	855	0.015
415	0.147	505	0.106	595	0.073	685	0.048	775	0.027	864	0.013
424	0.140	514	0.106	605	0.071	695	0.045	785	0.025	875	0.013
434	0.133	525	0.101	615	0.067	705	0.042	795	0.024	885	0.012
445	0.129	535	0.096	625	0.064	715	0.040	805	0.023	895	0.011
454	0.125	545	0.089	635	0.060	725	0.038	815	0.020		
465	0.124	555	0.089	645	0.059	735	0.035	825	0.020		
475	0.119	565	0.084	655	0.055	745	0.033	834	0.018		

Table 29: $[\mathbf{Cu_a}] = 6.1$ mM, $[\mathbf{L}] = 8.8$ mM, $[\mathbf{CX}]_0 = 311$ mM, $[\mathbf{A}]_0 = 380$ mM; (data fitted from 385-895 sec). A_{obs} uncorrected for experimental off-sets. Non-linear least squares fitting of $[\mathbf{CX.A}]_{obs} = O_{CX.A} \times \varepsilon_{CX.A}$ to $[\mathbf{CX.A}]_{obs} = [\mathbf{CX.A}]_0 exp(-k_1 t)$ gave $k_1 = 4.33(9) \times 10^{-3}\ s^{-1}$ [$R^2 = 0.98$]. $\varepsilon_{CX.A} = 0.697$ M was used; $[\mathbf{CX.A}]_{0,calc}$ (eq 8) 218 mM.

time (sec)	$O_{CX.A}$ (A_{obs})	time (sec)	$O_{CX.A}$ (A_{obs})	time (sec)	$O_{CX.A}$ (A_{obs})	time (sec)	$O_{CX.A}$ (A_{obs})	time (sec)	$O_{CX.A}$ (A_{obs})	time (sec)	$O_{CX.A}$ (A_{obs})
305	0.390	615	0.317	924	0.251	1235	0.199	1544	0.164	1855	0.141
314	0.388	625	0.316	934	0.248	1245	0.198	1554	0.163	1864	0.141
324	0.385	634	0.313	945	0.247	1254	0.197	1565	0.163	1874	0.140
334	0.383	645	0.311	955	0.244	1265	0.196	1574	0.161	1885	0.139
344	0.380	655	0.308	964	0.242	1274	0.195	1584	0.160	1894	0.139
355	0.378	664	0.306	974	0.241	1284	0.193	1595	0.160	1904	0.138
365	0.375	674	0.303	984	0.239	1295	0.192	1604	0.159	1914	0.138
374	0.373	685	0.302	994	0.237	1304	0.190	1614	0.158	1924	0.137
384	0.370	694	0.300	1005	0.235	1314	0.189	1624	0.158	1935	0.137
395	0.368	704	0.297	1014	0.233	1325	0.187	1634	0.156	1945	0.136
404	0.366	715	0.295	1024	0.232	1335	0.187	1645	0.155	1954	0.136
414	0.364	724	0.293	1035	0.230	1344	0.186	1654	0.155	1965	0.135
424	0.361	735	0.290	1044	0.229	1355	0.184	1664	0.154	1975	0.134
434	0.358	745	0.288	1054	0.227	1364	0.183	1675	0.153	1984	0.134
445	0.356	754	0.286	1064	0.225	1374	0.182	1685	0.153	1995	0.133
454	0.353	765	0.284	1074	0.223	1385	0.181	1694	0.152	2005	0.132
464	0.352	775	0.282	1085	0.222	1394	0.180	1704	0.151	2014	0.132
475	0.349	784	0.280	1095	0.220	1404	0.179	1714	0.150	2024	0.131
485	0.347	795	0.277	1104	0.218	1415	0.177	1724	0.149	2034	0.131
494	0.345	804	0.275	1115	0.217	1424	0.176	1735	0.149	2044	0.131
504	0.342	814	0.273	1125	0.216	1434	0.175	1744	0.148	2055	0.130
514	0.340	825	0.271	1134	0.214	1444	0.174	1754	0.147	2065	0.130
524	0.338	835	0.269	1145	0.212	1454	0.173	1765	0.147	2074	0.129
535	0.336	844	0.267	1155	0.211	1464	0.172	1774	0.146	2085	0.130
544	0.333	854	0.264	1164	0.210	1475	0.171	1784	0.145	2095	0.129
554	0.331	864	0.263	1174	0.208	1484	0.170	1795	0.145	2104	0.129
565	0.329	874	0.260	1185	0.206	1494	0.169	1805	0.144	2115	0.129
574	0.326	885	0.258	1194	0.205	1505	0.168	1814	0.144	2124	0.129

584	0.324	894	0.256	1205	0.203	1514	0.167	1824	0.143	2134	0.129
594	0.322	904	0.254	1215	0.202	1524	0.165	1834	0.143	2145	0.129
604	0.320	915	0.252	1224	0.201	1534	0.165	1844	0.142	2154	0.130

Table 30: $[\mathbf{Cu_a}] = 3.6$ mM, $[\mathbf{L}] = 1.7$ mM, $[\mathbf{CX}]_0 = 151$ mM, $[\mathbf{A}]_0 = 196$ mM; (data fitted from 305-2154 sec). A_{obs} uncorrected for experimental off-sets. Non-linear least squares fitting of $[\mathbf{CX.A}]_{obs} = O_{CX.A} \times \varepsilon_{\mathbf{CX.A}}$ to $[\mathbf{CX.A}]_{obs} = [\mathbf{CX.A}]_0 exp(-k_1 t)$ gave $k_1 = 6.74(4) \times 10^{-4}\ s^{-1}$ [$R^2 = 0.99$]. $\varepsilon_{\mathbf{CX.A}} = 0.697$ M was used; $[\mathbf{CX.A}]_{0,calc}$ (eq 8) 232 mM.

time (sec)	$O_{\mathbf{CX.A}}$ (A_{obs})	time (sec)	$O_{\mathbf{CX.A}}$ (A_{obs})	time (sec)	$O_{\mathbf{CX.A}}$ (A_{obs})	time (sec)	$O_{\mathbf{CX.A}}$ (A_{obs})	time (sec)	$O_{\mathbf{CX.A}}$ (A_{obs})	time (sec)	$O_{\mathbf{CX.A}}$ (A_{obs})
305	0.347	535	0.275	765	0.214	995	0.163	1225	0.128	1455	0.104
314	0.343	545	0.271	775	0.211	1005	0.162	1235	0.127	1465	0.104
325	0.338	555	0.271	785	0.210	1015	0.161	1245	0.125	1475	0.103
335	0.335	565	0.271	795	0.205	1025	0.159	1255	0.124	1485	0.102
345	0.333	575	0.263	805	0.204	1035	0.156	1265	0.123	1495	0.102
355	0.332	585	0.262	815	0.203	1045	0.154	1275	0.122	1505	0.101
365	0.330	595	0.260	825	0.199	1055	0.153	1285	0.121	1515	0.100
375	0.323	605	0.255	835	0.197	1065	0.152	1295	0.119	1525	0.099
385	0.323	615	0.255	845	0.195	1075	0.149	1305	0.118	1535	0.098
395	0.318	625	0.252	855	0.192	1085	0.147	1315	0.117	1545	0.098
405	0.315	635	0.250	865	0.191	1095	0.147	1325	0.117	1555	0.097
415	0.314	645	0.246	875	0.189	1105	0.144	1335	0.115	1565	0.097
425	0.310	655	0.241	885	0.186	1115	0.143	1345	0.114	1575	0.096
435	0.303	665	0.241	895	0.185	1125	0.141	1355	0.113	1585	0.096
445	0.304	675	0.236	905	0.182	1135	0.141	1365	0.112	1595	0.095
455	0.298	685	0.232	915	0.179	1145	0.139	1375	0.112	1605	0.094
465	0.298	695	0.231	925	0.178	1155	0.138	1385	0.111	1615	0.094
475	0.297	705	0.230	935	0.176	1165	0.136	1395	0.109	1625	0.093
485	0.290	715	0.228	945	0.173	1175	0.134	1405	0.109	1635	0.093
495	0.289	725	0.225	955	0.172	1185	0.133	1415	0.108	1645	0.092
505	0.282	735	0.224	965	0.170	1195	0.132	1425	0.107	1655	0.092
515	0.283	745	0.219	975	0.169	1205	0.131	1435	0.106	1665	0.091
525	0.280	755	0.216	985	0.165	1215	0.128	1445	0.106	1675	0.091

Table 31: $[\mathbf{Cu_a}] = 3.5$ mM, $[\mathbf{L}] = 3.5$ mM, $[\mathbf{CX}]_0 = 397$ mM, $[\mathbf{A}]_0 = 403$ mM; (data fitted from 305-1675 sec). A_{obs} uncorrected for experimental off-sets. Non-linear least squares fitting of $[\mathbf{CX.A}]_{obs} = O_{CX.A} \times \varepsilon_{\mathbf{CX.A}}$ to $[\mathbf{CX.A}]_{obs} = [\mathbf{CX.A}]_0 exp(-k_1 t)$ gave $k_1 = 1.066(5) \times 10^{-3}\ s^{-1}$ [$R^2 > 0.99$]. $\varepsilon_{\mathbf{CX.A}} = 0.697$ M was used; $[\mathbf{CX.A}]_{0,calc}$ (eq 8) 254 mM.

time (sec)	$O_{\mathbf{CX.A}}$ (A_{obs})	time (sec)	$O_{\mathbf{CX.A}}$ (A_{obs})	time (sec)	$O_{\mathbf{CX.A}}$ (A_{obs})	time (sec)	$O_{\mathbf{CX.A}}$ (A_{obs})	time (sec)	$O_{\mathbf{CX.A}}$ (A_{obs})	time (sec)	$O_{\mathbf{CX.A}}$ (A_{obs})
305	0.299	445	0.248	585	0.192	725	0.144	865	0.102	1005	0.075
315	0.295	455	0.243	595	0.189	735	0.140	875	0.100	1015	0.074
325	0.292	465	0.238	605	0.183	745	0.137	885	0.097	1025	0.073
335	0.288	475	0.237	615	0.182	755	0.134	895	0.095	1035	0.072

345	0.287	485	0.232	625	0.178	765	0.130	905	0.093	1045	0.071
355	0.284	495	0.229	635	0.174	775	0.127	915	0.090	1055	0.070
365	0.278	505	0.223	645	0.171	785	0.124	925	0.088	1065	0.069
375	0.272	515	0.220	655	0.168	795	0.121	935	0.086	1075	0.069
385	0.270	525	0.217	665	0.165	805	0.118	945	0.085	1085	0.069
395	0.267	535	0.211	675	0.161	815	0.115	955	0.083		
405	0.262	545	0.207	685	0.158	825	0.112	965	0.081		
415	0.256	555	0.205	695	0.154	835	0.110	975	0.079		
425	0.254	565	0.200	705	0.151	845	0.107	985	0.078		
435	0.251	575	0.197	715	0.147	855	0.104	995	0.076		

Table 32: $[\mathbf{Cu_a}] = 3.2$ mM, $[\mathbf{L}] = 6.5$ mM, $[\mathbf{CX}]_0 = 339$ mM, $[\mathbf{A}]_0 = 396$ mM; (data fitted from 305-1085 sec).). A_{obs} uncorrected for experimental off-sets. Non-linear least squares fitting of $[\mathbf{CX.A}]_{obs} = O_{CX.A} \times \varepsilon_{\mathbf{CX.A}}$ to $[\mathbf{CX.A}]_{obs} = [\mathbf{CX.A}]_0 exp(-k_1 t)$ gave $k_1 = 1.94(2) \times 10^{-3}\ s^{-1}$ [$R^2 = 0.99$]. $\varepsilon_{\mathbf{CX.A}} = 0.697$ M was used; $[\mathbf{CX.A}]_{0,calc}$ (eq 8) 227 mM.

time (sec)	$O_{\mathbf{CX.A}}$ (A_{obs})	time (sec)	$O_{\mathbf{CX.A}}$ (A_{obs})	time (sec)	$O_{\mathbf{CX.A}}$ (A_{obs})	time (sec)	$O_{\mathbf{CX.A}}$ (A_{obs})	time (sec)	$O_{\mathbf{CX.A}}$ (A_{obs})	time (sec)	$O_{\mathbf{CX.A}}$ (A_{obs})
305	0.338	355	0.305	405	0.269	455	0.233	505	0.199	555	0.171
315	0.332	365	0.298	415	0.262	465	0.227	515	0.193	565	0.167
325	0.326	375	0.292	425	0.255	475	0.220	525	0.187	575	0.162
335	0.318	385	0.284	435	0.248	485	0.212	535	0.181	585	0.158
345	0.312	395	0.276	445	0.241	495	0.206	545	0.176	595	0.155
										605	0.152

Table 33: $[\mathbf{Cu_a}] = 3.4$ mM, $[\mathbf{L}] = 11.7$ mM, $[\mathbf{CX}]_0 = 332$ mM, $[\mathbf{A}]_0 = 408$ mM; (data fitted from 305-605 sec).). A_{obs} uncorrected for experimental off-sets. Non-linear least squares fitting of $[\mathbf{CX.A}]_{obs} = O_{CX.A} \times \varepsilon_{\mathbf{CX.A}}$ to $[\mathbf{CX.A}]_{obs} = [\mathbf{CX.A}]_0 exp(-k_1 t)$ gave $k_1 = 2.76(3) \times 10^{-3}\ s^{-1}$ [$R^2 > 0.99$]. $\varepsilon_{\mathbf{CX.A}} = 0.697$ M was used; $[\mathbf{CX.A}]_{0,calc}$ (eq 8) 227 mM. Non-linear least squares fitting of $[\mathbf{CX.A}]_{obs} = O_{CX.A} \times \varepsilon_{\mathbf{CX.A}}$ to $[\mathbf{CX.A}]_{obs} = [\mathbf{CX.A}]_0 - k_0 t$ gave $k_0 = 4.56(6) \times 10^{-4}$ M s^{-1} [$R^2 = 0.99$]. This is at the cross-over point from first order to zero order behaviour in $[\mathbf{CX.A}]$ and near identical qualities of fit are attained.

time (sec)	$O_{\mathbf{CX.A}}$ (A_{obs})	time (sec)	$O_{\mathbf{CX.A}}$ (A_{obs})	time (sec)	$O_{\mathbf{CX.A}}$ (A_{obs})	time (sec)	$O_{\mathbf{CX.A}}$ (A_{obs})	time (sec)	$O_{\mathbf{CX.A}}$ (A_{obs})	time (sec)	$O_{\mathbf{CX.A}}$ (A_{obs})
305	0.279	384	0.252	465	0.213	545	0.174	625	0.131	705	0.096
315	0.280	395	0.240	475	0.207	555	0.162	635	0.125	715	0.093
325	0.275	404	0.241	485	0.202	565	0.159	645	0.121	725	0.089
335	0.268	415	0.234	495	0.199	575	0.155	655	0.115	735	0.087
345	0.267	425	0.229	505	0.193	584	0.149	665	0.112	745	0.085
355	0.261	434	0.229	515	0.185	595	0.144	675	0.106	754	0.083
365	0.264	445	0.224	525	0.178	604	0.143	685	0.104	765	0.080
375	0.251	455	0.214	535	0.177	615	0.135	695	0.099	775	0.079

Table 34: $[\mathbf{Cu_a}] = 3.4$ mM, $[\mathbf{L}] = 13.6$ mM, $[\mathbf{CX}]_0 = 362$ mM, $[\mathbf{A}]_0 = 428$ mM; (data fitted from 305-775 sec).). A_{obs} uncorrected for experimental off-sets. Non-linear least squares fitting of $[\mathbf{CX.A}]_{obs} = O_{CX.A} \times \varepsilon_{\mathbf{CX.A}}$ to $[\mathbf{CX.A}]_{obs} = [\mathbf{CX.A}]_0 exp(-k_1 t)$ gave $k_1 = 2.60(6) \times 10^{-3}$ s^{-1} $[R^2 = 0.98]$. $\varepsilon_{\mathbf{CX.A}} = 0.697$ M was used; $[\mathbf{CX.A}]_{0,calc}$ (eq 8) 248 mM. Non-linear least squares fitting of $[\mathbf{CX.A}]_{obs} = O_{CX.A} \times \varepsilon_{\mathbf{CX.A}}$ to $[\mathbf{CX.A}]_{obs} = [\mathbf{CX.A}]_0 - k_0 t$ gave $k_0 = 3.24(3) \times 10^{-4}$ M s^{-1} $[R^2 > 0.99]$. Cross-over into zero order behaviour in $[\mathbf{CX.A}]$ complete.

time (sec)	$O_{\mathbf{CX.A}}$ (A_{obs})	time (sec)	$O_{\mathbf{CX.A}}$ (A_{obs})	time (sec)	$O_{\mathbf{CX.A}}$ (A_{obs})	time (sec)	$O_{\mathbf{CX.A}}$ (A_{obs})	time (sec)	$O_{\mathbf{CX.A}}$ (A_{obs})	time (sec)	$O_{\mathbf{CX.A}}$ (A_{obs})
305	0.299	405	0.264	505	0.234	605	0.196	705	0.158	805	0.129
315	0.289	415	0.264	515	0.229	615	0.193	715	0.156	815	0.128
325	0.293	425	0.259	525	0.226	625	0.189	725	0.153	825	0.126
335	0.291	435	0.253	535	0.221	635	0.183	735	0.149	835	0.124
345	0.280	445	0.254	545	0.218	645	0.182	745	0.146	845	0.122
355	0.279	455	0.246	555	0.214	655	0.179	755	0.143	855	0.121
365	0.276	465	0.248	565	0.209	665	0.172	765	0.140		
375	0.275	475	0.244	575	0.207	675	0.170	775	0.137		
385	0.269	485	0.238	585	0.205	685	0.168	785	0.135		
395	0.268	495	0.233	595	0.199	695	0.163	795	0.132		

Table 35: $[\mathbf{Cu_a}] = 3.4$ mM, $[\mathbf{L}] = 15.4$ mM, $[\mathbf{CX}]_0 = 330$ mM, $[\mathbf{A}]_0 = 386$ mM; (data fitted from 305-855 sec).). A_{obs} uncorrected for experimental off-sets. Non-linear least squares fitting of $[\mathbf{CX.A}]_{obs} = O_{CX.A} \times \varepsilon_{\mathbf{CX.A}}$ to $[\mathbf{CX.A}]_{obs} = [\mathbf{CX.A}]_0 exp(-k_1 t)$ gave $k_1 = 1.63(3) \times 10^{-3}$ s^{-1} $[R^2 = 0.98]$. $\varepsilon_{\mathbf{CX.A}} = 0.697$ M was used; $[\mathbf{CX.A}]_{0,calc}$ (eq 8) 220 mM. Non-linear least squares fitting of $[\mathbf{CX.A}]_{obs} = O_{CX.A} \times \varepsilon_{\mathbf{CX.A}}$ to $[\mathbf{CX.A}]_{obs} = [\mathbf{CX.A}]_0 - k_0 t$ gave $k_0 = 2.35(2) \times 10^{-4}$ M s^{-1} $[R^2 > 0.99]$. Cross-over into zero order behaviour in $[\mathbf{CX.A}]$ complete.

2.4.3 Synthesis and Application of a Novel Copper(I) Trifluoroacetate Complex

2.4.3.1 Synthesis of Cu_b and its Derivatives

Copper (I) tetrakis(acetonitrile) trifluoroacetate, trifluoroacetic acid adduct (Cu_b)

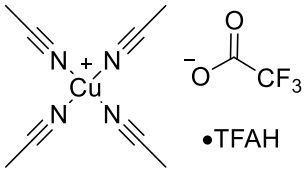

Cu_b

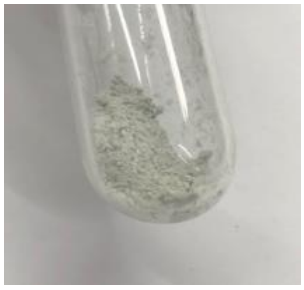

Cuprous oxide (0.55 g, 3.84 mmol) was suspended in acetonitrile (13.0 mL) and rapidly stirred, before the addition of trifluoroacetic acid (1.50 mL, 2.24 g, 19.6 mmol). During the addition, the suspension became homogenous and changed to a pale green/blue color. The solvent was removed *via* vacuum distillation and the residue dissolved in warm 4:1 diethyl ether:dichloromethane (15.0 mL). The mother liquor was removed from the dark colored residue *via* cannular filtration, and then chilled at -20 °C overnight, affording a colorless solid with a small amount of dark colored solid also present. After removal of the solvent and then drying *in vacuo*, **7** was obtained as a pale blue/green solid in 74% yield (2.59 g, 5.69 mmol). This solid proved useful for synthetic transformations but could be recrystallised again, from the same solvent mixture, to afford a colorless pure solid appropriate for kinetic studies. The ratio of TFAH in the adduct can be affected by drying *in vacuo*. Samples used for synthetic transformations and kinetic runs were confirmed as 1:1 adducts by ICP-OES and ^{1}H NMR spectroscopy. **M.p.** 57-59 °C with significant decomposition from the onset of heating; **^{1}H NMR** (500.1 MHz, $CDCl_3$): δ_H 12.66 (br s, 1H, TFA*H*), 2.15 (s, 12H, CC*H*$_3$); **^{19}F NMR** (470.6 MHz, $CDCl_3$): δ_F -68.98 (br s); **ν_{max}** (neat): 2944, 2308, 2276, 1778, 1722, 1685, 1591, 1555, 1444, 1373, 1328, 1197, 1137, 1034, 847, 806, 795, 781, 728, 699, 605, 519, 466, 436, 411 cm^{-1}; **HRMS(+)** (ESI+) found 144.9825 $C_4H_6CuN_2^+$ $[Cu(MeCN)_2]^+$ requires 144.9822 (|σ| 2.1 ppm); **HRMS(-)** (ESI-) found 112.9859 $C_2F_3O_2^-$ $[M]^-$ requires 112.9856 (|σ| 2.7 ppm); **Analysis ICP-OES** found: Cu, 13.78% $C_{12}N_4H_{13}O_4F_6Cu$, requires 13.97%. ICP analysis (typically indicating >98% purity) was preferred due to the significant thermolability of **Cu_b** during CHN combustion analysis.

Bis(tricyclohexylphosphine) copper(I) trifluoroacetate (2.64)

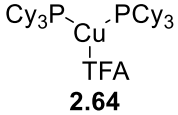

2.64

To a solution of **Cu_b** (61 mg, 0.134 mmol) in dichloromethane (1.8 mL), was added tricyclohexylphosphine (101 mg, 0.360 mmol) and the resulting very dark green solution was stirred at RT for 90 min, during which time it became colorless. After concentration of the reaction mixture *in vacuo*, it was dissolved in the minimum

diethyl ether and pentane was layered onto it. After diffusion at 4 ˚C, colorless crystals of the product formed in greater than quantitative yield (135 mg, 0.159 mmol, assumed to be occluding some solvent or TFAH). **M.p.**: 126-128 °C; **^{1}H NMR** (500.1 MHz, $CDCl_3$): δ_H 1.97-1.76 (m, 5H), 1.75-1.64 (m, 1H), 1.49-1.32 (m, 2H), 1.32-1.14 (m, 3H); **^{19}F NMR** (470.4 MHz, $CDCl_3$): δ_F -75.28; **^{31}P NMR** (202.4 MHz, $CDCl_3$): δ_P 11.72; **ν_{max}** (neat): 2931, 2857, 1777, 1736, 1681, 1449, 1387, 1354, 1329, 1301, 1276, 1181, 1124, 1084, 1042, 1005, 928, 890, 871, 852, 791, 705, 609, 589, 518, 500, 425 cm^{-1}; **HRMS** (ESI+) found 623.3911 $C_{36}H_{66}P_2Cu^+$ $[M]^+$ requires 623.3930 (|σ| 0.7 ppm); **HRMS** (ESI-) found 112.9856 $C_2O_2F_3^-$ requires 112.9856 (|σ|3.0 ppm).

$[Cu(MeCN)_4]_2[Cu_4TFA_{10}]$ (2.63)

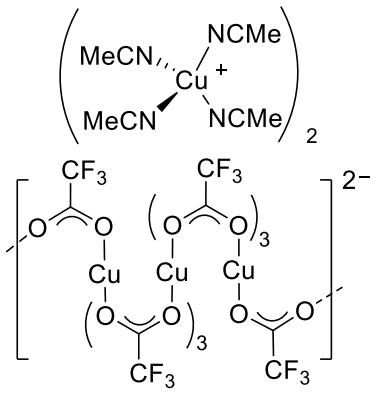

2.63

Cuprous oxide (0.25 g, 1.75 mmol) was suspended in diethyl ether (5.25 mL) and acetonitrile (0.75 mL) and rapidly stirred, before the addition of trifluoroacetic acid (1.50 mL, 2.24 g, 19.6 mmol). The reaction mixture remained heterogeneous, until further acetonitrile (0.75 mL) was added. This caused the reaction mixture to decolorize slowly and become homogeneous (with a small amount of flocculant yellow solid present). The reaction mixture was cannular filtered, then cooled to 4 ˚C for an hour before cooling to -20 ˚C for 18 h. Blue crystals formed overnight, which were dried *in vacuo* after removal of the solvent *via* cannular filtration. The product was isolated as a blue, crystalline solid in 21% yield (206 mg, 0.123 mmol). **M.p.** 118-120 °C; **^{1}H NMR** (400.1 MHz, $CDCl_3$): δ_H 2.11 (s); **ν_{max}** (neat): 3196, 3115, 3008, 2944, 2307, 2276, 1179, 1679, 1591, 1444, 1371, 1185, 1136, 1035, 840, 794, 722, 702, 608, 522, 466, 437 cm^{-1}; **HRMS** (ESI+) found 144.9819 $C_4H_6N_2Cu^+$ $[Cu(MeCN)_2]^+$ requires 144.9822 (|σ| 2.1 ppm); **HRMS** (ESI-) found 288.9002 $C_4F_6O_4Cu^+$ $[Cu(TFA)_2]^-$ requires 288.9002 (|σ| <0.1 ppm); **Anal:** Calcd. for $C_{28}H_{12}Cu_6F_{30}N_4O_{20}$ (lost 4 × MeCN upon drying) C, 20.07%; H, 0.72%; N, 3.34% found C, 19.58%; H, 0.88%; N, 3.32%.

2.4.3.2 1,4-Addition Trials Using Cu_b

General Procedure A: 1,4-Addition

A mixture of **Cu_b** (0.75 mol%) and **L** (1.5 mol%) were dissolved in toluene or dichloromethane and stirred at RT for 30 min. The resulting colorless solution was then cooled to T °C and stirred at this temperature for 10 min. $ZnEt_2$ (1.87 $mmol.g^{-1}$ in toluene, 1.2-2 equiv.) was then added

and the resulting mixture stirred for 10 minutes before the addition of the enone (1.0 equiv.). The reaction was stirred for t hours before quenching *via* the addition of 1 M HCl and warming to RT. The reaction was extracted with diethyl ether, washed with water, dried over anhydrous magnesium sulfate and then the solvent was removed *in vacuo*. The crude product was then purified *via* flash column chromatography (eluent: 12:1 pentane:diethyl ether) to afford the desired product.

(3*R*)-3-Ethyl-cyclohexanone (P)

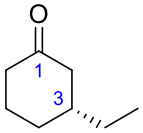

P

Synthesized according to **General Procedure A** using **Cu_b** (32.9 mg, 0.0723 mmol), **L** (80.7 mg, 0.150 mmol), dichloromethane (28.9 mL), $ZnEt_2$ (6.92 g, 12.9 mmol) and 2-cyclohexen-1-one (911 mg, 9.48 mmol) at -40 °C for 15 min. The reaction was purified *via* flash column chromatography (eluent: 8:1 pentane:diethyl ether) to afford the product as a colorless oil in 65% yield (782 mg, 6.20 mmol). This yield was improved to 88% by introducing a methanol quench before the addition of HCl, ensuring complete quenching of the zinc enolate before warming the reaction to RT. This prevents the partial dimerization of the ketone product and the zinc enolate from occurring. **R_f** (3:1 pentane:ethyl acetate): 0.84; **^{1}H NMR** (400.1 MHz, $CDCl_3$): δ_H 2.41 (dddd, 1H, *J* = 13.8, 4.0, 2.0, 2.0 Hz), 2.37-2.30 (m, 1H), 2.29-2.19 (m, 1H), 2.08-2.00 (m, 1H), 1.98 (dd, 1H, *J* = 13.0, 11.8 Hz), 1.93-1.84 (m, 1H), 1.73-1.56 (m, 2H), 1.43-1.25 (m, 3H), 0.89 (t, 3H, *J* = 7.5 Hz); **^{13}C NMR** (100.025 MHz, $CDCl_3$): δ_C 212.3 (C), 48.0 (CH_2), 41.7 (CH_2), 40.9 (CH), 31.0 (CH_2), 29.5 (CH_2), 25.4 (CH_2), 11.3 (CH_3); **ν_{max}** (neat): 2960, 2926, 2874, 2860, 1700, 1460, 1448, 1421, 1381, 1346, 1313, 1291, 1250, 1225, 1194, 1115, 1060, 1024, 1004, 964, 926, 890, 864, 769, 751, 517, 499 cm^{-1}; **HRMS** (ESI+) found 127.1112 $C_8H_{15}O^+$ $[M+H]^+$ requires 127.1117 (|σ| 3.9 ppm); **$[\alpha]_D^{25}$**: +16.0 (*er* 98:2, *c* = 2.00 in $CHCl_3$) [lit[184] -15.6 (3*S*, *er* 88:12, *c* = 1.00, $CHCl_3$)]. Data are in agreement with reported properties of **P**.[184]

(3*R*)-3-Methyl-cyclohexanone (2.65a)

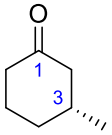

2.65a

Synthesized according to **General Procedure A** using **Cu_b** (8.5 mg, 0.0187 mmol), **L** (20.3 mg, 0.0376 mmol), toluene (6.0 mL), $ZnMe_2$ (1.5 M, 3.3 mL, 4.95 mmol) and 2-cyclohexen-1-one (0.24 mL, 238 mg, 2.48 mmol) at -40 °C for 18 hours. The reaction was purified *via* flash column chromatography (eluent: 12:1 pentane:diethyl ether) to afford the product as a colorless oil in 46% yield (129 mg, 1.15 mmol). **R_f** (8:1 pentane:diethyl ether): 0.36; **^{1}H NMR** (400.1 MHz, $CDCl_3$): δ_H 2.37-2.25 (m, 2H), 2.24-2.13 (m, 1H), 2.05-1.77 (m, 4H), 1.69-1.56 (m, 1H), 1.35-1.23 (m, 1H), 0.98 (d, 3H, *J* = 6.4 Hz); **^{13}C NMR** (100.025 MHz, $CDCl_3$):

δ_C 212.0 (C), 50.1 (CH_2), 41.2 (CH_2), 34.3 (CH), 33.4 (CH_2), 25.4 (CH_2), 22.1 (CH_3); ν_{max} (neat): 2958, 2826, 2866, 1709, 1455, 1419, 1386, 1293, 1270, 1170, 1137, 1107, 1077, 1050, 965, 947, 830, 799, 748, 727, 668, 617, 540, 502, 490 cm^{-1}; **HRMS** (ESI+) found 247.1669 $C_{14}H_{24}O_2Na^+$ $[2M+Na]^+$ requires 247.1663 (|σ| 2.4 ppm); $[\alpha]_D^{25}$: +12.0 (*er* > 99:1, *c* = 1.00 in $CHCl_3$) [lit[121] +14.2 (3*R*, *c* = 4.13, $CHCl_3$)]. Data are in agreement with reported properties of **2.65a**.[121]

(3*R*)-3-Ethyl-cycloheptanone (2.65c)

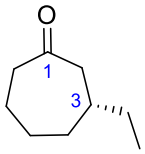

2.65c

Synthesized according to **General Procedure A** using Cu_b (8.5 mg, 0.0187 mmol), **L** (20.3 mg, 0.0376 mmol), toluene (7.8 mL), $ZnEt_2$ (1.5 mL, 2.81 mmol) and 2-cyclohepten-1-one (0.30 mL, 296 mg, 2.69 mmol) at -78 °C for 2 hours. The reaction was purified *via* flash column chromatography (eluent: 12:1 pentane:diethyl ether) to afford the product as a colorless oil in 40% yield (151 mg, 1.08 mmol). R_f (8:1 pentane:diethyl ether): 0.39; **^{1}H NMR** (400.1 MHz, $CDCl_3$): δ_H 2.52-2.32 (m, 4H), 1.95-1.81 (m, 3H), 1.68-1.52 (m, 2H), 1.45-1.19 (m, 4H), 0.89 (t, 3H, *J* = 7.4 Hz); **^{13}C NMR** (100.025 MHz, $CDCl_3$): δ_C 214.9 (C), 49.8 (CH_2), 44.1 (CH_2), 37.8 (CH), 36.6 (CH_2), 30.2 (CH_2), 28.7 (CH_2), 24.6 (CH_2), 11.6 (CH_3); ν_{max} (neat): 2960, 2924, 2875, 2856, 1697, 1457, 1446, 1408, 1381, 1348, 1320, 1252, 1198, 1165, 1074, 934, 731, 521, 490, 466 cm^{-1}; **HRMS** (ESI+) found 163.1093 $C_9H_{16}ONa^+$ $[M+Na]^+$ requires 163.1093 (|σ| < 0.1 ppm); **GC:** 6-Me-2,3-pe-γ-Cyclodextrin, 75 °C isothermal; retention times (*S*) enantiomer: 20.1 min (5.0%), (*R*) enantiomer: 20.5 min (95.0%), *er* 95:5; $[\alpha]_D^{25}$: +43.6 (*er* 95:5, *c* = 1.10 in $CHCl_3$) [lit[174] -52.7 (3*S*, *er* 93:7, *c* = 1.09, $CHCl_3$)]. Data is in agreement with reported properties of **2.65c**.[174]

(4*S*)-4-Phenyl-2-hexanone (2.65d)

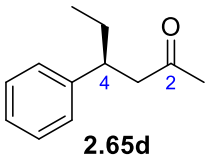

2.65d

Synthesized according to **General Procedure A** using Cu_b (8.5 mg, 0.0187 mmol), **L** (20.3 mg, 0.0376 mmol), toluene (7.8 mL), $ZnEt_2$ (1.5 mL, 2.81 mmol) and benzylideneacetone (365 mg, 2.50 mmol) at -40 °C for 4 hours. The reaction was purified *via* flash column chromatography (eluent: 8:1 pentane:diethyl ether) to afford the product as a colorless oil in 76% yield (337 mg, 1.91 mmol). R_f (8:1 pentane:diethyl ether): 0.32; **^{1}H NMR** (500.1 MHz, $CDCl_3$): δ_H 7.32-7.24 (m, 2H), 7.21-7.14 (m, 3H), 3.03 (dddd, 1H, *J* = 9.3, 7.2, 7.2, 5.3 Hz), 2.72 (2 × d, 2H, *J* = 7.2 Hz), 2.02 (s, 3H), 1.73-1.52 (m, 2H), 0.78 (t, 3H, *J* = 7.3 Hz); **^{13}C NMR** (125.025 MHz, $CDCl_3$): δ_C 208.2 (C), 144.4 (C), 128.6 (CH), 127.7 (CH), 126.5 (CH), 50.7 (CH_3), 43.1 (CH_2), 30.8 (CH), 29.5 (CH_2), 12.1 (CH_3); ν_{max} (neat): 3025, 2987, 2961, 2925, 2863, 1708, 1602, 1493, 1452, 1409, 1355, 1215, 1160, 1002, 751, 698, 666, 627, 579, 529, 494, 486, 453, 432 cm^{-1}; **HRMS** (ESI+) found 199.1098 $C_{12}H_{16}ONa^+$ $[M+Na]^+$

requires 199.1093 (|σ| 2.5 ppm); **HPLC:** Chiralpak OJ-H; mobile phase, hexane:2-propanol (99:1 v/v); flow rate, 0.5 mL.min^{-1}; retention times (*S*) enantiomer: 21.7 min (95.9%), (*R*) enantiomer: 27.4 min (4.1%), *er* 96:4; **[α]$_D^{25}$**: +24.2 (*er* 96:4, *c* = 1.65 in $CHCl_3$) [lit[198] +26.2 (4*S*, *er* 87.5:12.5, *c* = 1.00, $CHCl_3$)]. Data is in agreement with reported properties of **2.65d**.[198]

(3*S*)-1,3-Diphenyl-1-pentanone (2.65e)

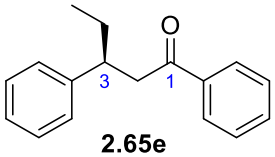

2.65e

Synthesized according to **General Procedure A** using **Cu$_b$** (8.5 mg, 0.0187 mmol), **L** (20.3 mg, 0.0376 mmol), toluene (7.8 mL), $ZnEt_2$ (1.5 mL, 2.81 mmol) and *trans*-chalcone (520 mg, 2.50 mmol) at -40 °C for 4 hours. The reaction was purified *via* flash column chromatography (eluent: 12:1 pentane:diethyl ether) to afford the product as a colorless oil in 90% yield (535 mg, 2.24 mmol). **R$_f$** (8:1 pentane:diethyl ether): 0.65; **^{1}H NMR** (500.1 MHz, $CDCl_3$): δ_H 7.92-7.89 (m, 2H), 7.53 (tt, 1H, *J* = 7.0, 1.5 Hz), 7.46-7.40 (m, 2H), 7.32-7.16 (m, 5H), 3.32-3.19 (m, 3H), 1.84-1.61 (m, 2H), 0.81 (t, 3H, *J* = 7.3 Hz); **^{13}C NMR** (125.025 MHz, $CDCl_3$): δ_C 199.3 (C), 144.8 (C), 137.4 (C), 133.0 (CH), 128.7 (CH), 128.5 (CH), 128.2 (CH), 127.8 (CH), 126.4 (CH), 45.8 (CH_2), 43.2 (CH), 29.4 (CH_2), 12.2 (CH_3); **ν$_{max}$** (neat): 3060, 3027, 2961, 2929, 2873, 1683, 1597, 1580, 1509, 1494, 1461, 1448, 1407, 1368, 1251, 1211, 1173, 1157, 1139, 1099, 1024, 977, 896, 859, 809, 749, 737, 690, 660, 589, 564, 542 cm^{-1}; **HRMS** (ESI+) found 261.1252 $C_{17}H_{18}ONa^+$ [M+Na]$^+$ requires 261.1250 (|σ| 0.8 ppm); **HPLC:** Chiralpak AD-H; mobile phase, hexane:2-propanol (95:5 v/v); flow rate, 0.5 mL.min^{-1}; retention times (*S*) enantiomer: 13.2 min (96.4%), (*R*) enantiomer: 16.8 min (3.6%), *er* 96:4; **[α]$_D^{25}$**: +5.3 (*er* 96:4, *c* = 1.50 in dichloromethane) [lit[199] -5.6 (3*R*, *er* 99.5:0.5, *c* = 1.49, dichloromethane)]. Data is in agreement with reported properties of **2.65e**.[199]

(4*S*)-4-Ethyl-2-nonanone (2.65f)

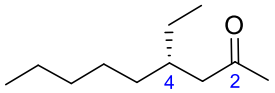

2.65f

Synthesized according to **General Procedure A** using **Cu$_b$** (8.5 mg, 0.0187 mmol), **L** (20.3 mg, 0.0376 mmol), toluene (7.8 mL), $ZnEt_2$ (1.5 mL, 2.81 mmol) and *trans*-3-nonen-2-one (0.41 mL, 348 mg, 2.48 mmol) at -78 °C for 1.5 hours. The reaction was purified *via* flash column chromatography (eluent: 12:1 pentane:diethyl ether) to afford the product as a colorless oil in 65% yield (274 mg, 1.61 mmol). **R$_f$** (8:1 pentane:diethyl ether): 0.63; **^{1}H NMR** (400.1 MHz, $CDCl_3$): δ_H 2.35-2.30 (m, 2H), 2.13 (s, 3H), 1.85 (hept, 1H, *J* = 6.2 Hz), 1.38-1.14 (m, 10H), 0.87 (t, 3H, *J* = 6.9 Hz), 0.84 (t, 3H, *J* = 7.4 Hz); **^{13}C NMR** (100.025 MHz, $CDCl_3$): δ_C 209.6 (C), 48.6 (CH_2), 35.5 (CH), 33.6 (CH_2), 32.3 (CH_2), 30.6 (CH_3), 26.5 (CH_2), 26.4 (CH_2), 22.8 (CH_2), 14.2 (CH_3), 11.0 (CH_3); **ν$_{max}$** (neat): 2959,

2925, 2873, 2857, 1714, 1460, 1410, 1355, 1270, 1231, 1164, 1000, 961, 768, 725, 600, 542, 519 cm^{-1}; **HRMS** (ESI+) found 171.1730 $C_{11}H_{23}O^+$ $[M+H]^+$ requires 171.1743 (|σ| 7.6 ppm); **GC:** 6-Me-2,3-pe-γ-Cyclodextrin, 75 °C isothermal; retention times (*S*) enantiomer: 18.2 min (79.3%), (*R*) enantiomer: 18.6 min (20.7%), *er* 79:21; **$[\alpha]_D^{25}$**: -2.6 (*er* 79:21, *c* = 3.00 in $CDCl_3$) [lit[200] -5.1 (4*S*, *er* 80:20, *c* = 3.00, $CDCl_3$)]. Data is in agreement with reported properties of **2.65f**.[200]

(3*R*)-3-Ethyl-octanal (2.65g)

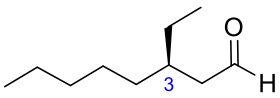

2.65g

Synthesized according to **General Procedure A** using **Cu_b** (8.5 mg, 0.0187 mmol), **L** (20.3 mg, 0.0376 mmol), toluene (10.0 mL), $ZnEt_2$ (2.4 mL, 4.49 mmol) and adding *trans*-2-octenal (0.37 mL, 313 mg, 2.48 mmol) dropwise over 15 min at -30 °C before stirring for a further 25 min. The reaction was quenched with water rather than HCl and then purified *via* flash column chromatography (eluent: 12:1 pentane:diethyl ether) to afford the product as a colorless oil in 39% yield (151 mg, 0.966 mmol). **R_f** (8:1 pentane:diethyl ether): 0.73; **^{1}H NMR** (500.1 MHz, $CDCl_3$): δ_H 9.75 (dd, 1H, *J* = 2.4, 2.4 Hz), 2.32-2.29 (m, 2H), 1.88 (hept, 1H, *J* = 6.4 Hz), 1.40-1.17 (m, 10H), 0.90-0.80 (m, 6H); **^{13}C NMR** (125.025 MHz, $CDCl_3$): δ_C 203.5 (CH), 48.3 (CH_2), 34.5 (CH), 33.8 (CH_2), 32.1 (CH_2), 26.7 (CH_2), 26.5 (CH_2), 22.7 (CH_2), 14.1 (CH_3), 11.0 (CH_3); **ν_{max}** (neat): 2959, 2920, 2872, 2858, 1725, 1686, 1460, 1379, 1231, 1138, 1060, 968, 948, 822, 749, 696, 651, 553, 542, 511, 464, 457 cm^{-1}; **HRMS** (ESI-) found 171.1387 $C_{10}H_{19}O_2^-$ $[M+O-H]^-$ requires 171.1391 (|σ| 2.3 ppm); **GC** (once converted into (4*R*-4-ethyl-2-nonanone)**:** 6-Me-2,3-pe-γ-Cyclodextrin, 75 °C isothermal; retention times (*S*) enantiomer: 18.2 min (42.3%), (*R*) enantiomer: 18.7 min (57.7%), *er* 58:42; **$[\alpha]_D^{25}$**: -28.0 (*er* 58:42, *c* = 1.00 in $CHCl_3$).

(3*S*)-3-Ethyl-4,4-dimethyl-cyclohexanone (2.65b)

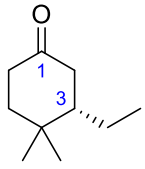

2.65b

Synthesized according to **General Procedure A** using **Cu_b** (8.5 mg, 0.0187 mmol), **L** (20.3 mg, 0.0376 mmol), toluene (6.8 mL), $ZnEt_2$ (2.4 mL, 4.49 mmol) and 4,4-dimethyl-2-cyclohexen-1-one (0.33 mL, 312 mg, 2.51 mmol) at -40 °C for 18 hours. The reaction was purified *via* flash column chromatography (eluent: 8:1 pentane:diethyl ether) to afford the product as a colorless oil in a quantitative yield (386 mg, 2.51 mmol). **R_f** (8:1 pentane:diethyl ether): 0.27; **^{1}H NMR** (500.1 MHz, $CDCl_3$): δ_H 2.44 (ddd, 1H, *J* = 14.7, 4.5, 2.1 Hz), 2.41-2.36 (m, 1H), 2.26 (dddd, 1H, *J* = 14.8, 4.9, 3.7, 2.2 Hz), 2.01 (ddd, 1H, *J* = 14.8, 12.1, 1.1 Hz), 1.75-1.51 (m, 3H), 1.39 (dddd, 1H, *J* = 12.1, 10.5, 4.4, 2.7 Hz), 1.07-0.98 (m, 1H, overlapping with Me peaks), 1.02 (s, 3H), 0.98 (s, 3H), 0.87 (t, 3H, *J* = 7.4 Hz); **^{13}C NMR** (125.025 MHz, $CDCl_3$): δ_C 212.5 (C), 49.0 (CH), 42.4 (CH_2), 40.7 (CH_2), 38.5 (CH_2),

33.1 (C), 28.9 (CH_3), 23.5 (CH_2), 19.7 (CH_3), 12.4 (CH_3); ν_{max} (neat): 2961, 2933, 2874, 1712, 1467, 1455, 1418, 1389, 1368, 1334, 1296, 1245, 1146, 1137, 1009, 777, 762, 529, 508 cm^{-1}; **HRMS** (ESI+) found 177.1252 $C_{10}H_{18}ONa^+$ $[M+Na]^+$ requires 177.1250 (|σ| 1.1 ppm); $[\alpha]_D^{25}$: +14.3 (*er* > 99:1, *c* = 1.40 in $CHCl_3$) [lit[174] -17.2 (3*R*, *er* 87.5:12.5, *c* = 1.38, $CHCl_3$)]. Data is in agreement with reported properties of **2.65b**.[174]

Product of Aldol reaction between 1,4-addition product (P) and intermediate enolate (E) (2.71)

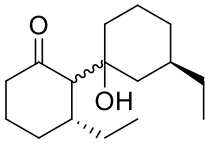

2.71

A mixture of Cu_b (8.5 mg, 0.0187 mmol), **L** (20.3 mg, 0.0376 mmol) and dichloromethane (7.8 mL) was stirred at RT for 30 min before cooling to -40 ˚C and stirring for a further 10 min. After this, $ZnEt_2$ (1.87 $mmol.g^{-1}$ in toluene, 1.5 mL, 2.81 mmol) was added, and the resulting mixture stirred for a further 10 min, before the addition of 2-cyclohexen-1-one (0.25 mL, 248 mg, 2.58 mmol). After stirring for 4 min, (3*R*)-3-ethyl-cyclohexanone (0.12 g, 0.951 mmol). The resulting mixture was stirred at the same temperature for a further 8 min before removing from the cold bath and then adding HCl (1 M, 5 mL). Once fully warmed to RT and quenched, the reaction mixture was diluted with water, extracted with diethyl ether, dried over anhydrous sodium sulfate and concentrated *in vacuo* to afford the crude product. This was then purified *via* flash column chromatography (8:1 pentane:diethyl ether) to afford the product as a colorless oil in 59% yield (141 mg, 0.559 mmol) and as a mixture of 2 diastereomers in an approximate ratio of 1:0.15. For clarity, all NMR signals are given with an exact integration as referenced to the signal at 0.70 ppm in the ^{1}H NMR and 66.0 ppm in the ^{13}C NMR. **^{1}H NMR** (500.1 MHz, $CDCl_3$): δ_H 2.51 (ddd, 0.97H, *J* = 14.6, 10.7, 7.2 Hz), 2.41-2.35 (m, 1.28H), 2.33-2.25 (m, 1H), 2.10-1.91 (m, 3.48H), 1.87-1.74 (m, 1.97H), 1.70 (ddd, 0.72H, *J* = 12.8, 3.7, 1.7 Hz), 1.63-1.36 (m, 4.73H), 1.35-1.23 (m, 2.57H), 1.21-1.09 (m, 2.93H), 1.01 (t, 0.96H, *J* = 12.6 Hz), 0.89-0.77 (m, 6.83H), 0.70 (qd, 1H, *J* = 12.6, 4.3 Hz); **^{13}C NMR** (125.025 MHz, $CDCl_3$): δ_C 216.5 (C, 0.45C), 212.3 (C, 0.07C), 73.44 (C, 0.58C), 66.0 (CH, 1.00C), 47.9 (CH_2, 0.26C), 43.4 (CH_2, 1.05C), 42.1 (CH_2, 1.13C), 41.6 (CH_2, 0.29C), 40.8 (CH, 0.25C), 38.3 (CH, 1.00C), 35.9 (CH_2, 1.06C), 34.4 (CH, 0.94C), 31.7 (CH_2, 1.04C), 31.0 (CH_2, 0.29C), 29.8 (CH_2, 0.95C), 29.4 (CH_2, 0.27C), 28.1 (CH_2, 1.18C), 26.5 (CH_2, 1.01C), 25.4 (CH_2, 0.29C), 21.7 (CH_2, 0.93C), 21.5 (CH_2, 1.08C), 12.0 (CH_3, 1.00C), 11.3 (CH_3, 0.91C), 11.2 (CH_3, 0.26C); ν_{max} (neat): 3497, 2959, 2927, 2873, 1684, 1459, 1448, 1422, 1380, 1357, 1347, 1312, 1239, 1228, 1158, 1129, 1115, 1090, 1061, 1028, 1015, 1000, 979, 907, 729, 647, 520, 494, 440 cm^{-1}; **HRMS** (ESI+) found 253.2155 $C_{16}H_{29}O_2^+$ $[M+H]^+$ requires 253.2162 (|σ| 2.8 ppm).

2.4.4 Kinetic Investigations Using Diethylzinc

2.4.4.1 Formation of CX·Zn Adduct

Formation of CX·Zn Adduct Experimental Procedure Example

To a flame-dried, three necked flask under argon, cyclohex-2-en-1-one (**CX**, 1.0458 g 1.0532 mL, 10.879 mmol) was dissolved in anaerobic, anhydrous toluene (20.0935 g, 23.1759 mL) and stirred at -40 ^{o}C over 10 minutes. Data collection using the ReactIR was then started, in the range 1900-1500 cm^{-1}, using manual sampling corrected for initial minor experimental off-sets (typically ~0.02-0.04 absorbance units). Two scans were taken *ca.* 2 min apart to ensure thermodynamic equilibrium had been attained. This procedure was repeated after each addition of diethylzinc (**Zn**, 0.962 M, 0.9906 $mmol.g^{-1}$, 2.190 g, 2.000 mmol) on the derived yellow solutions. After 10 additions, data collection was halted and the reaction was quenched *via* the addition of HCl_{aq} (1 M, 10 mL) providing colourless **CX** recovered in quantitative yield. The volumes used were estimated from standard densities for **CX** (0.993 g mL^{-1}) and toluene (0.867 g ml^{-1}), while that of 0.962 M diethylzinc (**Zn**) solutions in toluene was determined experimentally to be 1.030 $g.mL^{-1}$ in these titration runs. Reaction component volumes were assumed to be additive (*i.e.* partial molar volume/phase change effects were assumed minimal).

Formation of CX·Zn Adduct Data Analysis

Data were collected based on titration of known quantities of diethylzinc (**Zn**) into a known cyclohex-2-en-1-one (**CX**) solution. The quantity of **CX** remaining was determined by the, off-set corrected, absorbance (O_{CX}) as [**CX**] = $\varepsilon_{CX} \times O_{CX}$ where ε_{CX} is the molar constant of the ReactIR instrument. Values of ε_{CX} can be both measured against standard solutions and thus fitted against the **CX**/**Zn** mixtures. Data were fitted against 1:1 and 1:2 isotherms, whose derivations are shown in Figure 45 and Figure 46 respectively.

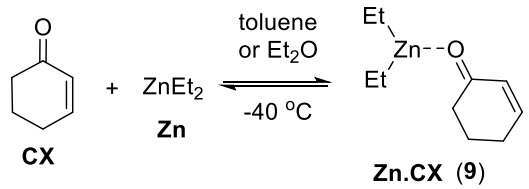

With equilibrium const:

$$K_1 = \frac{[\mathbf{ZnCX}]}{[\mathbf{CX}][\mathbf{Zn}]} \quad (1)$$

Mass balance: the **CX** and **Zn** species must total at any given moment:

$$[\mathbf{Zn_{TOT}}] = [\mathbf{Zn}] + [\mathbf{ZnCX}] \quad (2)$$

Sub (*2*) and (*3*) into (*1*):

$$[\mathbf{CX_{TOT}}] = [\mathbf{CX}] + [\mathbf{Zn.CX}] \quad (3)$$

$$K_1 = \frac{[\mathbf{ZnCX}]}{([\mathbf{CX_{TOT}}] - [\mathbf{Zn.CX}])([\mathbf{Zn_{TOT}}] - [\mathbf{Zn.CX}])} \quad (4)$$

...multiply out (4) and rearranging:

$$K_1[\mathbf{Zn.CX}]^2 + (-K_1[\mathbf{CX_{TOT}}] - K_1[\mathbf{Zn_{TOT}}] - 1)[\mathbf{Zn.CX}] + K_1[\mathbf{CX_{TOT}}][\mathbf{Zn_{TOT}}] = 0 \quad (5)$$

Eq (5) is a standard quadratic form with known solution:

$$ax^2 + bx + c = 0 \quad \text{with..} \quad x = \frac{-b \pm \sqrt{b2 - 4ac}}{2a} \quad \text{where } x = [\mathbf{Zn.CX}] \quad (6)$$

with:

$$a = K_1$$
$$b = (-K_1[\mathbf{CX_{TOT}}] - K_1[\mathbf{Zn_{TOT}}] - 1)$$
$$c = K_1[\mathbf{CX_{TOT}}][\mathbf{Zn_{TOT}}]$$

One of the root solutions of (*6*) must have a 'real world' meaning, viz:

K_1, $\varepsilon_{\mathbf{Zn.CX}}$ and [**Zn.CX**] must all be positive, where: [**Zn.CX**] = $\varepsilon_{\mathbf{Zn.CX}} \times O_{\mathbf{CX.A}}$
and $\varepsilon_{\mathbf{Zn.CX}}$ is the molar constant for **Zn.CX** and $O_{\mathbf{Zn.CX}}$ its absorbance

Thus, [**Zn.CX**] and [**CX**] can be calculated through (*6*) and (*7*):

$$[\mathbf{CX}] = [\mathbf{CX_{TOT}}] - [\mathbf{Zn.CX}] \quad (7)$$

*Figure 45: Derivation of the 1:1 predicted binding curve for **Zn·CX**, from **CX** and **Zn** at -40 ˚C.*

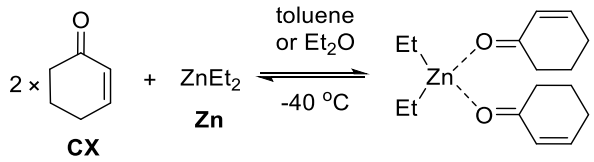

Zn.CX$_2$ (**10**)

With equilibrium const:

$$K_2 = \frac{[\mathbf{Zn.CX_2}]}{[\mathbf{Zn}][\mathbf{CX}]^2} \qquad (8)$$

Mass balance: the **CX** and **Zn** species must total at any given moment:

$$[\mathbf{Zn_{TOT}}] = [\mathbf{Zn}] + [\mathbf{Zn.CX_2}] \qquad (9)$$

Sub (*9*) and (*10*) into (*8*): $$[\mathbf{CX_{TOT}}] = [\mathbf{CX}] + 2[\mathbf{Zn.CX_2}] \qquad (10)$$

$$K_2 = \frac{[\mathbf{Zn.CX_2}]}{([\mathbf{Zn_{TOT}}] - [\mathbf{Zn.CX_2}])([\mathbf{CX_{TOT}}] - 2[\mathbf{Zn.CX_2}])^2} \qquad (11)$$

...multiply out (*11*) and rearranging:

$$-4K_2[\mathbf{Zn.CX_2}]^3 + (4K_2[\mathbf{Zn_{TOT}}] + 4K_2[\mathbf{CX_{TOT}}])[\mathbf{Zn.CX_2}]^2 + ... \\ .... (-4K_2[\mathbf{CX_{TOT}}][\mathbf{Zn_{TOT}}] - K_2[\mathbf{CX_{TOT}}]^2 - 1)[\mathbf{ZnCX_2}] + K_2[\mathbf{Zn_{TOT}}][\mathbf{CX_{TOT}}]^2 = 0 \qquad (12)$$

Eq (*12*) is a standard cubic form with known solution:

$$ax^3 + bx^2 + cx + d = 0 \quad \text{with..} \quad x = -\frac{1}{3a}\left(b + C + \frac{\Delta_0}{c}\right) \quad \text{where } x = [\mathbf{Zn.CX_2}] \qquad (13)$$

$$\Delta_0 = b^2 - 3ac \qquad \Delta_1 = 2b^3 - 9abc + 27a^2d \qquad C = \sqrt[3]{\frac{\Delta_0 \pm \sqrt{\Delta_1^2 - 4\Delta^3}}{2}}$$

with:
$a = -4K_2$
$b = (4K_2[\mathbf{Zn_{TOT}}] + 4K_2[\mathbf{CX_{TOT}}])$
$c = (-4K_2[\mathbf{Zn_{TOT}}][\mathbf{CX_{TOT}}] - K_2[\mathbf{CX_{TOT}}]^2 - 1)$
$d = K_2[\mathbf{Zn_{TOT}}][\mathbf{CX_{TOT}}]^2$

One of the root solutions of (*13*) must have a 'real world' meaning, viz:

K_2, $\varepsilon_{\mathbf{Zn.CX_2}}$ and $[\mathbf{Zn.CX_2}]$ must all be positive, where: $[\mathbf{Zn.CX_2}] = \varepsilon_{\mathbf{Zn.CX_2}} \times O_{\mathbf{Zn.CX_2}}$ and $\varepsilon_{\mathbf{Zn.CX_2}}$ is the molar constant for **Zn.CX$_2$** and $O_{\mathbf{Zn.CX_2}}$ its absorbance

Thus, [**CX.Zn**] and [**CX**] can be calculated through (*13*) and (*14*):

$$[\mathbf{CX}] = [\mathbf{CX_{TOT}}] - 2[\mathbf{Zn.CX_2}] \qquad (14)$$

*Figure 46: Derivation of the 1:2 predicted binding curve for **Zn·CX$_2$**, from **CX** and **Zn** at -40 ˚C.*

The calculated values of *K* and the qualities of fit were presented previously (see Table 15). As the absorbance is being used to precisely quantify the **CX** concentration great care was taken to eliminate minor off-sets in instrument backgrounds (in A_{obs}, ~0.03 which are common) before data analysis. Primary titration data, fitted to the model shown in Figure 45 (**CX·Zn**), are shown below – as the quality of fit was highest for this model.

$[\mathbf{Zn}_{TOT}]$ (mM)	$[\mathbf{CX}_{TOT}]$ (mM)	$O_{\mathbf{cx}}$ (A_{obs})	$[\mathbf{Zn.CX}]_{calc}$ (mM)	$[\mathbf{Zn}_{TOT}]$ (mM)	$[\mathbf{CX}_{TOT}]$ (mM)	$O_{\mathbf{cx}}$ (A_{obs})	$[\mathbf{Zn.CX}]_{calc}$ (mM)
0.0	469.1	0.330	0.0	289.5	321.6	0.133	133.3
51.9	426.1	0.286	33.2	318.3	308.9	0.123	138.6
98.2	405.8	0.246	60.0	348.7	296.4	0.108	142.5
139.7	387.5	0.221	81.2	373.6	284.6	0.104	144.8
183.1	368.4	0.197	100.4	397.7	274.1	0.096	146.0
222.1	351.2	0.164	114.8	421.1	263.7	0.092	146.2
256.2	336.2	0.140	125.2				

*Table 36: Titration of **Zn/CX** in toluene: $[\mathbf{Zn}_{TOT}]$ = 0-421 mM, $[\mathbf{CX}_{TOT}]$ = 469-264 mM (the concentration of **CX** falls due to the increase in volume as **Zn** is added), O_{CX} = the calculated absorbance for **CX**; A_{obs} corrected for instrument off-set. Non-linear least squares fitting of equation 5 (Figure 45) gave K = 4.5(3) M^{-1} (R^2=>0.99).*

$[\mathbf{Zn}_{TOT}]$ (mM)	$[\mathbf{CX}_{TOT}]$ (mM)	$O_{\mathbf{cx}}$ (A_{obs})	$[\mathbf{Zn.CX}]_{calc}$ (mM)	$[\mathbf{Zn}_{TOT}]$ (mM)	$[\mathbf{CX}_{TOT}]$ (mM)	$O_{\mathbf{cx}}$ (A_{obs})	$[\mathbf{Zn.CX}]_{calc}$ (mM)
0.0	388.3	0.211	0.0	375.0	318.5	0.142	57.5
75.5	374.2	0.195	15.1	426.4	309.0	0.133	62.3
141.7	361.9	0.183	26.0	474.4	300.0	0.127	66.2
206.6	350.0	0.170	8.0	519.7	291.6	0.120	69.4
268.8	338.3	0.159	36.9	562.3	283.7	0.115	72.0
322.4	328.3	0.151	45.4				

*Table 37: Titration of **Zn/CX** in diethyl ether: $[\mathbf{Zn}_{TOT}]$ = 0-562 mM, $[\mathbf{CX}_{TOT}]$ = 388-284 mM (the concentration of **CX** falls due to the increase in volume as **Zn** is added), O_{CX} = the calculated absorbance for **CX**; A_{obs} corrected for instrument off-set. Non-linear least squares fitting of equation 5 (Figure 45) gave K = 0.69(1) M^{-1} (R^2=>0.99).*

2.4.4.2 Measurement and Calculation of the Order in Each Reaction Component

General Experimental Procedure (Triple Dose Experiment)

To a flame-dried three necked flask under argon, (*R*,*S*,*S*)-phosphoramidite ligand **L** (41.7 mg, 77.3 µmol) and [Cu(MeCN)$_4$]TFA·TFAH (**Cu$_b$**, 17.7 mg, 38.9 µmol) were added to anhydrous anaerobic dichloromethane (21.2052 g, 15.944 mL) and the mixture stirred at room temperature for 30 minutes. The solution was cooled to -40 °C for 10 minutes, after which time diethylzinc (**Zn**, 2.128 M in toluene, 1.910 mmol.g^{-1}, 3.358 g, 3.288 mL of solution, 6.413 mmol) was added to the mixture and stirred at this temperature for an additional 10 minutes at -40 °C. During this period, data collection was started. At 1 min, cyclohex-2-en-1-one (**CX**, 488.9 mg, 0.4923 mL, 5.086 mmol) was added. At 13.5 min, this 1st dose had completed (>4 half-lives) and the reaction mixture was charged with additional **Zn** (2.749 g, 5.250 mmol) from the same stock solution. After equilibration, a 2nd dose of **CX** (498.1 mg, 5.1815 mmol) was added at 15 min and the data collection continued. After completion of the 2nd conjugate addition process at 23 min, additional **Zn** (2.658 g, 5.077 mmol) from the same stock solution was added. After equilibration, a 3rd dose of **CX** (485.2 mg, 5.0473 mmol) was added at 24.5 min and the data collection continued until the reaction completed. Kinetic data were obtained by the general methods described previously.

Primary Data

Time (sec)	O_E (A_{obs})	Time (sec)	O_E (A_{obs})	Time (sec)	O_E (A_{obs})	Time (sec)	O_E (A_{obs})	Time (sec)	O_E (A_{obs})
100	0.023	205	0.128	310	0.185	415	0.214	520	0.231
115	0.038	220	0.139	325	0.190	430	0.217	535	0.233
130	0.054	235	0.149	340	0.195	445	0.219	550	0.235
145	0.071	250	0.157	355	0.199	460	0.222		
160	0.087	265	0.165	370	0.203	475	0.224		
175	0.102	280	0.172	385	0.207	490	0.227		
190	0.115	295	0.179	400	0.211	505	0.229		

*Table 38: Dose 1; [**Cu$_b$**] = 1.97 mM, [**L**] = 3.92 mM, [**CX**]$_0$ = 258 mM, [**Zn**]$_0$ = 325 mM; t_0 = 100 s (40 s after addition of **CX**). A_{obs} corrected for instrument background ($A_{background}$ = 0.0544). Non-linear least squares fitting of $[E]_{obs} = O_E \times (1/\varepsilon_E)$ to $[E]_t = [E]_{40} + \Delta[E](1-\exp(-k_1 t))$ gave k_1 = 0.00608(5) s^{-1} [R^2 = 0.999]. An average ε_E across 12 separate runs of 0.756(6) M^{-1} was used in all fits.*

Time (sec)	O_E (A_{obs})	Time (sec)	O_E (A_{obs})	Time (sec)	O_E (A_{obs})	Time (sec)	O_E (A_{obs})	Time (sec)	O_E (A_{obs})
940	0.307	985	0.375	1030	0.405	1075	0.422	1120	0.432
955	0.336	1000	0.388	1045	0.412	1090	0.425	1135	0.434
970	0.358	1015	0.398	1060	0.417	1105	0.429		

*Table 39: Dose 2; [**Cu_b**] = 1.70 mM, [**L**] = 3.37 mM, [**CX**]$_0$ = 226 mM, [**Zn**]$_0$ = 287 mM; t_0 = 940 s (40 s after addition of **CX**). A_{obs} corrected for instrument background ($A_{background}$ = 0.0544). Non-linear least squares fitting of $[E]_{obs} = O_E \times (1/\varepsilon_E)$ to $[E]_t = [E]_{40} + \Delta[E](1-\exp(-k_1 t))$ gave k_1 = 0.0154(3) s^{-1} [R^2 = 0.999]. An average ε_E across 12 separate runs of 0.756(6) M^{-1} was used in all fits.*

Time (sec)	O_E (A_{obs})	Time (sec)	O_E (A_{obs})	Time (sec)	O_E (A_{obs})	Time (sec)	O_E (A_{obs})	Time (sec)	O_E (A_{obs})
1510	0.476	1555	0.521	1600	0.543	1645	0.556	1690	0.564
1525	0.495	1570	0.530	1615	0.548	1660	0.559	1705	0.566
1540	0.510	1585	0.537	1630	0.552	1675	0.562		

*Table 40: Dose 3; [**Cu_b**] = 1.50 mM, [**L**] = 2.97 mM, [**CX**]$_0$ = 194 mM, [**Zn**]$_0$ = 249 mM; t_0 = 1510 s (40 s after addition of **CX**). A_{obs} corrected for instrument background ($A_{background}$ = 0.0544). Non-linear least squares fitting of $[E]_{obs} = O_E \times (1/\varepsilon_E)$ to $[E]_t = [E]_{40} + \Delta[E](1-\exp(-k_1 t))$ gave k_1 = 0.0135(4) s^{-1} [R^2 = 0.999]. An average ε_E across 12 separate runs of 0.756(6) M^{-1} was used in all fits.*

Time (sec)	O_E (A_{obs})	Time (sec)	O_E (A_{obs})	Time (sec)	O_E (A_{obs})	Time (sec)	O_E (A_{obs})	Time (sec)	O_E (A_{obs})
940	0.232	985	0.283	1030	0.306	1075	0.319	1120	0.326
955	0.254	1000	0.293	1045	0.312	1090	0.321	1135	0.328
970	0.271	1015	0.301	1060	0.316	1105	0.324		

*Table 41: Dose 2; [**Cu_b**] = 1.70 mM, [**L**] = 3.37 mM, [**CX**]$_0$ = 226 mM, [**Zn**]$_0$ = 287 mM, [**E**]$_0$ = 222 mM; data fitted from 940-1135 s. A_{obs} corrected for instrument background ($A_{background}$ = 0.0545). Non-linear least squares fitting of $[E]_{obs} = O_E \times (1/\varepsilon_E)$ to $[E]_t = [E]_{40} + \Delta[E](1-\exp(-k_1 t))$ gave k_1 = 0.0154(3) s^{-1} [R^2 = 0.999]. An average ε_E across 12 separate runs of 0.76(1) M^{-1} was used in all fits.*

Time (sec)	O_E (A_{obs})	Time (sec)	O_E (A_{obs})	Time (sec)	O_E (A_{obs})	Time (sec)	O_E (A_{obs})	Time (sec)	O_E (A_{obs})
955	0.258	1015	0.312	1075	0.333	1135	0.344		

970	0.277	1030	0.319	1090	0.337	1150	0.346
985	0.292	1045	0.325	1105	0.340	1165	0.348
1000	0.303	1060	0.330	1120	0.342	1180	0.349

Table 42: Dose 2; $[\mathbf{Cu_b}] = 1.70$ mM, $[\mathbf{L}] = 3.62$ mM, $[\mathbf{CX}]_0 = 275$ mM, $[\mathbf{Zn}]_0 = 276$ mM, $[\mathbf{E}]_0 = 229$ mM; data fitted from 955-1180 s. A_{obs} corrected for instrument background ($A_{background} = 0.0443$). Non-linear least squares fitting of $[\mathbf{E}]_{obs} = O_E \times (1/\varepsilon_E)$ to $[\mathbf{E}]_t = [\mathbf{E}]_{40} + \Delta[\mathbf{E}](1-\exp(-k_1 t))$ gave $k_1 = 0.0139(3)\ s^{-1}$ [$R^2 = 0.999$]. An average ε_E across 12 separate runs of 0.76(1) M^{-1} was used in all fits.

Time (sec)	O_E (A_{obs})	Time (sec)	O_E (A_{obs})	Time (sec)	O_E (A_{obs})	Time (sec)	O_E (A_{obs})	Time (sec)	O_E (A_{obs})
940	0.205	1000	0.221	1060	0.230	1120	0.235	1180	0.238
955	0.210	1015	0.224	1075	0.232	1135	0.236	1195	0.239
970	0.214	1030	0.226	1090	0.233	1150	0.237		
985	0.218	1045	0.228	1105	0.234	1165	0.238		

Table 43: Dose 2; $[\mathbf{Cu_b}] = 1.76$ mM, $[\mathbf{L}] = 3.57$ mM, $[\mathbf{CX}]_0 = 72.3$ mM, $[\mathbf{Zn}]_0 = 295$ mM, $[\mathbf{E}]_0 = 233$ mM; data fitted from 940-1195 s. A_{obs} corrected for instrument background ($A_{background} = 0.0415$). Non-linear least squares fitting of $[\mathbf{E}]_{obs} = O_E \times (1/\varepsilon_E)$ to $[\mathbf{E}]_t = [\mathbf{E}]_{40} + \Delta[\mathbf{E}](1-\exp(-k_1 t))$ gave $k_1 = 0.0095(1)\ s^{-1}$ [$R^2 = 0.999$]. An average ε_E across 12 separate runs of 0.76(1) M^{-1} was used in all fits.

Time (sec)	O_E (A_{obs})	Time (sec)	O_E (A_{obs})	Time (sec)	O_E (A_{obs})	Time (sec)	O_E (A_{obs})	Time (sec)	O_E (A_{obs})
940	0.247	1000	0.294	1060	0.314	1120	0.325	1180	0.330
955	0.264	1015	0.301	1075	0.317	1135	0.326	1195	0.331
970	0.276	1030	0.306	1090	0.320	1150	0.327		
985	0.286	1045	0.311	1105	0.322	1165	0.329		

Table 44: Dose 2; $[\mathbf{Cu_b}] = 1.84$ mM, $[\mathbf{L}] = 3.81$ mM, $[\mathbf{CX}]_0 = 246$ mM, $[\mathbf{Zn}]_0 = 203$ mM, $[\mathbf{E}]_0 = 244$ mM; data fitted from 940-1195 s. A_{obs} corrected for instrument background ($A_{background} = 0.0149$). Non-linear least squares fitting of $[\mathbf{E}]_{obs} = O_E \times (1/\varepsilon_E)$ to $[\mathbf{E}]_t = [\mathbf{E}]_{40} + \Delta[\mathbf{E}](1-\exp(-k_1 t))$ gave $k_1 = 0.0127(3)\ s^{-1}$ [$R^2 = 0.999$]. An average ε_E across 12 separate runs of 0.76(1) M^{-1} was used in all fits.

Time (sec)	O_E (A_{obs})	Time (sec)	O_E (A_{obs})	Time (sec)	O_E (A_{obs})	Time (sec)	O_E (A_{obs})	Time (sec)	O_E (A_{obs})
1120	0.348	1180	0.381	1240	0.395	1300	0.402	1360	0.406

1135	0.360	1195	0.386	1255	0.397	1315	0.403
1150	0.366	1210	0.390	1270	0.399	1330	0.404
1165	0.374	1225	0.393	1285	0.401	1345	0.405

*Table 45: Dose 2; [**Cu$_b$**] = 1.75 mM, [**L**] = 3.65 mM, [**CX**]$_0$ = 233 mM, [**Zn**]$_0$ = 286 mM, [**E**]$_0$ = 232 mM; data fitted from 1120-1360 s. A_{obs} corrected for instrument background ($A_{background}$ = 0.0794). Non-linear least squares fitting of [**E**]$_{obs}$ = O_E× (1/ε_E) to [**E**]$_t$ = [**E**]$_{40}$ + Δ[**E**](1-exp(-k_1t)) gave k_1 = 0.0129(3) s^{-1} [R^2 = 0.999]. An average ε_E across 15 separate injections of 0.86(3) M^{-1} was used in all fits.*

Time (sec)	O_E (A_{obs})	Time (sec)	O_E (A_{obs})	Time (sec)	O_E (A_{obs})	Time (sec)	O_E (A_{obs})	Time (sec)	O_E (A_{obs})
1000	0.223	1045	0.248	1090	0.262	1135	0.273	1180	0.277
1015	0.233	1060	0.254	1105	0.265	1150	0.274	1195	0.278
1030	0.241	1075	0.258	1120	0.271	1165	0.276		

*Table 46: Dose 2; [**Cu$_b$**] = 1.56 mM, [**L**] = 3.02 mM, [**CX**]$_0$ = 190 mM, [**Zn**]$_0$ = 76.2 mM, [**E**]$_0$ = 191 mM; data fitted from 1000-1195 s. A_{obs} corrected for instrument background ($A_{background}$ = 0.0509). Non-linear least squares fitting of [**E**]$_{obs}$ = O_E× (1/ε_E) to [**E**]$_t$ = [**E**]$_{40}$ + Δ[**E**](1-exp(-k_1t)) gave k_1 = 0.0109(4) s^{-1} [R^2 = 0.999]. An average ε_E across 15 separate injections of 0.86(3) M^{-1} was used in all fits.*

Time (sec)	O_E (A_{obs})	Time (sec)	O_E (A_{obs})	Time (sec)	O_E (A_{obs})	Time (sec)	O_E (A_{obs})	Time (sec)	O_E (A_{obs})
1000	0.283	1045	0.325	1090	0.345	1135	0.355	1180	0.361
1015	0.301	1060	0.333	1105	0.349	1150	0.358		
1030	0.315	1075	0.340	1120	0.352	1165	0.360		

*Table 47: Dose 2; [**Cu$_b$**] = 1.70 mM, [**L**] = 3.44 mM, [**CX**]$_0$ = 221 mM, [**Zn**]$_0$ = 347 mM, [**E**]$_0$ = 219 mM; data fitted from 1000-1180 s. A_{obs} corrected for instrument background ($A_{background}$ = 0.0759). Non-linear least squares fitting of [**E**]$_{obs}$ = O_E× (1/ε_E) to [**E**]$_t$ = [**E**]$_{40}$ + Δ[**E**](1-exp(-k_1t)) gave k_1 = 0.0154(3) s^{-1} [R^2 = 0.999]. An average ε_E across 15 separate injections of 0.86(3) M^{-1} was used in all fits.*

Time (sec)	O_E (A_{obs})	Time (sec)	O_E (A_{obs})	Time (sec)	O_E (A_{obs})	Time (sec)	O_E (A_{obs})	Time (sec)	O_E (A_{obs})
940	0.301	985	0.342	1030	0.362	1075	0.373	1120	0.380
955	0.318	1000	0.350	1045	0.366	1090	0.375		
970	0.332	1015	0.357	1060	0.370	1105	0.378		

*Table 48: Dose 2; [**Cu$_b$**] = 0.871 mM, [**L**] = 1.81 mM, [**CX**]$_0$ = 233 mM, [**Zn**]$_0$ = 282 mM, [**E**]$_0$ = 234 mM; data fitted from 940-1120 s. A_{obs} corrected for instrument background ($A_{background}$ = 0.0871). Non-linear least squares fitting of $[E]_{obs} = O_E \times (1/\varepsilon_E)$ to $[E]_t = [E]_{40} + \Delta[E](1-\exp(-k_1 t))$ gave k_1 = 0.0138(3) s^{-1} [R^2 = 0.999]. An average ε_E across 15 separate injections of 0.86(3) M^{-1} was used in all fits.*

Time (sec)	O_E (A_{obs})	Time (sec)	O_E (A_{obs})	Time (sec)	O_E (A_{obs})	Time (sec)	O_E (A_{obs})	Time (sec)	O_E (A_{obs})
940	0.306	985	0.350	1030	0.367	1075	0.375	1120	0.381
955	0.327	1000	0.357	1045	0.370	1090	0.377	1135	0.382
970	0.341	1015	0.362	1060	0.373	1105	0.379	1150	0.383

*Table 49: Dose 2; [**Cu$_b$**] = 3.61 mM, [**L**] = 7.13 mM, [**CX**]$_0$ = 235 mM, [**Zn**]$_0$ = 278 mM, [**E**]$_0$ = 236 mM; data fitted from 940-1150 s. A_{obs} corrected for instrument background ($A_{background}$ = 0.104). Non-linear least squares fitting of $[E]_{obs} = O_E \times (1/\varepsilon_E)$ to $[E]_t = [E]_{40} + \Delta[E](1-\exp(-k_1 t))$ gave k_1 = 0.0175(1) s^{-1} [R^2 = 0.99]. An average ε_E across 15 separate injections of 0.86(3) M^{-1} was used in all fits.*

Time (sec)	O_E (A_{obs})	Time (sec)	O_E (A_{obs})	Time (sec)	O_E (A_{obs})	Time (sec)	O_E (A_{obs})	Time (sec)	O_E (A_{obs})
940	0.325	985	0.367	1030	0.389	1075	0.397		
955	0.341	1000	0.377	1045	0.390	1090	0.397		
970	0.358	1015	0.380	1060	0.393	1105	0.401		

*Table 50: Dose 2; [**Cu$_b$**] = 2.70 mM, [**L**] = 5.30 mM, [**CX**]$_0$ = 236 mM, [**Zn**]$_0$ = 272 mM, [**E**]$_0$ = 237 mM; data fitted from 940-1105 s. A_{obs} corrected for instrument background ($A_{background}$ = 0.132). Non-linear least squares fitting of $[E]_{obs} = O_E \times (1/\varepsilon_E)$ to $[E]_t = [E]_{40} + \Delta[E](1-\exp(-k_1 t))$ gave k_1 = 0.0170(1) s^{-1} [R^2 = 0.99]. An average ε_E across 15 separate injections of 0.86(3) M^{-1} was used in all fits.*

Time (sec)	O_E (A_{obs})	Time (sec)	O_E (A_{obs})	Time (sec)	O_E (A_{obs})	Time (sec)	O_E (A_{obs})	Time (sec)	O_E (A_{obs})
1000	0.292	1060	0.344	1120	0.362	1180	0.370	1240	0.376
1015	0.312	1075	0.350	1135	0.364	1195	0.372	1255	0.377
1030	0.326	1090	0.355	1150	0.367	1210	0.373	1270	0.378
1045	0.336	1105	0.358	1165	0.369	1225	0.375	1285	0.378

*Table 51: Dose 2; [**Cu$_b$**] = 1.86 mM, [**L**] = 2.40 mM, [**CX**]$_0$ = 235 mM, [**Zn**]$_0$ = 280 mM, [**E**]$_0$ = 235 mM; data fitted from 1000-1285 s. A_{obs} corrected for instrument background ($A_{background}$ = 0.0725). Non-linear least squares fitting of $[E]_{obs}$*

= O_E× (1/ε_E) to $[E]_t = [E]_{40} + \Delta[E](1-exp(-k_1t))$ gave k_1 = 0.0143(5) s^{-1} [R^2 = 0.99]. An average ε_E across 15 separate injections of 0.86(3) M^{-1} was used in all fits.

Time (sec)	O_E (A_{obs})	Time (sec)	O_E (A_{obs})	Time (sec)	O_E (A_{obs})	Time (sec)	O_E (A_{obs})	Time (sec)	O_E (A_{obs})
970	0.273	1030	0.322	1090	0.343	1150	0.352	1210	0.357
985	0.289	1045	0.329	1105	0.345	1165	0.354	1225	0.359
1000	0.304	1060	0.334	1120	0.347	1180	0.355		
1015	0.315	1075	0.339	1135	0.350	1195	0.356		

Table 52: Dose 2; $[\mathbf{Cu_b}] = 1.78$ mM, $[\mathbf{L}] = 1.59$ mM, $[\mathbf{CX}]_0 = 233$ mM, $[\mathbf{Zn}]_0 = 296$ mM, $[\mathbf{E}]_0 = 230$ mM; data fitted from 970-1225 s. A_{obs} corrected for instrument background ($A_{background}$ = 0.0903). Non-linear least squares fitting of $[\mathbf{E}]_{obs}$ = O_E× (1/ε_E) to $[\mathbf{E}]_t = [\mathbf{E}]_{40} + \Delta[\mathbf{E}](1-exp(-k_1t))$ gave k_1 = 0.0120(4) s^{-1} [R^2 = 0.99]. An average ε_E across 15 separate injections of 0.86(3) M^{-1} was used in all fits.

Time (sec)	O_E (A_{obs})	Time (sec)	O_E (A_{obs})	Time (sec)	O_E (A_{obs})	Time (sec)	O_E (A_{obs})	Time (sec)	O_E (A_{obs})
1000	0.259	1060	0.312	1120	0.333	1180	0.347		
1015	0.278	1075	0.322	1135	0.334	1195	0.349		
1030	0.294	1090	0.321	1150	0.339	1210	0.349		
1045	0.307	1105	0.329	1165	0.345	1225	0.354		

Table 53: Dose 2; $[\mathbf{Cu_b}] = 1.79$ mM, $[\mathbf{L}] = 4.12$ mM, $[\mathbf{CX}]_0 = 232$ mM, $[\mathbf{Zn}]_0 = 286$ mM, $[\mathbf{E}]_0 = 230$ mM; data fitted from 1000-1225 s. A_{obs} corrected for instrument background ($A_{background}$ = 0.107). Non-linear least squares fitting of $[\mathbf{E}]_{obs}$ = O_E× (1/ε_E) to $[\mathbf{E}]_t = [\mathbf{E}]_{40} + \Delta[\mathbf{E}](1-exp(-k_1t))$ gave k_1 = 0.012(1) s^{-1} [R^2 = 0.99]. An average ε_E across 15 separate injections of 0.86(3) M^{-1} was used in all fits.

3 Bibliography

[1] P. I. Dalko, L. Moisan, *Angew. Chem. Int. Ed.* **2004**, *43*, 5138–5175.

[2] J. von Liebig, *Liebigs Ann.* **1860**, *113*, 246–247.

[3] W. Langenbeck, *Liebigs Ann.* **1929**, *469*, 16–25.

[4] G. Jones, in *Organic Reactions*, **2011**, pp. 205–273.

[5] E. Ciganek, in *Organic Reactions*, **1997**, pp. 203–226.

[6] H. Pracejus, *Liebigs Ann.* **1960**, *634*, 9–22.

[7] Z. Wang, in *Comprehensive Organic Named Reactions and Reagents*, **1971**, pp. 1305–1309.

[8] P. I. Dalko, *Enantioselective Organocatalysis Reactions and Experimental Procedures* **2007**, 1–17.

[9] Y. Tu, Z. Wang, Y. Shi, *J. Am. Chem. Soc.* **1996**, *118*, 9806–9807.

[10] M. S. Sigman, E. N. Jacobsen, *J. Am. Chem. Soc.* **1998**, *120*, 4901–4902.

[11] B. List, R. a Lerner, C. F. Barbas III, *J. Am. Chem. Soc.* **2000**, *122*, 2395–2396.

[12] J. Wagner, R. a Lerner, C. F. Barbas, *Science* **1995**, *270*, 1797–1800.

[13] Y. M. a. Yamada, N. Yoshikawa, H. Sasai, M. Shibasaki, *Angew. Chem. Int. Ed.* **1997**, *36*, 1871–1873.

[14] W. S. Jen, J. J. M. Wiener, D. W. C. MacMillan, *J. Am. Chem. Soc.* **2000**, *122*, 9874–9875.

[15] D. W. C. MacMillan, *Nature* **2008**, *455*, 304–308.

[16] G. Wittig, H. Blumenthal, *Ber. Dtsch. Chem. Ges.* **1927**, *60*, 1085–1094.

[17] C. Mannich, H. Davidsen, *Chem. Ber.* **1936**, 2106–2112.

[18] G. Stork, R. Terrell, J. Szmuszkovicz, *J. Am. Chem. Soc.* **1954**, *76*, 2029–2030.

[19] H. Schiff, *Liebigs Ann.* **1864**, *131*, 118–119.

[20] A. Vilsmeier, A. Haack, *Chem. Ber.* **1927**, *60*, 119–122.

[21] S. Bahmanyar, K. N. Houk, H. J. Martin, B. List, *J. Am. Chem. Soc.* **2003**, *125*, 2475–2479.

[22] L. Hoang, S. Bahmanyar, K. N. Houk, B. List, *J. Am. Chem. Soc.* **2003**, *125*, 16–17.

[23] A. Armstrong, R. A. Boto, P. Dingwall, J. Contreras-García, M. J. Harvey, N. J. Mason, H. S. Rzepa, *Chem. Sci.* **2014**, *5*, 2057–2071.

[24] G. Dickmeiss, K. L. Jensen, D. Worgull, P. T. Franke, K. A. Jørgensen, *Angew. Chem. Int. Ed.* **2011**, *50*, 1580–1583.

[25] K. Frisch, A. Landa, S. Saaby, K. A. Jørgensen, *Angew. Chem. Int. Ed.* **2005**, *44*, 6058–6063.

[26] M. J. Gaunt, C. C. C. Johansson, A. McNally, N. T. Vo, *Drug Discovery Today* **2007**, *12*, 8–27.

[27] G. Zhong, *Angew. Chem. Int. Ed.* **2003**, *115*, 4379–4382.

[28] B. List, *J. Am. Chem. Soc.* **2002**, *124*, 5656–5657.

[29] M. Marigo, D. Fielenbach, A. Braunton, A. Kjærsgaard, K. A. Jørgensen, *Angew. Chem. Int. Ed.* **2005**, *44*, 3703–3706.

[30] M. P. Brochu, S. P. Brown, D. W. C. MacMillan, *J. Am. Chem. Soc.* **2004**, *126*, 4108–4109.

[31] N. Halland, A. Braunton, S. Bachmann, M. Marigo, K. A. Jørgensen, *J. Am. Chem. Soc.* **2004**, *126*, 4790–4791.

[32] E. N. Jacobsen, W. Zhang, A. R. Muci, J. R. Ecker, L. Deng, *J. Am. Chem. Soc.* **1991**, *113*, 7063–7064.

[33] B. D. Brandes, E. N. Jacobsen, *J. Org. Chem.* **1994**, *59*, 4378–4380.

[34] M. Lemay, L. Aumand, W. W. Ogilvie, *Adv. Synth. Catal.* **2007**, *349*, 441–447.

[35] M. Harmata, S. K. Ghosh, X. Hong, S. Wacharasindhu, P. Kirchhoefer, *J. Am. Chem. Soc.* **2003**, *125*, 2058–2059.

[36] E. Anniina, I. Majander, P. M. Pihko, *Chem. Rev.* **2007**, *107*, 5416–5470.

[37] H. King, Z. Meng, D. Denhart, R. Mattson, R. Kimura, D. Wu, Q. Gao, J. E. Macor, *Org. Lett.* **2005**, *7*, 3427–3440.

[38] M. Marigo, T. Schulte, J. Franzén, K. A. Jørgensen, *J. Am. Chem. Soc.* **2005**, *127*, 15710–15711.

[39] P. Dinér, M. Nielsen, M. Marigo, K. A. Jørgensen, *Angew. Chem. Int. Ed.* **2007**, *46*, 1983–1987.

[40] S. Bertelsen, P. Dinér, R. L. Johansen, K. A. Jørgensen, *J. Am. Chem. Soc.* **2007**, *129*, 1536–1537.

[41] H. Sundén, I. Ibrahem, L. Eriksson, A. Córdova, *Angew. Chem. Int. Ed.* **2005**, *44*, 4877–4880.

[42] C. Grondal, M. Jeanty, D. Enders, *Nat. Chem.* **2010**, *2*, 167–178.

[43] B. R. Buckley, M. C. Kimber, N. H. Slater, *Annu. Reports Prog. Chem.* **2012**, *108*, 98–109.

[44] H. Y. Jang, J. B. Hong, D. W. C. MacMillan, *J. Am. Chem. Soc.* **2007**, *129*, 7004–7005.

[45] T. D. Beeson, A. Mastracchio, J. Hong, K. Ashton, D. W. C. MacMillan, *Science* **2007**, *316*, 582–585.

[46] A. G. Wenzel, E. N. Jacobsen, *J. Am. Chem. Soc.* **2002**, *124*, 12964–12965.

[47] M. S. Taylor, E. N. Jacobsen, *J. Am. Chem. Soc.* **2004**, *126*, 10558–10559.

[48] E. A. Peterson, E. N. Jacobsen, *Angew. Chem. Int. Ed.* **2009**, *48*, 6328–6331.

[49] D. M. Flanigan, F. Romanov-Michailidis, N. A. White, T. Rovis, *Chem. Rev.* **2015**, *115*,

9307–9387.

[50] S. M. Langdon, M. M. D. Wilde, K. Thai, M. Gravel, *J. Am. Chem. Soc.* **2014**, *136*, 7539–7542.

[51] T. Ema, Y. Oue, K. Akihara, Y. Miyazaki, T. Sakai, *Org. Lett.* **2009**, *11*, 4866–4869.

[52] L. Hong, W. Sun, D. Yang, G. Li, R. Wang, *Chem. Rev.* **2016**, *116*, 4006–4123.

[53] P. G. Cozzi, F. Benfatti, L. Zoli, *Angew. Chem. Int. Ed.* **2009**, *48*, 1313–1316.

[54] J. H. Day, *Chem. Rev.* **1953**, *53*, 167–189.

[55] P. Preethalayam, K. S. Krishnan, S. Thulasi, S. S. Chand, J. Joseph, V. Nair, F. Jaroschik, K. V. Radhakrishnan, *Chem. Rev.* **2017**, *117*, 3930–3989.

[56] J. Thiele, *Ber. dtsch. chem. Ges.* **1900**, *33*, 666–673.

[57] K. J. Stone, R. D. Little, *J. Org. Chem.* **1984**, *49*, 1849–1853.

[58] I. Erden, F. Xu, A. Sadoun, W. Smith, G. Sheff, M. Ossun, *J. Org. Chem.* **1995**, *60*, 813–820.

[59] K. Chajara, H. Ottosson, *Tetrahedron Lett.* **2004**, *45*, 6741–6744.

[60] E. D. Bergmann, *Chem. Rev.* **1967**, *68*, 41–84.

[61] N. Coskun, I. Erden, *Tetrahedron* **20011**, *67*, 8607–8614.

[62] A. B. Flynn, W. W. Ogilvie, *Chem. Rev.* **2007**, *107*, 4698–4745.

[63] H. C. L. Abbenhuis, U. Burckhardt, V. Gramlich, A. Togni, A. Albinati, B. Mueller, *Organometallics* **1994**, *13*, 4481–4493.

[64] R. Mose, G. Preegel, J. Larsen, S. Jakobsen, E. H. Iversen, K. A. Jørgensen, *Nat. Chem.* **2017**, *9*, 487–492.

[65] W. Adam, L. P. Hadjiarapoglou, A. Meffert, *Tetrahedron Lett.* **1991**, *32*, 6697–6700.

[66] S. S. Chand, G. Gopalan, P. V. Santhini, P. Preethanuj, J. John, D. Harakat, F. Jaroschik, K. V. Radhakrishnan, *Org. Lett.* **2016**, *18*, 964–967.

[67] Z. Zhou, Z.-X. Wang, Y.-C. Zhou, W. Xiao, Q. Ouyang, W. Du, Y.-C. Chen, *Nat. Chem.* **2017**, *9*, 590–594.

[68] Z. J. Jia, C. Merten, R. Gontla, C. G. Daniliuc, A. P. Antonchick, H. Waldmann, *Angew. Chem. Int. Ed.* **2017**, *56*, 2429–2434.

[69] N. J. Sweeney, O. Mendoza, H. Müller-Bunz, C. Pampillón, F. J. K. Rehmann, K. Strohfeldt, M. Tacke, *J. Organomet. Chem.* **2005**, *690*, 4537–4544.

[70] K. Strohfeldt, M. Tacke, *Chem. Soc. Rev.* **2008**, *37*, 1174–1187.

[71] M. Cini, T. D. Bradshaw, S. Woodward, W. Lewis, *Angew. Chem. Int. Ed.* **2015**, *54*, 14179–14182.

[72] M. Cini, T. D. Bradshaw, W. Lewis, S. Woodward, *Eur. J. Org. Chem.* **2013**, 3997–4007.

[73] M. Tacke, L. T. Allen, L. P. Cuffe, W. M. Gallagher, Y. Lou, O. Mendoza, H. Müller-Bunz, F. J. K. Rehmann, N. Sweeney, *J. Organomet. Chem.* **2004**, *689*, 2242–2249.

[74] R. L. Halterman, *Chem. Rev.* **1992**, *92*, 965–994.

[75] C. G. Newton, D. Kossler, N. Cramer, *J. Am. Chem. Soc.* **2016**, *138*, 3935–3941.

[76] A. Gutnov, H. J. Drexler, A. Spannenberg, G. Oehme, B. Heller, *Organometallics* **2004**, *23*, 1002–1009.

[77] E. Cesarotti, H. B. Kagan, R. Goddard, C. Krüger, *J. Organomet. Chem.* **1978**, *162*, 297–309.

[78] G. Erker, A. a. H. van der Zeijden, *Angew. Chem. Int. Ed. English* **1990**, *29*, 512–514.

[79] S. L. Colletti, R. L. Halterman, *Organometallics* **1991**, *10*, 3438–3448.

[80] B. Ye, N. Cramer, *J. Am. Chem. Soc.* **2013**, *135*, 636–639.

[81] J. Zheng, W. J. Cui, C. Zheng, S. L. You, *J. Am. Chem. Soc.* **2016**, *138*, 5242–5245.

[82] D. Y. Kondakov, E. Negishi, *J. Am. Chem. Soc.* **1995**, *117*, 10771–10772.

[83] E. I. Negishi, *Arkivoc* **2011**, *8*, 34–53.

[84] E. Meléndez, *Crit. Rev. Oncol. Hematol.* **2002**, *42*, 309–315.

[85] M. Cini, T. D. Bradshaw, S. Woodward, *Chem. Soc. Rev.* **2017**, *46*, 1040–1051.

[86] M. Cini, S. Woodward, T. D. Bradshaw, S. Woodward, T. D. Bradshaw, *Metallomics* **2016**, *8*, 286–297.

[87] R. Nouch, M. Cini, M. Magre, M. Abid, M. Diéguez, O. Pàmies, S. Woodward, W. Lewis, *Chem. Eur. J.* **2017**, *23*, 17195–17198.

[88] L. Pasteur, *Ann. Chim. Phys.* **1850**, *28*, 56–99.

[89] Y. Tobe, *Mendeleev Commun.* **2003**, *13*, 93–94.

[90] R. Chowdhury, S. K. Ghosh, *Org. Lett.* **2009**, *11*, 3270–3273.

[91] S. K. Hendrie, J. Leonard, *Tetrahedron* **1987**, *43*, 3289–3294.

[92] B. Nyasse, L. Grehn, U. Ragnarsson, *Chem. Commun.* **1997**, 1017–1018.

[93] J. Carreras, A. Avenoza, J. H. Busto, J. M. Peregrina, *J. Org. Chem.* **2007**, *72*, 3112–3115.

[94] R. L. Elliott et al., *Bioorganic Med. Chem. Lett.* **1996**, *6*, 2283–2288.

[95] J. N. Freskos, G. W. Morrow, J. S. Swenton, *J. Org. Chem.* **1985**, *50*, 805–810.

[96] D. H. T. Phan, B. Kim, V. M. Dong, *J. Am. Chem. Soc.* **2009**, *131*, 15608–15609.

[97] C. I. Someya, S. Inoue, E. Irran, S. Krackl, S. Enthaler, *Eur. J. Inorg. Chem.* **2011**, 2691–2697.

[98] A. R. Katritzky, P. A. Harris, A. Kotali, *J. Org. Chem.* **1991**, *56*, 5049–5051.

[99] F. G. Bordwell, M. J. Bausch, *J. Am. Chem. Soc.* **1983**, *105*, 6188–6189.

[100] T. Chanda, S. Chowdhury, N. Anand, S. Koley, A. Gupta, M. S. Singh, *Tetrahedron Lett.*

2015, *56*, 981–985.

[101] J. Moritani, Y. Hasegawa, Y. Kayaki, T. Ikariya, *Tetrahedron Lett.* **2014**, *55*, 1188–1191.

[102] D. B. Knight, J. A. Harrelson, *J. Chem. Soc. Chem. Commun.* **1987**, 116–117.

[103] S. M. E. D. Hughes, C. K. Ingold, *J. Chem. Soc.* **1935**, 1196–1201.

[104] P. Brewster, E. D. Hughes, C. K. Ingold, P. A. D. S. Rao, *Nature* **1950**, *166*, 179–180.

[105] R. M. Pagni, *Found. Chem.* **2011**, *13*, 131–143.

[106] E. Sirignano, C. Saturnino, A. Botta, M. S. Sinicropi, A. Caruso, A. Pisano, R. Lappano, M. Maggiolini, P. Longo, *Bioorg. Med. Chem. Lett.* **2013**, *23*, 3458–3462.

[107] T. Widianti, Y. Hiraga, S. Kojima, M. Abe, *Tetrahedron Asymmetry* **2010**, *21*, 1861–1868.

[108] G. A. Molander, J. A. C. Romero, *Tetrahedron* **2005**, *61*, 2631–2643.

[109] V. Sandanayaka et al., *J. Med. Chem.* **2010**, *53*, 573–585.

[110] K. Nobuoka, S. Kitaoka, T. Kojima, Y. Kawano, K. Hirano, M. Tange, S. Obata, Y. Yamamoto, T. Harran, Y. Ishikawa, *Org. Chem. Int.* **2014**, *2014*, 1–9.

[111] M. Asami, *Bull. Chem. Soc. Jpn.* **1990**, *63*, 721–727.

[112] S. Des, D. Primaires, P. Canonne, I. P. I. Akssira, *Tetrahedron* **1988**, *44*, 2903–2912.

[113] W. Chen, Z.-H. Zhou, H.-B. Chen, *Org. Biomol. Chem.* **2017**, *15*, 1530–1536.

[114] E. C. Ashby, *Q. Rev. Chem. Soc.* **1967**, *2*, 259–285.

[115] G. H. Posner, *Org. React.* **1972**, 1–114.

[116] M. Conrad, M. Guthzeit, *Ber. dtsch. chem. Ges* **1884**, *17*, 1185–1188.

[117] T. Tokoroyama, *Eur. J. Org. Chem.* **2010**, 2009–2016.

[118] A. Michael, *J. für Prakt. Chemie* **1887**, *35*, 349–356.

[119] B. E. Rossiter, N. M. Swingle, *Chem. Rev.* **1992**, *92*, 771–806.

[120] W. Oppolzer, H. J. Loher, *Helv. Chim. Acta* **1981**, *64*, 2808–2811.

[121] R. K. Dieter, M. Tokles, *J. Am. Chem. Soc.* **1987**, *109*, 2040–2046.

[122] G. M. Villacorta, C. P. Rao, S. J. Lippard, *J. Am. Chem. Soc.* **1988**, *110*, 3175–3182.

[123] K. H. Ahn, R. B. Klassen, S. J. Lippard, *Organometallics* **1990**, *9*, 3178–3181.

[124] A. Alexakis, N. Krause, S. Woodward, *Copper-Catalyzed Asymmetric Synthesis*, **2014**.

[125] S. R. Harutyunyan, T. den Hartog, K. Geurts, A. J. Minnaard, B. L. Feringa, *Chem Rev* **2008**, *108*, 2824–2852.

[126] T. Thaler, P. Knochel, *Angew. Chem. Int. Ed.* **2009**, *48*, 645–648.

[127] A. Alexakis, J. E. Backvall, N. Krause, O. Pamies, M. Dieguez, *Chem Rev* **2008**, *108*, 2796–2823.

[128] D. Willcox, R. Nouch, A. Kingsbury, D. Robinson, J. V. Carey, S. Brough, S. Woodward, *ACS Catal.* **2017**, *7*, 6901–6908.

[129] F. López, A. J. Minnaard, B. L. Feringa, *Acc. Chem. Res.* **2007**, *40*, 179–188.

[130] A. Hajra, N. Yoshikai, E. Nakamura, *Org. Lett.* **2006**, *8*, 4153–4155.

[131] N. Germain, M. Magrez, S. Kehrli, M. Mauduit, A. Alexakis, *European J. Org. Chem.* **2012**, 5301–5306.

[132] L. Palais, A. Alexakis, *Chem. Eur. J.* **2009**, *15*, 10473–10485.

[133] S. H. Bertz, S. Cope, M. Murphy, C. A. Ogle, B. J. Taylor, *J. Am. Chem. Soc.* **2007**, *129*, 7208–7209.

[134] N. Yoshikai, E. Nakamura, *Chem. Rev.* **2012**, *112*, 2339–2372.

[135] E. Nakamura, S. Mori, *Angew. Chem. Int. Ed.* **2000**, *39*, 3750–3771.

[136] S. Mori, E. Nakamura, *Chem. Eur. J.* **1999**, *5*, 1534–1543.

[137] S. R. Harutyunyan, F. López, W. R. Browne, A. Correa, D. Peña, R. Badorrey, A. Meetsma, A. J. Minnaard, B. L. Feringa, *J. Am. Chem. Soc.* **2006**, *128*, 9103–9118.

[138] M. Vuagnoux-D'Augustin, A. Alexakis, *Eur. J. Org. Chem.* **2007**, 5852–5860.

[139] O. Knopff, A. Alexakis, *Org. Lett.* **2002**, *4*, 3835–3837.

[140] S. Woodward, *Synlett* **2007**, *10*, 1490–1500.

[141] R. Benn, H. Lehmkuhl, K. Mehler, A. Rufinska, *Angew. Chem. Int. Ed.* **1984**, *23*, 534–535.

[142] M. B. Smith, W. E. Becker, *Tetrahedron* **1966**, *22*, 3027–3036.

[143] P. G. Andersson, *Innovative Catalysis in Organic Synthesis*, **2012**.

[144] M. Kitamura, T. Miki, K. Nakano, R. Noyori, *Bull. Chem. Soc. Jpn.* **2000**, *73*, 999–1014.

[145] T. Pfretzschner, L. Kleemann, B. Janza, K. Harms, T. Schrader, *Chem. Eur. J.* **2004**, *10*, 6048–6057.

[146] K. Schober, H. Zhang, R. M. Gschwind, *J. Am. Chem. Soc.* **2008**, *130*, 12310–12317.

[147] H. Zhang, R. M. Gschwind, *Angew. Chem. Int. Ed.* **2006**, *45*, 6391–9394.

[148] F. Von Rekowski, C. Koch, R. M. Gschwind, *J. Am. Chem. Soc.* **2014**, *136*, 11389–11395.

[149] H. Zhang, R. M. Gschwind, *Chem. Eur. J.* **2007**, *13*, 6691–6700.

[150] M. Welker, S. Woodward, L. F. Veiros, M. J. Calhorda, *Chem. Eur. J.* **2010**, *16*, 5620–5629.

[151] J. Canisius, A. Gerold, N. Krause, *Angew. Chem. Int. Ed.* **1999**, *38*, 1644–1646.

[152] R. Molteni, R. Bertermann, K. Edkins, A. Steffen, *Chem. Commun.* **2016**, *52*, 5019–5022.

[153] F. A. Cotton, E. V. Dikarev, M. A. Petrukhina, *Inorg. Chem.* **2000**, *39*, 6072–6079.

[154] X. Lin, C. Hou, H. Li, Z. Weng, *Chem. Eur. J.* **2016**, *22*, 2075–2084.

[155] P. F. Rodesiler, E. L. Amma, *J. Chem. Soc. Chem. Commun.* **1974**, 599–600.

[156] E. A. Goreshnik, M. G. Mys'Kiv, *Russ. J. Coord. Chem. Khimiya* **2008**, *34*, 819–823.

[157] C. Wu, Y. Huang, Z. Zhang, Z. Weng, *Asian J. Org. Chem.* **2016**, *5*, 1406–1410.

[158] R. J. Davidson, E. W. Ainscough, A. M. Brodie, G. H. Freeman, G. B. Jameson, *Polyhedron* **2014**, *79*, 330–337.

[159] E. A. Goreshnik, Z. Mazej, V. V Karpyak, M. G. Mys, *Acta Chim. Slov.* **2008**, *55*, 775–778.

[160] F. Fenwick, *J. Am. Chem. Soc.* **1926**, *48*, 860–870.

[161] B. M. Rosen, X. Jiang, C. J. Wilson, N. H. Nguyen, M. J. Monteiro, V. Percec, *J. Polym. Sci. Part A Polym. Chem.* **2009**, *47*, 5606–5628.

[162] R. G. Salomon, *Encycl. Reagents Org. Synth.* **2005**.

[163] E. J. Parish, S. A. Kizito, *Encycl. Reagents Org. Synth.* **2001**.

[164] E. J. Parish, H. Qin, B. H. Lipshutz, T. B. Petersen, *Encycl. Reagents Org. Synth.* **2007**.

[165] J. Kubas, *Inorg. Synth.* **1990**, *28*, 68–70.

[166] T. Rühl, W. Rafique, V. T. Lien, P. J. Riss, *Chem. Commun.* **2014**, *50*, 6056–6059.

[167] M. Kubota, D. L. Johnston, *J. Inorg. Nucl. Chem.* **1967**, *29*, 769–773.

[168] P. K. Fraser, S. Woodward, *Chem. Eur. J.* **2003**, *9*, 776–783.

[169] J. Green, E. Sinn, S. Woodward, R. Butcher, *Polyhedron* **1993**, *12*, 991–1001.

[170] C. Börner, M. R. Dennis, E. Sinn, S. Woodward, *Eur. J. Org. Chem.* **2001**, 2435–2446.

[171] L. Palais, L. Babel, A. Quintard, S. Belot, A. Alexakis, *Org. Lett.* **2010**, *12*, 1988–1991.

[172] S. Afewerki, P. Breistein, K. Pirttilä, L. Deiana, P. Dziedzic, I. Ibrahem, A. Cordova, *Chem. Eur. J.* **2011**, *17*, 8784–8788.

[173] M. Fananas-Mastral, B. L. Feringa, *J. Am. Chem. Soc.* **2010**, *132*, 13152–13153.

[174] T. Soeta, K. Selim, M. Kuriyama, K. Tomioka, *Adv. Synth. Catal.* **2007**, *349*, 629–635.

[175] Y. Yamanoi, T. Imamoto, *J. Org. Chem.* **1999**, *64*, 2988–2989.

[176] L. Wang, Y. Li, C. Yip, L. Qiu, Z. Zhou, A. S. C. Chan, *Adv. Synth. Catal.* **2004**, *346*, 947–953.

[177] C. L. Winn, F. Guillen, J. Pytkowicz, S. Roland, P. Mangeney, A. Alexakis, *J. Organomet. Chem.* **2005**, *690*, 5672–5695.

[178] F. Guillen, C. L. Winn, A. Alexakis, *Tetrahedron Asymmetry* **2001**, *12*, 2083–2086.

[179] F. Zhang, A. S. C. Chan, *Tetrahedron Asymmetry* **1998**, *9*, 1179–1182.

[180] W. A. N. Bo, K. F. Yee, W. Lailai, X. U. Lijin, Z. Qinglu, X. Aiping, *Chinese J. Catal.* **2011**, *32*, 80–85.

[181] Y. Ebisu, K. Kawamura, M. Hayashi, *Tetrahedron: Asymmetry* **2012**, *23*, 959–964.

[182] A. Mandoli, L. A. Arnold, A. H. M. de Vries, P. Salvadori, B. L. Feringa, *Tetrahedron Asymmetry* **2001**, *12*, 1929–1937.

[183] A. Alexakis, J. Burton, J. Vastra, C. Benhaim, X. Fournioux, A. Van Den Heuvel, J. Leve, S. Rosset, *Eur. J. Org. Chem.* **2000**, 4011–4027.

[184] K. Kawamura, H. Fukuzawa, M. Hayashi, *Org. Lett.* **2008**, *10*, 3509–3512.

[185] O. Huttenloch, J. Spieler, H. Waldmann, *Chem. Eur. J.* **2000**, *6*, 671–675.

[186] S. J. Degrado, H. Mizutani, A. H. Hoveyda, B. College, C. Hill, *J. Am. Chem. Soc.* **2001**, *123*, 755–756.

[187] L. Liang, T. T. Au-yeung, A. S. C. Chan, *Org. Lett.* **2002**, *4*, 3799–3801.

[188] B. Breit, A. C. Laungani, *Tetrahedron: Asymmetry* **2003**, *14*, 3823–3826.

[189] Q. Zhao, L. Wang, A. Xing, *Tetrahedron: Asymmetry* **2010**, *21*, 2993–2998.

[190] S. Gou, Z. Ye, L. Shi, D. Qing, W. Zhang, Y. Wang, *Appl. Organomet. Chem.* **2010**, *24*, 517–522.

[191] G. Delapierre, T. Constantieux, J. M. Brunel, G. Buono, *Eur. J. Org. Chem.* **2000**, 2507–2511.

[192] V. Gutmann, *Coord. Chem. Rev.* **1976**, *18*, 225–255.

[193] R. Nouch, S. Woodward, D. Willcox, D. Robinson, W. Lewis, *Manuscript in preparation***.**

[194] L. A. Arnold, R. Imbos, A. Mandoli, A. H. M. De Vries, R. Naasz, B. L. Feringa, *Tetrahedron* **2000**, *56*, 2865–2878.

[195] H. Gilman, F. K. Cartledge, *J. Organomet. Chem.* **1964**, *2*, 447–454.

[196] C. R. Smith, D. J. Mans, T. V. RajanBabu, *Org. Synth.* **2008**, *85*, 238–247.

[197] E. J. Billo, *Excel for Chemists: A Comprehensive Guide*, John Wiley & Sons, **2011**.

[198] T. Inagaki, L. T. Phong, A. Furuta, J. I. Ito, H. Nishiyama, *Chem. Eur. J.* **2010**, *16*, 3090–3096.

[199] X. F. Cao, M. Hu, F. Li, W. C. Lu, G. A. Yu, S. H. Liu, *Helv. Chim. Acta* **2009**, *92*, 1007–1013.

[200] B. L. F. B. Macia, M. A. Fernandez-Ibanez, N. Mrsic, A. J. Minnaard, *Tetrahedron Lett.* **2008**, *49*, 1877–1880.